

GENETIC, PHYSIOLOGICAL AND BIOTECHNOLOGICAL ASSESSMENT OF  
MICROORGANISMS FOR RENEWABLE AND SUSTAINABLE ENERGY RESOURCE  
PRODUCTION

By  
KAAN YILANCIOĞLU

Submitted to the Graduate School of Engineering and Natural Sciences  
in partial fulfillment of  
the requirements for the degree of  
Doctor of Philosophy

SABANCI UNIVERSITY

June 2014

GERİ DÖNÜŞÜMLÜ VE SÜRDÜRÜLEBİLİR ENERJİ KAYNAĞI ÜRETİMİ İÇİN  
MİKROORGANİZMALARIN GENETİK, FİZYOLOJİK VE BİYOTEKNOLOJİK  
AÇIDAN DEĞERLENDİRİLMESİ

APPROVED BY:

Prof. Dr. Selim Çetiner .....  
(Dissertation Supervisor)

Prof. Dr. Meriç Albay .....

Assoc. Prof. Dr. Batu Erman .....

Assoc. Prof. Dr. Murat Çokol .....

Asst. Prof. Dr. Alpay Taralp .....

DATE OF APPROVAL: .../.../...

© Kaan Yilanciođlu 2014  
All Rights Reserved

GENETIC, PHYSIOLOGICAL AND BIOTECHNOLOGICAL ASSESSMENT OF  
MICROORGANISMS FOR RENEWABLE AND SUSTAINABLE ENERGY RESOURCE  
PRODUCTION

Kaan Yılancıoğlu

Biological Sciences and Bioengineering, PhD Thesis, 2014

Thesis Advisor: Prof. Dr. Selim Çetiner

Key words: Halophilic Microalgae, Renewable Energy, Algae Biotechnology, *Dunaliella*

**Abstract**

The term "algae" defines variety of photosynthetic organisms found throughout the world in various environmental conditions. Algae species are estimated to number in the tens of thousands. Because algae are photosynthetic, naturally able to replicate rapidly and produce high amount of oils, alcohols, and biomass, they have attracted the attention of researchers and industrial producers seeking alternatives to currently used fossil fuels. Algae thrive on organic carbon or CO<sub>2</sub>, nutrients such as nitrogen, phosphorus and other inorganic substances which enables algae to be used in bioremediation. Growth conditions, nutrients such as carbon and nitrogen, and many other factors affect the algal cell metabolism. Thus, manipulation of different cultivation conditions have been shown successful in increasing algal biomass and lipid productivity in order to substitute petroleum use. Algae biotechnology research goals especially include finding ways to increase the reproductive rate, improve metabolism of inputs, and enhance the production of desired oils, fuel-grade alcohols in useful species. In this thesis, newly isolated halophilic unicellular green algae species are assessed for potential renewable energy resource. Novel strategies for increasing cellular lipid production were established. Exogenous application of oxidative stress by hydrogen peroxide treatment was shown as a novel lipid accumulation inducer. Moreover, increased lipid accumulation response was also observed in heavy metal induced oxidative stress which makes combination of heavy metal bioremediation and oil production possible as a novel algae cultivation strategy. Directed evolution and natural selection strategies were applied to model organism *Saccharomyces cerevisiae* and *Dunaliella salina* for revealing underlying biochemical, genetic factors of increased cellular lipid production in order to provide useful strategies for future biofuel production.

GERİ DÖNÜŞÜMLÜ VE SÜRDÜRÜLEBİLİR ENERJİ KAYNAĞI ÜRETİMİ İÇİN  
MİKROORGANİZMALARIN GENETİK, FİZYOLOJİK VE BİYOTEKNOLOJİK AÇIDAN  
DEĞERLENDİRİLMESİ

Kaan Yılcıoğlu

Biyoloji Bilimleri ve Biyomühendislik, Doktora Tezi, 2014

Tez Danışmanı: Prof. Dr. Selim Çetiner

Anahtar kelimeler: Halofilik Mikroalg, Yenilenebilir Enerji, Alg Biyoteknolojisi, *Dunaliella*

**Özet**

Algler çeşitli çevresel koşullara adapte olmuş fotosentetik organizmalar olarak tanımlanmaktadır. Onbinlerce farklı çeşit alg türünün varolduğu düşünülmektedir. Alglerin hızlı çoğalmaları, yüksek miktarda yağ ve biyokütle üretimleri nedeni ile, kullanılmakta olan fosil yakıtların yerine geçebilecekleri düşünülmekte, bilim dünyasının ilgisi gün geçtikçe bu yöne kaymaktadır. Algler karbondioksit, nitrojen, fosfor gibi bileşikleri, besin üretimi için kullanmakta, bu özellikleri algleri biyoremediyasyon açısından kullanışlı hale getirmektedir. Çevresel koşullar metabolizmaları açısından önemlidir. Bu koşulların değiştirilmesi ile yapılan metabolik manipülasyonlar ile büyüme ve yağ üretim potansiyellerinin artırılması sözkonusudur. Biyoteknolojik araştırma hedefleri, yağ üretimi veya biyoteknolojik açıdan önemli diğer metabolitlerin üretimlerinin arttırımına yönelik yeni yöntemler bulunmasını kapsamaktadır. Bu çalışmada, yeni izole edilmiş halofilik tek hücreli yeşil alglerin geri dönüşümlü enerji kaynağı olarak kullanım potansiyelleri araştırılmış, hücresel yağ oranlarını arttırmaya yönelik özgün stratejiler geliştirilmiştir. Hidrojen peroksit uygulaması ile dışarıdan tetiklenen oksidatif stresin hücresel yağ arttırımında özgün bir uyaran olduğu gösterilmiştir. Ayrıca, ağır metal uygulaması ile tetiklenen oksidatif stress sonucunda hücresel lipid üretiminin arttığıda gözlemlenmiş, ağır metal biyoremediyasyonu ve yağ üretiminin kombinasyonu ile yeni bir üretim stratejisi ortaya çıkartılmıştır. Yönlendirilmiş evrim ve doğal seleksiyon stratejileri model organizma *Saccharomyces cerevisiae* and *Dunaliella salina* türlerine uygulanarak, arttırılmış hücresel lipid üretiminin biyokimyasal ve genetik temellerinin ortaya çıkarılması, böylece biyoyakıt üretiminde yararlı olabilecek stratejilerin bulunmasında yarar sağlanması amaçlanmıştır.

*To my family and beloved wife,  
past, present and future...*

## ACKNOWLEDGEMENTS

This thesis represents a tremendous amount of work, and required a tremendous amount of support from a lot of people. I take this opportunity with much pleasure to thank all of them.

The first and deepest thanks to my fatherly supervisor and mentor, Prof. Dr. Selim Çetiner for his patience and understanding in guiding me. The remarkable person instructed me a lot of things, especially about how to be a scientist and most importantly how to be a good and ethical individual. I always consider myself a lucky person to know him and to have the chance studying under his supervision and leadership. I want to give my gratitude to Assoc. Prof. Dr. Murat Çokol to lead me whenever I felt lost. I also want to thank to Prof. Selim Çetiner and Assoc. Prof. Murat Çokol for being such a family to me in this long and hardest way through the end.

I also want to thank to our collaborators and other remarkable people I met in this journey Prof. Dr. Meriç Albay and Assoc. Prof. Dr. Reyhan Akçaalan from Istanbul University for providing me important guidance and mentorship. Furthermore, I am thankful to Prof. Melek Öztürk, Assist. Prof. Alpay Taralp, Assoc. Prof. Batu Erman for their support and guidance, their time in this study.

My special thanks go to my beloved friend Can Timuçin for being me such a brother in my hard times, I thank for his support and priceless times of our conversations. I thank to Dr. Özgür Arıkan, Dr. Özgür Uzun and many other friends from Cerrahpasa School of Medicine that I could not mention here. They always supported me emotionally whenever I need them.

Finally my deepest thanks go to my dear family Neslihan, Kubilay and Dilay Yılancıoğlu who grew me up and provided me a good education, social and intellectual environment. I thank to my soul, beloved wife Sebnem Kuter Yilancioglu for being every good thing for me all the times and giving me everything I need from a spouse, her lovely heart and priceless support.

## TABLE OF C ONTENTS

<b>Chapter 1</b> .....	1
1.1 Introduction .....	1
1.1.1 Introduction to Algae Kingdom.....	1
1.1.2 Introduction to Algae Biotechnology .....	2
1.1.2.1 Historical View of Algae.....	2
1.1.2.2 Utilization of Algae .....	3
1.1.2.2.1 Human Food .....	4
1.1.2.2.2 Animal Feed.....	4
1.1.2.2.3 Aquaculture.....	4
1.1.2.2.4 Chemicals and Pharmaceuticals .....	5
1.1.2.2.5 Pigments .....	6
1.1.2.2.6 Diatomite .....	6
1.1.2.2.7 Fertilizers .....	6
1.1.2.2.8 Waste Water Treatment .....	6
1.1.2.2.9 Cosmetics.....	6
1.1.2.2.10 Fuel .....	6
1.1.3 Introduction to Renewable and Sustainable Energy Resources from Algae.....	8
1.1.3.1 Potential Advantages and Challenges of Algae as Feedstocks for Biofuels.....	13
1.1.3.2 Conversion of Lipids to Biofuel .....	14
1.1.3.3 Factors Affecting Triacylglycerol Accumulation and Fatty Acid Composition.....	15
1.1.3.4 Harvesting and Extraction of Algal Oil from Microalgae .....	16
1.1.3.5 Future of Algal Feedstock Based Biofuels .....	17
1.1.3.6 Bio-Oil and Bio-Syngas.....	18
1.1.3.7 Hydrogen From Algae .....	18
1.2 Materials and Methods .....	19
1.2.1 Algae Isolation and Purification .....	19
1.2.2 Morphological Identification .....	20

1.2.3 Molecular Identification .....	20
1.2.3.1 Isolation and Purification of DNA and Amplification of 18s RNA Gene .....	20
1.2.3.2 Sequencing and Phylogenetic Analysis.....	21
1.2.4 Optimization of Cultivation Conditions .....	21
1.2.4.1 Optical Density (Od <sub>600</sub> ) Standardization .....	21
1.2.4.2 Growth Media Optimization.....	21
1.2.4.3 pH Range Test .....	22
1.2.4.4 Salinity Range Test.....	22
1.2.5 Flow Cytometric Nile Red Method for Lipid Content Analysis .....	22
1.2.6 Algae Growth Kinetics .....	23
1.2.7 Fluorescent Microscopic Analyses .....	23
1.2.8 Lipid Extraction GC-MS Analysis of Fatty Acid Composition.....	23
1.3 Result and Discussion .....	24
1.3.1 Selection of Isolation Location and Sampling .....	24
1.3.2 ICP-OES Macro and Micro Element Analysis of the Lake Tuz.....	26
1.3.3 Obtaining Monocultures of Newly Isolated Hypersaline Algae Species.....	28
1.3.4 Optimization of Cultivation Conditions of Newly Isolated Algae Species .....	30
1.3.4.1 Optimization of NaCl Concentration.....	30
1.3.4.2 Optimization of pH Conditions .....	31
1.3.4.3 Optimization of Nitrogen Sources.....	33
1.3.5 Molecular Identification of Newly Isolated Halophilic Algal Species from Lake Tuz.	34
1.3.6 Entry of Genetic ID to NCBI GeneBank .....	36
1.3.7 Phylogenetic Analysis of the Newly Isolated <i>Dunaliella</i> Strains.....	39
1.3.7.1 ClustalW Analysis of 18S-RDNA Regions of Newly Isolated <i>Dunaliella</i> Strains Compared with Known <i>Dunaliella</i> Species .....	39
1.3.7.2 AFLP Analysis of Newly Isolated <i>Dunaliella</i> Strains .....	40
1.3.7.3 Blast Analysis of Newly Isolated <i>Dunaliella</i> Species.....	42
1.3.8 GC-MS Analysis of Fatty Acid Composition of New <i>Dunaliella</i> Isolates.....	44
1.3.9 Determination of Lipid Contents of The Isolated <i>Dunaliella</i> Strains Under Different Cultivation Conditions.....	45

1.3.9.1 The Effect of Different NaCl Concentrations on Lipid Accumulation in Isolated <i>Dunaliella</i> Species .....	47
1.3.9.2 The Effect of Different pHs on Lipid Accumulation in Isolated <i>Dunaliella</i> Species.....	49
1.3.9.3 The Effect of Different Nitrogen Source on Lipid Accumulation in Isolated <i>Dunaliella</i> Species .....	51
1.3.9.4 The Effect of Nitrogen Deprived Cultivation Conditions on Lipid Accumulation in Isolated <i>Dunaliella</i> Species.....	53
1.3.9.5 The Effect of Sea Water Cultivation Conditions on Lipid Accumulation in Isolated <i>Dunaliella</i> Species.....	55
1.3.9.6 Optimization of -80°C / -196°C Ultrafreeze Storage Conditions for Long and Short Term Storage .....	57
1.4 Conclusions.....	59
<b>Chapter 2.....</b>	<b>60</b>
2.1 Introduction .....	60
2.2 Algae Isolation and Purification.....	62
2.2.1 Organism and Culture Conditions .....	62
2.2.2 Isolation and Purification of DNA and Amplification Of 18S rRNA Encoding Gene .	63
2.2.3 Sequencing and Phylogenetic Analysis .....	64
2.2.4 Growth Analysis .....	64
2.2.5 Extraction and Measurements of Lipid Contents and Fluorescence Microscopy.....	64
2.2.6 Spectrofluorometric Microplate Analysis for Determination of Lipid and Reactive Oxygen Species Accumulation .....	65
2.2.7 Flow Cytometric Analysis for Determination of Lipid and Reactive Oxygen Species Accumulation .....	65
2.2.8 Protein, Chlorophyll, Carotenoid, TBARS Analyses and Enzymatic Assays .....	66
2.3 Results and Discussion.....	67
2.3.1 Isolation and Identification of the New <i>Dunaliella</i> Salina Strain.....	67
2.3.2 Growth Analysis of the New <i>Dunaliella</i> Strain Under Different Nitrogen Concentrations .....	69

2.3.3 Lipid Accumulation Analysis of the New <i>Dunaliella Salina</i> Strain Under Different Nitrogen Concentrations .....	70
2.3.4 Antioxidant Enzyme Activities, Pigment Composition and Protein Analyses Under Different Nitrogen Concentrations .....	73
2.3.5 Reactive Oxygen Species (ROS) Production Induces Lipid Accumulation .....	76
2.3.6 Effects of H <sub>2</sub> O <sub>2</sub> Induced Oxidative Stress on Lipid Accumulation in <i>Dunaliella Tertiolecta</i> and <i>Chlamydomonas Reinhardtii</i> .....	81
2.4 Conclusions .....	83

### Chapter 3

3.1 Introduction .....	85
3.2 Materials and Methods .....	87
3.2.1 Organism and Culture Conditions .....	87
3.2.2 Isolation and Purification of DNA and Amplification of 18S rRNA Encoding Gene .....	88
3.2.3 Sequencing and Phylogenetic Analysis .....	88
3.2.4 Adsorption Experiments and Analysis .....	88
3.2.5 Growth Analysis .....	89
3.2.6 Fluorometric Microplate Analysis for Determination of Lipid and Reactive Oxygen Species Accumulation .....	89
3.2.7 Flow Cytometric Analysis for Determination of Lipid and Reactive Oxygen Species Accumulation.....	90
3.2.8 FT-IR Spectroscopy .....	90
3.2.9 Protein, Chlorophyll, Carotenoid, TBARS Analyses and Fluorescence Microscopy .....	90
3.3 Results and Discussion.....	91
3.3.1 Isolation and Identification of the New <i>Dunaliella</i> Strain.....	91
3.3.2 Heavy Metal Adsorption by <i>Dunaliella Sp. Tuz Ks_02</i> .....	92
3.3.3 Growth Analysis of the New <i>Dunaliella Sp. Tuz Ks_02</i> Strain Under Cu (II), Zn (II), Ni (II) Consisting Cultivation Conditions .....	97
3.3.4 Cellular Lipid and ROS Accumulation Analyses of the New <i>Dunaliella Sp. Tuz Ks_02</i> Strain Under Cu (II), Zn (II), Ni (II) Consisting Cultivation Conditions.....	99

3.3.5 Metabolic Activity and Pigment Analysis of the New <i>Dunaliella Sp. Tuz Ks_02</i> Strain Under Cu (II), Zn (II), Ni (II) Consisting Cultivation Conditions.....	106
3.4 Conclusions .....	109
<b>Chapter 4</b> .....	110
4.1 Introduction .....	110
4.1.1 Genetic Engineering of Microorganisms .....	110
4.1.1.1 General Aspects .....	110
4.1.1.2 Algae Genome Projects.....	111
4.1.1.3 Lipid Metabolism and Metabolic Engineering .....	112
4.1.1.4 Existing Problems in Genetic Engineering .....	117
4.1.1.5 Directed Evolution .....	118
4.2 Materials And Methods.....	121
4.2.1 Semi-Quantitative RT-PCR Analysis of Fatty Acid Synthesis Genes under Nitrogen Depleted Cultivation Conditions .....	121
4.2.1.1 rDNA Isolation and RT Reaction.....	121
4.2.1.2 Semi-Quantitative RT-PCR Analysis .....	121
4.2.2 Obtaining Fatty Acid Metabolism Specific Inhibitor Resistant Algae and Yeast Strains .....	123
4.2.3 Flow Cytometric Analysis of Lipid Content.....	123
4.2.4 Fluorometric Microplate Lipid Content Analysis.....	124
4.2.5 Fluorometric FDA Growth Kinetics Analysis .....	124
4.2.6 Illumina Whole Genome Sequencing .....	125
4.2.7 Analysis of Illumina Sequencing Data.....	125
4.3 Results and Discussion.....	126
4.3.1 Semi-Quantitative RT-PCR Analysis of Fatty Acid Synthesis Genes under Nitrogen Depleted Cultivation Conditions in Algae.....	126
4.3.1.1 Determination of Target Gene for Directed Evolution Experiments .....	126
4.3.2 Obtaining Acetyl-CoA Carboxylase Specific Inhibitor Quinalofob Resistant Algae Strains .....	129

4.3.3 Fluorometric Microplate and Flow-Cytometric Nile Red Lipid Content Analysis of Acetyl-CoA Carboxylase Inhibitor Resistant Algae Strains.....	131
4.3.4 Obtaining Ergosterol Biosynthesis Inhibitor, Fenpropimorph Resistant Yeast Strains .....	136
4.3.4.1 Flow Cytometric Lipid Content Analysis of Resistant Yeast Strains .....	139
4.3.4.2 Illumina Sequencing Data Analysis .....	140
4.3.4.2.1 Finding Candidate Genes Which Might be Responsible for Increased Lipid Accumulation in Fenpropimorph Resistant Yeast Strains .....	140
4.3.4.2.1.1 <i>Saccharomyces Cerevisiae</i> FenR-A Strain Whole Genome Sequence Analysis.....	141
4.3.4.2.1.2 <i>Saccharomyces Cerevisiae</i> FenR-B Strain Whole Genome Sequence Analysis.....	145
4.3.4.2.1.1 <i>Saccharomyces Cerevisiae</i> FenR-C Strain Whole Genome Sequence Analysis.....	146
5 References .....	150

## TABLE OF ABBREVIATIONS

FAME: Fatty Acid Methyl Esters

DCW: Dry Cell Weight

TAG: Triacylglycerol

BBM: Bold's Basal Medium

PCR: Polymerase Chain Reaction

OD: Optical Density

BLAST: Basic Local Alignment Search Tool

NCBI: National Center for Biotechnology Information

PPT: Parts Per Million

PSU: Practical Salinity Unit

NR- Nile Red

FACS: Fluorescence Assisted Cell Sorting

Div.day: Divisions Per Day

*Gen' t*: Generation Time

GC-MS- Gas Chromotography Mass Spetroscopy

ICP-OES: Inductively Coupled Plasma Atomic Emission Spectroscopy

AFLP: Amplified Fragment Lenght Polymorphism

UPMGA: Unweighted Pair-Group Method with Arithmetic Averaging

RFU: Relative Fluorescence Units

MFI: Mean Fluorescence Intensity

MDA: Malondialdehyde

ROS: Reactive Oxygen Species

FDA: Fluorescein diacetate

DCFH-DA: Diclorodihydrofluorescein

SSC: Side Scatter

FCS: Forward Scatter

SOD: Superoxide dismutase  
CAT: Catalyse  
APX: Ascorbate Peroxidase  
FT-IR: Fourier Transform Infrared Spectroscopy  
TBARS: Thiobarbituric Acid Reactive Substances  
ER: Endoplasmic Reticulum  
ACCCase: Acetyl-CoA Carboxylase  
ACP: Acyl carrier Protein  
CoA: Coenzyme A  
DAGAT: Diacylglycerol acyltransferase  
DHAP: Dihydroxyacetone Phosphate  
ENR: Enoyl-ACP Reductase  
FAT: Fatty Acyl-ACP Thioesterase  
G3PDH: Glycerol-3-Phosphate Dehydrogenase  
GPAT: Glycerol-3-Phosphate Acyltransferase  
HD: 3-Hydroxyacyl-ACP Dehydratase  
KAR: 3-Ketoacyl-ACP Reductase  
KAS, 3-Ketoacyl-ACP Synthase  
LPAAT: Lyso-Phosphatidic Acid Acyltransferase:  
LPAT: Lyso-Phosphatidylcholine Acyltransferase  
MAT: Malonyl-CoA: ACP Transacylase  
PDH: Pyruvate Dehydrogenase Complex  
HRP: Horseradish Peroxidase  
BC: Biotin Carboxylase  
ACP: Acyl Carrier Protein  
MCTK: Malonyl-CoA ACP Transacylase  
KAS: 3-Ketoacyl- ACP Synthase  
FATA: Acyl-ACP Thioesterase  
SAD: Stearoyl-ACP-Desaturase  
FAD:  $\omega$ -3 Fatty Acid Desaturase  
ACT: Actin

MIC: Minimum Inhibitory Concentration

YPD: Yeast Peptone Dextrose

SNP: Single Nucleotide Polymorphism

BEN: Benomyl

BRO: Bromopyruvate

DYC: Dyclonine

FEN: Fenpropimorph

HAL: Haloperidol

MM: Methyl-Methane Sulfonate

PEN: Pentamidine

RAP: Rapamycin

STA: Staurosporine

TER: Terbinafine

TUN: Tunicamycin

INDEL: Insertion or Deletion Mutations

## LIST OF FIGURES

### CHAPTER 1

<b>Figure 1.</b> Trans-esterification reaction.....	15
<b>Figure 2.</b> Sampling stations at Lake Tuz chosen for the isolation of hemophilic algae species.	25
<b>Figure 3.</b> Microphotographs of unialgal monocultures of isolated hypersaline algae species. C-F are showing <i>Dunaliella sp. (KS_02)</i> and A-B-D-E are showing <i>Dunaliella salina (KS_01)</i> where B-E are showing red <i>Dunaliella</i> cells under stress conditions. ....	29
<b>Figure 4.</b> Microphotographs of isolated algae species. A-B; <i>Dunaliella salina (KS_01)</i> , C-D; <i>Dunaliella sp. (KS_02)</i> . ....	30
<b>Figure 5.</b> Growth analysis of newly isolated <i>Dunaliella</i> species cultivated under different NaCl concentrations. ....	31
<b>Figure 6.</b> Growth analysis of newly isolated <i>Dunaliella</i> species cultivated under different pH cultivation conditions.....	32
<b>Figure 7.</b> Growth analysis of newly isolated <i>Dunaliella</i> species cultivated under cultivation conditions with different nitrogen sources. ....	33
<b>Figure 8.</b> PCR amplification of 18s-rDNA regions of several <i>Dunaliella</i> species using <i>Dunaliella</i> specific primers MA1-MA2-MA3. First 4 lanes are representing 18s-rDNA regions <i>Dunaliella tertiolecta</i> , <i>Dunaliella salina</i> and Tuz Lake isolates <i>Dunaliella sp. (KS_02)</i> , <i>Dunaliella sp. (KS_01)</i> respectively (MA1-MA2). Last 4 lanes representing 18s-rDNA regions <i>Dunaliella tertiolecta</i> , <i>Dunaliella salina</i> and Tuz Lake isolates <i>Dunaliella sp. (KS_02)</i> , <i>Dunaliella sp.(KS_01)</i> in the same order (MA1-MA3).....	35
<b>Figure 9.</b> PCR amplification of 18s-rDNA regions of several <i>Dunaliella</i> species using <i>Dunaliella</i> specific primers MA1-MA2. First 8 lanes are representing 18s-rDNA regions (~1700-2000bp) of <i>Dunaliella salina</i> , <i>Dunaliella tertiolecta</i> and Tuz Lake isolates <i>Dunaliella sp. (KS_02)</i> , <i>Dunaliella sp.(KS_01)</i> respectively after PCR amplification. Last 4 lanes shows 18srDNA bands after PCR purification process needed for direct PCR amplicon sequencing reaction. ....	36
<b>Figure 10.</b> GeneBank accession of <i>Dunaliella salina strain Tuz_KS_01</i> .....	37

<b>Figure 11.</b> GeneBank accession of <i>Dunaliella sp. Tuz_KS_02</i> .....	38
<b>Figure 12.</b> ClustalW analysis of newly isolated <i>Dunaliella</i> species <i>KS_01</i> and <i>KS_02</i> and known <i>Dunaliella</i> species obtained from UTEX Collection Culture of Algae. ....	39
<b>Figure 13.</b> Representative AFLP gel image. Lane 1; Lane 2; Lane 3; Lane 4; Lane 5, Marker; <i>Dunaliella tertiolecta</i> , <i>Dunaliella salina</i> , <i>Dunaliella sp. KS_01</i> and <i>KS_02</i> respectively .....	41
<b>Figure 14.</b> Phylogram of newly isolated <i>Dunaliella</i> species <i>KS_01</i> ( <i>B</i> ) and <i>KS_02</i> ( <i>S</i> ) and known <i>Dunaliella</i> species obtained from UTEX Collection Culture of Algae .....	42
<b>Figure 15.</b> Taxonomic report for <i>Dunaliella salina</i> strain <i>Tuz_KS_01</i> (GeneBank accession no. <u><b>JX880083</b></u> ) based on BLAST analysis. ....	43
<b>Figure 16.</b> Taxonomic report for <i>Dunaliella sp. Tuz_KS_02</i> (GeneBank accession no. <u><b>JX880082</b></u> ) based on BLAST analysis. ....	43
<b>Figure 17.</b> GC-MS analysis of fatty acid composition of <i>Dunaliella salina KS_01</i> .....	44
<b>Figure 18.</b> GC-MS analysis of fatty acid composition of <i>Dunaliella sp. KS_02</i> .....	45
<b>Figure 19.</b> Flow cytometric Nile red lipid content analysis of newly isolated <i>Dunaliella sp.</i> under different cultivation conditions ( <i>KS_01</i> -Up/Left, <i>KS_02</i> -Bottom/Left).....	48
<b>Figure 20.</b> Fluorescent microscopic Nile red lipid content analysis of newly isolated <i>Dunaliella sp.</i> under different cultivation conditions (Big-Up/Left, Small-Bottom/Left) .....	49
<b>Figure 21.</b> Effect of different pH levels on lipid accumulation of newly isolated <i>Dunaliella</i> species.....	50
<b>Figure 22.</b> Fluorescent microscopic Nile red lipid content analysis of newly isolated <i>Dunaliella sp.</i> under different pH cultivation conditions. Upper six are showing <i>Dunaliella KS_02</i> where lower six microphotographs are showing <i>Dunaliella KS_01</i> cells .....	51
<b>Figure 23.</b> Effect of different nitrogen sources on lipid accumulation of newly isolated <i>Dunaliella</i> species. Left; <i>KS_01</i> ( <i>D. sp. B</i> ), Right; <i>KS_02</i> ( <i>D. sp. S</i> ).....	53
<b>Figure 24.</b> Effect of nitrogen limitation on growth rates of newly isolated <i>Dunaliella</i> species. Upper Right-Left; <i>KS_01</i> , Lower Right-Left; <i>KS_02</i> .....	54
<b>Figure 25.</b> Effect of nitrogen limitation on lipid accumulation of newly isolated <i>Dunaliella</i> species. Left; <i>KS_01</i> ( <i>D. sp. B</i> ), Right; <i>KS_02</i> ( <i>D. sp. S</i> ).....	55
<b>Figure 26.</b> Effect of sea water cultivation conditions on lipid accumulation of newly isolated <i>Dunaliella</i> species. Right; <i>KS_01</i> ( <i>D. sp. B</i> ), Left; <i>KS_02</i> ( <i>D. sp. S</i> ).....	56

**Figure 27.** Effect of sea water cultivation conditions on lipid accumulation of newly isolated *Dunaliella* species.....57

**Figure 28.** Optimization of short and long term ultrafreeze storage protocols for newly isolated *Dunaliella* species. Bar graph; Fluorometric FDA cell survival analysis, Top Table; Cell survival upon freeze-thaw process at -196°C, Bottom Table; Cell survival upon freeze-thaw process at -80°C.....58

## CHAPTER 2

**Figure 1.** Phylogenetic analysis of *Dunaliella salina* strain *Tuz\_KS\_01* (GeneBank accession no. JX880083). Dendrogram was generated using the neighbor-joining analysis based on 18S rDNA gene sequences. The phylogenetic tree shows the position of *Dunaliella salina* strain *Tuz\_KS\_01* (GeneBank accession no. JX880083) relative to other species and strains of *Dunaliella* deposited in NCBI GeneBank ..... 68

**Figure 2.** Effects of different nitrogen concentrations on the growth and biomass productivity of *Dunaliella salina* strain *Tuz\_KS\_01* (GeneBank accession no. JX880083). 0.05mM, 0.5mM and 5mM NaNO<sub>3</sub> are referred as low, medium and high nitrogen concentrations respectively. Shown OD<sub>600</sub> optical density and biomass values are the means of three replicates. Error bars correspond to ± 1 SD of triplicate optical density measurements ..... 70

**Figure 3.** Lipid content analysis of *Dunaliella salina* strain *Tuz\_KS\_01* under different nitrogen conditions. **A)** Zebra-plot of SSC (Side Scatter) and FSC (Forward Scatter) expressing cellular granulation and cellular size, respectively, under a representative nitrogen depletion condition (0.05mM). **B)** A representative histogram of flow-cytometric analysis of lipid contents under different nitrogen concentrations **C)** Mean fluorescent intensities (MFI) of flow cytometric analysis. **D)** Fluorometric microplate Nile Red analysis of early logarithmic, late logarithmic and stationary growth phases. Data represent the mean values of triplicates. Standard error for each triplicate is shown as tilted lines for clarity, where the minimum and maximum y values of each line corresponds to ± 1 SE..... 72

**Figure 4.** Oxidative stress and lipid accumulation under different nitrogen concentrations. **A)** Fluorometric microplate DCFH-DA analysis under different nitrogen concentrations. **B)** TBARS analysis for lipid peroxidation under different nitrogen concentrations. **C)**

Fluorometric microplate Nile-Red analysis under different nitrogen concentrations. Data represent the mean values of triplicates  $\pm$  1 SE.....73

**Figure 5.** Antioxidant enzyme activities under different nitrogen concentrations. **A-C)** Spectrophotometric enzymatic assays for catalase (CAT), ascorbate peroxidase (APX) and superoxide dismutase (SOD). Data demonstrate the mean values of triplicates  $\pm$  1 SE ..... 75

**Figure 6.** Pigment and protein contents of *Dunaliella salina* strain under different nitrogen concentrations. **A)** Chlorophyll A, B and total carotenoid contents under different nitrogen concentrations. **B)** Protein contents of *Dunaliella salina strain Tuz\_KS\_01* cells cultivated under different nitrogen concentrations Data demonstrate the mean values of triplicates  $\pm$  1 SE76

**Figure 7.** Effect of H<sub>2</sub>O<sub>2</sub>, a known oxidative stress inducer, on *Dunaliella salina strain Tuz\_KS\_01*. **A)** Zebra-plot of SSC (Side Scatter) and FSC (Forward Scatter) expressing cellular granulation and cellular size under a representative H<sub>2</sub>O<sub>2</sub> condition (4 mM). **B)** Histogram of flow-cytometric analysis of ROS accumulation under different H<sub>2</sub>O<sub>2</sub> concentrations. **C)** Percentage increase of ROS production based on flow-cytometric DCFH-DA analysis. **D)** Fluorometric microplate fluorescent diacetate (FDA) survival analysis cultivated under different H<sub>2</sub>O<sub>2</sub> concentrations. **E)** Fluorometric microplate Nile-Red analysis under different H<sub>2</sub>O<sub>2</sub> concentrations. Data represent the mean values of triplicates  $\pm$  1 SE..... 79

**Figure 8.** Fluorescence microphotographs of *Dunaliella salina strain Tuz\_KS\_01* stained with Nile-Red fluorescence dye and screened under 400X magnification. **A)** Control group, 5mM nitrogen concentration cultivation condition. **B)** Nitrogen limitation group, 0.05mM nitrogen concentration cultivation condition **C)** Oxidative stress group, 4mM H<sub>2</sub>O<sub>2</sub> cultivation condition. Gravimetric lipid content analysis and Nile-Red fluorescence measurement correlation. **D)** Gravimetric and fluorometric Nile-Red lipid content analysis of *Dunaliella salina strain Tuz\_KS\_01* under 0.05mM nitrogen and 4mM H<sub>2</sub>O<sub>2</sub> cultivation conditions. Data represent the mean values of triplicates  $\pm$  1 SE **E)** Correlation plot of gravimetric and fluorometric Nile-Red lipid content analysis ( $r^2=0.82$ ). ..... 80

**Figure 9.** Effect of H<sub>2</sub>O<sub>2</sub> induced oxidative stress on cellular lipid accumulation of different algae species. **A)** Fluorometric DCFH-DA and FDA analyses showing percentage change of ROS production and percentage change of cell survivability of *Chlamydomonas reinhardtii* cells cultivated under different H<sub>2</sub>O<sub>2</sub> concentrations. **B)** Fluorometric Nile red analysis showing the effect of different H<sub>2</sub>O<sub>2</sub> concentrations on cellular lipid accumulation of *Chlamydomonas*

*reinhardtii* cells. **C)** Fluorometric DCFH-DA and FDA analyses showing percentage change of ROS production and percentage change of cell survivability of *Dunaliella tertiolecta* cells cultivated under different H<sub>2</sub>O<sub>2</sub> concentrations. **D)** Fluorometric Nile Red analysis showing the effect of different H<sub>2</sub>O<sub>2</sub> concentrations on cellular lipid accumulation of *Dunaliella tertiolecta* cells. Data represent the mean values of triplicates ± 1 SE ..... 82

**Figure 10.** Flow cytometric Nile red, cellular granulation and bio-volume analysis of *Chlamydomonas reinhardtii* cells cultivated under different H<sub>2</sub>O<sub>2</sub> concentrations. **A)** A representative histogram of flow-cytometric analysis of lipid contents under different H<sub>2</sub>O<sub>2</sub> concentrations. **B)** Zebra-plot of SSC (Side Scatter) and FSC (Forward Scatter) expressing cellular granulation and cellular size, respectively, under different H<sub>2</sub>O<sub>2</sub> concentrations. Data represent the mean values of triplicates ± 1 SE ..... 83

### CHAPTER 3

**Figure 1.** Phylogenetic analysis of *Dunaliella sp. Tuz Lake KS\_02* (GeneBank accession no. JX880082). Dendrogram was generated using the neighbor-joining analysis based on 18S rDNA gene sequences. The phylogenetic tree shows the position of *Dunaliella sp. Tuz KS\_02* relative to other *Dunaliella salina* strains deposited in NCBI GeneBank ..... 92

**Figure 2.** Heavy metal sorption analyses of *Dunaliella sp. Tuz KS\_02* **a)** Effect of pH on the sorption of Zn(II), Cu(II), and Ni(II) **b)** Kinetic modeling of sorption of Zn(II), Cu(II), and Ni(II) onto the *Dunaliella sp. Tuz KS\_02* **c)** The pseudo-second-order kinetic model for the sorption of Zn(II), Cu(II), and Ni(II) onto the *Dunaliella sp. Tuz KS\_02*. The error bars correspond to ± 1 SD of triplicates. .... 97

**Figure 3.** Fluorometric (left) and spectrophotometric (right) growth analyses of *Dunaliella sp. Tuz KS\_02*. Data represented as relevant fluorescence units and optical density at 600nm wave length for fluorometric and spectrophotometric measurements respectively. The error bars correspond to ± 1 SD of triplicates. .... 99

**Figure 4.** Fluorometric microplate lipid accumulation (Nile Red) and ROS production (DCFH-DA) analyses of *Dunaliella sp. Tuz KS\_02* cultivated under Cu (II), Zn (II) and Ni (II) treatments ..... 102

**Figure 5.** Flowcytometric lipid accumulation (Nile Red) and ROS production (DCFH-DA) analyses of *Dunaliella sp. Tuz KS\_02* cultivated under Cu (II), Zn (II) and Ni (II) treatments. **a-**

**b)** Zebra-plot of SSC (Side Scatter) and FSC (Forward Scatter) expressing cellular granulation and cellular size, respectively, under the heavy metal treatment conditions **c)** Histogram of flow-cytometric analysis of lipid contents under Cu (II), Zn (II) and Ni (II) treatments **d)** Histogram of flow-cytometric analysis of cellular ROS production under Cu (II), Zn (II) and Ni (II) treatments. Data represent the mean values of triplicates. Standard error for each triplicate corresponds to  $\pm 1$  SE. .... 103

**Figure 6.** Fluorescence microscope images of *Dunaliella sp. Tuz KS\_02* cultivated under Cu (II), Zn (II) and Ni (II) treatments. Cells were stained with DCFH-DA, an indicator of ROS production and TBARS assay was used for showing MDA end-product, an indicator of lipid peroxidation mainly resulted from H<sub>2</sub>O<sub>2</sub> reactants. **a-b-c-d)** Representative fluorescent images of non-treated control, Cu (II), Zn (II), Ni (II) groups stained with DCFH-DA respectively **e)** TBARS analysis of *Dunaliella sp. Tuz KS\_02* cultivated under Cu (II), Zn (II) and Ni (II) treatments. Data represent the mean values of triplicates. Standard error for each triplicate corresponds to  $\pm 1$  SE. .... 104

**Figure 7.** Representative FT-IR analysis of *Dunaliella sp. Tuz KS\_02* cultivated under Cu (II), Zn (II) and Ni (II) treatments. **a)** Spectra were collected over the wavenumber range 4000–600 cm<sup>-1</sup>. Spectra were baseline corrected using the automatic baseline correction algorithm **b)** Scatter plots of transmittance (%) of TAG, polysaccharide, oligosaccharide and amide groups **c)** Overall histogram of transmittance (%) of Cu (II), Zn (II) and Ni (II) treatments in comparison with control group. Data represent the mean values of triplicates. Standard error for each triplicate corresponds to  $\pm 1$  SE. .... 105

**Figure 8.** Flowcytometric metabolic activity analysis of *Dunaliella sp. Tuz KS\_02* cultivated under Cu (II), Zn (II) and Ni (II) treatments. **a)** Zebra-plot of SSC (Side Scatter) and FSC (Forward Scatter) expressing cellular granulation and cellular size, respectively, under the heavy metal treatment conditions **b-c-d-e-f)** Histogram and corresponding bar graphs of representative flow-cytometric analysis of metabolic activities of *Dunaliella* cells under Cu (II), Zn (II) and Ni (II) treatments in comparison with no dye and untreated control groups. .... 107

**Figure 9.** Total protein and pigment contents of *Dunaliella sp. Tuz Lake KS\_02* strain cultivated under Cu (II), Zn (II) and Ni (II) treatments. Data demonstrate the mean values of triplicates  $\pm 1$  SE. .... 108

## CHAPTER 4

- Figure 1.** Fatty acid synthesis pathway in Baker's yeast, *Saccharomyces cerevisiae* ..... 113
- Figure 2.** Simplified scheme of the metabolites and representative pathways in microalgal lipid biosynthesis. Free fatty acids are synthesized in the chloroplast, while TAGs may be assembled at the ER. ACCase, acetyl-CoA carboxylase; ACP, acyl carrier protein; CoA, coenzyme A; DAGAT, diacylglycerol acyltransferase; DHAP, dihydroxyacetone phosphate; ENR, enoyl-ACP reductase; FAT, fatty acyl-ACP thioesterase; G3PDH, glycerol-3-phosphate dehydrogenase; GPAT, glycerol-3-phosphate acyltransferase; HD, 3-hydroxyacyl-ACP dehydratase; KAR, 3-ketoacyl-ACP reductase; KAS, 3-ketoacyl-ACP synthase; LPAAT, lyso-phosphatidic acid acyltransferase; LPAT, lyso-phosphatidylcholine acyltransferase; MAT, malonyl-CoA:ACP transacylase; PDH, pyruvate dehydrogenase complex; TAG, triacylglycerols ..... 114
- Figure 3.** Pathways of lipid biosynthesis and acyl chain desaturation which are known or hypothesized to occur in green microalgae. The assignment of candidate genes encoding enzymes catalyzing the reactions were also shown in the diagram in this study Abbreviations: ACP, acyl carrier protein; CoA, coenzyme A; DGDG, digalactosyldiacylglycerol; FA, fatty acid; MGDG, monogalactosyldiacylglycerol; SQDG, sulfoquinovosyldiacylglycerol ..... 127
- Figure 4.** Semi-quantitative RT-PCR experiments on *Dunaliella salina* KS\_01 hypersaline green microalgae under nitrogen depleted conditions compared with normal cultivation conditions. BC: Biotin carboxylase; ACP: Acyl carrier protein; MCTK: Malonyl-CoA: ACP transacylase; KAS: 3-ketoacyl- ACP synthase; FATA: Acyl-ACP thioesterase; SAD: Stearoyl-ACP-desaturase; FAD:  $\omega$ -3 fatty acid desaturase..... 128
- Figure 5.** Selective pressure to fatty acid synthetic pathway by using specific chemical inhibitors through phenotypic selection..... 129
- Figure 6.** Selection of Acetyl-CoA carboxylase inhibitor quizalofop resistant/tolerant *Dunaliella salina* KS\_01 cells by application of selective pressure. .... 131
- Figure 7.** Nile red microplate fluorometric lipid content analysis of acetyl-CoA carboxylase inhibitor quizalofop resistant/tolerant *Dunaliella salina* KS\_01 cells upon application of selective pressure. .... 133
- Figure 8.** Growth and lipid content analysis of *Dunaliella salina* KS\_01 cells upon application of selective pressure with acetyl-CoA carboxylase inhibitor Diclofop. .... 134

<b>Figure 9.</b> Growth and lipid content analysis of <i>Dunaliella salina</i> KS_01 cells upon application of selective pressure with acetyl-CoA carboxylase inhibitor Fenoxaprop. ....	135
<b>Figure 10.</b> A) Nile red flow-cytometry analysis of lipid contents of <i>Dunaliella salina</i> KS_01 cells upon application of selective pressures with acetyl-CoA carboxylase inhibitors Quizialofob, Diclofop and Fenoxaprop. Control groups (C), Quizialofob (Q), Diclofop (D) and Fenoxaprop (F) resistant cells on March, 2013. B) Control groups (C), Quizialofob (Q), and Diclofop (D) and Fenoxaprop (F) resistant cells on May, 2013. C) Control groups (C), Quizialofob (Q) resistant cells treated with 15µM Q and 20µM Q.....	136
<b>Figure 11.</b> Cross-resistance of three Fenpropimorph-resistant strains. ....	138
<b>Figure 12.</b> Flow-cytometric lipid content analysis of fenpropimorph resistant yeast strains. A, B, C, D is demonstrating; non-resistant control, resistant A strain, resistant B strain and resistant C strain respectively. ....	140
<b>Figure 13.</b> Sphingolipid biosynthesis pathway. Hypothesis for increased lipid accumulation response of fenpropimorph resistant <i>Saccharomyces cerevisiae</i> .....	149

## LIST OF TABLES

### CHAPTER 1

<b>Table 1.</b> Some biotechnologically important algae species .....	10
<b>Table 2.</b> Chemical composition of algae expressed on a dry matter basis .....	11
<b>Table 3.</b> Vegetable oil yields.....	12
<b>Table 4.</b> Detailed ICP-OES settings used in the study.....	27
<b>Table 5.</b> ICP-OES macro and micro element analysis of Lake Tuz. ....	28

### CHAPTER 3

<b>Table 1.</b> The kinetic sorption modelling parameters of Cu (II), Ni (II) and Zn (II) on the <i>Dunaliella sp. Tuz KS_02</i> .....	96
--	----

### CHAPTER 4

<b>Table 1.</b> Primers for semi-quantitative real time PCR in this study .....	121
---	-----

## CHAPTER 1

### 1.1 INTRODUCTION

#### 1.1.1 Introduction to Algae Kingdom

Algae are mostly eukaryotes, which typically, but not necessarily, live in aquatic biotopes, they can also live in soil. They are including ~40,000 species, a heterogeneous group that describes a life-form, not a systematic unit; this is one reason why a broad spectrum of phenotypes exists in this group. They can be described as "lower" plants but they never have true stems, roots and leaves, and they are normally capable of photosynthesis. The nontaxonomic term "algae" groups several eukaryotic phyla, including the *Rhodophyta* (red algae), *Chlorophyta* (green algae), *Phaeophyta* (brown algae), *Bacillariophyta* (diatoms), and *Dinoflagellates*, as well as the prokaryotic phylum *Cyanobacteria* (blue-green algae). There are coccoid, capsoid, amoeboid, palmelloid, colonial, plasmodial, filamentous, parenchymatous (tissue-like), and thalloid organizational levels; some algae at the last-mentioned level developed complex structures that resemble the leaves, roots, and stems of vascular plants. The size of algae ranges from tiny single-celled species to gigantic multicellular organisms. The smallest eukaryotic alga, *Ostreococcus tauri* (Prasinophyceae) has a cell diameter of less than 1  $\mu\text{m}$  which makes it the smallest known free-living eukaryote having the smallest eukaryotic genome; in contrast, the brown alga *Macrocystis pyrifera* (Phaeophyceae), also known as the giant kelp, grows up to 60 meters and is often the dominant organism in kelp forests. Algae can also live in other habitats which include very extreme environments. Some of these habitats are very extreme: There is an outstanding salt tolerance of halophilic algae like *Dunaliella salina* (Chlorophyceae), which is capable of

growing in environments that are nearly saturated with NaCl. Cryophilic green algae like *Chlamydomonas nivalis* (Chlorophyceae) are very tolerant to low temperature, poor nutrition, permanent freeze-thaw cycles and high irradiation, they color snow fields orange or red. A principal alga of hot acidic waters is the red alga *Cyanidium caldarium* (Bangiophyceae), which can grow, albeit slowly, at a pH of zero and at temperatures up to ~56°C. Aerial, sub-aerial and aeroterrestrial algae like *Apatococcus lobatus* (Chlorophyta) are normally spread by airborne spores and grow in the form of biofilms in aerophytic biotopes (bark of trees, rocks, soils, and other natural or man-made surfaces). Hypolithic algae, like *Microcoleus vaginatus* (Cyanobacteria), can live in arid environments like the Death Valley or the Negev desert.

Other species of algae can live in symbiotic relationships with animals or fungi. Symbioses between sponges and algae are abundant in nutrient-poor waters of tropical reefs. Lichens, like the common yellow colored *Xanthoria parietina*, are “composite organisms” made of a fungus (mostly *Ascomycota*) and a photosynthetic alga; they prosper in some of the most inhospitable habitats.

Algae species are producing approximately 52,000,000,000 tons of organic carbon per year, which is ~50% of the total organic carbon produced on earth each year [1], but this is not the only reason why algae are so important in terms of biology.

## **1.1.2 Introduction to Algae Biotechnology**

### **1.1.2.1 Historical View of Algae**

- The first traceable use of microalgae by humans dates back 2000 years to the Chinese, who used Nostoc to survive during famine.
- The first report on collection of a macroalga, “nori”, dates back to the year 530, and the first known documentation of cultivation of this alga occurred in 1640
- At about the same time, in the year 1658, people in Japan started to process collected Chondrus, Gelidium, and Gracilaria species to produce an agar-like product
- In the eighteenth century, iodine and soda were extracted from brown algae, like Laminaria, Macrocystis and Fucus
- In the 1860s, Alfred Nobel invented dynamite by using diatomaceous earth (diatomite), which consists of the fossil silica cell walls of diatoms, to stabilize and

absorb nitroglycerine into a portable stick; so dynamite was, in all respects, one of the most effective algal products.

- In the 1940s, microalgae became more and more important as live feeds in aquaculture, At that time, the idea of using microalgae for wastewater treatment was launched and the systematic examination of algae for biologically active substances, particularly antibiotics , began.
- In the 1960s, the commercial production of *Chlorella* as a novel health food commodity was a success in Japan and Taiwan because of its high nutritional characteristics.
- The energy crises in the 1970s triggered considerations about using microalgal biomasses as renewable fuels and fertilizers.
- In the 1980s, there were already 46 large-scale algae production plants in Asia mainly producing *Chlorella sp.* large scale production of *Cyanobacteria* began in India, and large commercial production facilities in the USA and Israel started to process the halophilic green alga *Dunaliella salina* as a source of  $\beta$ -carotene
- In the 1980s, the use of microalgae as a source of common and fine chemicals was the beginning of a new trend.
- In the 1990s in the USA and India, several plants started with large-scale production of *Haematococcus pluvialis* as a source of the carotenoid astaxanthin, which is used in pharmaceuticals, nutraceuticals, agriculture, and animal nutrition.
- Present, Algae is still considered for various important industrial fields. Genetically modified algae is researched by a broad scientific community to obtain desired traits which ease the production and increase the efficiency of algae cultivation in industrial zones.

### **1.1.2.2 Utilization of Algae**

Today, about 107 tons of algae are harvested each year by algal biotechnology industries for different purposes. Number of commercial companies selling different algae species and various kinds of algal products. Today's commercial algal biotechnology is still a non-transgenic industry that basically produces food, feed, food and feed additives, cosmetics, and pigments. Algal biotechnology is also called blue biotechnology because of the marine and aquatic applications.

#### **1.1.2.2.1 Human Food**

Algal nutritional supplements can positively effect the human health because of its large profile of natural vitamins, essential fatty acids and minerals. The microalgal market is dominated by *Chlorella* and *Spirulina* [2] mainly because of their high protein content, nutritive value, and not least, because they are easy to grow. The biomass of these alga is marketed as liquid, capsules or tablets. An alga called nori, actually *Porphyra spp.*, which is used e.g. for making sushi, currently provides an industry in Asia with a yearly turnover of ~US\$ 1 x 10<sup>9</sup>. Algae is consumed as a food in many asian countries including the biggest producer country, China. Other species used as human food are *Monostroma spp.*, *Ulva spp.*, *Laminaria spp.*, *Undaria spp.*, *Hizikia fusiformis*, *Chondrus crispus*, *Caulerpa spp.*, *Alaria esculenta*, *Palmaria palmata*, *Callophyllis variegata*, *Gracilaria spp.* and *Cladosiphon okamuranus* [3].

#### **1.1.2.2.2 Animal Feed**

It was widely accepted that algal biomass as a feed supplement is suitable [4]. Mostly the microalgae *Spirulina* and, to some extent, *Chlorella* are used in this domain for many types of animals: cats, dogs, aquarium fish, ornamental birds, horses, poultry, cows and breeding bulls [5]. Within the same animal spectrum, macroalgae like *Ulva spp.*, *Porphyra spp.*, *Palmaria palmata*, *Gracilaria spp.*, and *Alaria esculenta* are used as feed. All of these algae are able to enhance the nutritional content of conventional feed preparations. Thus they effect animal health in a positive manner.

#### **1.1.2.2.3 Aquaculture**

Microalgae are utilized in aquaculture as live feeds for all growth stages of bivalve molluscs (e.g. oysters, scallops, clams and mussels), for the larval and early juvenile stages of abalone, crustaceans and some fish species, and for zooplankton used in aquaculture food chains.

#### 1.1.2.2.4 Chemicals and Pharmaceuticals

Algae include a largely novel and valuable compounds such as  $\omega$ 3 polyunsaturated fatty acids, algal docosahexaenoic acid from *Cryptocodinium cohnii*,  $\gamma$ -linolenic acid from *Spirulina*, arachidonic acid from *Porphyridium*, and eicosapentaenoic acid from *Nannochloropsis*, *Phaeodactylum* or *Nitzschia*. This also seems to be the main application area of future commercial algal transgenics. Current exploitation mainly aims to utilize fatty acids, pigments, vitamins and other bioactive compounds. Other fatty acids or lipids are isolated from *Phaeodactylum tricornutum* as a food additive, from *Odontella aurita* for pharmaceuticals, cosmetics, and baby food, and from *Isochrysis galbana* for animal nutrition. Macroalgae, mainly *Gelidium spp.* and *Gracilaria spp.*, but also *Gelidiella* and *Ahnfeltia spp.*, are used as a source of hydrocolloid agar, an unbranched polysaccharide obtained from their cell walls. The gelatinous agar (plus nutrients) is used as a standard medium in almost all microbiological, molecular biological, or medical laboratories. Moreover, agar is used in many foods (ice creams, soups, icings, jellies etc.), pharmaceuticals and feed as a gelling agent. It is also used as a vegetarian gelatin substitute, as a clarifying agent in the brewing industry and other fermentation industries, and as a laxative in addition to a couple of other purposes. Other products such as carrageenans are used as gelling agents, stabilizers, texturants, thickeners, and viscosifiers for a wide range of food products. Alginates, the salts of alginic acid and their derivatives, are extracted from the cell walls of brown macroalgae like *Laminaria* carboxylated polysaccharides are used for a wide variety of applications in food production as thickeners, stabilizers, emulsifier, and gelling agents. Alginates are required for production of dyes for textile printing, latex paint, and welding rods. The water absorbing properties of alginates are utilized in slimming aids and in the production of textiles and paper. Calcium alginate is used in different types of medical products, including burn dressings that promote healing and can be removed painlessly. Due to its biocompatibility, it is also used for cell immobilization and encapsulation. In addition, alginates are widely used in prosthetics and dentistry for making molds. In addition, they are often components of cosmetics. Extracts from the cyanobacterium *Lyngbya majuscula* are used as immune modulators in pharmaceuticals and nutrition management [6].

#### **1.1.2.2.5 Pigments**

Carotenes can be also named as the hydrocarbon carotenoids, oxygenated derivatives of these hydrocarbons can be described as xanthophylls. The most popular xanthophyll is astaxanthin, which is extracted in large scale amounts from the green microalga *Haematococcus pluvialis*. Other prominent xanthophylls are lutein, canthaxanthin, and zeaxanthin. Phycobiliproteins are not only used as pigments, but have also been shown to have health-promoting properties. They are also used in research laboratories as labels for biomolecules [7].

#### **1.1.2.2.6 Diatomite**

Diatomite has many applications such as hydroponic medium, as a soil conditioner, as a lightweight building material, as a mechanical insecticide, as a pet litter, as a thermal insulator, as a fertilizer, as a refractory, as an important component of dynamite.

#### **1.1.2.2.7 Fertilizers**

Seaweeds like *Phymatolithon spp.*, *Ecklonia spp.*, and *Ascophyllum nodosum* are utilized to produce fertilizers and soil conditioners, especially for the horticultural industry.

#### **1.1.2.2.8 Waste Water Treatment**

Algae can be used in wastewater treatment to reduce the content of nitrogen and phosphorus in sewage and certain agricultural wastes. Another application is the removal of toxic metals from industrial wastewater.

#### **1.1.2.2.9 Cosmetics**

Components of algae are frequently used in cosmetics as thickening agents, water-binding agents, and antioxidants.

#### **1.1.2.2.10 Fuel**

Microalgae are microscopic heterotrophic or autotrophic photosynthesizing organisms. They seem to have enormous potential to be a source of biofuel because of many class of

microalgae contain large amounts of high-quality lipids that can be converted into biodiesel. From many different feedstocks including grease, vegetable oils, waste oils, animal fats and microalgae, biodiesel, one of the major biofuel, can be produced. The reaction is called transesterification that triglycerides are converted into fatty acid methyl esters (FAMEs) in the presence of an alcohol such as methanol or ethanol, and also an alkaline or acidic catalyst. From the reaction, two immiscible layers appear. One of the layers is the biodiesel as primary product and the second layer is glycerol as a by-product.

Market fluctuations of fossil fuels, requirement of reducing CO<sub>2</sub> emission to the atmosphere have increased the interest of finding a new sustainable energy source called biofuels. Biofuels are mainly produced from living organisms such as soybean, canola, palm, rapeseed and sugarcane which are terrestrial plants. This strategy has become controversial because of the lack of sustainability of plant-based biofuels, also the need of extensive lands that are already in use for cultivation of crop plants for food and feed makes this strategy impossible to replace the fossil fuels. Such many factors described above, the necessity of searching for other sources of biodiesel production that are both sustainable and economical. Microalgae are microscopic organisms that can be heterotrophic or autotrophic and also photosynthesizing. They can inhabit different types of environments, including freshwater, seawater, brackish water, soil and many others. More than 40,000 different species of microalgae have been identified, most of them have a high lipid content accounting for between %20-50 of their total biomass. In contrast to terrestrial plants used for biofuel production, microalgae have the potential to synthesize 30-fold more oil per hectare than other plants [8].

Microalgae have many advantages, including biodiesel from microalgae contains low sulfur, is highly biodegradable and is associated with minimal nitrous oxide release compared to other sources of biodiesel production. In addition, microalgal farming is more cost-effective than conventional farming. Especially their high growth rate makes them valuable among others. They show a reliable potential to satisfy the big demand for transportation fuels in world market.

In the 1970s, after the petroleum crisis, U.S. government start a project of identifying the optimal type of algae for biodiesel production. As a result, more than 3000 algae species, including the species belonging to the *chlorophyceae*, *cyanophceae*, *prymnesiophyseae*, *eustigmatophyceae*, *bacillariophyceae*, *prasinophyceae*. Some of them were found to be cultivable on a large scale for biodiesel production. Presently very few species of microalgae are being used for producing biodiesel. Some of the commercially used microalgae species

are; *Cyanobacteria*, *Spirulina platensis* (mostly protein production for food supplemental), *Chlorophyceae Chlorella protothecoids* (heterotrophic cultivation in photobioreactors for biomass), *Tetraselmis suecica* (food source in aquaculture hatcheries), *Haematococcus pluvialis* (pigment production such as astaxanthin). These species mostly being used for the production of economically valuable products such as antioxidant pigment named astaxanthin or carotenoids, their use for production of biodiesel is controversial because of their need of large amounts of freshwater (*Spirulina*, *Chlorella*, *Haematococcus*) and too low lipid content (*Tetraselmis*).

There is still a need for identifying the fast growing microalga strains in natural and extreme environments with high content of fatty acids, neutral lipids, and polar lipids for production of biodiesel, the isolation and characterization of new microalga strains with the potential of more efficient lipid/oil production from either natural and extreme environments remain the focus of continuing research.

### **1.1.3 Introduction to Renewable and Sustainable Energy Resources from Algae**

Concern are growing about the supply of fossil fuels, thus other sources of energy are being attracted. Biofuels have been one of the options being considered for the hot debate. A number of sources for the production of biofuels have been considered. Biofuels are new type fuels that are produced from various kinds of living organisms and their byproducts. For being classified as a sustainable biofuel, the fuel should consist of over 80 % renewable materials. First generation biofuels are derived from edible biomass, primarily corn and soybeans in the United States, and sugarcane in Brazil. These biofuels have various problems. First, there is not enough farmland to provide more than about 10 % fuel needs of the developing countries. The use of first generation biofuels also increases the price of animal feed and ultimately raises the cost of food because of the competition with agriculture. In addition, when the total emissions of growing, harvesting, and processing corn are factored into the cost of biofuel, it becomes clear that first generation biofuels are not environmentally friendly and feasible [9]. Bioethanol is currently produced from corn and sugarcane while biodiesel is being made from palm oil, soybean oil, and oilseed rape [10].

Second generation biofuels are made from cellulosic biomass. Sources include wood residues like sawdust and other cellulosic sources like construction debris, agricultural residues like corn stalks and wheat straw, fast growing grasses and woody materials that are grown for the sole purpose of making biofuel. The advantage of second generation biofuels is

that they are abundant and do not interfere with the production of food. Most of these energy crops can be grown on marginal lands that would not otherwise be used as farmland [11].

Cellulosic biomass is able to be sustainably collected and being produced for fuel. The U.S. Department of Agriculture and the Department of Energy have already estimated that the U.S. can produce at least 1.3 billion dry tons of cellulosic biomass every year without decreasing the amount of biomass that is available for food, animal feed or exports. It is also estimated that more than 100 billion gallons of fuel can be produced from this amount of biomass. It is important to point that cellulosic biomass can be converted into any type of fuel including ethanol, gasoline, diesel, and jet fuel by using different chemical processes.

Third generation biofuel includes fuel produced from algae and cyanobacteria. Algae grown in open-ponds could be far more efficient than higher plants in capturing solar energy especially when grown in bioreactors. If algal production could be scaled up, less than 6 million hectares would be needed worldwide to have the current fuel demand. This consists of less than 0.4% of arable land which would be an achievable goal from global agriculture. In addition, many of the most efficient algal species are marine which means that no freshwater would be necessary in their culture such as *Dunaliella* species. Some of the biotechnologically important algae strains are demonstrated in Table 1.

Microalgae contain lipids and fatty acids as membrane components, metabolites, storage products, and sources of energy. Microalgae which include algal strains, diatoms, and cyanobacteria have been found to contain high levels of lipids - over 30%. Due to the high lipid content, these microalgae strains are of great interest in the search for sustainable sources for the production of biodiesel. It has been found that algae can contain between 2% and 40% lipids by weight which can be transformed into biofuel. In Table 2, cellular compositions of some important algae species are shown.

**Table 1.** Some biotechnologically important Algae species

<b>Some Biotechnologically Important Algae Species</b>	
<i>Neochloris oleoabundans</i>	Class Chlorophyceae
<i>Scenedesmus dimorphus</i>	Class Chlorophyceae. Preferred species for oil production for biodiesel.
<i>Euglena gracilis</i>	Food and feed Production
<i>Phaeodactylum tricornutum</i>	Diatom
<i>Pleurochrysis carterae</i>	
<i>Prymnesium parvum</i>	Toxic algae
<i>Tetraselmis chui</i>	Marine unicellular alga
<i>Tetraselmis suecica</i>	
<i>Isochrysis galbana</i>	Cosmetics
<i>Nannochloris oculata</i>	Biofuel Production
<i>Botryococcus braunii</i>	Can produce long chain hydrocarbons representing 86%
<i>Dunaliella tertiolecta</i>	Oil yield of about 37%. Fast growing
<i>Nannochloris sp.</i>	Aquaculture
<i>Spirulina species</i>	Food and Feed Production

The composition of algal oils are very diverse and have been demonstrated to be very high in unsaturated fatty acids which is suitable for biofuel production. Some of these unsaturated fatty acids that are found in different algal species include: arachidonic acid, eicosapentaenoic acid, docosahexaenoic acid, gamma-linolenic acid, and linoleic acid. When it is comparing the lipid yield of algae to vegetable sources, algae could yield between 20,000 and 100,000 liters oil per hectare.

**Table 2.** Chemical composition of algae expressed on a dry matter basis

Chemical composition of algae expressed on a dry matter basis (%)				
Strain	Protein	Carbohydrates	Lipids	Nucleic acid
<i>Scenedesmus obliquus</i>	50-56	10-17	12-14	3-6
<i>Scenedesmus quadricauda</i>	47	-	1.9	-
<i>Scenedesmus dimorphus</i>	8-18	21-52	16-40	-
<i>Chlamydomonas reinhardtii</i>	48	17	21	-
<i>Chlorella vulgaris</i>	51-58	12-17	14-22	4-5
<i>Chlorella pyrenoidosa</i>	57	26	2	-
<i>Spirogyra sp.</i>	6-20	33-64	11-21	-
<i>Dunaliella bioculata</i>	49	4	8	-
<i>Dunaliella salina</i>	57	32	6	-
<i>Euglena gracilis</i>	39-61	14-18	14-20	-
<i>Prymnesium parvum</i>	28-45	25-33	22-38	1-2
<i>Tetraselmis maculata</i>	52	15	3	-
<i>Porphyridium cruentum</i>	28-39	40-57	9-14	-
<i>Spirulina platensis</i>	46-63	8-14	4-9	2-5
<i>Spirulina maxima</i>	60-71	13-16	6-7	3-4.5
<i>Synechoccus sp.</i>	63	15	11	5
<i>Anabaena cylindrica</i>	43-56	25-30	4-7	-

Oil yield of algae per hectare has been shown much higher than other oil producing plant species shown in Table 3. Estimated oil yeald from algae is 1,000 to 6,500 US gallons/acre which is far more yield compared to other terrestrial candidates.

**Table 3.** Vegetable oil yields

Vegetable Oil Yields					
Crop	liters oil/ha	US gal/acre	Crop	liters oil/ha	US gal/acre
corn (maize)	172	18	camelina	583	62
cashew nut	176	19	sesame	696	74
oats	217	23	safflower	779	83
lupine	232	25	rice	828	88
kenaf	273	29	tung oil	940	100
calendula	305	33	sunflower	952	102
cotton	325	35	cocoa (cacao)	1026	110
hemp	363	39	peanut	1059	113
soybean	446	48	opium poppy	1163	124
coffee	459	49	rapeseed	1190	127
linseed (flax)	478	51	olive	1212	129
hazelnut	482	51	castor bean	1413	151
euphorbia	524	56	pecan nut	1791	191
pumpkin seed	534	57	jojoba	1818	194
coriander	536	57	jatropha	1892	202
mustard seed	572	61	macadamia nut	2246	240

*Botryococcus braunii* which is a green, colonial microalgae has been found to produce unusual hydrocarbons and ether lipids. These hydrocarbons are classified as n-alkadienes and trienes, triterpenoid botrycococcenes and methylated squalenes, as well as a tetraterpenoid, lycopadiene. In addition to these compounds and classic lipids like fatty acids, glycerolipids, and sterols, these algae synthesize several ether lipids closely related to hydrocarbons.

Algae are of great interest in the production of biofuels due to the fact that a number of species of freshwater and marine algae contain large amounts of high quality polyunsaturated fatty acids which can be produced for aquaculture operations. Algae can grow heterotrophically on cheap organic substrates, without light, and under well-controlled cultivation conditions. Several strategies are important when determining ways to increase the use of algae for commercial production of polyunsaturated fatty acids in the near future.

These include continued selection and screening of oleaginous species, improvement of strains using genetic engineering, optimization of the culture conditions, and the development of efficient cultivation systems. It is also important to determine whether the polyunsaturated fatty acids are located within the membrane lipids, or in the cytosol [12].

Algae can produce a large number of different types of lipids which include but are not limited to, neutral lipids, polar lipids, were esters, sterols, and hydrocarbons, as well as prenyl derivatives such as tocopherols, carotenoids, terpenes, quinones, and phytylated pyrrole derivatives like chlorophylls [13].

When algae are grown under optimal conditions, they synthesize fatty acids principally for esterification into glycerol based membrane lipids which make up about 5-20% of their dry cell weight (DCW). Fatty acids include medium (C10-14), long chain (C16-18) and very long chain (>C20) fatty acid derivatives. The major components of the membrane glycerolipids are different kinds of fatty acids that are polyunsaturated and are derived through aerobic desaturation and chain elongation from the precursor fatty acids palmitic and oleic acids [13].

When there are unfavorable environmental or stress conditions for growth, many algae change their lipid biosynthetic pathways toward the formation and accumulation of neutral lipids (20-50% DCW), mainly in the form of triacylglycerol (TAG). TAGs, unlike the glycerolipids found in membranes, do not perform a structural role but instead serve mainly as a storage form of carbon and energy. There is evidence that suggests that in algae, the TAG biosynthesis pathway may play a more active role in the stress response, in addition to functioning as carbon and energy storage under environmental stress conditions. After being synthesized, TAGS are deposited in densely packed lipid bodies that are located in the cytoplasm of algal cells.

#### **1.1.3.1 Potential Advantages and Challenges of Algae as Feedstocks for Biofuels**

Numerous algae species have been found to grow rapidly and produce large amounts of TAG. Under the light of this fact, it has been proposed that algae could be used as cell factories to produce oils and other lipids for biofuels and other industrially important biomaterials. There are a various potential advantages of algae as feed stocks. Algae can synthesize and accumulate large quantities of neutral lipids besides polar and non-polar lipids. The growth rate of algal species is very high compared to terrestrial agricultural plants. Some species have 1-3 doublings per day. Algae thrive in saline/brackish water/coastal seawater for

which there are few competing demands. Land that is not suitable for conventional agriculture can be used to grow algal species. Algae could utilize growth nutrients like nitrogen and phosphorus from a number of wastewater sources which also provides the benefit of wastewater bio-remediation. Algae can sequester CO<sub>2</sub> from flue gases that are emitted from fossil fuel fired power plants and other sources which reduce the emission of a major greenhouse gas. Other by-products including biopolymers, proteins, polysaccharides, pigments, animal feed, fertilizer and H<sub>2</sub> are value added co-products or by-products that are produced from the growth of algae. Algae can also grow throughout the year with an annual biomass productivity that surpasses that of terrestrial plants by about tenfold [13].

Based on the photosynthetic efficiency and the growth potential for algae, theoretical calculations indicate that an annual oil production of about 200 barrels of algal oil per hectare of land may be achievable from mass algal cultures. Unfortunately, production of biofuel from algae has not proceeded beyond the small laboratory or field testing stage due to the fact that the lipid yields obtained from algal mass culture efforts have, to date, performed at around 10-20 times lower than the theoretical maximum. This fact has historically made algal oil production technology prohibitively expensive.

In order for algae to be a viable source for biofuel on a commercial scale, many fundamental biological questions relating to the biosynthesis and regulation of fatty acids and TAG in algae need to be answered. It is important that physiological and genetic manipulations of growth and lipid metabolism must be implementable, and critical engineering breakthroughs related to algal mass culture and downstream processing are needed.

### **1.1.3.2 Conversion of Lipids to Biofuel**

Biodiesel which could be produced by the chemical reaction, trans-esterification, of triglycerides with catalyst methanol produces the corresponding mono-alkyl fatty acid esters. This biodiesel is widely accepted an alternative to petroleum based diesel fuels. The properties of biodiesel are mainly determined by the structure of the fatty acid esters that are present. The most important characteristics include the ignition quality, how it flows in the cold, and its oxidative stability. Saturation and the fatty acid makeup do not appear to have much of an impact on the production of biodiesel by the trans-esterification process; they do have an effect on the properties of the fuel product. It is interesting to point out that saturated

fats produce a biodiesel with superior oxidative stability and a high ignition quality, but with poor low temperature properties. Biodiesels that are produced using these saturated fats are more likely to gel at ambient temperatures. If the biodiesel is produced from feedstocks that are high in polyunsaturated fatty acids (PUFAs), the fuel has good cold flow properties, but they are susceptible to oxidation which leads to long term storage problems [13].

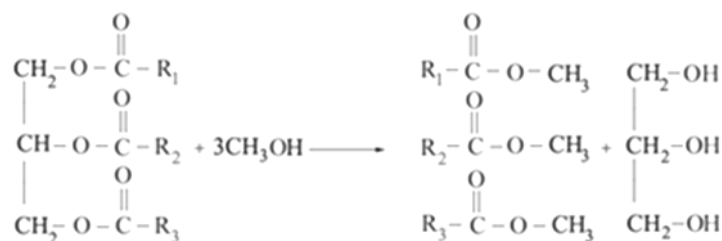


**Figure 1.** Trans-esterification reaction

### 1.1.3.3 Factors Affecting Triacylglycerol Accumulation and Fatty Acid Composition

Since the occurrence and the extent to which TAG is produced appears to be species/strain- specific, and is ultimately controlled by the genetic make-up of the organisms, algae produce only small amounts of TAG under optimal condition.

Synthesis and accumulation of large amounts of TAG occur when the cell is placed under stress conditions that are imposed by chemical or physical environmental stimuli, either acting individually or in combination. The major chemical stimuli include nutrient starvation, salinity, and growth medium pH. The major physical stimuli include temperature and light intensity. In addition, the age of the culture affects the TAG content and the fatty acid composition.

Nitrogen limitation is the single most critical nutrient affecting lipid metabolism in algae. A general trend towards the accumulation of lipids in response to nitrogen deficiency has been observed in many species of various algal taxa. Silicon is equally important in the lipid production of diatoms. It has been found that higher levels of TAG are produced in silicon deficient diatoms. Other types of nutrient deficiency that promote lipid accumulation include phosphate limitation and sulfate limitation [13].

Temperature has also been found to have a major effect on the fatty acid make-up of algae. It has been found that as temperature decreases there is an increase in unsaturated fatty acids. Likewise, when the temperature is increased there is an increase in saturated fatty acids. Temperature has also been shown to affect the total lipid content in algae. However, no general trend has been established yet.

Algae that are grown at different light intensities show remarkable changes in their gross chemical composition, pigment content and photosynthetic activity. Usually, low light intensity causes the formation of polar lipids, particularly the membrane polar lipids that are associated with the chloroplast. However, high light intensity causes a decrease in the total polar lipid content with a concomitant increase in the amount of neutral storage lipids, mainly TAGs. The degree of fatty acid saturation can also be altered by the intensity of the light. High light levels alter the fatty acid synthesis to produce more of the saturated and mono-unsaturated fatty acids that mainly make up neutral lipids.

#### **1.1.3.4 Harvesting & Extraction of Algal Oil from Microalgae**

Concentration of high density algal cultures is typically carried out by concentrating the culture using either chemical flocculation or centrifugation. Chemicals such as aluminum sulfate or iron (III) chloride are added to cause the cells to coagulate and precipitate to the bottom or float to the surface. Then the algal biomass is recovered by removing the supernatant or skimming the cells off the surface. Once this process has taken place, the coagulated algae are no longer suitable as food for filter feeders due to the increase in the particle size.

A cream separator is then used to centrifuge large volumes of the algal culture. The type of algae being cultured determines the flow rate and the rate of centrifugation. The cells are removed from the centrifuge and reconstituted in a small amount of water. This suspension can be stored for 1 – 2 weeks in the refrigerator. The sample can also be frozen, but it must be treated with glucose or dimethylsulfoxide. These chemicals act as cryoprotective agents to maintain the integrity of the cells during the freezing process.

Mechanical methods for the extraction of oil from algae include the expression/expeller press and ultrasonic assisted extraction. When the expression/expeller press is used, the algae are dried and the oil is pressed out with an oil press. With ultrasonic assisted extraction, ultrasonic waves are used to create cavitation bubbles in the solvent

material. As these bubbles collapse near the cell walls shock waves and liquid jets are created that cause the cell walls to break and release the contents of the cell into the solvent. The simplest method for extraction is mechanical crushing. Due to the different characteristics of algal strains, a number of different types of press configurations including screw, expeller, and piston are used. In some cases, chemical extraction methods are combined with mechanical crushing.

Organic solvents can be used to chemically extract the oil. Solvents that are commonly used include benzene, ether and hexane. These chemicals are hazardous and must be treated with care. The hexane solvent extraction method can be used alone or in conjunction with the oil press/expeller method. After the oil has been extracted from the algae using the expeller, the remaining pulp is then mixed with hexane in order to remove any remaining oil. The hexane and oil are then separated by the use of a distillation apparatus. When these two methods are combined, more than 95% of the total oil present in the algae is extracted. Another method called soxhlet extraction uses hexane or petroleum ether to remove the oils through a process of repeated washing in special glassware. Another chemical method called supercritical fluid extraction uses liquefied CO<sub>2</sub> under pressure. The CO<sub>2</sub> is heated to the point at which it has the properties of both a liquid and a gas; this liquefied fluid then acts as a solvent in extraction in the oil.

#### **1.1.3.5 Future of Algal Feedstock Based Biofuels**

In order to better understand and manipulate algae for the production of biofuels, it is important to undertake research to further elucidate the biosynthesis of algal lipids in particular TAGs. It is clear that algae can provide the natural raw materials in the form of lipid rich feedstock, but it is important to better understand the details of lipid metabolism in order to effectively manipulate the process physiologically and genetically. To date funding has been an issue for full scale development of algae based biofuel technology.

In order to fully exploit the potential of algae as a source for biofuels, it is necessary to pioneer new engineering innovations and breakthroughs in algal mass culture as well as downstream processing. However the most important issue is the need for research on the fundamental biological questions that are related to the regulation of lipid metabolism.

There are several biological challenges and opportunities. At the biochemical level, it is important to understand the synthetic pathways in algae that are responsible for the

production of fatty acid and TAG. In addition, it is important to understand how algal cells control the flux of photosynthetically fixed carbon and its partitioning into different groups of major macromolecules. It is also necessary to understand the relationship between the cell cycle and TAG accumulation. The isolation and characterization of algae from unique aquatic environments is also necessary in order to provide insights into the unique mechanisms that algae possess for more efficient lipid production. Metabolic engineering through the use of genetic manipulation should be undertaken in order to optimize the production of algal oils. Large scale culture systems must be designed in order to allow for the maximum yield of lipids from algal strains. Ways to reduce the cost and energy consumption associated with the processing of algal biomass must also be explored. Methods for efficient lipid extraction from algal biomass must be designed in order to make the process feasible.

#### **1.1.3.6 Bio-oil and Bio-syngas**

When any type of biomass is processed under conditions of high temperature in the absence of oxygen, the products that are produced are found in three phases – the vapor phase, the liquid phase, and the solid phase. Bio-oil is a complex mixture of the liquid phase. It has been found that the overall energy to biomass ratio of a well-controlled pyrolytic process could produce up to 95.5% bio oils and syngas [14]. Syngas is an abbreviation for synthesis gas. This gas is produced from the gasification of a carbon containing fuel to a gaseous produce that has some heating value.

It has been shown that bio-oils are suitable for powering external combustion and internal combustion engines or for use by co-firing with fossil diesel or natural gas. Unfortunately, bio-oils have several undesirable features like a high oxygen content, low heat content, high viscosity at low temperature, and chemical instability. Research to overcome these obstacles is ongoing. Work by a group in China has shown that hydrogen can be reliably produced by steam-reforming bio-oil. It has also been determined that microalgae biomass produces a higher quality bio-oil than biomass from other sources.

#### **1.1.3.7 Hydrogen from Algae**

Hydrogen is another possible fuel source that has been considered as an alternative to gasoline. The advantage of hydrogen is that water is the only by-product of the reaction of hydrogen with oxygen, but the difficulty has been finding a viable source of hydrogen. One

possible source is the green alga, *Chlamydomonas reinhardtii* which is found around the world as green pond scum. This alga has the potential to produce large amounts of hydrogen because it can directly split water into hydrogen and oxygen using the enzyme, hydrogenase. It is thought that this alga evolved to take advantage of very different environments. In an aerobic environment with plenty of sunlight, the alga undergoes photosynthesis. However If the alga is forced to live in an anaerobic environment or is deprived of an essential nutrient like sulfur, it switches to another mechanism of metabolism and produces hydrogen instead.

Scientists have discovered that when the algae are deprived of essential sulfate salts, they no longer maintain the protein complex necessary for the production of oxygen photosynthetically and instead switch to the hydrogen-producing metabolic pathway. However, there are problems that must be resolved before large amounts of hydrogen can be produced. The alga cannot grow in a sulfur deprived condition for very long before it needs to revert to the oxygen producing mode. It has been reported that the algae can grow for 4 days before it needs to return to normal metabolic pathways. During the period of sulfate deprivation, the algae were found to produce  $1.23 \times 10^{-4}$  moles of hydrogen for every liter of growing medium at a temperature of 25°C and a pressure of 1 atmosphere. The optimal growth temperature for most species of algae is between 20 °C to 30°C. Much more work is necessary in order to make algae a viable method for the production of hydrogen.

## **1.2 Materials and Methods**

### **1.2.1 Algae Isolation and Purification**

The algae species used in this study was isolated from the hypersaline lake “Tuz”, which is located in the Middle Anatolia, Turkey. Collection of water samples was done and isolation location was recorded by using a GPS device as 39°4'23.97"K - 33°24'33.11"E in the southern east part of Sereflikochisar province. 10 ml water samples were collected and enriched with the same volume of Bold's Basal Medium (BBM) modified by addition of 5% NaCl. BBM was pH 7.4 and consisted of 5 mM NaNO<sub>3</sub> along with CaCl<sub>2</sub>•2H<sub>2</sub>O 0.17 mM, MgSO<sub>4</sub>•7H<sub>2</sub>O 0.3 mM, K<sub>2</sub>HPO<sub>4</sub> 0.43 mM, KH<sub>2</sub>PO<sub>4</sub> 1.29 mM, Na<sub>2</sub>EDTA•2H<sub>2</sub>O 2 mM, FeCl<sub>3</sub>•6H<sub>2</sub>O 0.36 mM, MnCl<sub>2</sub>•4H<sub>2</sub>O 0.21 mM, ZnCl<sub>2</sub> 0.037 mM, CoCl<sub>2</sub>•6H<sub>2</sub>O 0.0084 mM, Na<sub>2</sub>MoO<sub>4</sub>•2H<sub>2</sub>O 0.017 mM, Vitamin B12 0.1 mM and 5 mM NaCO<sub>3</sub> was supplied as carbon source.

Water samples were plated on petri dishes with modified BBM 5% NaCl and 1% bacteriological agar, besides the same water samples were also subjected to dilutions with fresh modified BBM 5% NaCl in 48-well plates (1:2, 1:4, 1:8, 1:16, 1:32, 1:64) to obtain monocultures. After 2 and 4 weeks cultivation periods of 48-well plate liquid cultures and agar plates, respectively, clones were isolated. These clones were transferred to fresh mediums in 100 ml canonical flasks in a final volume of 25 ml for obtaining cell stocks at 25°C under continuous shaking and photon irradiance of 80 rpm and 150  $\mu\text{Em}^{-2}\text{s}^{-1}$ .

### **1.2.2 Morphological Identification**

Water samples were plated onto agar-solidified 5% NaCl Bold's Basal Medium (BBM), and colony-forming units of algae were isolated. Representative colonies selected for further study were subcultured in either liquid 5% NaCl BBM or agar-solidified BBM plates. Unialgal stock cultures of selected isolates were maintained on agar-solidified slants. Each isolate was identified.

Specimens were examined using an Olympus photomicroscope with Nomarski DIC optics and photographed using an Olympus DP25 camera. Taxonomic identifications were made using a standard keys or primary literature under light microscope.

### **1.2.3 Molecular Identification**

#### **1.2.3.1 Isolation and Purification of DNA and Amplification of 18S rRNA Gene**

DNA isolation was done by using DNeasy Plant Mini Kit (Qiagen) as instructed by the manufacturer. Quantification of the genomic DNA obtained and assessment of its purity was done on a Nanodrop Spectrophotometer ND-1000 (Thermo Scientific) and on 1% agarose gel electrophoresis. MA1 [5'-GGGATCCGTAGTCATATGCTTGCTCTC-3'] and MA2 [5'-GGAATTCCTTCTGCAGGTTTCACC-3'] were designed from 18S rDNA genes and were previously reported by Olmos et al (Olmos, Paniagua, Contreras, 2000). PCR reactions were carried out in a total volume of 50  $\mu\text{l}$  containing 50 ng of chromosomal DNA in dH<sub>2</sub>O and 200 ng MA1 and MA2 conserved primers. The amplification was carried out using 30 cycles in a MJ Mini™ Personal Thermal Cycler (BioRad), with a T<sub>m</sub> of 52°C for all reactions. One cycle consisted of 1 minute at 95°C, 1 minute at 52°C and 2 minutes at 72°C.

### **1.2.3.2 Sequencing and Phylogenetic Analysis**

MA1–MA2 PCR products were utilized to carry out sequencing reactions after purification with a QIAquick PCR purification kit (Qiagen). The sequencing reactions were run by MCLAB (San Francisco, CA), employing primers MA1–MA2 in both reverse and forward directions. DNA sequences were imported to BLAST for identification and to search for phylogenetic relationship correlations between other known 18S rDNA gene sequences of related species/strains deposited in NCBI Gene Bank.

### **1.2.4 Optimization of Cultivation Conditions**

#### **1.2.4.1 Optical Density (OD<sub>600</sub>) Standardization**

Standardization based on the OD<sub>600</sub> of isolate stocks was carried out prior to optimization studies of growth media, temperature, pH and salinity. First, all isolates were centrifuged and supernatant discarded. Next, 5 ml of autoclaved and filter sterilized 5% NaCl BBM was added to all stocks and the pellet was resuspended. Then, 1000 µl of each were taken and placed in a cuvette to measure their OD<sub>600</sub> in an Eppendorf BioPhotometer Plus spectrophotometer and correlated to gradually increased concentration and/or number of algae cells. 5% NaCl BBM was used as the blank in all cases.

#### **1.2.4.2 Growth Media Optimization**

Four different media were tested for growth preference of the isolates, namely F/2, BG-11 SW and Johnson's Medium and 5% NaCl BBM. BD Falcon 24-well (6\*4) Multiwell Plates were used as the growth system. The experimental setup was established as follows: the first column was always unseeded media (negative control/blank), the subsequent columns were used to grow the isolates. The first, second, third and fourth rows contained F/2, BG-11 SW, Johnson's Medium and 5% NaCl BBM, respectively, and each plate was done in duplicate.

For this test, initial OD<sub>600</sub> was set to 0.03. Plates were stored at 25 °C, no agitation, 16:8 light/dark photoperiod and 100 µmol/s/m<sup>2</sup> light intensity. Automatic plate reader was used to measure the final OD<sub>600</sub> in each well.

### **1.2.4.3 pH Range Test**

For each isolate, six different pH conditions were tested in their corresponding best media, namely 6, 7, 8, 9, 10 and 11. In this case the Corning Costar 24 Well Cell Culture Clusters (6\*4) with at bottom lids were used as the growth system. The experimental setup was established as follows: columns 1 through 6 were set as pH 6, 7, 8, 9, 10 and 11, respectively. Row 1 was always used to place unseeded media (negative control/blank), the remaining 3 rows were used to place the isolates. All plates were done in duplicate.

pH was adjusted for each media using 1 M HCl and/or 5 N NaOH as needed and measuring with a Mettler Toledo Seven Multi Inlab Routine Pro pH Meter, while constantly agitating with a Velp Scientifica ARE Heating Magnetic Stirrer. For this test, initial OD<sub>600</sub> was set to 0.03. Plates were stored at 25 °C, no agitation, 16:8 light/dark photoperiod and 100 µmol/s/m<sup>2</sup> light intensity. Observations were made every week for 1 month using a automatic plate reader.

### **1.2.4.4 Salinity Range Test**

For each isolate, six different salinity conditions were tested in their corresponding best media, namely 2.5, 3.0, 3.5, 4.0, 5 and 10 percent (%), that are approximately equivalent to 25, 30, 35, 40, 50 and 100 PSU or PPM (‰). In this case the Corning Costar 24 Well Cell Culture Clusters (6\*4) with at bottom lids were used as the growth system.

The experimental setup was established as follows: columns 1 through 6 were set as conditions 25, 30, 35, 40, 50 and 100 PSU, respectively. Row 1 was always used to place unseeded media (negative control/blank), the remaining 3 rows were used to place the isolates. All plates were done in duplicate.

For this test, initial OD<sub>600</sub> was set to 0.03. Plates were stored at 25 °C, no agitation, 16:8 light/dark photoperiod and 100 µmol/s/m<sup>2</sup> light intensity. Observations were made every week for 1 month using a automatic plate reader.

### **1.2.5 Flowcytometric Nile Red Method for Lipid Content Analysis**

5 µl of Nile Red (Sigma, USA) from stock solution (0.5 mg/mL) was added to 1 ml of a cell suspension at an OD<sub>600</sub> of 0.3 after washing cells twice with fresh medium. This mixture was gently vortexed and incubated for 20 minutes at room temperature in dark. Nile

Red uptake was determined using a BD-FACS Canto flow cytometer (Becton Dickinson Instruments) equipped with a 488 nm argon laser. Upon excitation by a 488 nm argon laser, NR exhibits intense yellow-gold fluorescence when dissolved in neutral lipids. The optical system used in the FACS Canto collects yellow and orange light (560–640 nm, corresponding to neutral lipids). Approximately 10,000 cells were analysed using a log amplification of the fluorescent signal. Non-stained cells were used as an autofluorescence control. Nile Red fluorescence was measured using a 488 nm laser and a 556 LP+585/42 band pass filter set on a FACS Canto Flow Cytometer. Data were recorded as mean fluorescence intensity (MFI).

### 1.2.6 Algae Growth Kinetics

Specific growth rate and biomass productivity was calculated according to the equation;  $K' = \ln(N_2 / N_1) / (t_2 - t_1)$  where  $N_1$  and  $N_2$ , biomass at time1 ( $t_1$ ) and time2 ( $t_2$ ) respectively ( $t_2 > t_1$ ) [13]. Divisions per day and the generation (doubling) time were calculated according to the equations:

$$\text{Divisions per day} = \text{Div.day}^{-1} = K' / \ln 2$$

$$\text{Generation time} = \text{Gen}' t = 1 / \text{Div.day}^{-1}$$

### 1.2.7 Fluorescent Microscopic Analyses

Fluorescence microscopy analysis of Nile Red, cells were stained with 5 $\mu$ l 0.5mg/mL Nile Red (Sigma, USA) stock solution after fixing cells with 5% paraformaldehyde and imaged by epi-fluorescence microscopy with a Leica DMR microscope (Leica Microsystems).

### 1.2.8 Lipid Extraction and GC-MS Analysis of Fatty Acid Compositions

The lipid was extracted according to Bligh and Dyer wet extraction method. Briefly, to a 15 ml glass vial containing 100 mg dried algal biomass, 2 ml methanol and 1 ml chloroform were added and kept for 24 h at 25 °C. The mixture was then vortexed for 5 minutes. One milliliter of chloroform was again added, and the mixture shaken vigorously for 1 min. Subsequently, 1.8 ml of distilled water was added and the mixture vortexed again for 2 min. The aqueous and organic phases were separated by centrifugation for 10 min at 2,000 rpm.

The lower (organic) phase was transferred into a clean vial. Evaporation occurred in a thermo-block at 95 °C, and the residue was further dried at 104 °C for 30 min.

1% (V/V) dilutions of each oil sample dissolved in chloroform were subjected to GC/MS analysis by injecting 2 µL sample into a Rtx<sup>®</sup>-5MS fused silica column (30 m, 0.25 mm ID, 0.10 µm df). The injection temperature was set to 200 °C and column temperature program began at 50 °C for 5 min. Column temperature was further increased by 15 °C/min to 300 °C where it was kept for 5 minutes to complete the run. The GC was coupled to a quadrupole mass spectrometer, the interface temperature and ion source temperature was adjusted to 280 °C. MS analysis was started at 2.5 minute which was set to solvent cut time.

### **1.3 Results and Discussion**

#### **1.3.1 Selection of Isolation Location and Sampling**

We selected the sampling sites for obtaining new halophilic microalgae species from the biggest salt lake of Turkey located in the Middle Anatolian region in July 2011. Due to its extremophilic conditions such as high temperature and very high concentration of NaCl especially in summers, the lake was chosen.

Lake Tuz is the second largest lake in Turkey with its 1,665 km<sup>2</sup> (643 sq mi) surface area and one of the largest hypersaline lakes in the world. It is located in the Central Anatolia Region, 105 km (65 mi) northeast of Konya, 150 km (93 mi) south-southeast of Ankara and 57 km (35 mi) northwest of Aksaray.

The lake, occupying a tectonic depression in the central plateau of Turkey, is fed by two major streams, groundwater, and surface water, but has no outlet. Arable fields surround the lake, except in the south and southwest where extensive seasonally flooded salt-steppe occurs. Brackish marshes have formed where channels and streams enter the lake. Arable fields surround the lake, except in the south and southwest where extensive seasonally flooded salt-steppe occurs.

For most of the year, it is very shallow (approx. 0.4 m (1 ft)). During winter part of the salt is dissolved in the fresh water that is introduced to the lake by precipitation and surface runoff (to 32.9% salinity). During the summer the lake dries up exposing an average of 30 cm thick salt layer in August. This mechanism is used as a basis for the process of the salt mines in the lake. The three mines operating in the lake produce 63% of the salt consumed in

Turkey. The salt mining generates industrial activity in the region, mainly related to salt processing and refining [15].

In 2001, Lake Tuz was declared a specially protected area, including all of the lake surface and surrounding waterbeds and some of the important neighboring steppe areas. The main Turkish breeding colony of Greater Flamingo (*Phoenicopterus roseus*) is present on a group of islands in the southern part of the lake. Greater White-fronted Goose (*Anser albifrons*) is the second largest breeder here. Lesser Kestrel (*Falco naumanni*) is a common breeder in surrounding villages.

Because of extremophilic algae species such as temperature and salt resistant species are gaining interest by the scientific community in terms of biotechnological use especially for biofuel production. We chosen three sampling stations with given following GPS locations at the northern part of the lake.  $38^{\circ}57'7.93''\text{K} - 33^{\circ}25'5.28''\text{E}$ ;  $39^{\circ} 4'23.97''\text{K} - 33^{\circ}24'33.11''\text{E}$ ;  $39^{\circ} 0'4.83''\text{K} - 33^{\circ}27'19.29''\text{E}$  as shown in Figure 2.

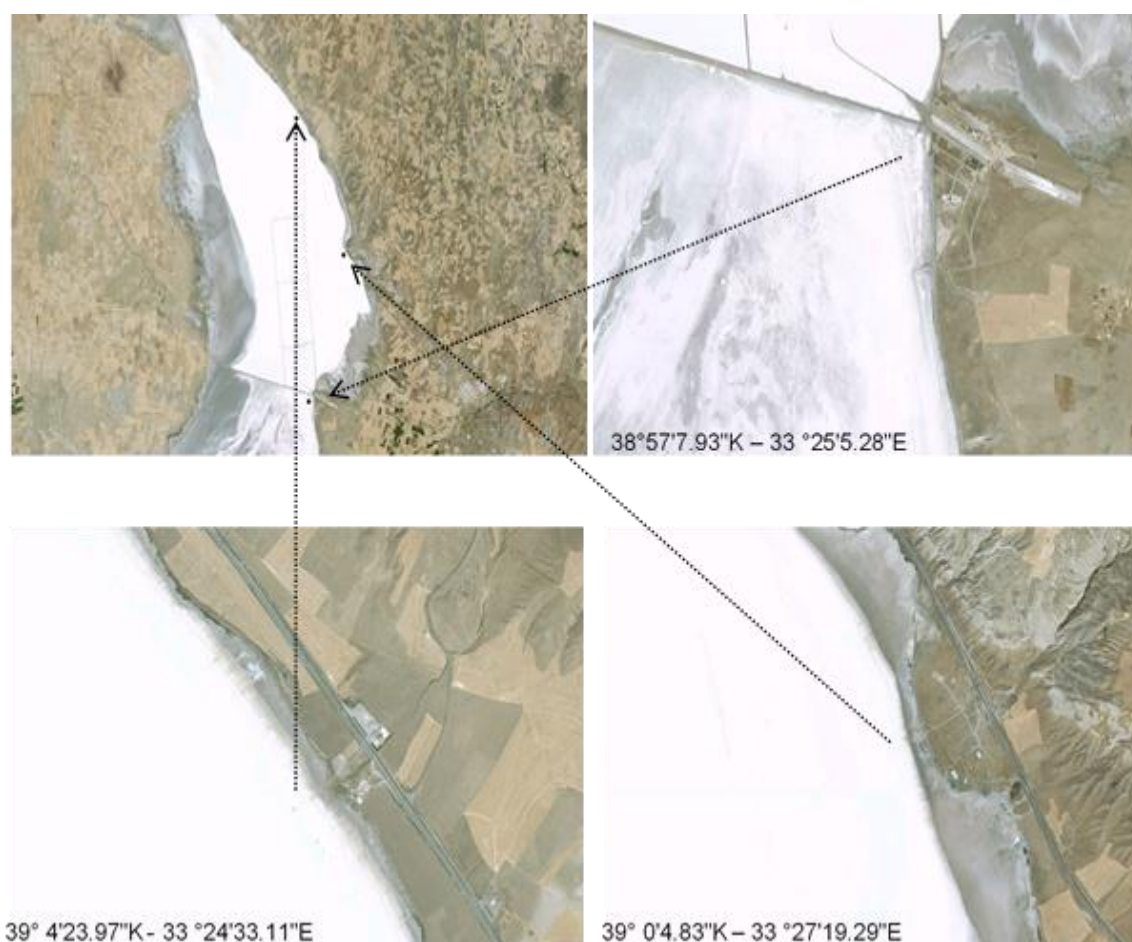


**Figure 2.** Sampling stations at Lake Tuz chosen for the isolation of hemophilic algae species.

Water samples were collected from selected spots which are located by using GPS device. Each sample was enriched with Bold's Basal Medium, Johnson's Medium and Erdshreiber's Medium adjusted to concentrations of 5-10-15-20 % NaCl in 50ml falcon tubes. Single colony isolation studies were done by using streak plating in addition to serial dilution monoculture isolation method for obtaining unialgal cultures. Morphological characterization studies of isolated species were done under light microscope using algal morphological features such as cell shape, cell size, chloroplast and nucleus location, flagella type, stigma, color with using keys and previously described literature. Water samples obtained from Lake Tuz were also analyzed for determination of mineral composition for adjustment of cultivation conditions and better understanding of natural nutrient needs of wild-type species using ICP-OES.

### **1.3.2 ICP-OES Macro and Micro Element Analysis of the Lake Tuz**

Samples were analyzed without preliminary treatment, such as microwave digestion or UV decomposition. No pre-treatment is simpler, quicker and minimizes possibilities of sample contamination compared to digestion, moreover, analytical limits of detection are reported to be better.

To minimize possible matrix effects, suitable dilutions were made using 2% (V/V) nitric acid by 3 fold for ICP-OES measurements. To correct for instrumental drift, internal standards were added, Y for ICP-OES.

For ICP-OES measurements we used a Varian 715-ES radial ICP-OES, equipped with a V-groove pneumatic nebulizer and a Sturman-Masters spray chamber. Detailed ICP-OES settings are shown in Table 4.

ICP-OES	Varian 715-ES					
RF power (W)	1300					
Elements measured and wavelengths (nm)	Al	396.1	Fe	238.2	Na	589.5
	B	249.7	K	766.4	Y	371.0
	Ca	396.8	Mg	279.5	Zn	213.8
	Cu	327.3	Mn	257.6		
Ar gas flow (L min <sup>-1</sup> )	15 (cooling), 1.50 (plasma)					
Nebulizer Ar pressure (kPa)	200					
Viewing height (mm)	12					
Replicate read time (s)	5					
Replicates measured	6					

**Table 4.** Detailed ICP-OES settings used in the study.

ICP-OES analysis of Lake Tuz was used for the further optimization studies of cultivation conditions of newly isolated algae species. As shown in Table 5, salinity of the Lake was found around 12 percent. Essential amount of Cd was also found. Other heavy metals were not found in the water samples. Concentrations of cultivation media ingredients were adjusted to specific concentrations of macro and micro elements found in ICP-OES analysis.

<b>Macro-Micro Element</b>	<b>Concentration (ppm)</b>
<i>Na</i> <sup>2+</sup>	<b>11 4383 ± 3123</b>
<i>K</i> <sup>+</sup>	<b>4 094 ± 177</b>
<i>Br</i>	<b>70 ± 5</b>
<i>Ca</i> <sup>2+</sup>	<b>408 ± 10</b>
<i>Cd</i> <sup>2+</sup>	<b>0.0025 ± 0.0011</b>
<i>Co</i> <sup>2+</sup>	<b>0.02 ± 0.001</b>
<i>Mn</i> <sup>2+</sup>	<b>0.02 ± 0.008</b>
<i>Mg</i> <sup>2+</sup>	<b>4 892 ± 237</b>
<i>S</i> <sup>2-</sup>	<b>3 898 ± 183</b>
<i>Mo</i> <sup>2+</sup>	<b>0.02 ± 0.01</b>
<i>Cu</i> <sup>+</sup>	<b>0.008 ± 0.004</b>
<i>P</i> <sup>3-</sup>	<b>0.64 ± 0.006</b>
<i>Zn</i> <sup>2+</sup>	<b>0.01 ± 0.007</b>
<i>Pb</i> <sup>+</sup>	<b>ND</b>
<i>Al</i> <sup>3+</sup>	<b>ND</b>
<i>Cr</i> <sup>3+</sup>	<b>ND</b>
<i>Fe</i> <sup>2+</sup>	<b>ND</b>
<i>Ni</i> <sup>2+</sup>	<b>ND</b>

**Table 5.** ICP-OES macro and micro element analysis of Lake Tuz.

### **1.3.3 Obtaining Monocultures of Newly Isolated Hypersaline Algae Species**

Approximately two weeks after initial incubation, most of the plates showed colonial formations on agar plates. In some cases the fungal growth was so dense that no colonies could be rescued and those plates were discarded. For subsequent subculturing rounds, microorganisms showed growth after only seven days in the agar surface, probably due to acclimatization in the new conditions. Even though single colony picking and subculturing was done with extreme care, many of the new plates still showed mixtures of two organisms. After approximately three subculturing rounds, most plates showed organism uniformity.

Two different algae species were isolated and monocultures were obtained. The microalgae, which is unicellular, biflagellate and tolerant up to 20% NaCl was identified as

*Dunaliella salina* based on the morphological characterization prior to molecular identification. We observed that cell color was green under normal conditions and the color changed to red under stress conditions. Morphologically, ovoid, spherical and cylindrical cell shapes were observed. Stigma was not clearly visible or diffuse. Large pyrenoid with distinct amylosphere was observed and refractile granules are absent. Cellular size was measured as ~20  $\mu\text{m}$ . These observed characteristics were consistent with previous morphological characteristics of *Dunaliella salina*. The other species is also unicellular, biflagellate and tolerant up to 20% NaCl but cellular color was not changed to red from green under stress conditions unlike the first strain. The alga was characterized as *Dunaliella sp.*. Algae species were given IDs as KS\_01 and KS\_02 for big *Dunaliella salina* species and small *Dunaliella sp.* species respectively as shown in Figure 3 and Figure 4.

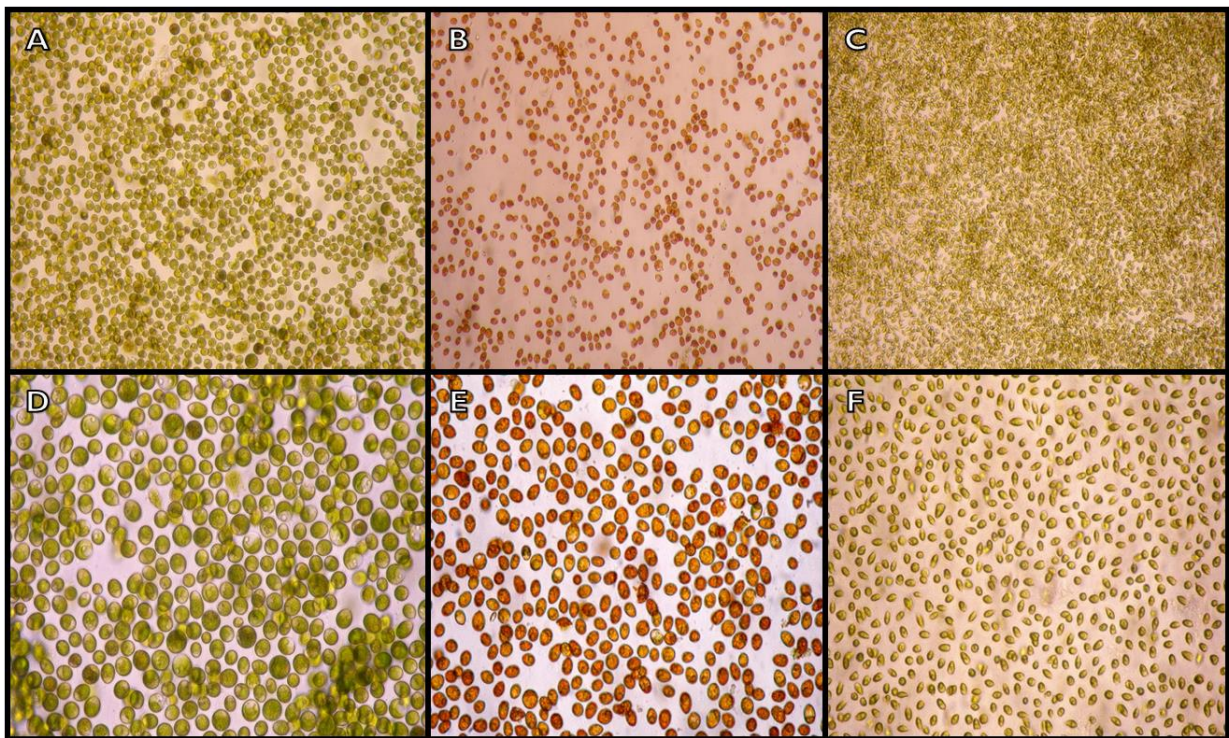


**Figure 3.** Microphotographs of unialgal monocultures of isolated hypersaline algae species. C-F are showing *Dunaliella sp.* (KS\_02) and A-B-D-E are showing *Dunaliella salina* (KS\_01) where B-E are showing red *Dunaliella* cells under stress conditions.

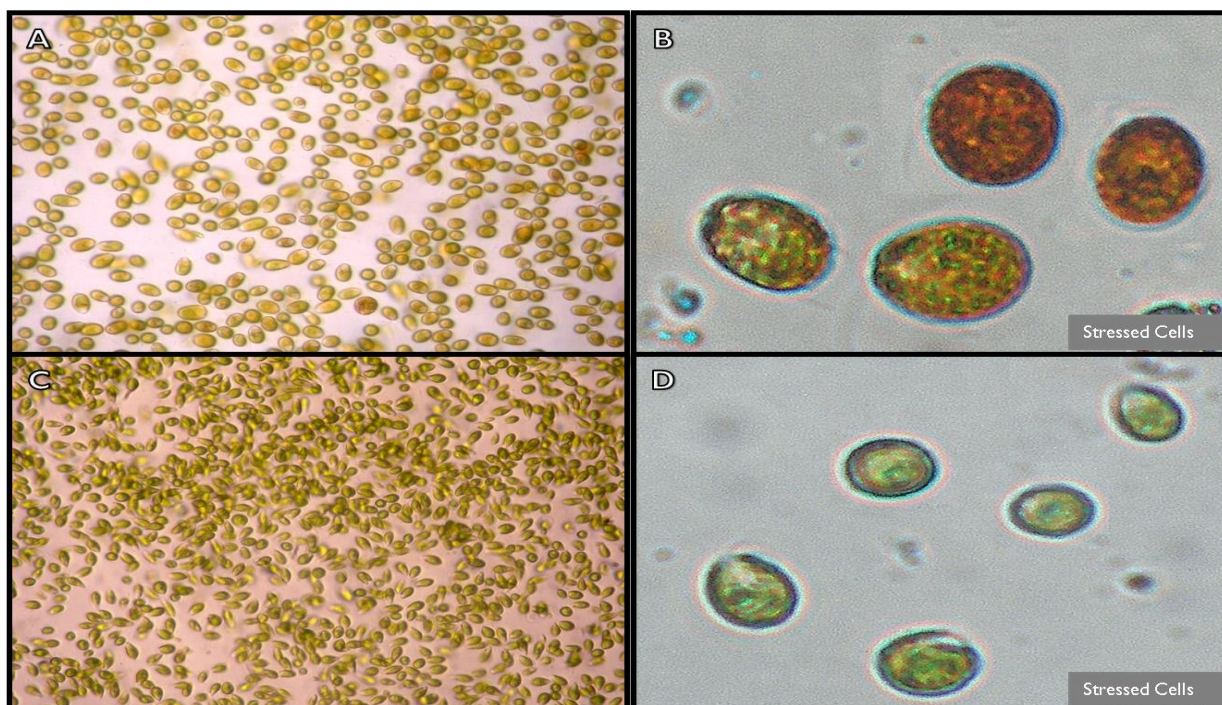


**Figure 4.** Microphotographs of isolated algae species. A-B; *Dunaliella salina* (KS\_01), C-D; *Dunaliella sp.* (KS\_02).

### 1.3.4 Optimization of Cultivation Conditions of newly Isolated Algae Species

#### 1.3.4.1 Optimization of NaCl Concentration

NaCl concentration is one of the most important factors for cultivation of hypersaline green algae species. According to the results shown in Figure 5, we have chosen 5 % NaCl concentrations as default for further cultivations of both newly isolated *Dunaliella* species.

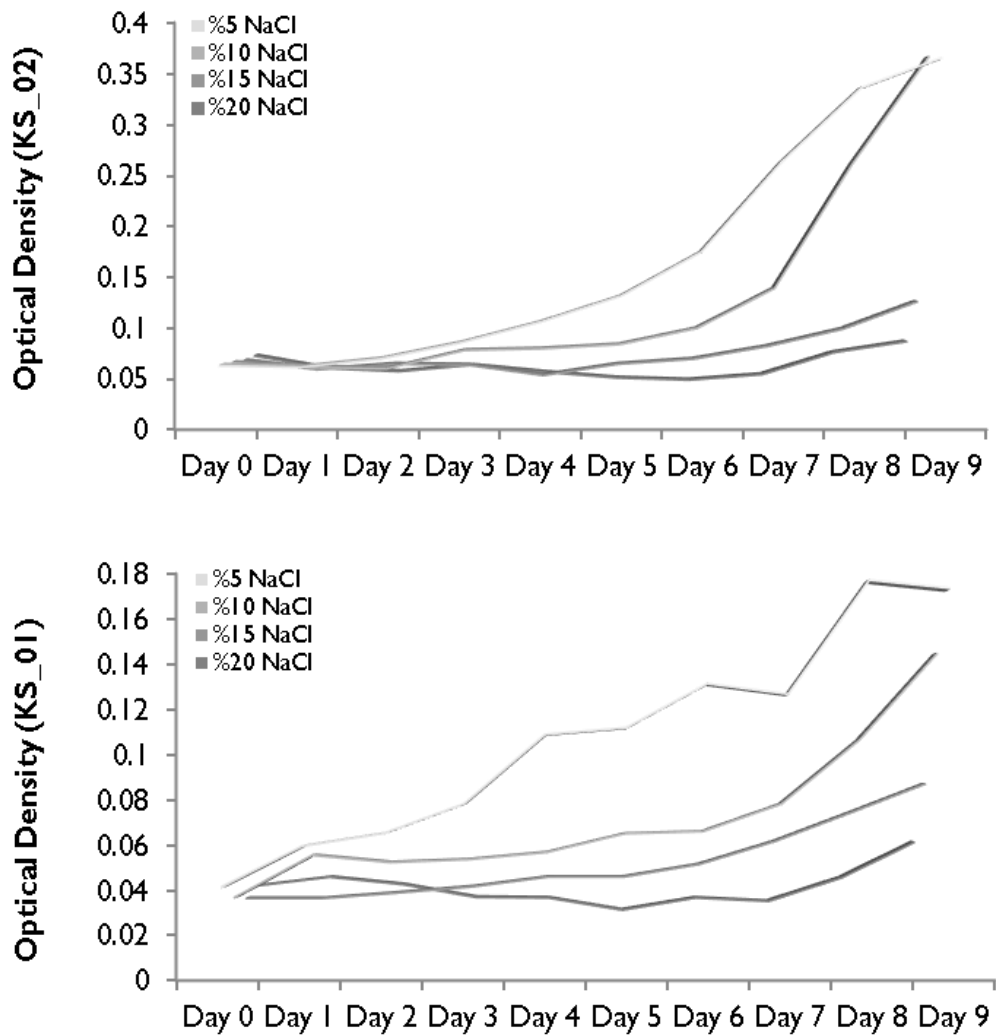


**Figure 5.** Growth analysis of newly isolated *Dunaliella* species cultivated under different NaCl concentrations.

#### 1.3.4.2 Optimization of pH Conditions

Another important factors for cultivation of hypersaline green algae species is pH. Thus we optimized pH conditions for optimized growth of newly isolated *Dunaliella* species. According to the results shown in Figure 6, we have chosen pH 8 as default for further cultivations of both newly isolated *Dunaliella* species.

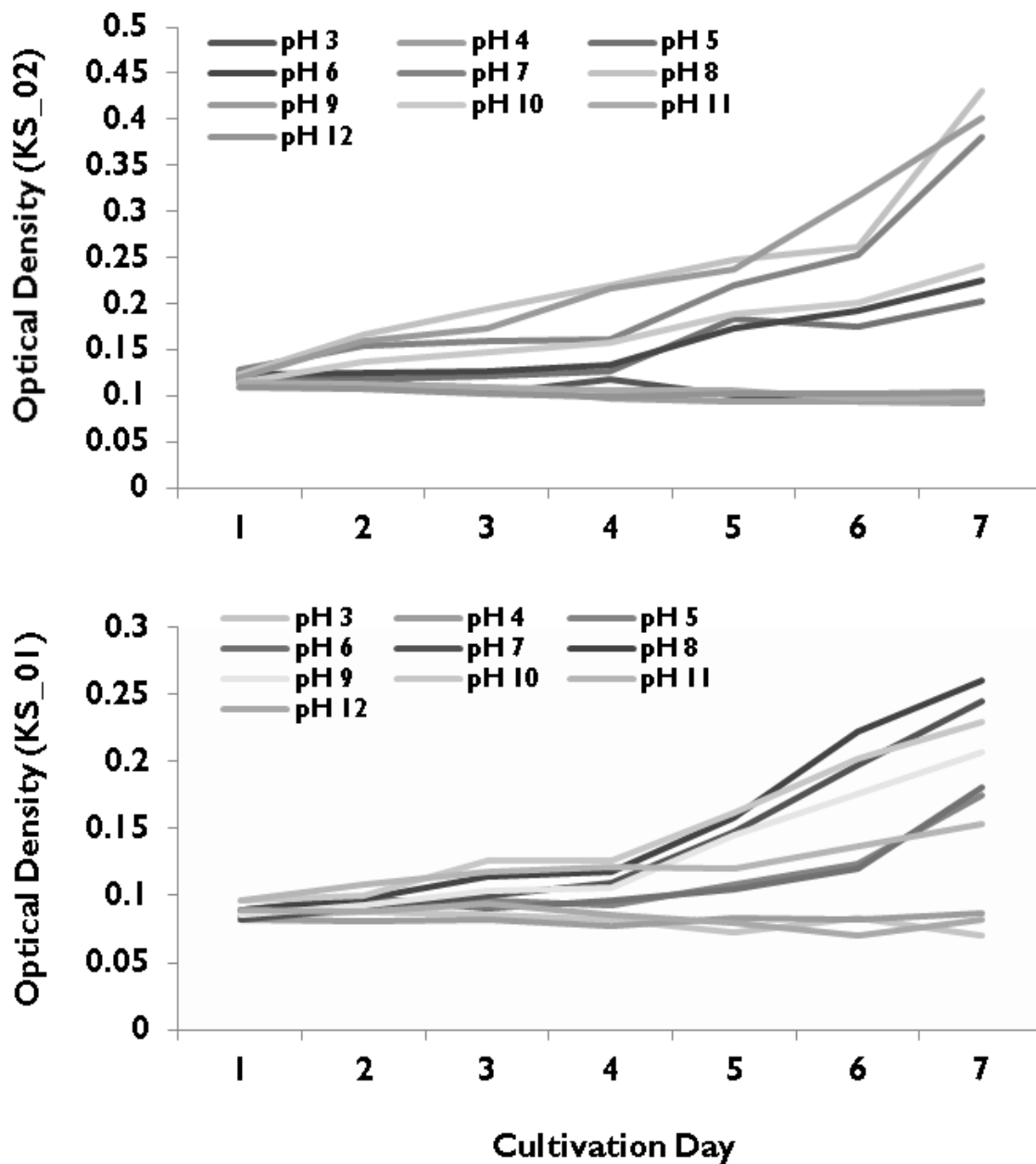


**Figure 6.** Growth analysis of newly isolated *Dunaliella* species cultivated under different pH cultivation conditions.

### 1.3.4.3 Optimization of Nitrogen Sources

Nitrogen source is another important factor for cultivation media in terms of either growth or lipid accumulation of algae species. We also determined which nitrogen sources would be better for cultivation of newly isolated *Dunaliella* species by optimization studies under cultivation conditions with different nitrogen sources namely  $\text{NaNO}_3$ ,  $\text{KNO}_3$ ,  $\text{NH}_4\text{Cl}$  and Urea. According to the results  $\text{NaNO}_3$  and  $\text{KNO}_3$  were found similar among different nitrogen sources as shown in Figure 7. Thus  $\text{NaNO}_3$  was selected for further cultivations.

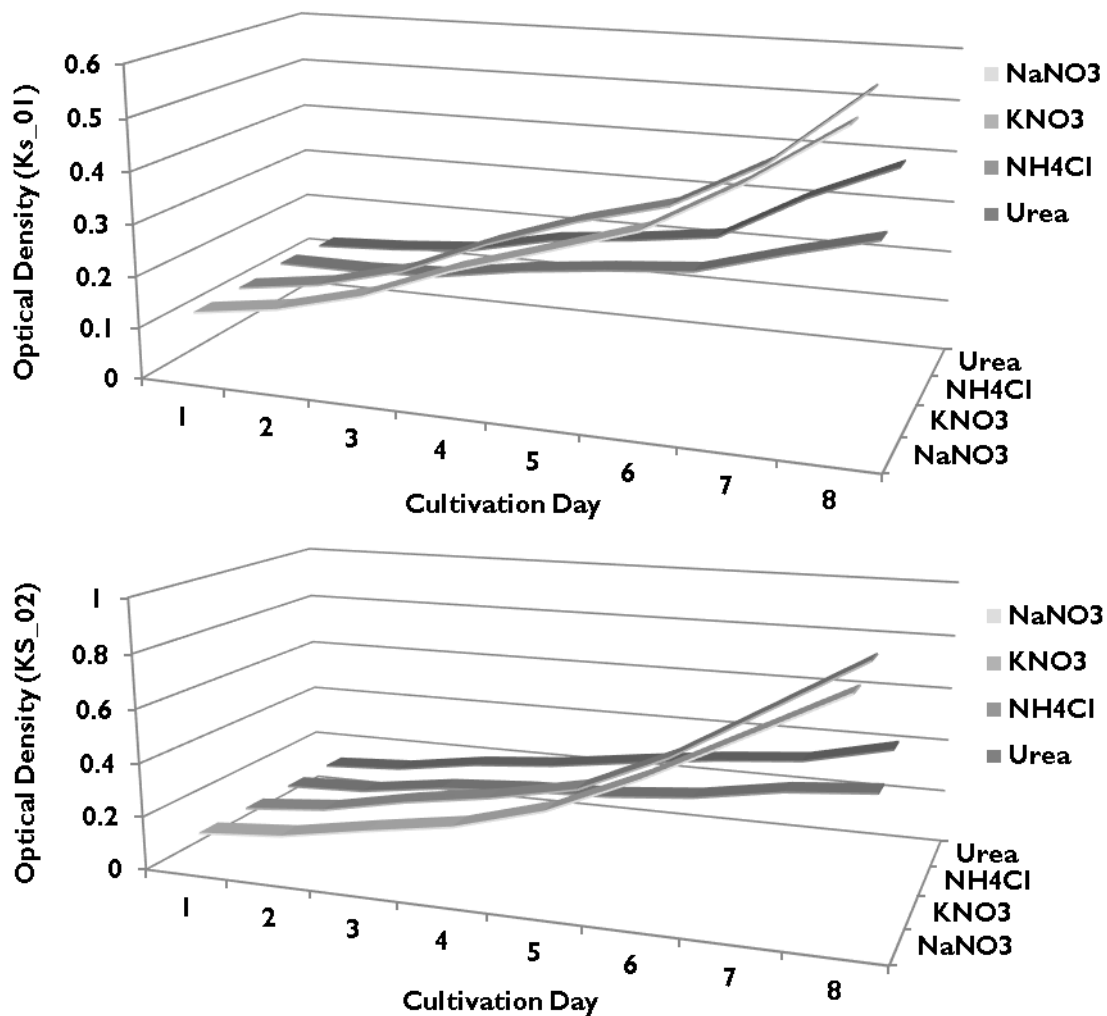


**Figure 7.** Growth analysis of newly isolated *Dunaliella* species cultivated under cultivation conditions with different nitrogen sources.

### 1.3.5 Molecular Identification of Newly Isolated Halophilic Algal Species from Lake Tuz

After isolation, obtaining monocultures and subsequent morphological identifications of new *Dunaliella* species. We did also molecular identifications of isolates for supporting our morphological identification results.

MA1 and MA2 PCR primers described in methods section were designed from 18S rDNA genes and were previously reported by Olmos et al. [16]. PCR reactions were carried out in a total volume of 50 µl containing 50 ng of chromosomal DNA in dH<sub>2</sub>O and 200 ng MA1 and MA2 conserved primers. The amplification was carried out using 30 cycles with a T<sub>m</sub> of 52 °C for all reactions. One cycle consisted of 1 minute at 95 °C, 1 minute at 52 °C and 2 minutes at 72 °C.

MA1–MA2 PCR products were utilized to carry out sequencing reactions after PCR purification. The sequencing reactions were run by MCLAB (San Francisco, CA), employing primers MA1–MA2 in both reverse and forward directions. DNA sequences were imported to BLAST for identification and to search for phylogenetic relationship correlations between other 18S rDNA gene sequences of *Dunaliella* species/strains deposited in NCBI Gene Bank. Dendrogram data generated by BLAST was converted into newick format and submitted to Phyfi [17] for generating phylogenetic tree.

As shown in Figure 8 and Figure 9, 18s-rDNA regions of several *Dunaliella* species using *Dunaliella* specific primers MA1-MA2-MA3 were successfully amplified. MA1 and MA2 primers were then selected for further amplification and sequencing reactions.

As a result of amplification reaction, approximately 1700-2000 basepairs 18s-rDNA regions were obtained. For comparing and determination of *Dunaliella* specific primers MA1-MA2-MA3, *Dunaliella tertiolecta* and *Dunaliella salina* species were also subjected to molecular identification as positive controls.

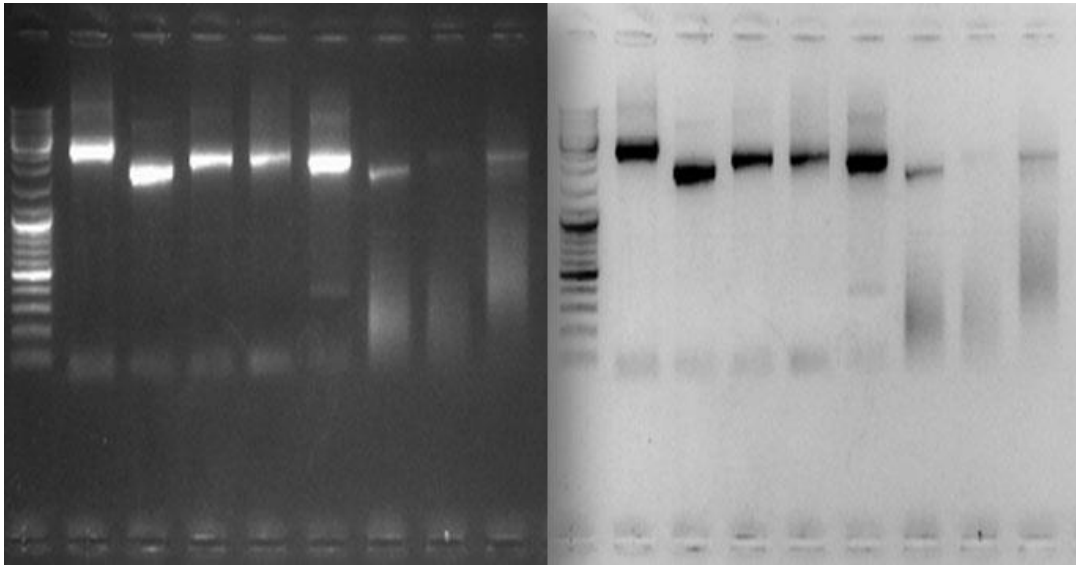


**Figure 8.** PCR amplification of 18s-rDNA regions of several *Dunaliella* species using *Dunaliella* specific primers MA1-MA2-MA3. First 4 lanes are representing 18s-rDNA regions *Dunaliella tertiolecta*, *Dunaliella salina* and Tuz Lake isolates *Dunaliella sp.* (KS\_02), *Dunaliella sp.* (KS\_01) respectively (MA1-MA2). Last 4 lanes representing 18s-rDNA regions *Dunaliella tertiolecta*, *Dunaliella salina* and Tuz Lake isolates *Dunaliella sp.* (KS\_02), *Dunaliella sp.*(KS\_01) in the same order (MA1-MA3)

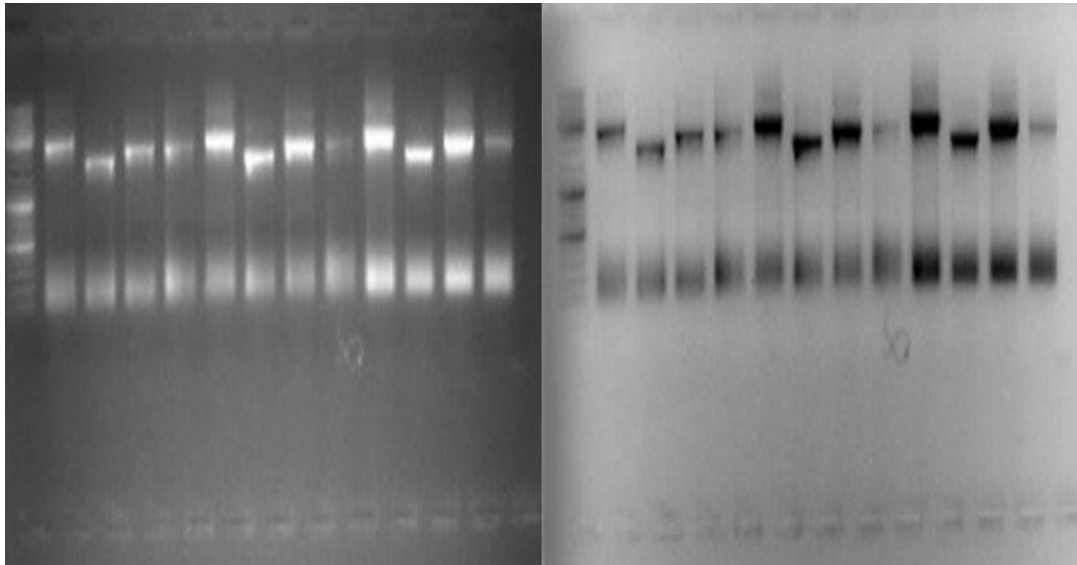


**Figure 9.** PCR amplification of 18s-rDNA regions of several *Dunaliella* species using *Dunaliella* specific primers MA1-MA2. First 8 lanes are representing 18s-rDNA regions (~1700-2000bp) of *Dunaliella salina*, *Dunaliella tertiolecta* and Tuz Lake isolates *Dunaliella sp. (KS\_02)*, *Dunaliella sp.(KS\_01)* respectively after PCR amplification. Last 4 lanes shows 18srDNA bands after PCR purification process needed for direct PCR amplicon sequencing reaction.

### 1.3.6 Entry of Genetic ID to NCBI GeneBank

The partial sequences of the 18S rDNA encoding genes of isolated *Dunaliella* species were submitted to National Center for Biotechnology Information (NCBI) GeneBank database as *Dunaliella salina strain Tuz\_KS\_01* (GeneBank accession no. **JX880083**) and *Dunaliella sp. Tuz\_KS\_02* (GeneBank accession no. **JX880082**) as shown in Figure 10-11 respectively.

## Dunaliella salina strain Tuz\_KS\_01 18S ribosomal RNA gene, partial sequence

GenBank: JX880083.1

[FASTA](#) [Graphics](#)

Go to:

```
LOCUS       JX880083                475 bp    DNA        linear    PLN 18-NOV-2012
DEFINITION  Dunaliella salina strain Tuz_KS_01 18S ribosomal RNA gene, partial
            sequence.
ACCESSION   JX880083
VERSION     JX880083.1  GI:414090947
KEYWORDS    .
SOURCE      Dunaliella salina
  ORGANISM  Dunaliella salina
            Eukaryota; Viridiplantae; Chlorophyta; Chlorophyceae;
            Chlamydomonadales; Dunaliellaceae; Dunaliella.
REFERENCE   1 (bases 1 to 475)
  AUTHORS   Yilancioglu,K. and Cetiner,S.M.
  TITLE     Identification and Characterization of a New Strain of the
            Unicellular Green Alga Dunaliella salina from Hypersaline Tuz Lake,
            Turkey and Evaluation of Biotechnological Potentials
  JOURNAL   Unpublished
REFERENCE   2 (bases 1 to 475)
  AUTHORS   Yilancioglu,K. and Cetiner,S.M.
  TITLE     Direct Submission
  JOURNAL   Submitted (28-SEP-2012) Biological Sciences and Bioengineering,
            Sabanci University, Faculty of Engineering and Natural Sciences,
            Orta Mahalle, Orhanli, Istanbul, Tuzla 34956, Turkey
COMMENT     ##Assembly-Data-START##
            Sequencing Technology :: Sanger dideoxy sequencing
            ##Assembly-Data-END##
FEATURES             Location/Qualifiers
     source           1..475
                     /organism="Dunaliella salina"
                     /mol_type="genomic DNA"
                     /strain="Tuz_KS_01"
                     /isolation_source="hypersaline lake"
                     /db_xref="taxon:3046"
                     /country="Turkey: Tuz Lake"
     rRNA             <1..>475
                     /product="18S ribosomal RNA"
ORIGIN
1 ccacaaagga atggttggac aacaccggtg gagcctgcgg cttaatTTga ctcaacacgg
61 gaaaacttac caggtccaga cacggggagg attgacagat tgagagctct ttcttgattc
121 tgtgggtggt ggtgcatggc cgttcttagt tggTgggttg ccttgTcagg ttgattccgg
181 taacgaacga gacctcagcc tgctaaatag tcacgtctac ctcggttagc gcctgacttc
241 ttagagggac tattggcgtt tagccaatgg aagtgtgagg caataacagg tctgtgatgc
301 ccttagatgt tctgggcccg acgcgcgcta cactgatgca ttcaacgagc ctatccttgg
361 ccgagaggtc cgggtaatct ttgaaactgc atcgtgatgg ggatagatta ttgcaattat
421 tagtcttcaa cgaggaatgc ctagtaagcg cgagtcatca gctcaggttg ctccc
```

**Figure 10.** GeneBank accession of *Dunaliella salina* strain Tuz\_KS\_01

## Dunaliella sp. Tuz\_KS\_02 18S ribosomal RNA gene, partial sequence

GenBank: JX880082.1

[FASTA](#) [Graphics](#)

[Go to:](#)

```
LOCUS       JX880082                815 bp    DNA        linear    PLN 18-NOV-2012
DEFINITION  Dunaliella sp. Tuz_KS_02 18S ribosomal RNA gene, partial sequence.
ACCESSION  JX880082
VERSION    JX880082.1  GI:414090946
KEYWORDS   .
SOURCE     Dunaliella sp. Tuz_KS_02
  ORGANISM Dunaliella sp. Tuz_KS_02
            Eukaryota; Viridiplantae; Chlorophyta; Chlorophyceae;
            Chlamydomonadales; Dunaliellaceae; Dunaliella.
REFERENCE  1 (bases 1 to 815)
  AUTHORS  Yilancioglu,K. and Cetiner,S.M.
  TITLE    Identification and Characterization of a New Strain of the
            Unicellular Green Alga Dunaliella sp. from Hypersaline Tuz Lake,
            Turkey and Evaluation of Biotechnological Potentials
  JOURNAL  Unpublished
REFERENCE  2 (bases 1 to 815)
  AUTHORS  Yilancioglu,K. and Cetiner,S.M.
  TITLE    Direct Submission
  JOURNAL  Submitted (28-SEP-2012) Biological Sciences and Bioengineering,
            Sabanci University, Faculty of Engineering and Natural Sciences,
            Orta Mahalle, Orhanli, Istanbul, Tuzla 34956, Turkey
COMMENT    ##Assembly-Data-START##
            Sequencing Technology :: Sanger dideoxy sequencing
            ##Assembly-Data-END##
FEATURES   Location/Qualifiers
   source   1..815
            /organism="Dunaliella sp. Tuz_KS_02"
            /mol_type="genomic DNA"
            /strain="Tuz_KS_02"
            /isolation_source="hypersaline lake"
            /db_xref="taxon:1258556"
            /country="Turkey: Tuz Lake"
   rRNA     <1..>815
            /product="18S ribosomal RNA"
ORIGIN
1  caaattgctgg gaaagcccct aaagctttgc taaccaagtt gagtgtgaaa gcactcaatg
61  gccagggttaa tgaccttggg tatggtaaaa tcagcaaaga tgcaacaatg ggcaatccgc
121 agccaagctc ctacagtctg ttaggctatg gagaaggttc agagactaaa tggcagtggg
181 ccaactttgg cttaaagata agtccgtccc agctgaaagg ctgtctgcta gaggaagacc
241 attctaggtc tgagagctag tagagggtag gagaaaagga gaagtatcct gcttggagga
301 aacgggagcc tgcggcttaa ttgactcaa cacgggaaaa cttaccaggt ccagacacgg
361 ggaggattga cagattgaga gctctttctt gattctgtgg gtggtggtgc atggccgttc
421 ttagttggtg ggttgccctg tcaggttgat tccggtaacg aacgagacct cagcctgcta
481 aatagtcacg tctacctcgg taggcgctcg acttcttaga gggactattg gcgtttagcc
541 aatggaagtg tgaggcaata acaggtctgt gatgccctta gatgttctgg gccgcacggc
601 cgctacactg atgcattcaa cgagcctatc cttggccgag aggtccgggt aatctttgaa
661 actgcatcgt gatggggata gattattgca attattagtc ttcaacgagg aatccttagt
721 aagcgcgagt catcagctcg cgttgattac gtcctgccc tttgtacaca ccgcccgtcg
```

Figure 11. GeneBank accession of *Dunaliella sp. Tuz\_KS\_02*

### 1.3.7 Phylogenetic Analysis of the Newly Isolated *Dunaliella* Strains

#### 1.3.7.1 ClustalW Analysis of 18s-rDNA Regions of Newly Isolated *Dunaliella* Strains compared with Known *Dunaliella* Species

As mentioned in previous section, *Dunaliella tertiolecta* and *Dunaliella salina* were also genotyped as positive controls along newly isolated *Dunaliella* species *KS\_01* and *KS\_02*. In order to show genetic relatedness of known *Dunaliella* species with new isolates ClustalW analysis was performed and phylogenetic tree was plotted based on this data.

According to the results, *Dunaliella* species *KS\_01* and *KS\_02* showed close genetic relatedness to known *Dunaliella* species shown in Figure 12.

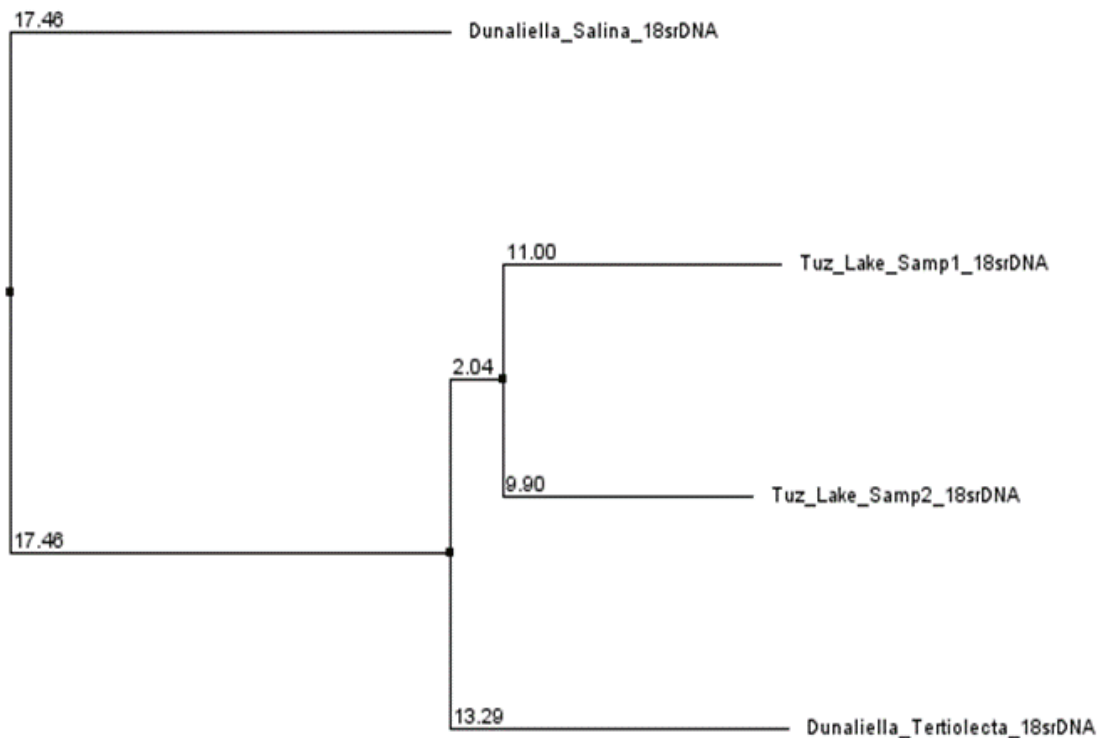


**Figure 12.** ClustalW analysis of newly isolated *Dunaliella* species *KS\_01* and *KS\_02* and known *Dunaliella* species obtained from UTEX Collection Culture of Algae, Texas, USA.

### 1.3.7.2 AFLP Analysis of newly Isolated *Dunaliella* Strains

AFLP analysis was conducted using the LI-COR® template preparation and 2-dye selective amplification kits (LI-COR Biosciences, USA), and visualized with Li-COR 4300 DNA analyzer (LI-COR, USA). Briefly, Genomic DNA (250ng) was digested with 1µL of mixture of EcoRI/MseI (1.25units/µL) at 37 °C for 2 hours and then ligated to EcoRI/MseI adapters with 1.5µL (1unit/µL) of T4 DNA ligase at 25°C for 2 hours. For the pre-amplification reaction, 1:10 diluted ligation reaction mixture was used. The pre-amplification mixture was prepared according to the manufacturer's instructions and the PCR reaction was performed as follows: 30 cycles at 94°C for 15s, 56°C for 30s and 72°C for 1min, then 72°C for 3min. For the selective amplification, infrared fluorescence dye (IRD-700nm and IRD-800nm) labeled EcoRI primers and non-labeled MseI primers were utilized. Selective amplification mixture was prepared according to the manufacturer's instructions and then PCR reaction was performed by a touchdown program as follows: 13 cycles at 94°C for 15s, 65°C for 30s – 0.7°C / cycle, and 72°C for 1 min, then 30 cycles at 94°C for 15s, 56°C for 30s, 72°C for 1min, then 72°C for 3min. The products from selective amplification were run on 6% denaturing polyacrylamide gel using an automated LI-COR 4300 DNA analyzer as instructed by the manufacturer.

Polymorphic bands obtained from AFLP analyses was scored manually as present (1) or absent (0) across all known and isolated *Dunaliella* species genotypes for AFLP primer-pair combination and then the values were used to generate binary data matrices. The MVSP software package version 3.1 was used for calculation of Jaccard's similarity coefficients across all the genotypes for AFLP analyses. A dendrogram for AFLP analysis was constructed using the unweighted pair-group method with arithmetic averaging (UPGMA) by using MVSP software package version 3.1.

A representative AFLP gel image is shown in Figure 13. According to the results, *Dunaliella species KS\_01* and *KS\_02* demonstrated again a close genetic relatedness to known *Dunaliella* species shown in Figure 14.

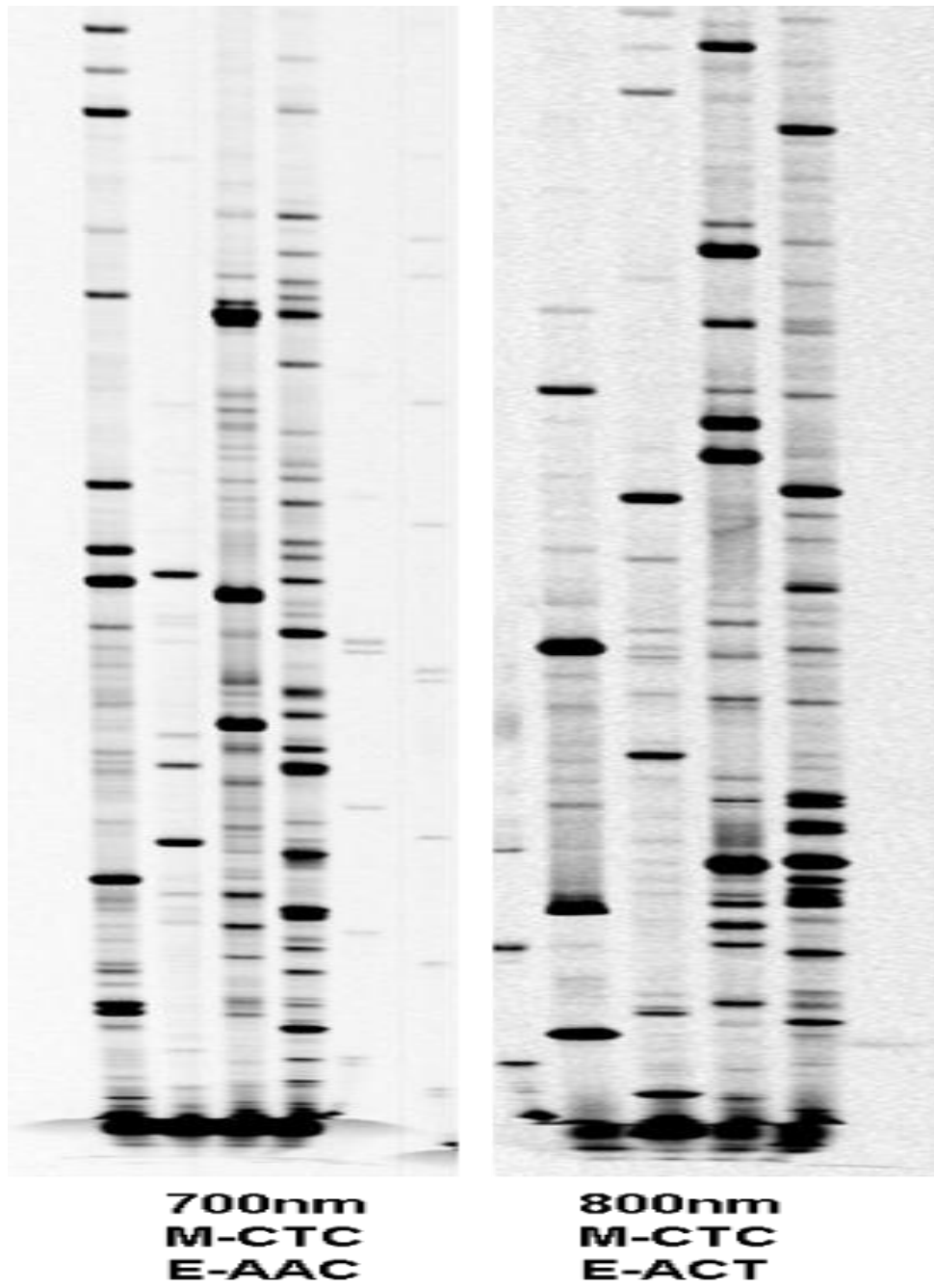


**Figure 13.** Representative AFLP gel image. Lane 1; Lane 2; Lane 3; Lane 4; Lane 5, Marker; *Dunaliella tertiolecta*, *Dunaliella salina*, *Dunaliella species KS\_01* and *KS\_02* respectively

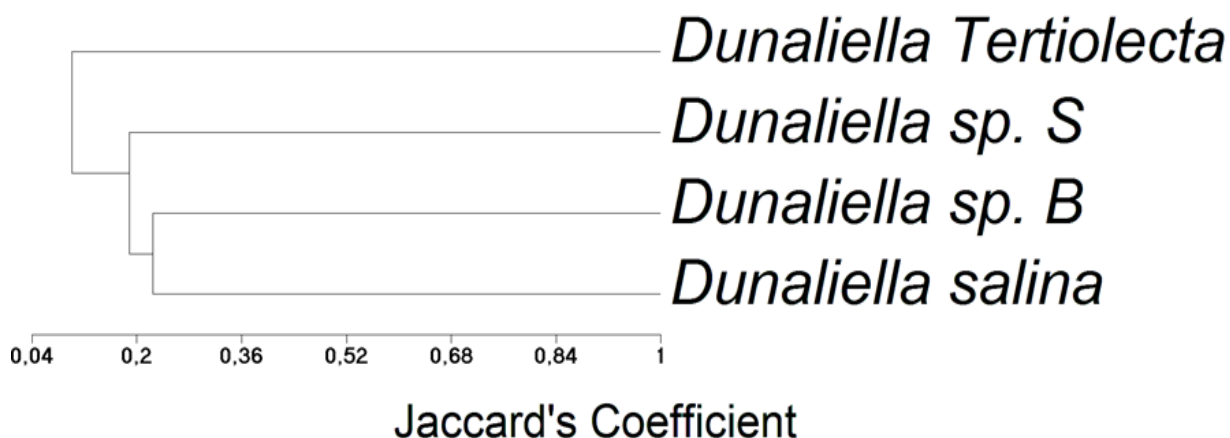


**Figure 14.** Phylogram of newly isolated *Dunaliella* species *KS\_01* (*B*) and *KS\_02* (*S*) and known *Dunaliella* species obtained from UTEX Collection Culture of Algae, Texas, USA.

### 1.3.7.3 BLAST Analysis of Newly Isolated *Dunaliella* Species

The partial sequences of the 18S rDNA encoding genes of isolated *Dunaliella* species were submitted to National Center for Biotechnology Information (NCBI) GeneBank database as *Dunaliella salina* strain *Tuz\_KS\_01* (GeneBank accession no. **JX880083**) and *Dunaliella* sp. *Tuz\_KS\_02* (GeneBank accession no. **JX880082**). According to Basic Local Alignment Search Tool (BLAST) analysis, the isolated sequence had very high percentage of identity with other deposited 18S rDNA sequences of *Dunaliella* species shown in the taxonomic reports in Figure 15 and Figure 16 for *Dunaliella salina* strain *Tuz\_KS\_01* and *Dunaliella* sp. *Tuz\_KS\_02* respectively. Molecular identification showed a high percentage identity to *Dunaliella* strains.

## Lineage Report

Eukaryota	[eukaryotes]			
Chlorophyceae	[green algae]			
Chlamydomonadales	[green algae]			
Dunaliellaceae	[green algae]			
Dunaliella	[green algae]			
Dunaliella salina	-----	878	25 hits	[green algae]
Dunaliella sp. G5L020	.....	815	1 hit	[green algae]
Dunaliella sp. SAS11133	.....	813	1 hit	[green algae]
Dunaliella sp. ABR11NW-G22	.....	813	1 hit	[green algae]
Dunaliella sp. BUM11123	.....	813	1 hit	[green algae]
Dunaliella sp. ABR11NW-G4	.....	813	1 hit	[green algae]
Dunaliella sp. ABR11NW-Sh6.3	.....	813	1 hit	[green algae]
Dunaliella sp. ABR11NW-Ch5	.....	813	1 hit	[green algae]
Dunaliella sp. ABR11NW-G3	.....	813	1 hit	[green algae]
Dunaliella sp. ABR11NW UI/1	.....	813	1 hit	[green algae]
Dunaliella sp. ABR11NW M1/1	.....	813	1 hit	[green algae]
Dunaliella tertiolecta	.....	813	7 hits	[green algae]
Dunaliella sp. SPMO 300-4	.....	813	1 hit	[green algae]
Dunaliella sp. SPMO 210-3	.....	813	1 hit	[green algae]
Dunaliella sp. SPMO 201-6	.....	813	1 hit	[green algae]
Dunaliella sp. SPMO 112-2	.....	813	1 hit	[green algae]
Dunaliella sp. SPMO 112-1	.....	813	1 hit	[green algae]
Dunaliella sp. SPMO 109-1	.....	813	1 hit	[green algae]
Dunaliella sp. FL1	.....	813	1 hit	[green algae]
Dunaliella sp. CCMP220	.....	813	1 hit	[green algae]
Dunaliella primolecta	.....	813	1 hit	[green algae]
Dunaliella sp. CCMP1641	.....	813	1 hit	[green algae]
Dunaliella sp. CCMP1923	.....	813	1 hit	[green algae]
Dunaliella parva	.....	813	1 hit	[green algae]
Dunaliella bioculata	.....	813	1 hit	[green algae]
Dunaliella sp. KMMCC 1074	.....	809	1 hit	[green algae]
Dunaliella peircei	.....	809	1 hit	[green algae]
Dunaliella sp. Persian Gulf	.....	808	1 hit	[green algae]
uncultured Dunaliella	-----	828	52 hits	[green algae]
Chlamydomonadales sp. AB-2012	.....	813	1 hit	[green algae]
uncultured Pyrobrotys	.....	808	1 hit	[green algae]
Chlorosarcinopsis gelatinosa	-----	813	1 hit	[green algae]
uncultured Paulsenella	-----	808	1 hit	[dinoflagellates]
Dunaliella salina strain Tuz KS 01	18S ribosomal RNA gene,			
Dunaliella sp. G5L020	18S ribosomal RNA gene, partial sequ			
Dunaliella sp. SAS11133	18S ribosomal RNA gene, partial seq			
Dunaliella sp. ABR11NW-G22	18S ribosomal RNA gene, partial			
Dunaliella sp. BUM11123	18S ribosomal RNA gene, partial seq			
Dunaliella sp. ABR11NW-G4	18S ribosomal RNA gene, partial s			
Dunaliella sp. ABR11NW-Sh6.3	18S ribosomal RNA gene, partial			
Dunaliella sp. ABR11NW-Ch5	18S ribosomal RNA gene, partial			
Dunaliella sp. ABR11NW-G3	18S ribosomal RNA gene, partial s			
Dunaliella sp. ABR11NW UI/1	18S ribosomal RNA gene, partial			
Dunaliella sp. ABR11NW M1/1	18S ribosomal RNA gene, partial			
Dunaliella tertiolecta strain CCMP 1320	18S ribosomal RNA g			
Dunaliella sp. SPMO 300-4	18S ribosomal RNA gene, partial s			
Dunaliella sp. SPMO 210-3	18S ribosomal RNA gene, partial s			
Dunaliella sp. SPMO 201-6	18S ribosomal RNA gene, partial s			
Dunaliella sp. SPMO 112-2	18S ribosomal RNA gene, partial s			
Dunaliella sp. SPMO 112-1	18S ribosomal RNA gene, partial s			
Dunaliella sp. SPMO 109-1	18S ribosomal RNA gene, partial s			
Dunaliella sp. FL1	18S ribosomal RNA gene, partial sequence			
Dunaliella sp. CCMP 220	18S ribosomal RNA gene, partial seq			
Dunaliella primolecta strain UTEX LB 1000	18S ribosomal RNA			
Dunaliella sp. CCMP 1641	18S ribosomal RNA gene, partial se			
Dunaliella sp. CCMP 1923	18S ribosomal RNA gene, partial se			
Dunaliella parva strain SAG 19-1	18S ribosomal RNA gene, pa			
Dunaliella bioculata strain UTEX LB 199	18S ribosomal RNA g			
Dunaliella sp. KMMCC 1074	18S ribosomal RNA gene, partial s			
Dunaliella peircei strain UTEX LB 2192	18S ribosomal RNA g			
Dunaliella sp. Persian Gulf	18S ribosomal RNA gene, partial			
Uncultured Dunaliella isolate LT37 E12	18S ribosomal RNA ge			
Chlamydomonadales sp. AB-2012	18S ribosomal RNA gene, parti			
Uncultured Pyrobrotys isolate LT42 Aa10	18S ribosomal RNA g			
Chlorosarcinopsis gelatinosa strain CCMP 1511	18S ribosomal			
Uncultured Paulsenella isolate LT62 M23	18S ribosomal RNA g			

**Figure 15.** Taxonomic report for *Dunaliella salina* strain *Tuz\_KS\_01* (GeneBank accession no. **JX880083**) based on BLAST analysis.

## Lineage Report

Chlamydomonadales	[green algae]			
Dunaliellaceae	[green algae]			
Dunaliella	[green algae]			
Dunaliella sp. Tuz KS 02	-----	1506	1 hit	[green algae]
Dunaliella sp. SPMO 600-1	.....	1308	1 hit	[green algae]
Dunaliella sp. SPMO 300-5	.....	1308	1 hit	[green algae]
Dunaliella sp. BSF2	.....	1293	1 hit	[green algae]
Dunaliella sp. SPMO 200-8	.....	1280	1 hit	[green algae]
Dunaliella salina	.....	1279	27 hits	[green algae]
Dunaliella parva	.....	1279	1 hit	[green algae]
Dunaliella sp. SPMO 601-1	.....	1266	1 hit	[green algae]
Dunaliella peircei	.....	1092	1 hit	[green algae]
Dunaliella sp. SPMO 201-5	.....	1088	1 hit	[green algae]
Dunaliella sp. KMMCC 1074	.....	1066	1 hit	[green algae]
Dunaliella sp. ABR11NW G2/1	.....	1062	1 hit	[green algae]
Dunaliella sp. ABR11NW G1/1	.....	1026	1 hit	[green algae]
Dunaliella viridis	.....	942	2 hits	[green algae]
Dunaliella sp. SAS11133	.....	887	1 hit	[green algae]
Dunaliella sp. ABR11NW-G22	.....	887	1 hit	[green algae]
Dunaliella sp. BUM11123	.....	887	1 hit	[green algae]
Dunaliella sp. ABR11NW-G4	.....	887	1 hit	[green algae]
Dunaliella sp. ABR11NW-Sh6.3	.....	887	1 hit	[green algae]
Dunaliella sp. ABR11NW-Ch5	.....	887	1 hit	[green algae]
Dunaliella sp. ABR11NW-G3	.....	887	1 hit	[green algae]
Dunaliella sp. ABR11NW UI/1	.....	887	1 hit	[green algae]
Dunaliella sp. ABR11NW M1/1	.....	887	1 hit	[green algae]
Dunaliella tertiolecta	.....	887	4 hits	[green algae]
Dunaliella sp. SPMO 300-4	.....	887	1 hit	[green algae]
Dunaliella sp. SPMO 210-3	.....	887	1 hit	[green algae]
Dunaliella sp. SPMO 201-6	.....	887	1 hit	[green algae]
Dunaliella sp. SPMO 112-2	.....	887	1 hit	[green algae]
Dunaliella sp. SPMO 112-1	.....	887	1 hit	[green algae]
Dunaliella sp. SPMO 109-1	.....	887	1 hit	[green algae]
uncultured Dunaliella	-----	1042	51 hits	[green algae]
uncultured Halosarcinochlamys	-----	887	1 hit	[green algae]
Chlamydomonadales sp. AB-2012	.....	887	1 hit	[green algae]
Dunaliella sp. Tuz KS 02	18S ribosomal RNA gene, partial se			
Dunaliella sp. SPMO 600-1	18S ribosomal RNA gene, partial s			
Dunaliella sp. SPMO 300-5	18S ribosomal RNA gene, partial s			
Dunaliella sp. BSF2	18S ribosomal RNA gene, partial sequence			
Dunaliella sp. SPMO 200-8	18S ribosomal RNA gene, partial s			
Dunaliella bardawil strain Y2	18S ribosomal RNA gene, parti			
Dunaliella parva	18S rDNA gene			
Dunaliella sp. SPMO 601-1	18S ribosomal RNA gene, partial s			
Dunaliella peircei strain UTEX LB 2192	18S ribosomal RNA ge			
Dunaliella sp. SPMO 201-5	18S ribosomal RNA gene, partial s			
Dunaliella sp. KMMCC 1074	18S ribosomal RNA gene, partial s			
Dunaliella sp. ABR11NW G2/1	18S ribosomal RNA gene, partial			
Dunaliella sp. ABR11NW G1/1	18S ribosomal RNA gene, partial			
Dunaliella viridis strain CONCO02 (Gonzalez)	18S ribosomal			
Dunaliella sp. SAS11133	18S ribosomal RNA gene, partial seq			
Dunaliella sp. ABR11NW-G22	18S ribosomal RNA gene, partial			
Dunaliella sp. BUM11123	18S ribosomal RNA gene, partial seq			
Dunaliella sp. ABR11NW-G4	18S ribosomal RNA gene, partial s			
Dunaliella sp. ABR11NW-Sh6.3	18S ribosomal RNA gene, partial			
Dunaliella sp. ABR11NW-Ch5	18S ribosomal RNA gene, partial			
Dunaliella sp. ABR11NW-G3	18S ribosomal RNA gene, partial s			
Dunaliella sp. ABR11NW UI/1	18S ribosomal RNA gene, partial			
Dunaliella sp. ABR11NW M1/1	18S ribosomal RNA gene, partial			
Dunaliella tertiolecta strain CCMP 1320	18S ribosomal RNA g			
Dunaliella sp. SPMO 300-4	18S ribosomal RNA gene, partial s			
Dunaliella sp. SPMO 210-3	18S ribosomal RNA gene, partial s			
Dunaliella sp. SPMO 201-6	18S ribosomal RNA gene, partial s			
Dunaliella sp. SPMO 112-2	18S ribosomal RNA gene, partial s			
Dunaliella sp. SPMO 112-1	18S ribosomal RNA gene, partial s			
Dunaliella sp. SPMO 109-1	18S ribosomal RNA gene, partial s			
Uncultured Dunaliella isolate LT37 D22	18S ribosomal RNA ge			
Uncultured Halosarcinochlamys isolate LT42 Aa06	18S ribosom			
Chlamydomonadales sp. AB-2012	18S ribosomal RNA gene, parti			

**Figure 16.** Taxonomic report for *Dunaliella sp. Tuz\_KS\_02* (GeneBank accession no. **JX880082**) based on BLAST analysis.

### 1.3.8 GC-MS Analysis of Fatty Acid Composition of New *Dunaliella* Isolates

Fatty acid composition is one of the most important factors for biodiesel production from algae. Thus, we characterized the fatty acid profiles of newly isolated *Dunaliella* species by using GC-MS. For each oil sample, individual fatty acid percentages were estimated from total integrated peak areas. Irrelevant peaks were not included to the calculations. As shown in Figure 17 and Figure 18, total saturated fatty acid percentages much higher than that of unsaturated fatty acids in each *Dunaliella* species which is favorable to biodiesel production. This result indicates that oil extracted from new isolates of *Dunaliella* species have higher oxidative stability. Data also indicates that fatty acid profiles are significantly divergent between two algal species, Last of all C18:0 and C20:0 were found as the most abundant oil types in all samples which demonstrate an appropriate oil characteristic for biodiesel production.

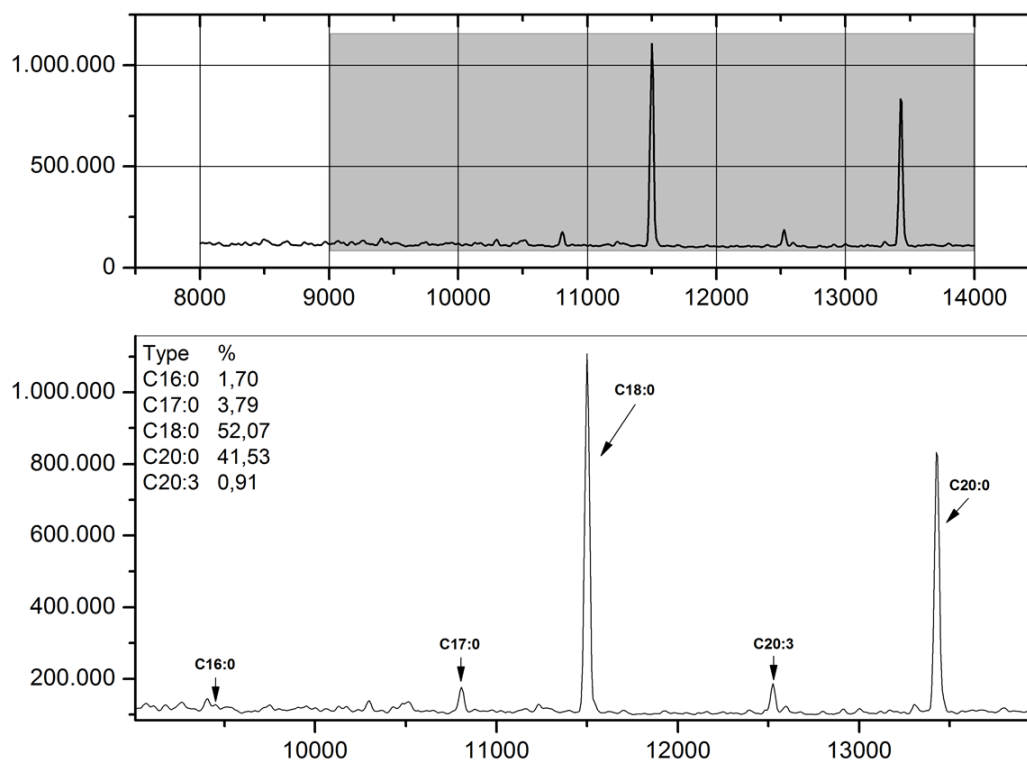


**Figure 17.** GC-MS analysis of fatty acid composition of *Dunaliella salina* strain Tuz\_KS\_01

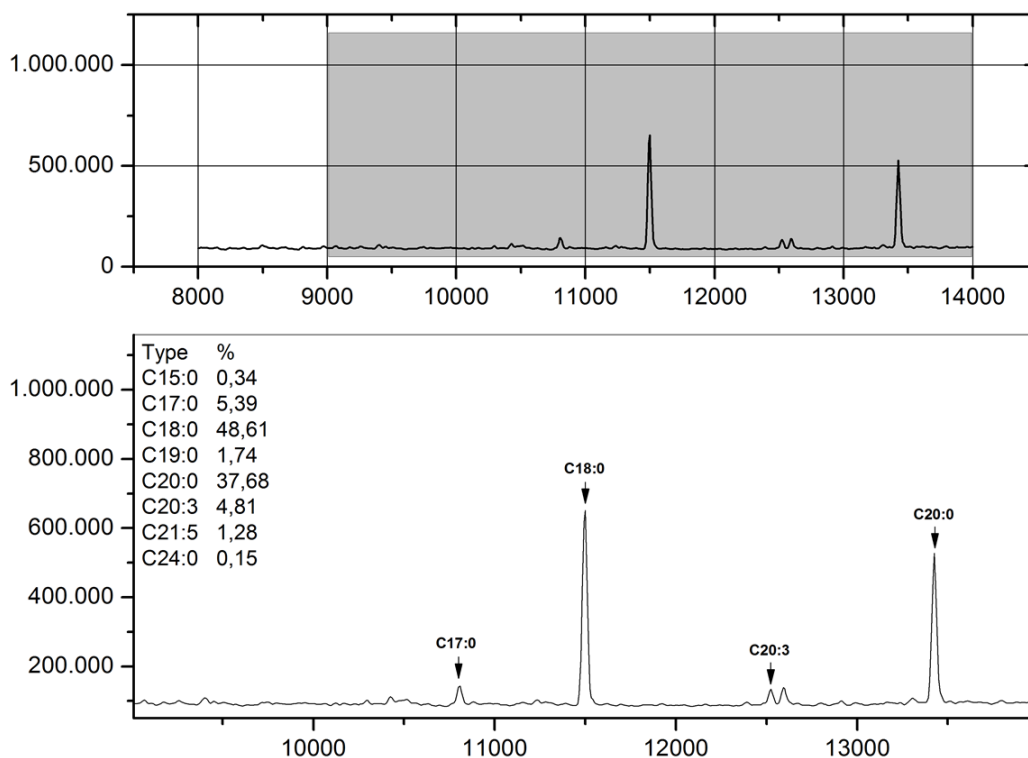


**Figure 18.** GC-MS analysis of fatty acid composition of *Dunaliella sp. Tuz\_KS\_02*

### 1.3.9 Determination of Lipid Contents of the Isolated *Dunaliella* Strains Under Different Cultivation Conditions

The global state of increasing energy consumption and demand pressure the scientific community to find new sustainable energy resources. Among different prospective options, biodiesel has recently garnered interest because of its environmental benefits and renewable characteristics.

The use of alkyl esters of long-chain fatty acids in diesel engines without expensive modifications makes biodiesel an attractive candidate when compared to other options such as hydrogen or solar power. Microalgae, due to their fast growth and small production area compared to other terrestrial plants, have been proposed as a very good potential feedstock of sustainable biodiesel production. Furthermore, using oilseed crops instead of algae for biofuel production creates a negative tension with food security because of the projected increased need for agricultural food production on the horizon [8].

Another desirable characteristic of algae is that environmental changes or stress conditions result in alterations in the lipid biosynthetic pathways and the formation and accumulation of increasing amounts of lipids (%20-50 of DCW), generally in the form of triacylglycerol (TAG). Unlike other lipids, TAGs do not perform a structural role but mainly serve as a storage form of carbon and energy. After synthesis, TAGs are deposited in densely packed lipid bodies in the cytoplasm of algal cells. Therefore, after following the isolation of algal lipids, biodiesel can be produced simply by trans-esterification of the TAGs with methanol and a catalyzer, generally NaOH [18].

Many algal species are already known for their lipid contents and hence their potentials for use in the production of biofuel [19]. Examples of such algae are *Botryococcus braunii* [20], *Nannochloropsis oculata* [21], *Dunaliella tertiolecta* [22], *Haematococcus pluvialis* [23], and *Chlorella vulgaris* [24] in terms of the effects of nutrient deficiencies and different cultivation conditions on their lipid accumulation and biomass production rates. It is also known that different nitrogen sources can be successfully utilized by most of microalgae species [25]. Therefore, some nitrogen sources may promote higher lipid accumulation and different fatty acid profiles. However, limited information has been demonstrated to date.

According to Ho et al. (2010) the optimal biomass and lipid productivity, of *Scenedesmus obliquus* were determined as 292.50 mgL<sup>-1</sup>Day<sup>-1</sup>, 78.73 mgL<sup>-1</sup>Day<sup>-1</sup> (38.9% lipid content per dry weight of biomass), respectively. In addition, under the nutrient-deficient condition, the micro-alga lipid was found mainly composed of C16-C18 fatty acids (accounting for 89% of total fatty acids), a composition thought suitable for biodiesel production [26]. Another study analyzed the potential of *Scenedesmus obliquus* for biodiesel production: according to the study, the lipid contents of experimental groups under nitrogen depleted conditions increased up to 40-fold higher when compared to that of control groups [27].

On the basis of previous findings, it is clearly stated that adjusting different cultivation conditions suggests itself as one of the most prominent strategy for more efficient biodiesel production. High biomass and lipid productive, well-adaptive characteristics prompted us to choose algae species for biofuel production. Additional benefit of previous studies has led us to focus on our comparison of the effects of different cultivation conditions on growth, lipid accumulation so as to attain a better understanding of cultivation characteristics of this important species and support potential, future biodiesel production.

### **1.3.9.1 The effect of Different NaCl Concentrations on Lipid Accumulation in Isolated *Dunaliella* Species**

In order to evaluate the effect of different NaCl concentration on lipid accumulation of newly isolated *Dunaliella* species. We cultivated both isolates with 5, 10, 15, and 20 percent NaCl consisting BBM mediums. According to results, increasing NaCl concentrations were found to increase cellular lipid accumulation in newly isolated algae species shown in Figure 19. Increase of initial NaCl concentration from 5% to 10% did not decrease cell concentration, which might be due to salt tolerant character of *Dunaliella* cells. However, initial NaCl concentration higher than 10% markedly inhibited cell growth. Consequently, initial NaCl concentration less than 5% was considered to be appropriate to achieve high cell concentration.

Although the cultivations with initial NaCl concentration of 5% and 10% showed similar time course of cell concentrations, lipid content of cells cultivated with 10% initial NaCl was higher than that with 5% NaCl as shown in Figure 19. Consequently, the reason for higher lipid content might be not nitrate limitation but high NaCl concentration. However, further increase in initial NaCl concentration should not be a good strategy, because a marked decrease in cell concentration by further increase in initial NaCl concentration was anticipated from the results.

In order to see cellular differences in *Dunaliella* cells under different NaCl concentrations we also conducted fluorescent microscopic Nile red analysis. Cellular morphology was not affected from increased NaCl concentrations in both isolates but cellular lipid contents were increased as shown in Figure 20.

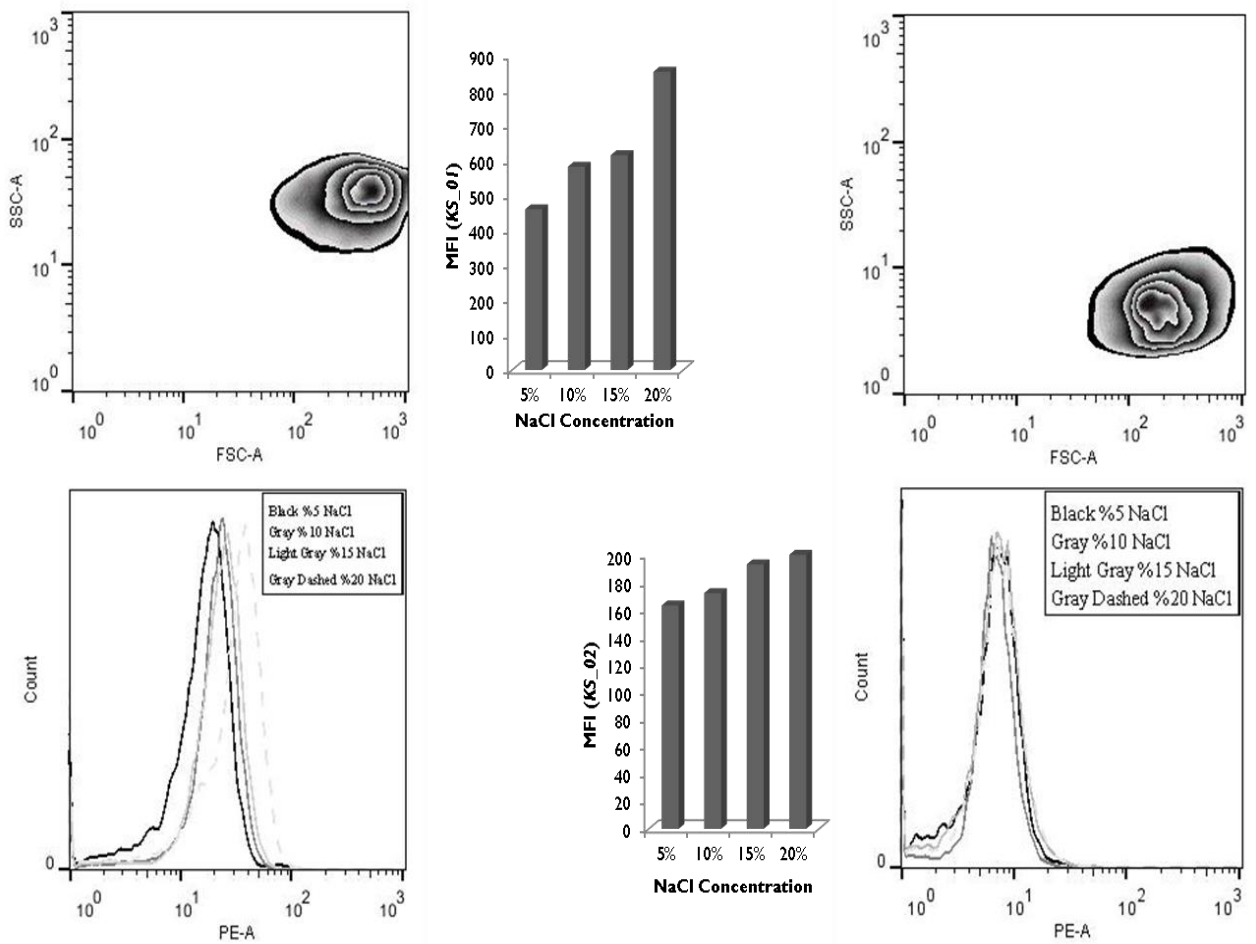


**Figure 19.** Flow cytometric Nile red lipid content analysis of newly isolated *Dunaliella sp.* under different cultivation conditions (KS\_01-Up/Left, KS\_02-Bottom/Left)

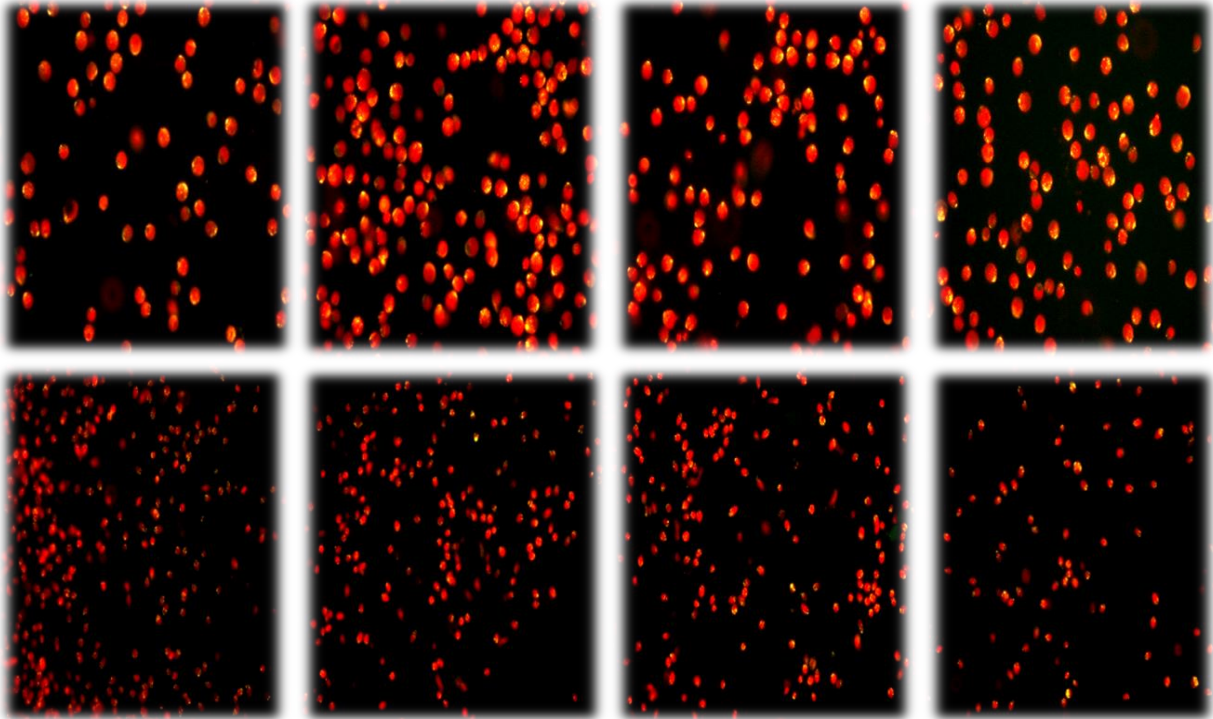


**Figure 20.** Fluorescent microscopic Nile red lipid content analysis of newly isolated *Dunaliella sp.* under different cultivation conditions (Big-Up/Left, Small-Bottom/Left)

### **1.3.9.2 The Effect of Different pHs on Lipid Accumulation in Isolated *Dunaliella* Species**

We tested the hypothesis that increased pH alters the amount of cellular lipid contents. In order to evaluate the effect of different pHs on lipid accumulations, we used both isolated *Dunaliella* species namely *KS\_01* and *KS\_02*. We tested 10 different pHs ranging from 3 to 12 by adding NaOH and HCl to the cultivation media. The total lipid content was reduced in high and low pHs compared to neutral pH conditions. Our data support the hypothesis that cellular lipid contents are reduced when pH increases to high levels, lipid contents are also decreased when pH was reduced to low levels. The favorable pH level was found to near neutral levels for better lipid accumulation in isolated *Dunaliella KS\_02* species shown in Figure 21 and Figure 22. The results suggest that regulating the pH during algae cultivation could be used to refine the lipid composition in the harvested algal biomass.

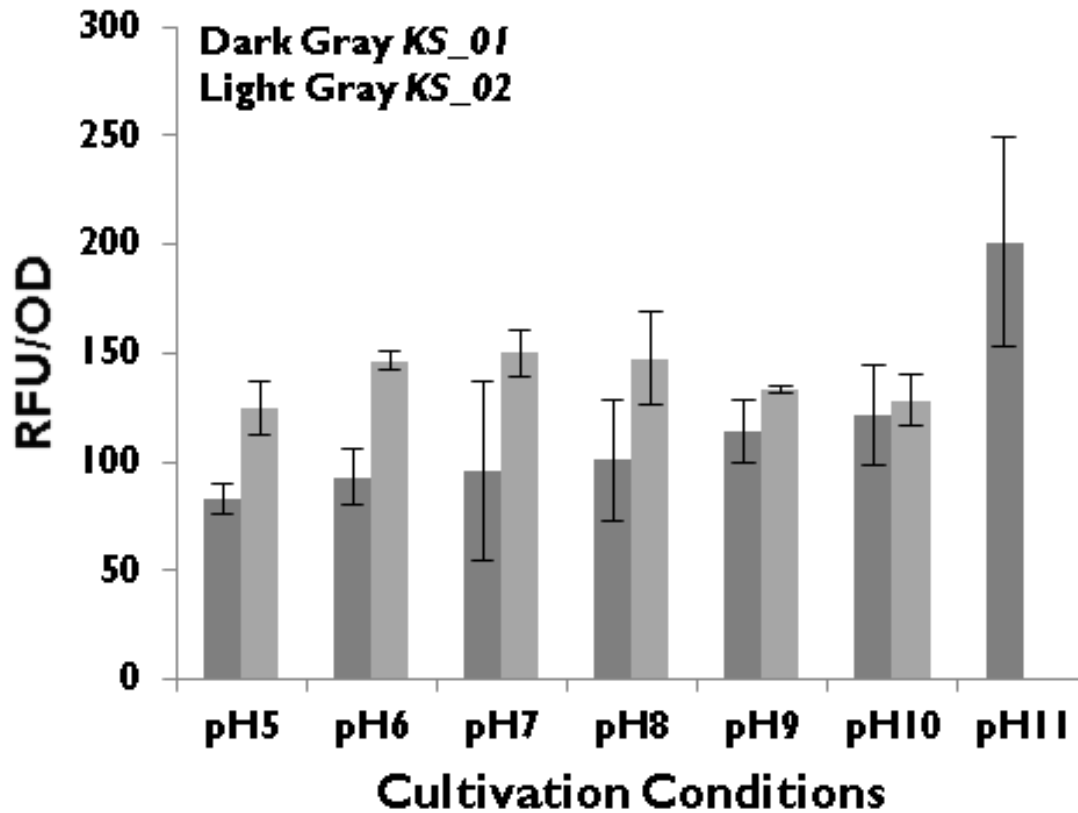


**Figure 21.** Effect of different pH levels on lipid accumulation of newly isolated *Dunaliella* species.

According to results, unlike *Dunaliella KS\_02* species, cellular lipid content of *Dunaliella KS\_01* species was found to be increased in response to higher pH levels shown in figure 21 and Figure 22. It was also demonstrated that *Dunaliella KS\_01* cells were found to be more resistant to higher pH conditions as the species can survive and grow in pH 11 where *Dunaliella KS\_02* cells were found to be totally dead.

For both species, cellular morphology were not altered in different pH levels but altered lipid contents can be seen in fluorescence microphotographs as increased yellow dots inside the cells.

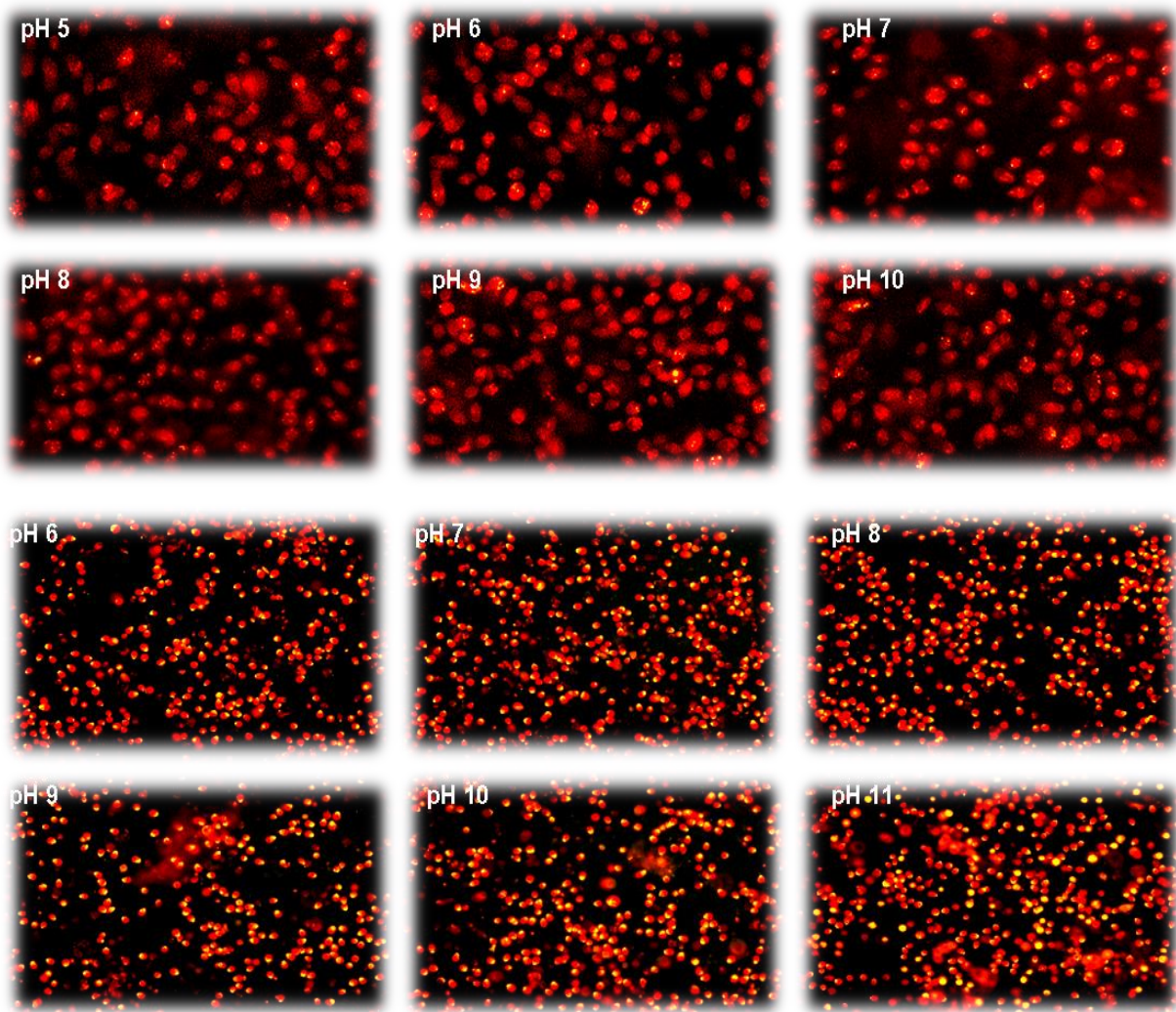


**Figure 22.** Fluorescent microscopic Nile red lipid content analysis of newly isolated *Dunaliella sp.* under different pH cultivation conditions. Upper six are showing *Dunaliella KS\_02* where lower six microphotographs are showing *Dunaliella KS\_01* cells

### **1.3.9.3 The Effect of Different Nitrogen Sources on Lipid Accumulation in Isolated *Dunaliella* Species**

Utilization of different nitrogen sources and their effects on cellular lipid accumulation of isolated hypersaline green algae strains were analyzed. Previous studies have demonstrated the influence of altered nutrient conditions on biomass and lipid productivity in various algae species [28-30]. According to the previous findings, the strategy of altering nutrient conditions especially limitations of nitrogen and phosphorus may result in increased lipid accumulation. Several studies have demonstrated the green algae species as a promising

species in biodiesel production and their lipid contents are affected different nitrogen regimes [26,27]. We showed that different nitrogen source utilization result in altered lipid accumulation in newly isolated *Dunaliella* species suggesting that altered nutrient conditions might be also one of the important factors for deciding biodiesel production efficiency.

All tested nitrogen sources were found to be successfully promoting growth of both isolated species. Nitrogen depletion is well-known factor which increases lipid production in many algal species shown in various studies [26,28-30], however relatively low information has been presented about different nitrogen source utilization and the effects on cellular metabolic response. Therefore, we focused specifically on the influence of different nitrogen source utilization. The Nile-red fluorometric assay was previously shown to be a powerful method for comparing lipid contents of many tissues and various cells of different organisms, especially algal species [31-34]. Thus in this study we again used Nile red method for lipid content comparison. According to results lipid content of both *Dunaliella KS\_01* and *Dunaliella KS\_02* cells were affected by different nitrogen sources. For *Dunaliella KS\_01* cells, the most lipid content increasing nitrogen source was found as  $\text{KNO}_3$  where  $\text{NH}_4\text{Cl}$  was found the most lipid content increasing nitrogen source for *Dunaliella KS\_02* cells shown in Figure 23.

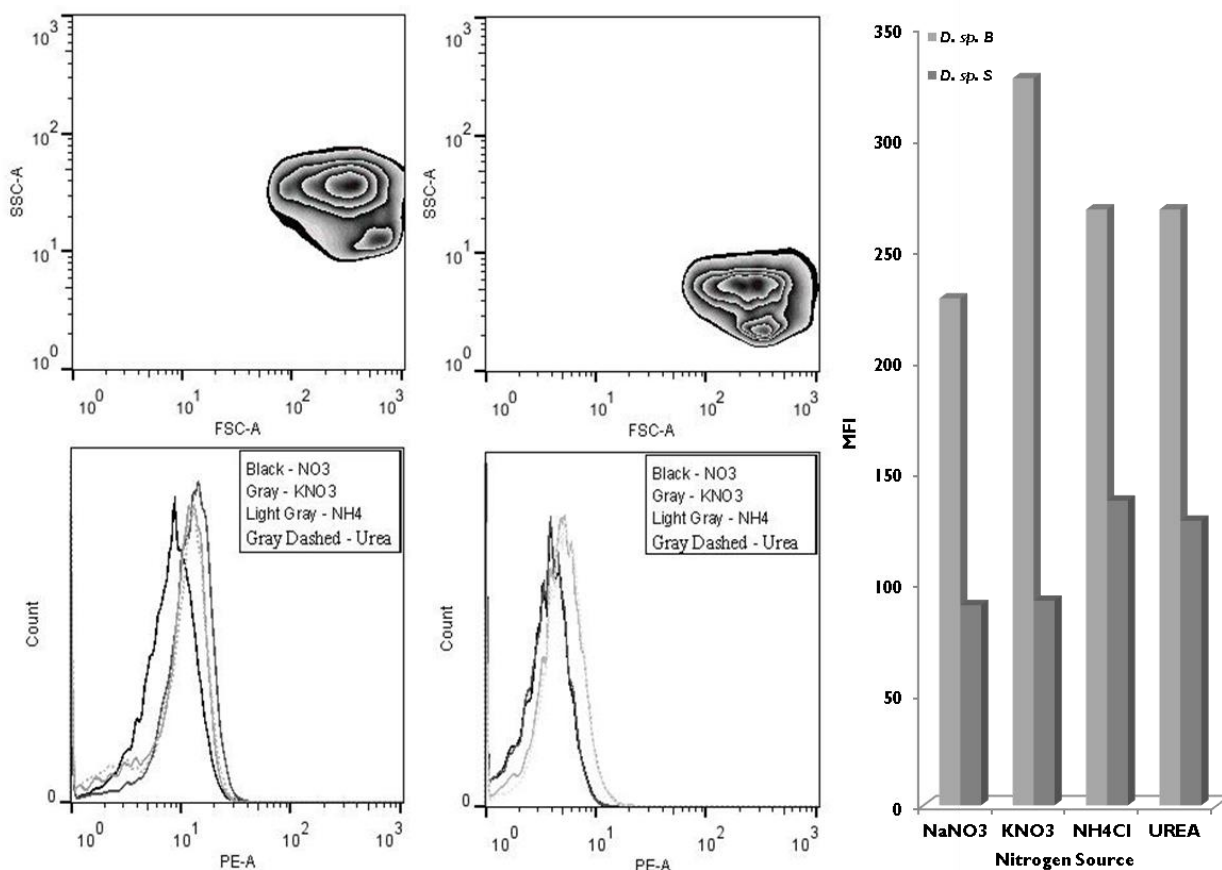


**Figure 23.** Effect of different nitrogen sources on lipid accumulation of newly isolated *Dunaliella* species. Left; *KS\_01* (*D. sp. B*), Right; *KS\_02* (*D. sp. S*)

#### 1.3.9.4 The Effect of Nitrogen Deprived Cultivation Conditions on Lipid Accumulation in Isolated *Dunaliella* Species

Nitrogen deprivation or limitation in cultivation media is a well-known lipid accumulator strategy in algae culture systems. We conducted nitrogen limitation experiments on newly isolated *Dunaliella* species in order to understand the responses of the cells in case of nitrogen limitation cultivation process for future biodiesel production. For this, we conducted spectrophotometric and fluorometric analysis for screening growth and lipid accumulation responses of isolated species. As shown in Figure 24, growth rate is dramatically decreases for both isolated species under nitrogen limitation where the lipid contents are increased.

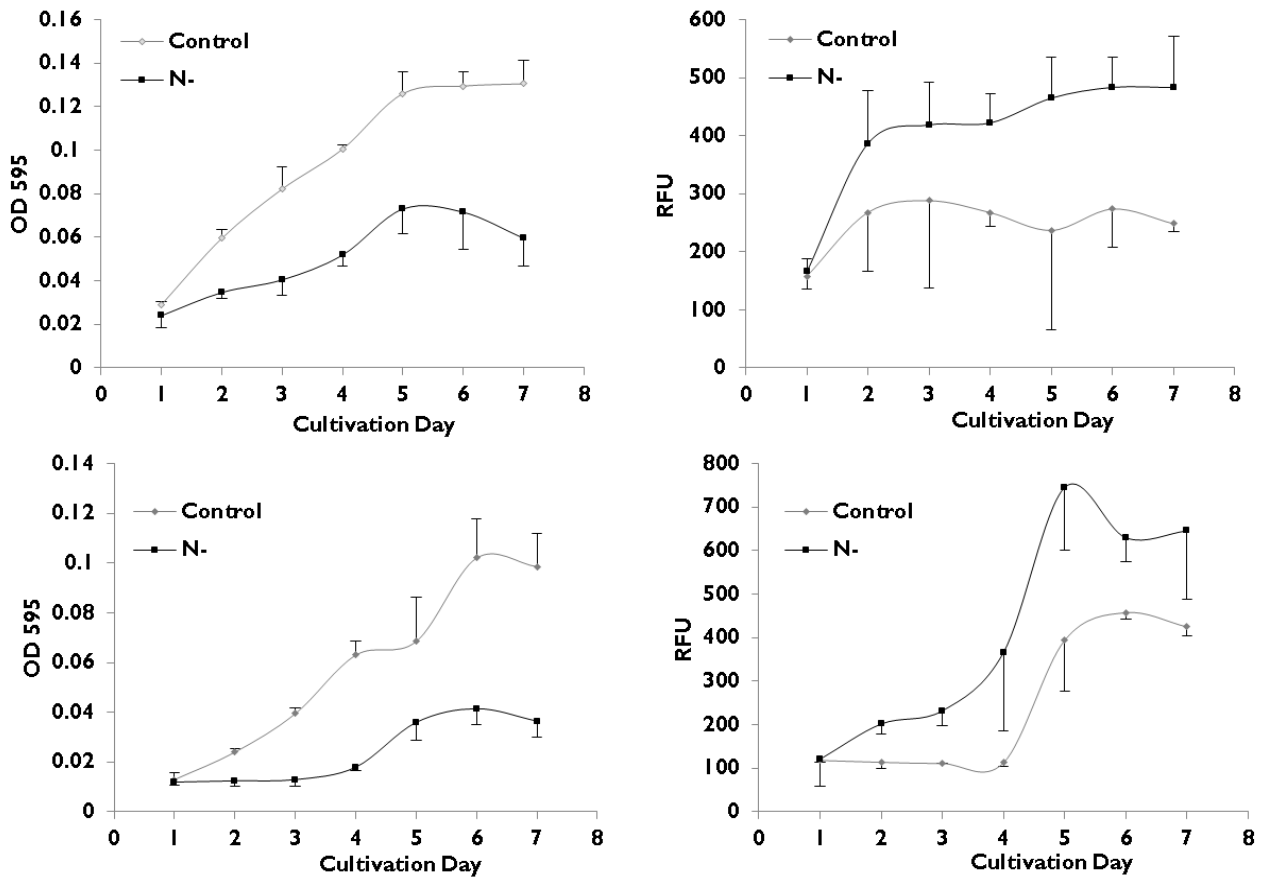


**Figure 24.** Effect of nitrogen limitation on growth rates of newly isolated *Dunaliella* species. Upper Right-Left; *KS\_01*, Lower Right-Left; *KS\_02*

In order to assess the effect of nitrogen limitation on lipid contents flow cytometric Nile red analysis was conducted. As shown in Figure 25, nitrogen depletion results to increased lipid accumulations in both isolated hypersaline algae species *KS\_01* and *KS\_02*.

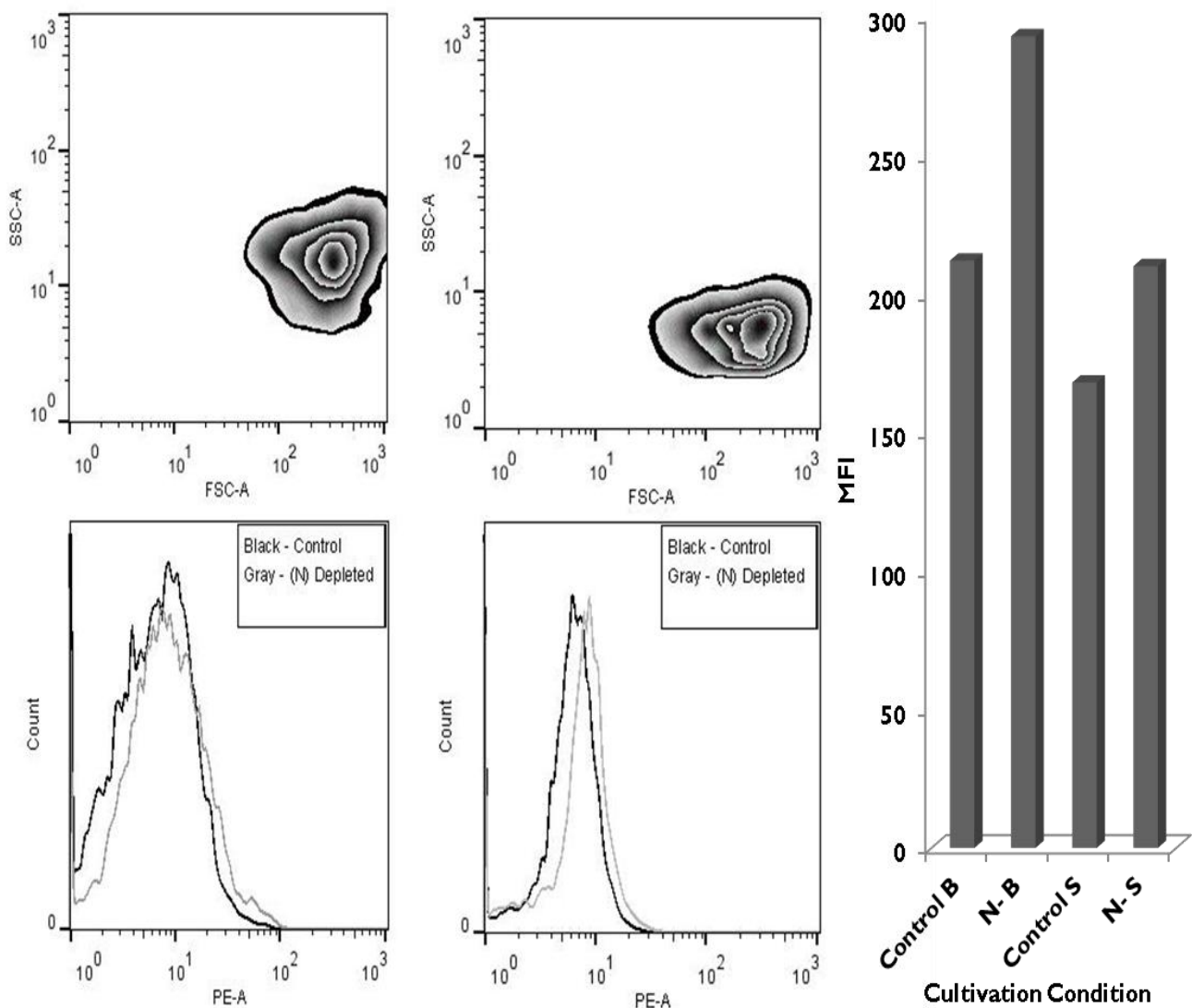


**Figure 25.** Effect of nitrogen limitation on lipid accumulation of newly isolated *Dunaliella* species. Left; *KS\_01* (*D. sp. B*), Right; *KS\_02* (*D. sp. S*)

### 1.3.9.5 The Effect of Sea Water Cultivation Conditions on Lipid Accumulation in Isolated *Dunaliella* Species

*Dunaliella* species are resistant to hypersaline conditions which enable them to be cultivated in unusable water bodies such as sea water. This characteristic of *Dunaliella* species might be crucial for their production due to freshwater resources are very limited especially for other purposes than using freshwaters for human consumption. In order to

assess possible lipid production of newly isolated *Dunaliella* species in sea water for especially biodiesel production, we analyzed lipid accumulation response of the isolated species under different cultivation conditions (with using sea water and modified sea water by adding exogenous nitrogen source). According to results, lipid contents of isolated species were found to be increased under sea water cultivation conditions besides modified sea water with exogenous nitrogen sources resulted to similar effect on cellular lipid accumulation as un-modified sea water cultivation condition did. Both sea water and modified sea water increased lipid accumulation shown in Figure 26 and Figure 27, this result suggest that sea water might be used as cultivation media for newly isolated *Dunaliella* species for its future biotechnological productions.

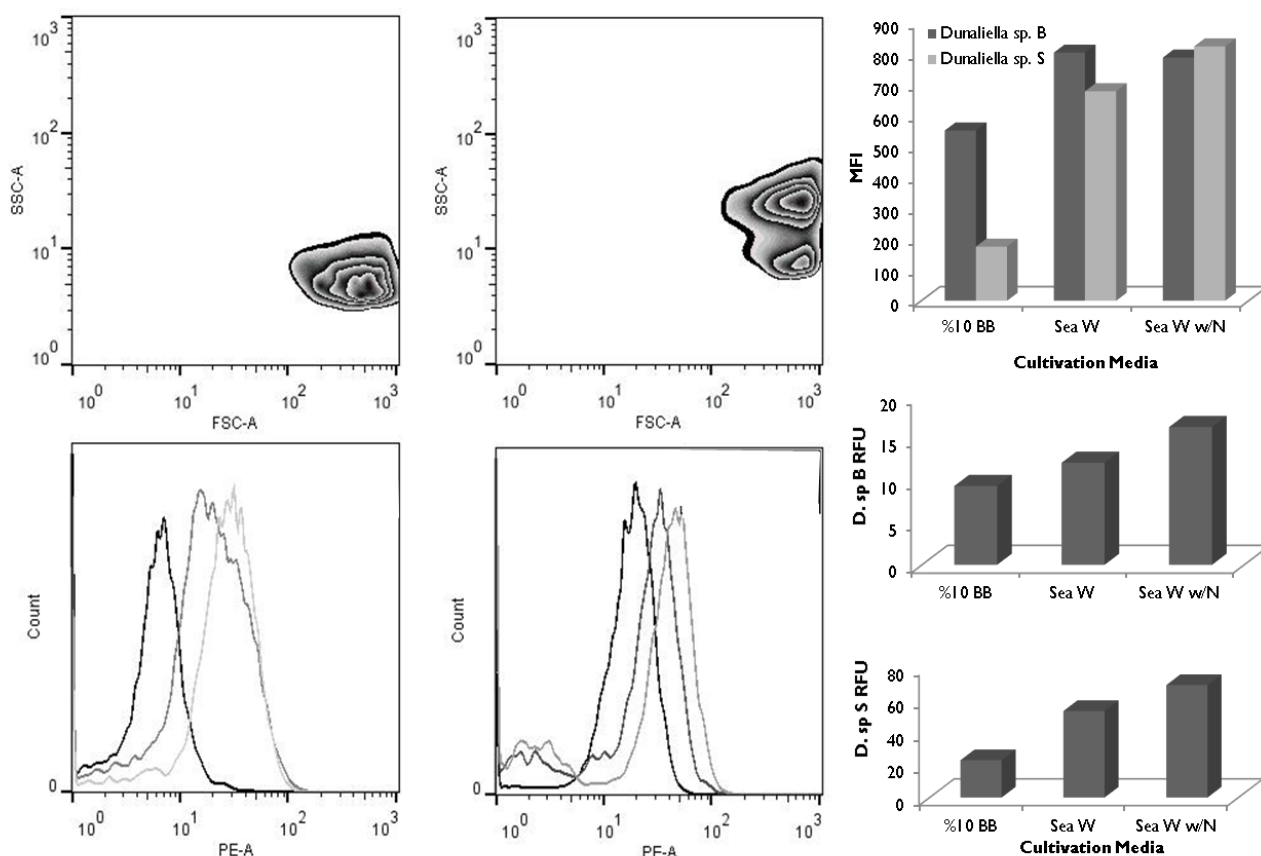


**Figure 26.** Effect of sea water cultivation conditions on lipid accumulation of newly isolated *Dunaliella* species. Right; KS\_01 (*D. sp. B*), Left; KS\_02 (*D. sp. S*)

For both species, cellular morphology were not altered in sea water cultivation conditions but altered lipid contents can be seen in fluorescence microphotographs as increased yellow dots inside the cells.

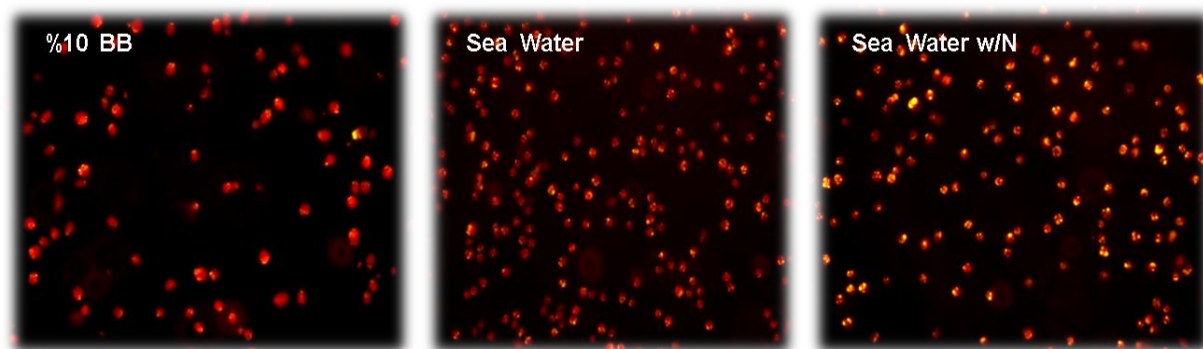


**Figure 27.** Effect of sea water cultivation conditions on lipid accumulation of newly isolated *Dunaliella* species.

#### **1.3.9.6 Optimization of -80°C /-196°C Ultrafreeze Storage Conditions for Long and Short term Storage**

In order to long and short term storage of newly isolated *Dunaliella* strains, we conducted optimization experiments for -80°C /-196°C ultrafreeze storage conditions. For this, we used following protocols below;

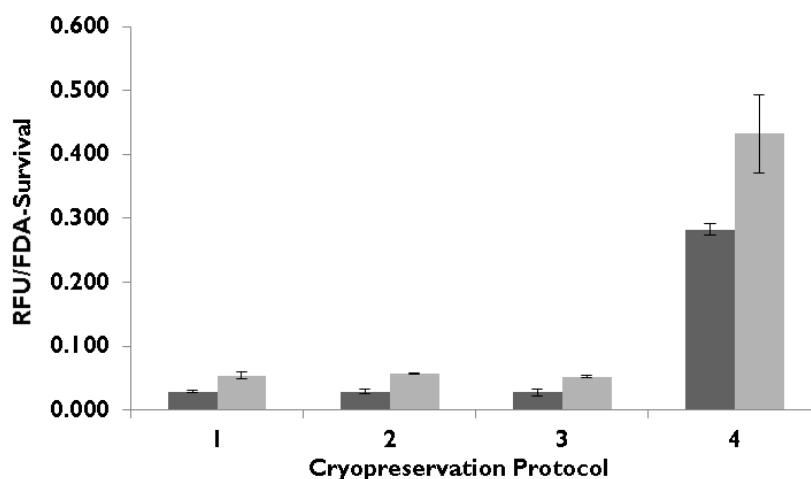
Long term storage protocols used;

- 1) %20 Methanol Direct Freezing at -196C
- 2) %5 DMSO Direct Freezing at -196C
- 3) 3 Step %20 Methanol Freezing Method (+20C-15min/-80C-1.5H/-196C-∞)
- 4) 3 Step %5 DMSO Freezing Method (+20C-15min/-80C-1.5H/-196C-∞)

Short term storage protocols used;

- 1) %20 Methanol Direct Freezing at -80C
- 2) %5 DMSO Direct Freezing at -80C
- 3) 2 Step %20 Methanol Freezing Method (+20C-15min/-80C Over Night)
- 4) 2 Step %5 DMSO Freezing Method (+20C-15min/-80C Over Night)

According to results, for both long and short term storage protocols, protocol number 4 was found viable as shown in Figure 28.



Method	Cell Survival (KS_01-KS_02)	Cell Stability	Cell Motion	Cell Size
1	0%	Not Intact	No	Bigger-Granulated
2	0%	Not Intact	No	Bigger-Granulated
3	0%	Not Intact	No	Bigger-Granulated
4	>%50	Intact	Yes	Smaller-Oblique-Healthy

Method	Cell Survival (KS_01-KS_02)	Cell Stability	Cell Motion	Cell Size
1	0%	Not Intact	No	Bigger-Amorphous
2	0%	Not Intact	No	Bigger-Amorphous
3	0%	Not Intact	No	Bigger-Amorphous
4	>%50	Intact	Yes	Smaller-Oblique-Healthy

**Figure 28.** Optimization of short and long term ultrafreeze storage protocols for newly isolated *Dunaliella* species. Bar graph; Fluorometric FDA cell survival analysis, Top Table; Cell survival upon freeze-thaw process at  $-196^{\circ}\text{C}$ , Bottom Table; Cell survival upon freeze-thaw process at  $-80^{\circ}\text{C}$ .

## 1.4 Conclusions

We isolated two different hypersaline *Dunaliella* species namely *Dunaliella salina* KS\_02 and *Dunaliella sp.* KS\_01 from Lake Tuz and for the first time molecular identifications were done on the strains and sequences were deposited in NCBI GeneBank database. Cultivation conditions and best lipid accumulator conditions were optimized for future productions of the strains. Ultrafreeze storage conditions were also established. Due to the limitation of freshwaters and the need for finding new biofuel resources, the use of hypersaline species are gaining importance, we recommend further molecular, biochemical and physiological studies on these species for understanding and developing new biotechnologically important information.

## CHAPTER 2

### **Oxidative stress is a mediator for increased lipid accumulation in a newly isolated *Dunaliella salina* strain**

#### **2.1 INTRODUCTION**

Green algae offer sustainable, clean and eco-friendly energy resource. However, production efficiency needs to be improved. Increasing cellular lipid levels by nitrogen depletion is one of the most studied strategies. Despite this, the underlying physiological and biochemical mechanisms of this response have not been well defined. Algae species adapted to hyper saline conditions can be cultivated in salty waters which are not useful for agriculture or consumption. Due to their inherent extreme cultivation conditions, use of hyper saline algae species is better suited for avoiding culture contamination issues. In this study, we identified a new halophilic *Dunaliella salina* strain by using 18S ribosomal RNA gene sequencing. We found that growth and biomass productivities of this strain were directly related to nitrogen levels, as the highest biomass concentration under 0.05mM or 5mM nitrogen regimes were 495 mg/l and 1409 mg/l, respectively. We also confirmed that nitrogen limitation increased cellular lipid content up to 35% under 0.05mM nitrogen concentration. In order to gain insight into the mechanisms of this phenomenon, we applied fluorometric, flow cytometric and spectrophotometric methods to measure oxidative stress and enzymatic defence mechanisms. Under nitrogen depleted cultivation conditions, we observed increased lipid peroxidation by measuring an important oxidative stress marker, malondialdehyde and enhanced activation of catalase, ascorbate peroxidase and superoxide dismutase antioxidant enzymes. These observations indicated that oxidative stress is accompanied by increased lipid content in the green alga. In addition, we also showed that at optimum cultivation conditions, inducing oxidative stress by application of exogenous H<sub>2</sub>O<sub>2</sub> leads to increased cellular lipid content up to 44% when compared with non-treated control groups. Our results support that

oxidative stress and lipid overproduction are linked. Importantly, these results also suggest that oxidative stress mediates lipid accumulation. Understanding such relationships may provide guidance for efficient production of algal biodiesels.

The idea of using biofuels has gained prominence, since they provide a cleaner alternative to the currently used fossil fuels. It has recently been estimated that utilization of biofuels will result in a 30% decrease in CO<sub>2</sub> emissions in the United States. Biofuels can be derived from different kinds of resources including microalgae, animal fats, soybeans, corns and other oil crops. While none of these options currently has the efficiency to produce the required amounts of biofuel [1], microalgae are considered the most promising venue of biofuel production due to their ease of cultivation, sustainability, and compliance in altering their lipid content resulting in higher biofuel production.

High lipid accumulation and biomass productivity are the two manifestly desired phenotypes in algae for biodiesel production. However, various studies conducted under nutrient depleted conditions have demonstrated that biomass productivity and lipid accumulation are negatively related [2]. These studies have established that stress conditions, which by definition reduce the biomass production, increase lipid content of algae. This problem was addressed by using a two-stage reactor where algal species such as *Oocystis* sp. and *Amphora* sp. are grown in optimal conditions for maximum biomass, followed by stress conditions for maximum lipid accumulation [3]. Within this context, nitrogen depletion can be still considered as a strategy for increasing lipid accumulation since it has been still defined as one of the best lipid accumulator stress condition in algae to date. However the mechanistic insights of this phenomenon are still needed.

Nitrogen deprivation as a stress condition is known to maximize the lipid content up to 90% [4]. However, underlying mechanisms have not been well described in terms of its physiological and molecular aspects. Despite the fact that oxygen itself is not harmful for cells, the presence of reactive oxygen species (ROS) may lead to oxidative damage to the cellular environment, ultimately leading to toxicity resulting from excessive reactive oxygen stress [5]. Redox reactions of the reactive forms of oxygen including hydrogen peroxide (H<sub>2</sub>O<sub>2</sub>), superoxide (O<sub>2</sub><sup>-</sup>) or hydroxyl (OH<sup>-</sup>) radicals with cellular lipids, proteins, and DNA result in oxidative stress [6]. A previous study showed that nitrogen depletion results in the co-occurrence of ROS species and lipid accumulation in diatoms [7]. Association of increased reactive oxygen species levels and cellular lipid accumulation under different environmental stress conditions was also shown in green microalgae [8] ROS is known to be an important factor in cellular response and it is well established that ROS increases when microalgae are

exposed to various stresses. However, a mechanistic understanding of the connection between ROS increase and increased lipid accumulation in algae species requires further investigation [9].

Nitrogen depleted conditions trigger reactive oxygen species accumulation, increased cellular lipid content and protein production impairment. However, the temporal order and the causal links between these events are yet to be explored. Here, we aimed at finding the relationship between oxidative stress and increased cellular lipid content under nitrogen depleted conditions in a hyper saline green alga in order to have a better understanding of this phenomenon.

*Dunaliella* genus [10] is one of the microalgae genus that has been considered for lipid production. *Dunaliella* species are particularly attractive due to their strong resistance characteristics to various unfavorable environmental conditions such as high salinity. Obtaining such strong algal species for lipid production under conditions that are otherwise not useful is an important economical consideration in terms of biodiesel production. In addition, cultivation of algae species in freshwaters may not be feasible due to the limited supply and population expansion. Understanding the mechanisms behind increased lipid accumulation in halophilic *Dunaliella* in response to different stress conditions, especially nitrogen depletion, is crucial to enable key manipulations at the genetic, biochemical and physiological level for decreasing biodiesel production costs.

## **2.2 Materials and Methods**

### **2.2.1 Organism and Culture Conditions**

*Dunaliella tertiolecta* (*D.t.* #LB999) and *Chlamydomonas reinhardtii* (*C.r.* #90) were obtained from UTEX, Collection Culture of Algae, USA and cultivated artificial sea water medium and soil extract medium as instructed by the culture collection protocols respectively. The alga used in this study was isolated from the hypersaline lake “Tuz”, which is located in Middle Anatolia, Turkey with the research permission of Republic of Turkey Ministry of Food, Agriculture and Livestock (Permit issue: B.12.0.TAG.404.03.10.03.03-1607). Field studies did not involve endangered or protected species. Collection of water samples was done and isolation location was recorded using a GPS device as 39°4'23.97"K - 33°24'33.11"E at the southern east part of Sereflikochisar province. 10 ml water samples were

collected and enriched with the same volume of Bold's Basal Medium (BBM) modified by addition of 5% NaCl. BBM was pH 7.4 and consisted of 5 mM NaNO<sub>3</sub> along with CaCl<sub>2</sub>·2H<sub>2</sub>O 0.17 mM, MgSO<sub>4</sub>·7H<sub>2</sub>O 0.3 mM, K<sub>2</sub>HPO<sub>4</sub> 0.43 mM, KH<sub>2</sub>PO<sub>4</sub> 1.29 mM, Na<sub>2</sub>EDTA·2H<sub>2</sub>O 2 mM, FeCl<sub>3</sub>·6H<sub>2</sub>O 0.36 mM, MnCl<sub>2</sub>·4H<sub>2</sub>O 0.21 mM, ZnCl<sub>2</sub> 0.037 mM, CoCl<sub>2</sub>·6H<sub>2</sub>O 0.0084 mM, Na<sub>2</sub>MoO<sub>4</sub>·2H<sub>2</sub>O 0.017 mM, Vitamin B<sub>12</sub> 0.1 mM and 5 mM NaCO<sub>3</sub> was supplied as carbon source.

Water samples were plated on petri dishes with modified BBM 5% NaCl and 1% bacteriological agar, while same water samples were also subjected to dilutions with fresh modified BBM 5% NaCl in 48-well plates (1:2, 1:4, 1:8, 1:16, 1:32, 1:64) to obtain monocultures. After 2 and 4 weeks cultivation periods of 48-well plate liquid cultures and petri dishes, respectively, clones were isolated. These clones were transferred to fresh mediums in 100 ml canonical flasks in a final volume of 25 ml for obtaining cell stocks at 25 °C under continuous shaking and photon irradiance of 80 rpm and 150 μEm<sup>-2</sup>s<sup>-1</sup>.

All experiments were carried out under same cultivation conditions in 250 ml batch cultures but different nitrogen concentrations, 0.05, 0.5 and 5 mM NaNO<sub>3</sub> were used for low, medium and high nitrogen concentrations, respectively. Concentrations ranging between 200 μM and 8 mM were used for H<sub>2</sub>O<sub>2</sub> experiments.

### **2.2.2 Isolation and Purification of DNA and Amplification of 18S rRNA Encoding Gene**

DNA isolation was done by using DNeasy Plant Mini Kit (Qiagen) as instructed by the manufacturer. Quantification of the genomic DNA obtained and assessment of its purity was done on a Nanodrop Spectrophotometer ND-1000 and on 1% agarose gel electrophoresis. MA1 [5'-CGGGATCCGTCATATGCTTGTCTC-3'] and MA2 [5'-GGAATTCCTTCTGCAGGTTTCACC-3'] were designed from 18S rDNA genes and were previously reported by Olmos et al [9]. PCR reactions were carried out in a total volume of 50 μl containing 50 ng of chromosomal DNA in dH<sub>2</sub>O and 200 ng MA1 and MA2 conserved primers. The amplification was carried out using 30 cycles in a MJ Mini™ Personal Thermal Cycler (BioRad), with a T<sub>m</sub> of 52 °C for all reactions. One cycle consisted of 1 minute at 95 °C, 1 minute at 52 °C and 2 minutes at 72 °C.

### 2.2.3 Sequencing and Phylogenetic Analysis

MA1–MA2 PCR products were utilized to carry out sequencing reactions after purification with a QIAquick PCR purification kit (Qiagen). The sequencing reactions were run by MCLAB (San Francisco, CA), employing primers MA1–MA2 in both reverse and forward directions. DNA sequences were imported to BLAST for identification and to search for phylogenetic relationship correlations between other 18S rDNA gene sequences of *Dunaliella* species/strains deposited in NCBI Gene Bank. Dendrogram data generated by BLAST was converted into Newick format and submitted to Phyfi [10] for generating phylogenetic tree.

### 2.2.4 Growth Analysis

Specific growth rate and biomass productivity was calculated according to the equation;  $K' = \ln(N2 / N1) / (t2 - t1)$  where N1 and N2, biomass at time1 (t1) and time2 (t2) respectively ( $t2 > t1$ ) [11]. Divisions per day and the generation (doubling) time were calculated according to the equations below:

$$\text{Divisions per day} = \text{Div. day}^{-1} = K' / \ln 2$$

$$\text{Generation time} = \text{Gen 't} = 1 / \text{Div. day}^{-1}$$

### 2.2.5 Extraction and Measurements of Lipid Contents and Fluorescence

#### Microscopy

Lipid was extracted according to Bligh and Dyer wet extraction method. Briefly, to a 15 ml glass vial containing 100 mg dried algal biomass, 2 ml methanol and 1 ml chloroform were added and kept for 24 h at 25 °C. The mixture was then vortexed and sonicated for 10 minutes. One milliliter of chloroform was again added, and the mixture shaken vigorously for 1 min. Subsequently, 1.8 ml of distilled water was added and the mixture vortexed again for 2 min. The aqueous and organic phases were separated by centrifugation for 15 min at 2,000 rpm. The lower (organic) phase was transferred into a previously weighed clean vial (V1). Evaporation occurred in a thermo-block at 95 °C, and the residue was further dried at 104 °C for 30 min. The weight of the vial was again recorded (V2). Lipid content was calculated by subtracting V1 from V2, and expressed as dcw %. The correspondence between Nile Red

fluorescence intensity and % lipid content was determined by plotting relative fluorescence units against % cellular lipid content obtained from triplicate samples. For fluorescence microscopy analysis of Nile Red, cells were stained with 5  $\mu$ l 0.5mg/mL Nile Red (Sigma, USA) stock solution after fixing cells with 5% paraformaldehyde and imaged by epifluorescence microscopy with a Leica DMR microscope (Leica Microsystems).

### **2.2.6 Spectrofluorometric Microplate Analysis for Determination of Lipid and Reactive Oxygen Species Accumulation**

A stock solution of Nile Red (NR) (Sigma, 72485) was prepared by adding 5 mg of NR to 10 ml of acetone. The solution was kept in a dark colored bottle and stored in the dark at -20 °C. 1 ml of algal cells from a culture of 250 ml glass erlenmeyer flasks containing 100 ml growth media with different nitrogen concentrations were transferred to 1.5 ml eppendorf tubes for 5 min centrifugation at 5,000 rpm, washed twice with fresh medium, and measured in a spectrophotometer at 600 nm. Each sample was adjusted to an OD<sub>600</sub> of 0.3 in a 1 ml final volume by dilution with fresh medium. 5  $\mu$ l of Nile Red solution was added to each tube and mixed well, followed by 20 min incubation in the dark. Finally, cellular neutral lipids were quantified using a 96-well microplate spectrofluorometry (SpectraMAX GEMINI XS) with an excitation wavelength of 485 nm and an emission wavelength of 612 nm.

Vital staining for determination of cell survival under H<sub>2</sub>O<sub>2</sub> treatment was done by using fluorescein diacetate (FDA) (Sigma, USA). Determination of ROS production related to oxidative stress was done by using DCFH-DA (Sigma, USA). 0.5 mg/ml stock solutions for both stains were prepared in acetone and the same protocol was used for FDA (Sigma, USA) and DCFH-DA (Sigma, USA) staining as described above for Nile Red staining. Data were recorded as relevant fluorescence units [12] for all spectrofluorometric staining experiments.

### **2.2.7 Flow Cytometric Analysis for Determination of Lipid and Reactive Oxygen Species Accumulation**

5  $\mu$ l of Nile Red (Sigma, USA) from stock solution (0.5 mg/mL) was added to 1 ml of a cell suspension at an OD<sub>600</sub> of 0.3 after washing cells twice with fresh medium. This mixture was gently vortexed and incubated for 20 minutes at room temperature in dark. Nile Red uptake was determined using a BD-FACS Canto flow cytometer (Becton Dickinson Instruments) equipped with a 488 nm argon laser. Upon excitation by a 488 nm argon laser,

NR exhibits intense yellow-gold fluorescence when dissolved in neutral lipids. The optical system used in the FACS Canto collects yellow and orange light (560–640 nm, corresponding to neutral lipids). Approximately 10,000 cells were analyzed using a log amplification of the fluorescent signal. Non-stained cells were used as an auto fluorescence control. Nile Red fluorescence was measured using a 488 nm laser and a 556 LP+585/42 band pass filter set on a FACS Canto Flow Cytometer. Data were recorded as mean fluorescence intensity (MFI).

DCFH-DA (Sigma, USA) from stock solution (0.5 mg/ml) was used as described for Nile Red staining. Nonfluorescent DCFH-DA is taken up and converted into dichlorodihydrofluorescein (DCF) by the action of cellular esterases. Fluorescence from oxidized DCF was measured using a 488 nm laser and a 556/Long Pass filter set on a BD-FACS Canto Flow Cytometer. Data were expressed as mean fluorescence intensity (MFI). The data of both staining methods were evaluated using Flowjo Ver. 7.6.1 (Tree Star, Inc.).

### **2.2.8 Protein, Chlorophyll, Carotenoid, TBARS Analyses and Enzymatic Assays**

Total protein isolation was done according to Barbarino et al [13]. Protein content was determined following the method described by Bradford [14]. Cellular chlorophyll and carotenoid isolations were done using the methanol extraction method. Calculation of chlorophyll and carotenoid contents were carried out using the formula for methanol extraction described by Wellburn [15]. Lipid peroxidation analysis upon different nitrogen concentration regimes was analysed by using thiobarbituric acid reactive substances (TBARS) method described by Sabatini et al [16]. For superoxide dismutase (SOD) analysis 50 mg biomass was homogenized in 2 ml 0.5 M phosphate buffer (pH 7.5) and centrifuged at 13,000 rpm for 10 min at 4 °C. SOD activity was determined in the supernatant by inhibition of nitroblue tetrazolium (NBT) using a reaction mixture of 1.5 ml Na<sub>2</sub>CO<sub>3</sub> (1 M), 200 µl methionine (200 mM), 100 µl NBT (2.25 mM), 100 µl EDTA (3 mM), 100 µl riboflavin (60 µM) and 1.5 ml phosphate buffer (pH 7.8, 0.1 M). The absorbance was recorded at 560 nm. One unit of SOD per gram of protein was defined as the amount causing 50% inhibition of photochemical reduction of NBT [17]. For catalase (CAT) analysis, 50 mg biomass was homogenized in 2 ml phosphate buffer (0.5 M, pH 7.5), centrifuged at 12,000 rpm at 4°C for 30 min and supernatant was taken for CAT activity. A reaction mixture containing 1.6 ml phosphate buffer (pH 7.3), 100 µl EDTA (3 mM), 200 µl H<sub>2</sub>O<sub>2</sub> (0.3%) and 100 µl supernatant (containing enzyme extract) was taken in a cuvette and CAT activity in supernatant was determined by monitoring the disappearance of H<sub>2</sub>O<sub>2</sub>, by measuring a decrease in absorbance

at 240 nm against a blank of same reaction mixture without 0.3% H<sub>2</sub>O<sub>2</sub> [18]. For analysis of ascorbate peroxidase (APX), 50 mg biomass was homogenized in 2 ml phosphate buffer (0.5 M, pH 7.5) and centrifuged at 12,000 rpm at 4 °C for 30 min. The supernatant was taken for APX activity. A reaction mixture containing 1 ml phosphate buffer (pH 7.3), 100 µl EDTA (3 mM), 1 ml ascorbate (5 mM), 200 µl H<sub>2</sub>O<sub>2</sub> (0.3%) and 100 µl supernatant (containing enzyme extract) was prepared in a cuvette. The reaction was followed for 3 min at a wavelength of 290 nm against a blank of same reaction mixture without 0.3% H<sub>2</sub>O<sub>2</sub> [19].

## 2.3 Results and Discussion

### 2.3.1 Isolation and identification of the new *Dunaliella salina* strain

We isolated a new hypersaline microalga from the biggest salt lake of Turkey located in the Middle Anatolian region in July 2011. The microalga, which is unicellular, biflagellate, tolerant up to 20% NaCl was identified as *Dunaliella salina* based on the morphological characterization prior to molecular identification.

This strain was deposited in -196 °C ultra-freeze conditions at Sabanci University algae culture collection as *Dunaliella salina* strain *Tuz\_KS\_01*. Molecular identification was based on 18S rDNA gene sequence amplification and sequencing. A single 18S rDNA PCR amplicon was about ~1800 bp in size, in accordance with Olmos et al. [9]. The partial sequence of the 18S rDNA encoding gene was submitted to National Center for Biotechnology Information (NCBI) GeneBank database as *Dunaliella salina* strain *Tuz\_KS\_01* (GeneBank accession no. **JX880083**). According to Basic Local Alignment Search Tool (BLAST) analysis, the isolated sequence had very high percentage of identity with other deposited 18S rDNA sequences of *Dunaliella* species shown in the phylogenetic tree plotted in Figure 1. Molecular identification showed a high percentage identity to *Dunaliella salina* strains (Identity 93%, Query Coverage 70%).

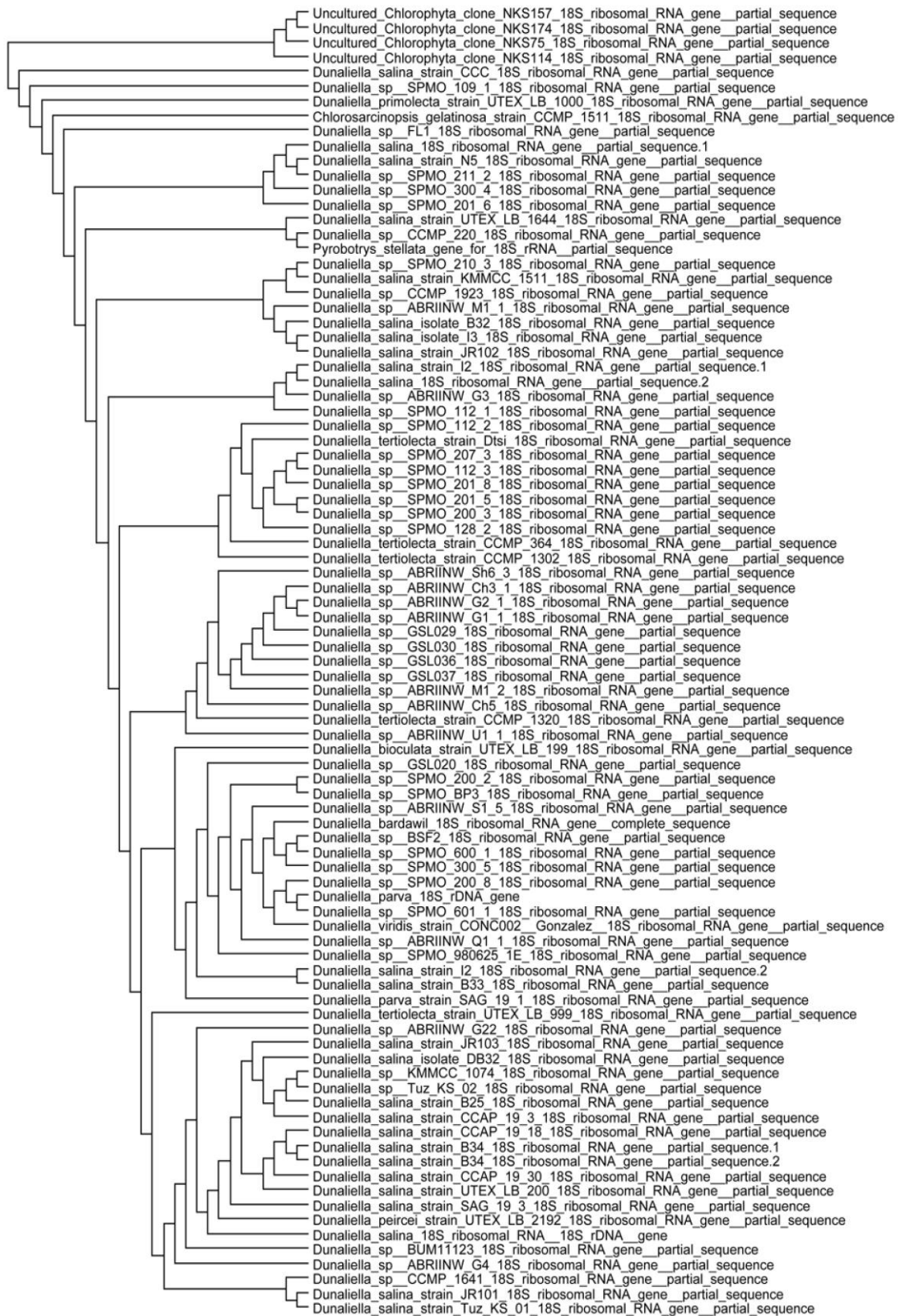


**Figure 1** Phylogenetic analysis of *Dunaliella salina* strain *Tuz\_KS\_01* (GeneBank accession no. **JX880083**). Dendrogram was generated using the neighbor-joining analysis

based on 18S rDNA gene sequences. The phylogenetic tree shows the position of *Dunaliella salina* strain *Tuz\_KS\_01* (GeneBank accession no. **JX880083**) relative to other species and strains of *Dunaliella* deposited in NCBI GeneBank.

### **2.3.2 Growth analysis of the new *Dunaliella* strain under different nitrogen concentrations**

The newly isolated halotolerant *Dunaliella salina* strain was cultivated under different nitrogen concentrations for growth analysis. 0.05 mM, 0.5 mM and 5 mM NaNO<sub>3</sub> concentrations were considered as low, medium and high nitrogen concentrations. Specific growth rates and/or average biomass productivities (ABP) were found to be 370 mg/dayL, 430 mg/dayL, 520 mg/dayL for low, medium and high nitrogen groups respectively. The highest biomass concentration under low nitrogen regimes was 495 mg/l, compared with 994 mg/l and 1409 mg/l for medium and high nitrogen regimes shown in Figure 2. Other kinetic growth data including doubling time/generation time and division per day were also calculated. Doubling times were calculated as 1.84, 1.59, and 1.32 whereas division of cells per day was calculated as 0.54, 0.62, and 0.75 for low, medium and high nitrogen concentration groups respectively.

Biomass productivity is one of the most important parameters for the feasibility of utilizing algal oil for biodiesel production. Hence, numerous studies have been conducted in various algal species. Tang et al. (2011) demonstrated that *Dunaliella tertiolecta* had a highest biomass concentration of ~400 mg/l [20]. In another study conducted by Ho et al. (2010) the optimal biomass productivity of freshwater alga *Scenedesmus obliquus* were found to be 292.50 mg/dayL [21]. Griffiths et al. (2012) studied 11 different algal species including freshwater, marine and halotolerant species and demonstrated their biomass productivities [22]. Compared to the reported biomass productivities in previous studies, both the highest biomass concentration and average biomass productivity of isolated *Dunaliella salina* strain *Tuz\_KS\_01* showed very good potential, even though small batch cultivation process was utilized instead of using more sophisticated and efficient cultivation systems.

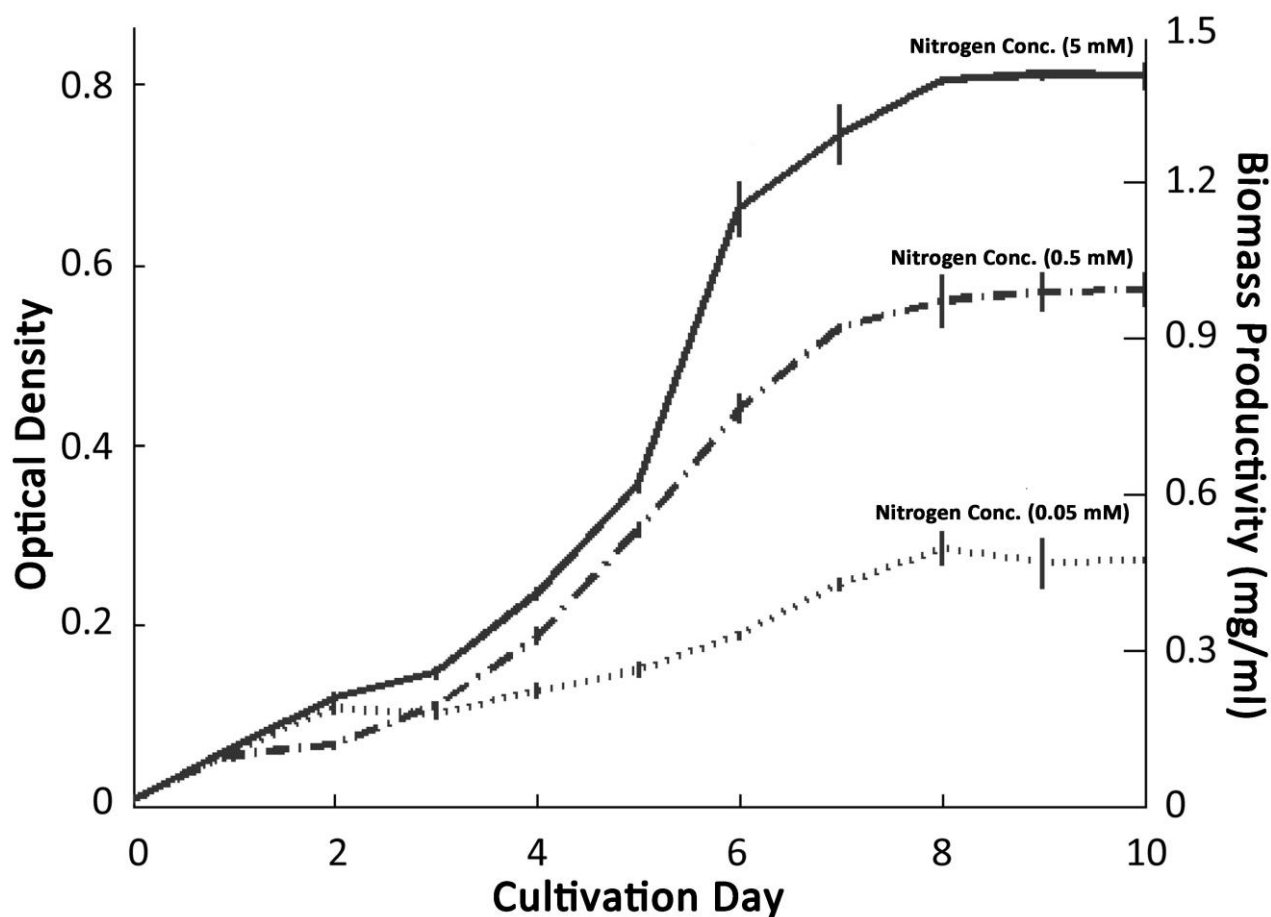


**Figure 2** Effects of different nitrogen concentrations on the growth and biomass productivity of *Dunaliella salina* strain *Tuz\_KS\_01* (GeneBank accession no. [JX880083](#)). 0.05 mM, 0.5 mM and 5 mM NaNO<sub>3</sub> are referred as low, medium and high nitrogen concentrations respectively. Shown OD<sub>600</sub> optical density and biomass values are the means of three replicates. The error bars correspond to  $\pm 1$  SD of triplicate optical density measurements.

### 2.3.3 Lipid accumulation analysis of the new *Dunaliella salina* strain under different nitrogen concentrations

Experimental groups were subjected to flow cytometric Nile red analysis for measuring lipid accumulation at single cell level in stationary growth phase. Cell populations were chosen according to cellular size and granulation as quantified by forward and side scatter values of populations, respectively which is demonstrated in Figure 3A. Figure 3B shows a representative flow cytometric analysis of lipid contents under different nitrogen

concentrations, indicating high lipid content under low nitrogen condition. Figure 3C shows the mean and standard error for three biological replicates, clearly exhibiting a negative relationship between lipid accumulation and nitrogen levels. Therefore, cultivation under low nitrogen conditions stimulates lipid accumulation in *Dunaliella salina* strain *Tuz\_KS\_01*, in agreement with previous studies [23,24].

In addition, we measured lipid accumulation of the green alga under different nitrogen levels using spectrofluorophotometer [25] at early-logarithmic, late-logarithmic and stationary growth phases. While the cellular lipid accumulation in early and late logarithmic phases did not show a drastic change, we observed a marked increase of lipid content in the stationary phase, which was significantly higher under low nitrogen cultivation conditions shown in Figure 3D.

Nitrogen depletion is well known to result in increased lipid accumulation in algal species [26], even though its association with other related factors has not been well defined. To demonstrate the oxidative stress under nitrogen limited cultivation conditions, fluorometric DCFH-DA and related TBARS lipid peroxidation assays were utilized. According to these results, increased ROS production (Figure 4A) and lipid peroxidation (Figure 4B) were both observed under nitrogen limited conditions, in association with increased lipid accumulation especially at stationary phase shown in Figure 4C.

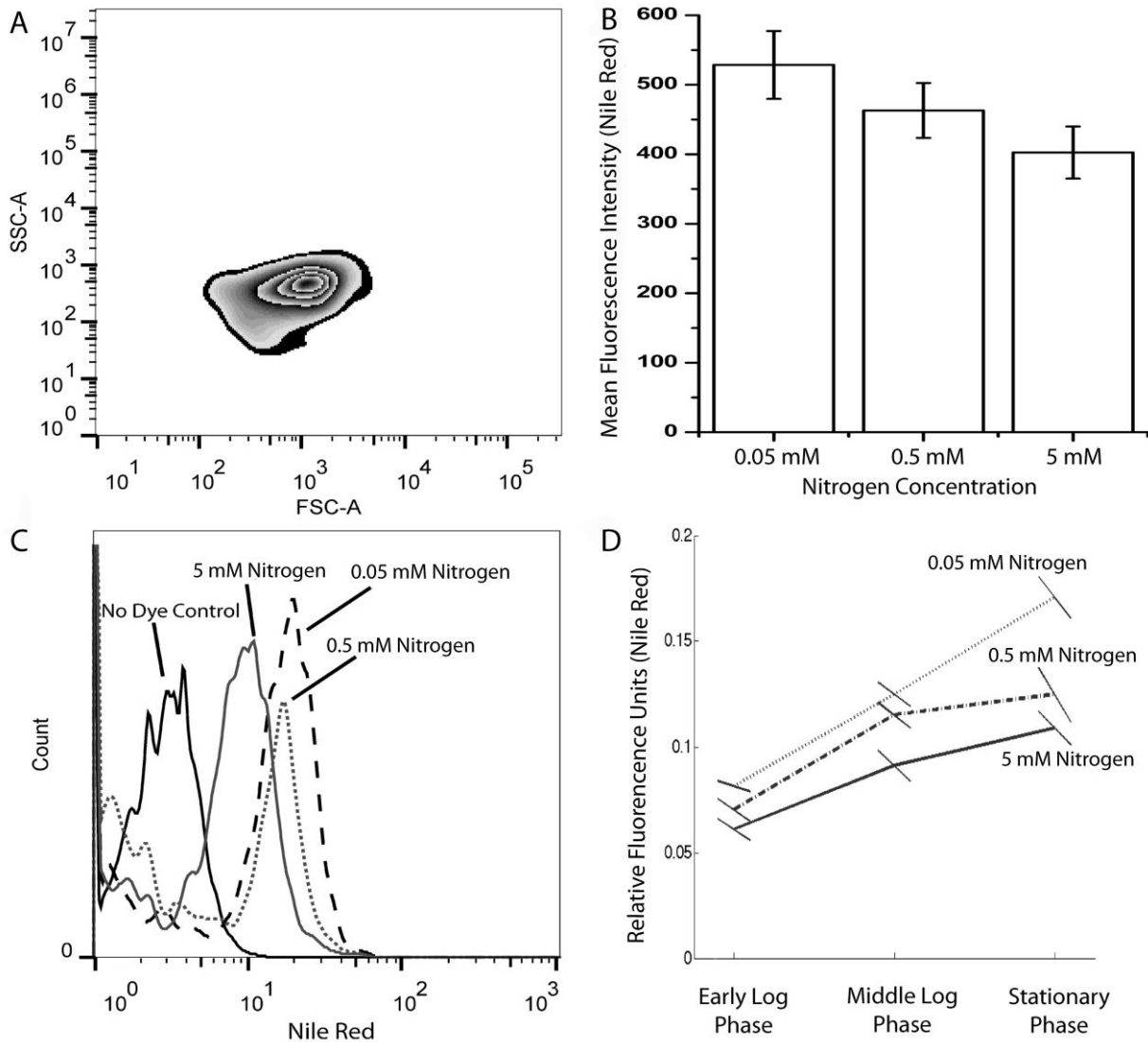


**Figure 3** Lipid content analysis of *Dunaliella salina* strain *Tuz\_KS\_01* under different nitrogen conditions. **A**) Zebra-plot of SSC (Side Scatter) and FSC (Forward Scatter) expressing cellular granulation and cellular size, respectively, under a representative nitrogen depletion condition (0.05 mM). **B**) A representative histogram of flow-cytometric analysis of lipid contents under different nitrogen concentrations **C**) Mean fluorescent intensities (MFI) of flow cytometric analysis. **D**) Fluorometric microplate Nile Red analysis of early logarithmic, late logarithmic and stationary growth phases. Data represent the mean values of triplicates. Standard error for each triplicate is shown as tilted lines for clarity, where the minimum and maximum y values of each line corresponds to  $\pm 1$  SE.

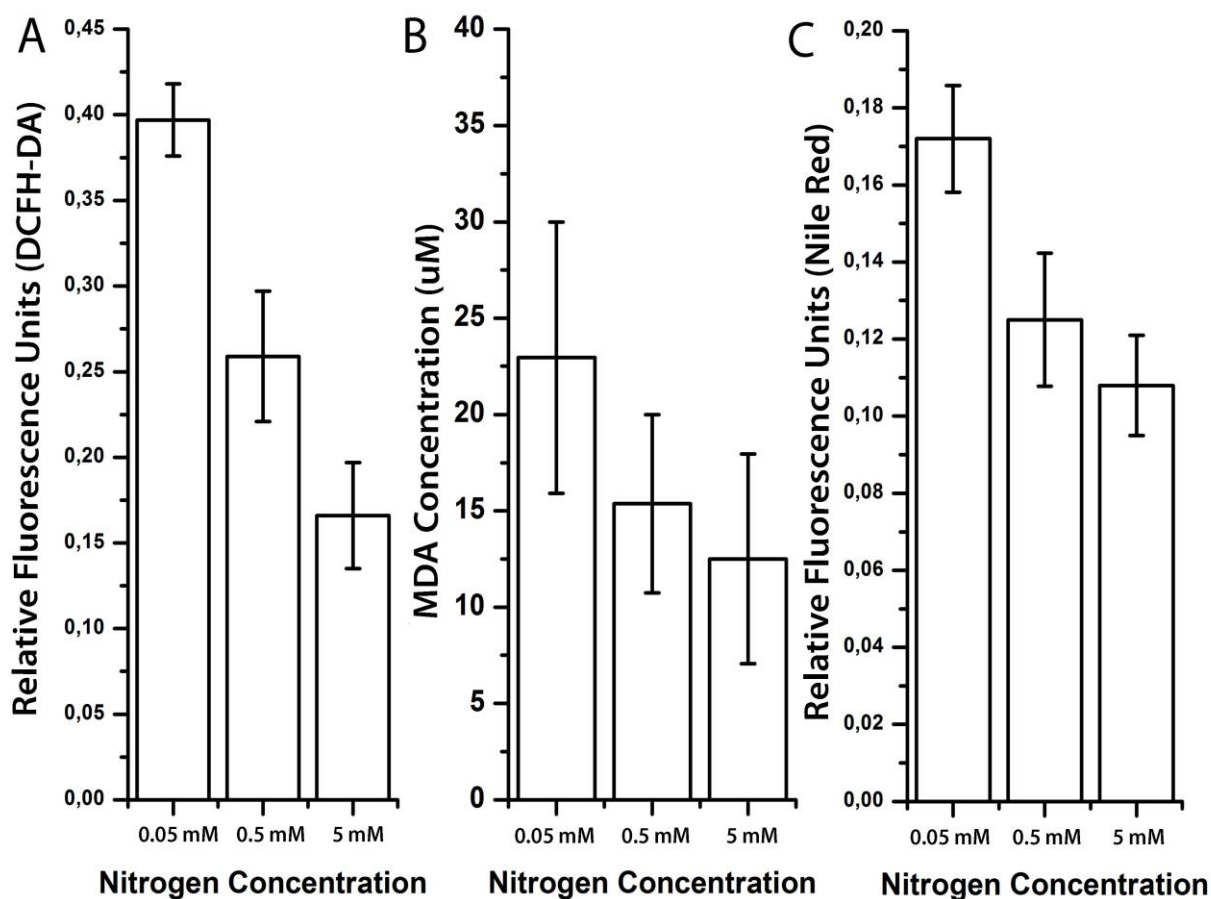


**Figure 4** Oxidative stress and lipid accumulation under different nitrogen concentrations. **A)** Fluorometric microplate DCFH-DA analysis under different nitrogen concentrations. **B)** TBARS analysis for lipid peroxidation under different nitrogen concentrations. **C)** Fluorometric microplate Nile-Red analysis under different nitrogen concentrations. Data represent the mean values of triplicates  $\pm$  1 SE.

#### **2.3.4 Antioxidant enzyme activities, pigment composition and protein analyses under different nitrogen concentrations**

ROS accumulation is prevented by a powerful intrinsic antioxidant system in photosynthetic organisms, involving enzymes such as superoxide dismutase (SOD), catalase (CAT), ascorbate peroxidase (APX) [37]. Next, we analyzed these three oxidative stress indicator antioxidant enzymes to demonstrate the effect of nitrogen depletion on the intracellular oxidative stress status as also supplementary to DCFH-DA measurements.

Intracellular SOD converts O<sub>2</sub><sup>-</sup> to O<sub>2</sub> and H<sub>2</sub>O<sub>2</sub>, acting as the first line of defence against oxidative stress [38]. We observed that SOD activity of cells increased under low nitrogen concentrations, especially at stationary growth phase. This data suggests that superoxides may be elevated under nitrogen depleted conditions, necessitating increased SOD activity (Figure 5A). CAT is a heme-containing enzyme that catalyzes the conversion of H<sub>2</sub>O<sub>2</sub> into oxygen and water [37]. APX is involved in the ascorbate-glutathione cycle occurring in chloroplasts, cytoplasm, mitochondria and peroxisomes [39]. We observed elevated levels of CAT and APX activity under nitrogen depleted conditions (Figure 5B, 5C). These data strongly indicate that oxidative stress is induced under nitrogen depletion in *Dunaliella salina* strain *Tuz\_KS\_01*.

Next, we analyzed the chlorophyll, carotenoid and protein content change in response to nitrogen depletion in *Dunaliella salina* strain *Tuz\_KS\_01*. Chlorophyll content is an indicator of both photosynthetic efficiency, rate and nitrogen [40] status. Carotenoids can perform an essential role in photoprotection by quenching the triplet chlorophyll and scavenging singlet oxygen and other reactive oxygen species [41]. We observed that chlorophyll A and B levels sharply declined in low nitrogen conditions, as expected (Figure 6A). In contrast, we observed no decrease in total carotenoid contents under nitrogen depletion conditions. This observation suggests that cells increase carotenoid content to overcome with oxidative stress induced by singlet oxygens, similar to SOD activity increase discussed above (Figure 6A).

Upon nitrogen starvation, algal cells reduce the synthesis of protein and nucleic acid synthesis and carbon flow is directed from protein synthesis to fatty acid and carbohydrate synthesis [42]. We found that neutral lipids increase while the protein content of algal cells was reduced under nitrogen depletion conditions (Figure 6B). This indicates that carbon flow direction is to fatty acid synthesis under nitrogen limitation at stationary phase, in accordance with the literature [43].

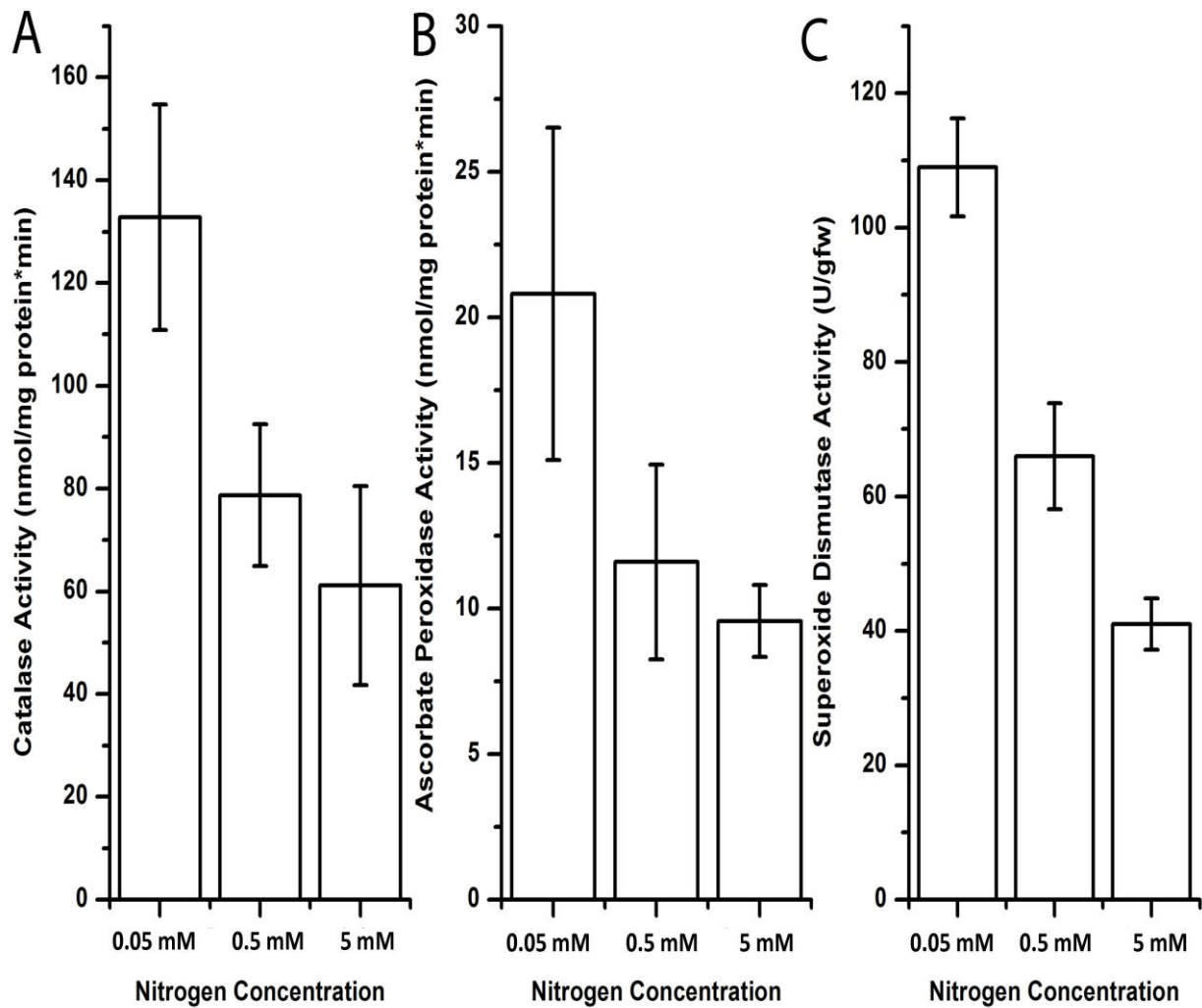


**Figure 5** Antioxidant enzyme activities under different nitrogen concentrations. **A-C)** Spectrophotometric enzymatic assays for catalase (CAT), ascorbate peroxidase (APX) and superoxide dismutase (SOD). Data demonstrate the mean values of triplicates  $\pm$  1 SE.

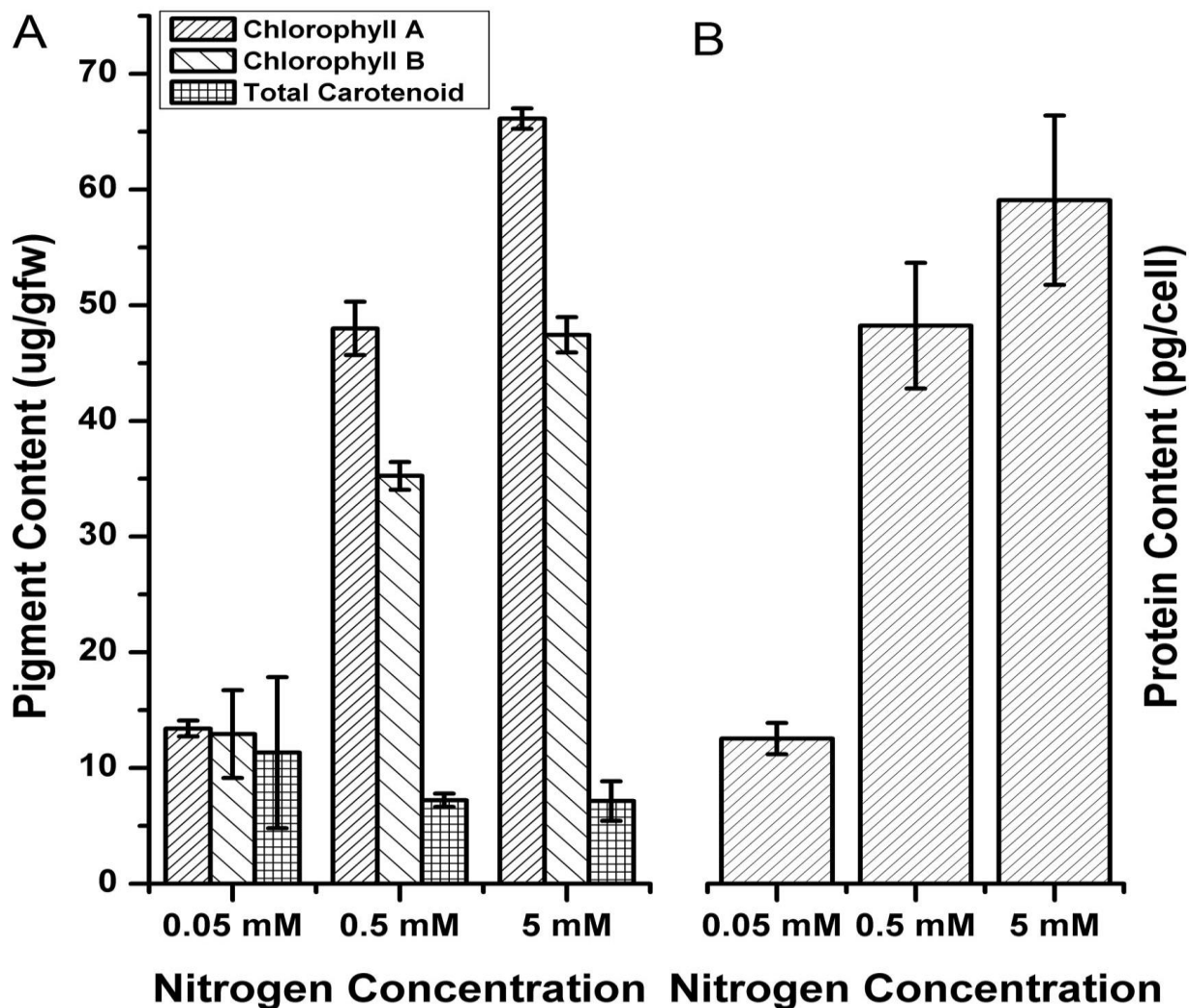


**Figure 6** Pigment and protein contents of *Dunaliella salina* strain under different nitrogen concentrations. **A)** Chlorophyll A, B and total carotenoid contents under different nitrogen concentrations. **B)** Protein contents of *Dunaliella salina* strain *Tuz\_KS\_01* cells cultivated under different nitrogen concentrations. Data demonstrate the mean values of triplicates  $\pm$  1 SE.

### 2.3.5 Reactive oxygen species (ROS) production induces lipid accumulation

Our analysis thus far hints that lipid accumulation might be partially triggered by ROS accumulation and oxidative stress under nitrogen depleted condition (Figure 4). In order to test this hypothesis, we used  $H_2O_2$ , a well-known oxidative stress inducer [44]. We treated cells at exponential growth phase in high nitrogen containing media (5 mM) with different concentrations of  $H_2O_2$  and we measured ROS, via using flowcytometric DCFH-DA method,

a robust fluorescent assay [45]. In addition, cell viability was measured by using FDA fluorescent assay while using Nile red staining method for determination of lipid contents under different H<sub>2</sub>O<sub>2</sub> concentrations. Although cellular size and granularity under H<sub>2</sub>O<sub>2</sub> treated conditions were similar to previous experimental conditions (Figure 7A and 3A), cell survival under higher H<sub>2</sub>O<sub>2</sub> concentrations were observed significantly reduced due to the oxidative stress induction (Figure 7B-7C). Although reduction of cell survival is to ~20% at 4 mM H<sub>2</sub>O<sub>2</sub> concentration, at this high concentration of H<sub>2</sub>O<sub>2</sub>, new isolate *Dunaliella salina* strain *Tuz\_KS\_01* showed highly tolerant characteristics to oxidative stress (Figure 7D).

Lipid accumulation of algae is known to increase by various factors including temperature, excessive light, and pH, which may also related to oxidative stress induced by ROS accumulation [33,46]. We used fluorometric Nile red analysis for analysis of lipid accumulation under different H<sub>2</sub>O<sub>2</sub> treatments. We observed increased lipid accumulation with increasing concentrations of H<sub>2</sub>O<sub>2</sub> (Figure 7E). This result supports that the lipid accumulation observed under nitrogen depletion conditions is at least partly mediated by oxidative stress. Importantly, this result also suggests a method for obtaining high lipid from green alga, namely by growing cells in high nitrogen (optimal) conditions followed by oxidative stress induction at stationary phase. Such a method may be economically more feasible than two stage reactors described above.

We next wished to visually observe the effect of nitrogen depletion and H<sub>2</sub>O<sub>2</sub> treatment on lipid accumulation. After cultivation, we collected and stained cells with Nile red and observed with fluorescence microscopy. We used three different conditions: 1) control, 2) 0.05 mM nitrogen and 3) 4 mM H<sub>2</sub>O<sub>2</sub>. Microscopy results were in strong agreement with our previous results, as lipid accumulation (increased size and number of cytoplasmic lipid droplets) after nitrogen depletion or H<sub>2</sub>O<sub>2</sub> treatment were higher than the control (Figure 8A-8B-8C).

Moreover, in order to validate the lipid increasing effect of nitrogen limitation and H<sub>2</sub>O<sub>2</sub> induced oxidative stress, solvent extraction gravimetric lipid analysis in nitrogen depleted (0.05 mM) and H<sub>2</sub>O<sub>2</sub> containing media (4 mM) were done. We found that, nitrogen limitation led to increased lipid accumulation up to 35%, and H<sub>2</sub>O<sub>2</sub> induced oxidative stress led to increased lipid accumulation up to 44% as shown in Figure 8D. We also measured the lipid content by Nile red fluorescence analysis for each of these conditions. Consistent with previous studies, we found that gravimetric and fluorometric measurements were correlated ( $r^2=0.82$ ) (Figure 8E) [17]. These data suggest that exogenously induced oxidative stress triggered by the application of H<sub>2</sub>O<sub>2</sub> resulted to increased lipid accumulation. Therefore, as

previously shown by the fluorometric analyses above, oxidative stress and increased lipid accumulation association is coupled under nitrogen limitation conditions. Induction of lipid accumulation by applying exogenous oxidative stress inducers such as H<sub>2</sub>O<sub>2</sub> may assist more effective lipid production compared with biomass production lowering nitrogen starvation strategy.

ROS production resulting from various stress factors is known to affect nearly all cellular processes by impairing the structural stability of functional macromolecules including DNA, proteins and structural lipids. Since the green algae life-cycle is reliant on its photosynthetic activity and cellular integrity, it is crucial to protect against oxidative stress. Otherwise cells cannot tolerate oxidative damage and eventually die [47-49]. Even though there is limited explanation about the correlation between ROS production and lipid accumulation in algae cultivated under nitrogen depleted conditions. Our results indicate that nitrogen depletion results in ROS accumulation and lipid peroxidation especially at stationary growth phase. This relationship might also be related to survival response of the alga against excessive oxidative stress conditions [7].

Although a few recent studies have suggested an association of ROS levels and cellular lipid accumulation [7, 8], underlying mechanistic principles are not clear. ROS is well demonstrated to modify cellular responses against different stressors in corresponding signal transduction pathways. ROS levels increase in microalgae cells when exposed to the different environmental stresses [9]. In a recent study, nitrogen depletion was shown to correlate with increased ROS accumulation and increased cellular lipid accumulation in a freshwater algae. This study showed that increased MDA concentration is an indicator of membrane peroxidation which implied increased ROS levels. It was suggested that H<sub>2</sub>O<sub>2</sub> induced exogenous oxidative stress was an effective factor for neutral lipid induction in *C. sorokiniana C3* [50].

Microalgae can modify its photosynthetic system under stress, resulting in a decrease in the gene expression of various proteins forming up the photosystem complexes I and II [51]. Such adjustments are thought to occur for minimizing oxidative stress via decreasing photosynthesis rate [52]. Nitrogen deprivation is closely associated with the degradation of ribulose-1, 5-bisphosphate carboxylase oxygenase to recycle nitrogen [53]. Degradation of this protein may result in alterations in photosynthesis rate, which is consistent with the observed decrease in chlorophyll content under nitrogen depleted condition [54]. As a result of decreased photosynthesis rate, overall anabolic reaction flux is severely constrained. In this

context, algae cells may favor storage of energetic molecules, such as lipids, instead of consumption.

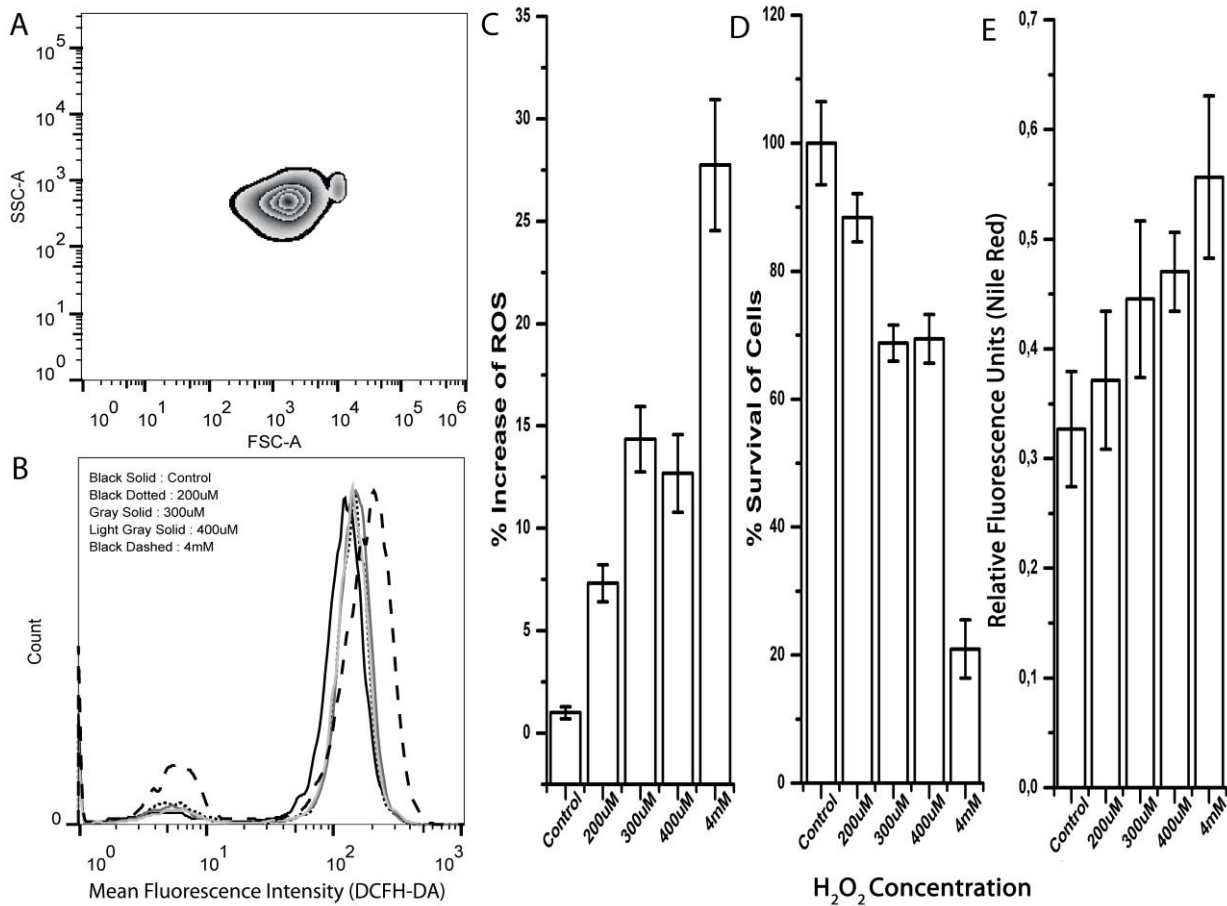


**Figure 7** Effect of H<sub>2</sub>O<sub>2</sub>, a known oxidative stress inducer, on *Dunaliella salina* strain *Tuz\_KS\_01*. **A)** Zebra-plot of SSC (Side Scatter) and FSC (Forward Scatter) expressing cellular granulation and cellular size under a representative H<sub>2</sub>O<sub>2</sub> condition (4 mM). **B)** Histogram of flow-cytometric analysis of ROS accumulation under different H<sub>2</sub>O<sub>2</sub> concentrations. **C)** Percentage increase of ROS production based on flow-cytometric DCFH-DA analysis. **D)** Fluorometric microplate fluorescent diacetate (FDA) survival analysis cultivated under different H<sub>2</sub>O<sub>2</sub> concentrations. **E)** Fluorometric microplate Nile-Red analysis under different H<sub>2</sub>O<sub>2</sub> concentrations. Data represent the mean values of triplicates ± 1 SE.

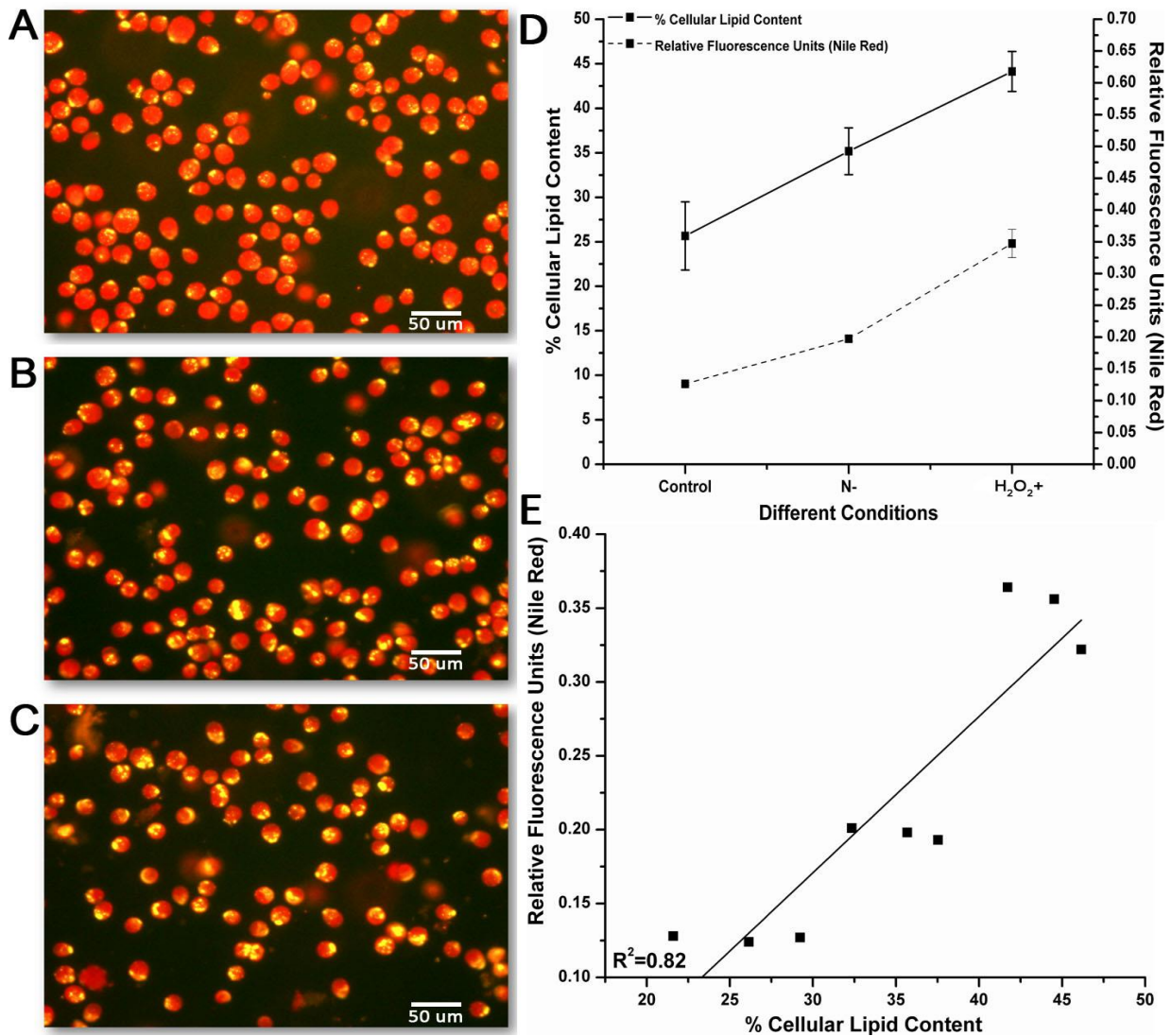


**Figure 8** Fluorescence microphotographs of *Dunaliella salina* strain *Tuz\_KS\_01* stained with Nile-Red fluorescence dye and screened under 400X magnification. **A)** Control group, 5 mM nitrogen concentration cultivation condition. **B)** Nitrogen limitation group, 0.05 mM nitrogen concentration cultivation condition **C)** Oxidative stress group, 4mM  $\text{H}_2\text{O}_2$  cultivation condition. Gravimetric lipid content analysis and Nile-Red fluorescence measurement correlation. **D)** Gravimetric and fluorometric Nile-Red lipid content analysis of *Dunaliella salina* strain *Tuz\_KS\_01* under 0.05 mM nitrogen and 4 mM  $\text{H}_2\text{O}_2$  cultivation conditions. Data represent the mean values of triplicates  $\pm 1$  SE **E)** Correlation plot of gravimetric and fluorometric Nile-Red lipid content analysis ( $r^2=0.82$ ).

### 2.3.6 Effects of H<sub>2</sub>O<sub>2</sub> Induced Oxidative Stress on Lipid Accumulation in *Dunaliella tertiolecta* and *Chlamydomonas reinhardtii*

Green algae, *Dunaliella tertiolecta* and *Chlamydomonas reinhardtii* were chosen for further investigation and confirmation of the H<sub>2</sub>O<sub>2</sub> induced oxidative stress effects on cellular lipid accumulation. We cultivated cells in high nitrogen containing media (5 mM) with different concentrations of H<sub>2</sub>O<sub>2</sub> as described for *Dunaliella salina* strain Tuz\_KS\_01. We measured ROS by using the DCFH-DA method, cell viability by using the FDA fluorescent assay, and lipid content by using the fluorometric Nile Red method, as described above. *Dunaliella tertiolecta* cells were found to be more tolerant to H<sub>2</sub>O<sub>2</sub>, therefore higher concentrations of H<sub>2</sub>O<sub>2</sub> were used to demonstrate the cellular response. *Chlamydomonas reinhardtii* cells were treated within the range from 200 μM to 4 mM H<sub>2</sub>O<sub>2</sub> concentrations while *Dunaliella tertiolecta* cells were treated within the range of 2 mM to 8 mM H<sub>2</sub>O<sub>2</sub> concentrations. As shown in Figure 9, we found that in response to H<sub>2</sub>O<sub>2</sub> in both species ROS accumulation and lipid contents increased, while cell survival dramatically decreased at high H<sub>2</sub>O<sub>2</sub> concentrations. In addition, by using flow cytometric analysis, we observed that lipid increase in response to oxidative stress was accompanied with increased granulation and biovolume in *Chlamydomonas* cells (Figure 10). Neither *Dunaliella tertiolecta* nor *Dunaliella salina* strain Tuz\_KS\_01 cells showed biovolume increase upon treatment of H<sub>2</sub>O<sub>2</sub> at any experimented concentration.

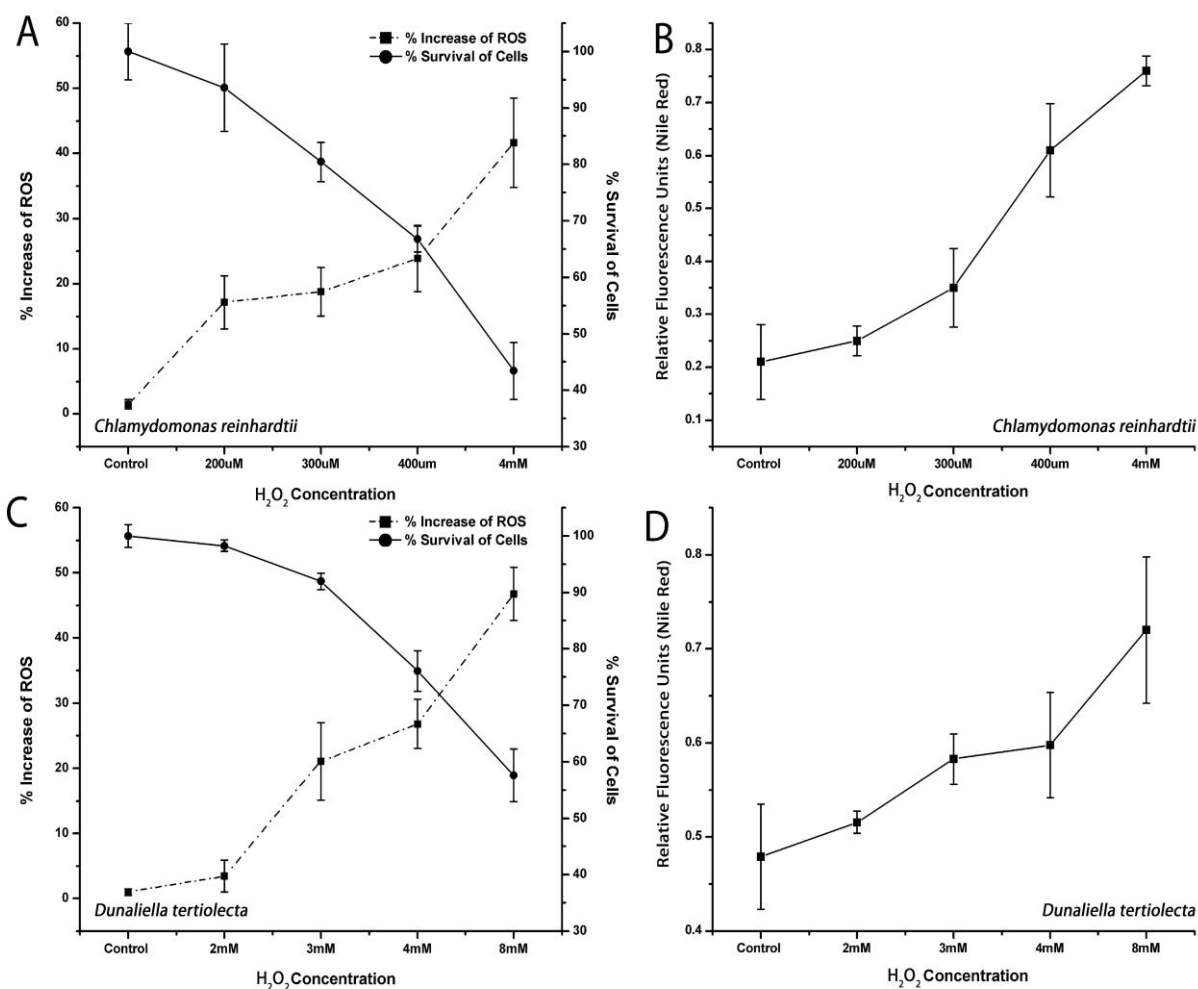


**Figure 9** Effect of H<sub>2</sub>O<sub>2</sub> induced oxidative stress on cellular lipid accumulation of different algae species. **A)** Fluorometric DCFH-DA and FDA analyses showing percentage change of ROS production and percentage change of cell survivability of *Chlamydomonas reinhardtii* cells cultivated under different H<sub>2</sub>O<sub>2</sub> concentrations. **B)** Fluorometric Nile red analysis showing the effect of different H<sub>2</sub>O<sub>2</sub> concentrations on cellular lipid accumulation of *Chlamydomonas reinhardtii* cells. **C)** Fluorometric DCFH-DA and FDA analyses showing percentage change of ROS production and percentage change of cell survivability of *Dunaliella tertiolecta* cells cultivated under different H<sub>2</sub>O<sub>2</sub> concentrations. **D)** Fluorometric Nile Red analysis showing the effect of different H<sub>2</sub>O<sub>2</sub> concentrations on cellular lipid accumulation of *Dunaliella tertiolecta* cells. Data represent the mean values of triplicates ± 1 SE.

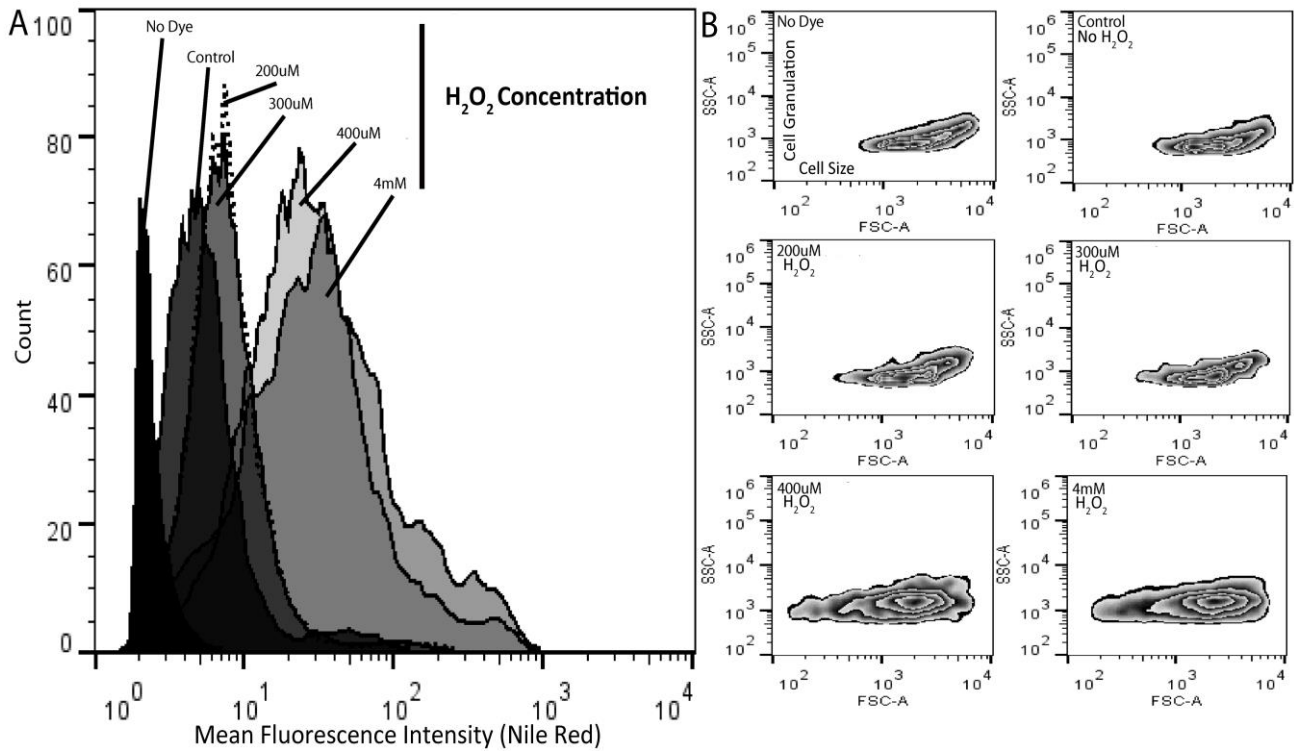


**Figure 10** Flow cytometric Nile red, cellular granulation and biovolume analysis of *Chlamydomonas reinhardtii* cells cultivated under different  $H_2O_2$  concentrations. **A)** A representative histogram of flow-cytometric analysis of lipid contents under different  $H_2O_2$  concentrations. **B)** Zebra-plot of SSC (Side Scatter) and FSC (Forward Scatter) expressing cellular granulation and cellular size, respectively, under different  $H_2O_2$  concentrations. Data represent the mean values of triplicates  $\pm 1$  SE.

## 2.4 Conclusions

Nitrogen depletion has been shown to be an effective inducer of lipid production of various unicellular green algae by previous studies. But few studies have examined the physiological and biochemical mechanisms underlying this response. In this study, we isolated a new halophilic green alga species. We presented evidence supporting previous observations that nitrogen depletion causes oxidative stress and lipid accumulation. In addition, we showed that oxidative stress by itself can cause lipid accumulation, suggesting

that lipid accumulation under nitrogen depletion is mediated by oxidative stress. These observations are helpful for utilization of green alga for biodiesel production.

## CHAPTER 3

### **Combinatorial Biotechnological Assessment and a New Strategy for Increasing Lipid Accumulation in Hyper Saline Algae by Applying Heavy Metal Induced Oxidative Stress**

#### **3.1 INTRODUCTION**

Bioremediation and biofuel technologies are the most important practices of algae biotechnology. However, crucial assessments of combinatory applications have not been done widely. Herein, we analyzed heavy metal bioadsorption potential of newly isolated hyper saline *Dunaliella* sp. and its lipid accumulation potential under high concentration heavy metal consisting cultivation conditions. The strain was found as a good heavy metal accumulator microalga. Moreover, interestingly we found that cultivation in heavy metal consisting media caused increased lipid accumulation in *Dunaliella* cells. As a mechanistic explanation for this phenomenon, we analyzed reactive oxygen species production under tested conditions. We demonstrated increased level of ROS accumulation along with increased malonaldehyde levels, an indicator of lipid peroxidation, in a parallel pattern of increased cellular lipid accumulation. Survival and metabolic analysis of *Dunaliella* cells suggest that its potential production in heavy metal contaminated saline systems is highly possible.

Marine waters are polluted by a variety of heavy metals due to increasing industrialization in coastal regions. Toxic effects of heavy metals pose serious problems for the ecosystem [1]. Industrial and mining effluents can contain extremely high concentrations of metals. Continued anthropogenic input of metals into marine environment has increased the concentrations of these metals to dangerous levels. Unlike other contaminants, metals persist without degradation and danger marine and saline ecosystems. In order to remediate contaminated water bodies, several methods are suggested such as ion-exchange, membrane filtration, chemical precipitation, and reverse osmosis. However, all of these methods present some disadvantages varying from relatively high application costs to various secondary risks

to the environment [2]. Therefore, utilization of bioremediation technologies instead of conventional counterparts become indispensable [3]. There exist various reports on bioaccumulation of heavy metals by mostly freshwater and several marine microalgae species. Marine diatome, *Phaeodactylum tricornerutum* has been reported to uptake  $\text{Cd}^{2+}$  from saline waters [4]. Another study showed that the unicellular green alga *Chlamydomonas reinhardtii* accumulates  $\text{Cu}^{2+}$  and  $\text{Pb}^{2+}$  using different metal uptake mechanisms and accumulates heavy metals efficiently [5]. Similarly, marine brown algae *Laminaria japonica* has been demonstrated to effectively bioaccumulate  $\text{Cd}^{2+}$ ,  $\text{Cu}^{2+}$ ,  $\text{Ni}^{2+}$ , and  $\text{Zn}^{2+}$  ions from aqueous solutions [6]. However, most of the studies have been conducted with freshwater algae species. Marine or hypersaline microalgae species are also crucial to be assessed in terms of their bioaccumulation potentials of heavy metals since marine and saline water bodies are also important subjects to remediation practices.

Another important biotechnological field which microalgae are considered to be beneficial is renewable energy industry. Extensive research confirms that microalgae oil, a powerful candidate of biodiesel feedstock may replace fossil fuels [7,8]. Herein, a further goal to integrate microalgae oil production and bioremediation is also possible. Recent survey suggests that biodiesel production from algae can be integrated with bioremediation. Therefore, water pollution can be minimized and high yield of biodiesel could be obtained using microalgae species [9]. However, limited number of empirical studies have assessed the feasibility of algae production in a combinatory aspect which subjects both bioremediation, algal growth/biomass production and lipid accumulation. Thus, we set our major aim to fill in the gap within this important biotechnological research field.

Various microalgae species have been studied for the assessment of their capability to produce lipids. Of all these, *Dunaliella* species were reported to yield oil with high quantities [10]. In addition, the ease of their cultivation even in marine or saline systems, and their strong resistance characteristics to extreme salinity and temperature conditions make the species favourable for biodiesel production [11]. In the light of above, *Dunaliella* species may demonstrate a good potential in combination of biofuel production and bioremediation processes especially in unusable saline systems.

In photosynthetic organisms, several peroxidases and oxidases can be activated in response to various environmental stresses including heavy metal exposure. This enzymatic activation can generate reactive oxygen species (ROS). Metabolic processes including lipid synthesis might be affected by increasing intracellular ROS levels [12-14]. In the light of above, effects of heavy metal inducing oxidative stress on cellular lipid accumulation in the

hypersaline green alga *Dunaliella sp.* were evaluated along with its bioaccumulation potentials of  $\text{Cu}^{2+}$ ,  $\text{Ni}^{2+}$ , and  $\text{Zn}^{2+}$  in order to evaluate possible combination of bioremediation and biodiesel feedstock, lipid production in a pilot study. Thereby, the saline algae species may have a good potential in bioremediation and biofuel production in a combinatory process.

## **3.2 Materials and Methods**

### **3.2.1 Organism and Culture Conditions**

The alga used in this study was isolated from the hypersaline lake “Tuz”, which is located in the Middle Anatolia, Turkey. Collection of water samples was done and isolation location was recorded by using a GPS device as  $39^{\circ}4'23.97''\text{K}$  -  $33^{\circ}24'33.11''\text{E}$  in the southern east part of Sereflikochisar province. 10 ml water samples were collected and enriched with the same volume of Bold's Basal Medium (BBM) modified by addition of 5% NaCl. BBM was pH 7.4 and consisted of 5 mM  $\text{NaNO}_3$  along with  $\text{CaCl}_2 \cdot 2\text{H}_2\text{O}$  0.17 mM,  $\text{MgSO}_4 \cdot 7\text{H}_2\text{O}$  0.3 mM,  $\text{K}_2\text{HPO}_4$  0.43 mM,  $\text{KH}_2\text{PO}_4$  1.29 mM,  $\text{Na}_2\text{EDTA} \cdot 2\text{H}_2\text{O}$  2 mM,  $\text{FeCl}_3 \cdot 6\text{H}_2\text{O}$  0.36 mM,  $\text{MnCl}_2 \cdot 4\text{H}_2\text{O}$  0.21 mM,  $\text{ZnCl}_2$  0.037 mM,  $\text{CoCl}_2 \cdot 6\text{H}_2\text{O}$  0.0084 mM,  $\text{Na}_2\text{MoO}_4 \cdot 2\text{H}_2\text{O}$  0.017 mM, Vitamin B12 0.1 mM and 5 mM  $\text{NaCO}_3$  was supplied as carbon source.

Water samples were plated on petri dishes with modified BBM 5% NaCl and 1% bacteriological agar, besides the same water samples were also subjected to dilutions with fresh modified BBM 5% NaCl in 48-well plates (1:2, 1:4, 1:8, 1:16, 1:32, 1:64) to obtain monocultures. After 2 and 4 weeks cultivation periods of 48-well plate liquid cultures and agar plates, respectively, clones were isolated. These clones were transferred to fresh mediums in 100 ml canonical flasks in a final volume of 25 ml for obtaining cell stocks at 25 °C under continuous shaking and photon irradiance of 80 rpm and  $150 \mu\text{Em}^{-2}\text{s}^{-1}$ .

All experiments were carried out under same cultivation conditions in 250 ml batch cultures with different heavy metals. 5 ppm Cu(II), 10 ppm Zn(II) and Ni(II) concentrations were used for the experiments.

### **3.2.2 Isolation and Purification of DNA and Amplification of 18S rRNA Encoding Gene**

DNA isolation was done by using DNeasy Plant Mini Kit (Qiagen) as instructed by the manufacturer. Quantification of the genomic DNA obtained and assessment of its purity was done on a Nanodrop Spectrophotometer ND-1000 and on 1% agarose gel electrophoresis. MA1 [5'-CGGGATCCGTAGTCATATGCTTGTCTC-3'] and MA2 [5'-GGAATTCCTTCTGCAGGTTTACC-3'] were designed from 18S rDNA genes and were previously reported by Olmos et al (Olmos, Paniagua, Contreras, 2000). PCR reactions were carried out in a total volume of 50 µl containing 50 ng of chromosomal DNA in dH<sub>2</sub>O and 200 ng MA1 and MA2 conserved primers. The amplification was carried out using 30 cycles in a MJ Mini™ Personal Thermal Cycler (BioRad), with a T<sub>m</sub> of 52°C for all reactions. One cycle consisted of 1 minute at 95°C, 1 minute at 52°C and 2 minutes at 72°C.

### **3.2.3 Sequencing and Phylogenetic Analysis**

MA1–MA2 PCR products were utilized to carry out sequencing reactions after purification with a QIAquick PCR purification kit (Qiagen). The sequencing reactions were run by MCLAB (San Francisco, CA), employing primers MA1–MA2 in both reverse and forward directions. DNA sequences were imported to BLAST for identification and to search for phylogenetic relationship correlations between other known 18S rDNA gene sequences of related species/strains deposited in NCBI Gene Bank.

### **3.2.4 Adsorption Experiments and Analysis**

Experiments for the effect of varied pH on adsorption efficiency were carried out by adjusting pH values of 5 mg/L Cu(II), 10 mg/L Zn(II) and Ni(II) solution from 5 to 9 with the addition of 2.25 mg/ml cell concentration. The pH of solutions was adjusted to specified values with diluted HCl or NaOH, and the mixtures were shaken in an incubator shaker at 100 rpm mixing rate for 96 h at 25 °C. At the end of the experiment, the solution was separated from the cell adsorbent by using 0.22 µm PVDF membrane filter. In kinetic experiments, 100 mL of 5 mg/L Cu(II), 10 mg/L Zn(II) and Ni(II) solutions with 2.25 g/L wet algae biomass as adsorbent material at pH 7 were used and sampled at different time intervals. Heavy metal concentrations of the solutions were measured with a Varian, Vista-Pro CCD simultaneous

inductively coupled plasma ICP-OES spectrophotometer. Samples before and after adsorption experiments were analyzed to obtain residual heavy metal concentrations. Each adsorption experiment in the present study was repeated three times and average values were reported below.

### **3.2.5 Growth Analysis**

The optical densities of the cultures cultivated with different heavy metals was determined under wavelength 600 nm against non-treated control group. Growth was also measured by using fluorescein diacetate (FDA) vital staining (Sigma, USA) by using spectrofluorometric method as described below for Nile Red staining. Experiments were done in triplicates and data are shown with standard error.

### **3.2.6 Fluorometric Microplate Analysis for Determination of Lipid and Reactive Oxygen Species Accumulation**

A stock solution of Nile Red (NR) (Sigma, 72485) was prepared by adding 5 mg of NR to 10 ml of acetone. The solution was kept in a dark colored bottle and stored in the dark at -20°C. 1 ml of algal cells from a culture of 250 ml glass erlenmeyer flasks containing 100 ml growth media with different heavy metals were transferred to 1.5 ml eppendorf tubes for 5 min centrifugation at 5,000 rpm, washed twice with fresh medium, and measured in a spectrophotometer at 600 nm. Each sample was adjusted to an OD<sub>600</sub> of 0.3 in a 1 ml final volume by dilution with fresh medium. 5 µl of Nile Red solution was added to each tube and mixed well, followed by 20 min incubation in the dark. Finally, cellular neutral lipids were quantified using a 96-well microplate spectrofluorometry (SpectraMAX GEMINI XS) with an excitation wavelength of 485 nm and an emission wavelength of 612 nm.

Determination of ROS production related to oxidative stress was done by using DCFH-DA (Sigma, USA). 0.5 mg/mL stock solutions for the stains were prepared in acetone and the same protocol was used for FDA (Sigma, USA) and DCFH-DA (Sigma, USA) staining as described above for Nile Red staining. Data were recorded as relevant fluorescence units for all spectrofluorometric staining experiments.

### **3.2.7 Flow Cytometric Analysis for Determination of Lipid and Reactive Oxygen Species Accumulation**

5 µl of Nile Red (Sigma, USA) from stock solution (0.5 mg/mL) was added to 1 ml of a cell suspension at an OD<sub>600</sub> of 0.3 after washing cells twice with fresh medium. This mixture was gently vortexed and incubated for 20 minutes at room temperature in dark. Nile Red uptake was determined using a BD-FACS Canto flow cytometer (Becton Dickinson Instruments) equipped with a 488 nm argon laser. Upon excitation by a 488 nm argon laser, NR exhibits intense yellow-gold fluorescence when dissolved in neutral lipids. The optical system used in the FACS Canto collects yellow and orange light (560–640 nm, corresponding to neutral lipids). Approximately 10,000 cells were analysed using a log amplification of the fluorescent signal. Non-stained cells were used as an autofluorescence control. Nile Red fluorescence was measured using a 488 nm laser and a 556 LP+585/42 band pass filter set on a FACS Canto Flow Cytometer. Data were recorded as mean fluorescence intensity (MFI).

DCFH-DA (Sigma, USA) from stock solution (0.5 mg/ml) was used as described for Nile Red staining. Nonfluorescent DCFH-DA is taken up and converted into dichlorodihydrofluorescein (DCF) by the action of cellular esterases. Fluorescence from oxidized DCF was measured using a 488 nm laser and a 556/Long Pass filter set on a BD-FACS Canto Flow Cytometer. Data were expressed as mean fluorescence intensity (MFI). The data of both staining methods were evaluated using Flowjo Ver. 7.6.1 (Tree Star, Inc.).

### **3.2.8 FT-IR spectroscopy**

For FT-IR spectroscopy, heat dried biomasses of different heavy metal treated samples were taken from each replicate of experimental groups against non-treated control group. Spectra were collected over the wavenumber range 4000–600 cm<sup>-1</sup>. Each sample was analysed in triplicate. Spectra were baseline corrected using the automatic baseline correction algorithm (Dean et al. 2010).

### **3.2.9 Protein, Chlorophyll, Carotenoid, TBARS Analyses and Fluorescence Microscopy**

Total protein isolation was done according to Barbarino et al (Barbarino, Lourenco, 2005). Protein content was determined following the method described by Bradford (Bradford, 1976). Cellular chlorophyll and carotenoid isolations were done using the

methanol extraction method. Calculation of chlorophyll and carotenoid contents were carried out using the formula for methanol extraction described by Wellburn (Wellburn, 1994). Lipid peroxidation analysis upon different nitrogen concentration regimes was analysed by using thiobarbituric acid reactive substances (TBARS) method as described (Sabatini, 2009). For fluorescence microscopy analysis of oxidative stress, cells were stained with 5µl, 0.5mg/mL DCFH-DA (Sigma, USA) stock solution after fixing cells with 5% paraformaldehyde and imaged by epi-fluorescence microscopy with a Leica DMR microscope using a 490nm excitation/530nm emission wavelength filter cube (Leica Microsystems).

### **3.3 Results and Discussion**

#### **3.3.1 Isolation and identification of the new *Dunaliella* strain**

We isolated a new hypersaline microalgae strain from salt lake located in the Middle Anatolia region of Turkey in July 2011. The microalga, which is unicellular, biflagellate was found to be tolerant up to 20% NaCl similar to *Dunaliella* species.

The strain was deposited at -196 °C ultra-freeze conditions at Sabanci University algae culture collection under the name of *Dunaliella sp. Tuz KS\_02*. Molecular identification was based on 18S rDNA gene sequence amplification and sequencing. A single 18S rDNA PCR amplicon was about ~1800 bp in size, in accordance with previous studies. [15]. The partial sequence of the 18S rDNA encoding gene was submitted to National Center for Biotechnology Information (NCBI) GeneBank database as *Dunaliella sp. Tuz KS\_02* (accession number of JX880082). According to Basic Local Alignment Search Tool (BLAST) analysis, the isolated sequence showed very high percentage of identity with other deposited 18S rDNA sequences of *Dunaliella* species. Molecular identification showed high percentage identity to *Dunaliella salina* (Identity 92%, Query Coverage 96%) in accordance with the high morphological identity. The position of *Dunaliella sp. Tuz Lake KS\_02* relative to other *Dunaliella salina* strains deposited in NCBI GeneBank can be seen in Figure 1.

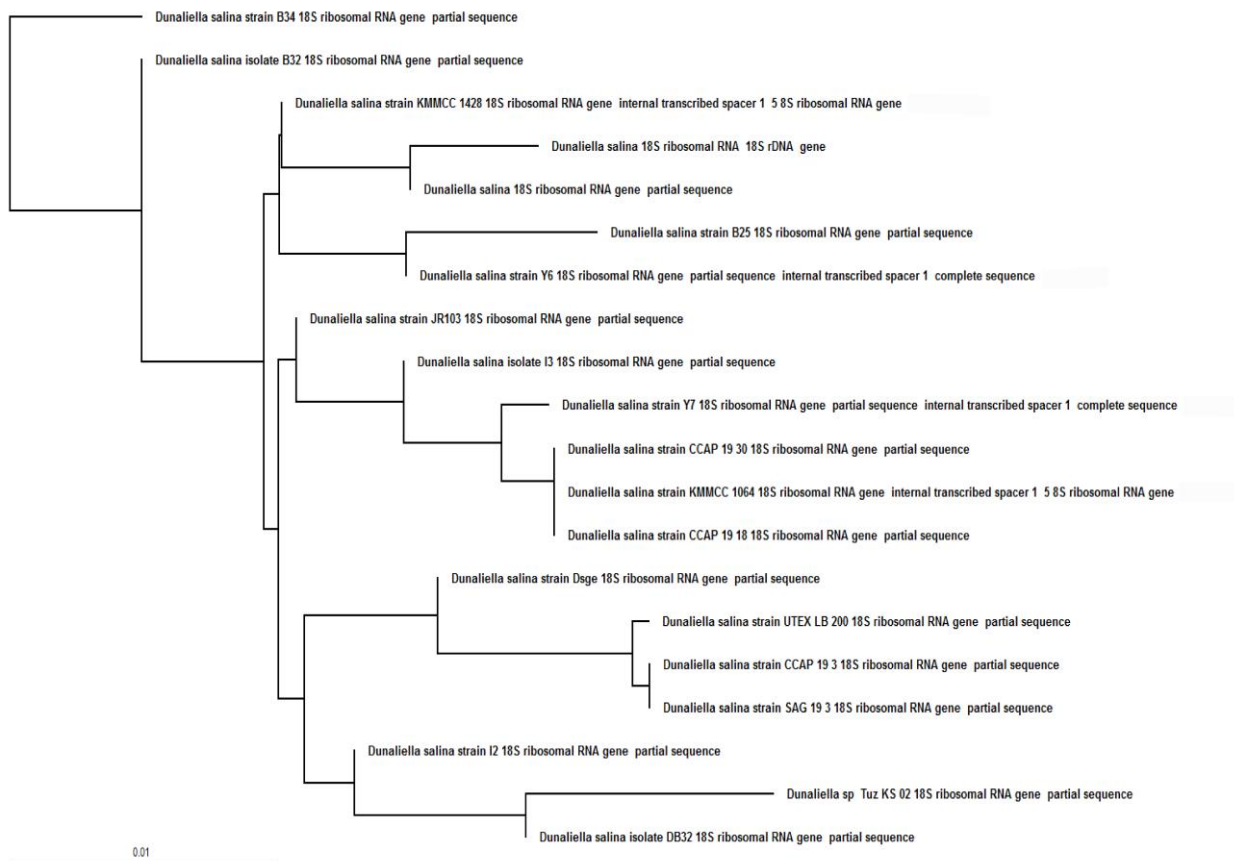


**Figure 1** Phylogenetic analysis of *Dunaliella sp. Tuz Lake KS\_02* (GeneBank accession no. JX880082). Dendrogram was generated using the neighbor-joining analysis based on 18S rDNA gene sequences. The phylogenetic tree shows the position of *Dunaliella sp. Tuz KS\_02* relative to other *Dunaliella salina* strains deposited in NCBI GeneBank.

### 3.3.2 Heavy metal adsorption by *Dunaliella sp. Tuz KS\_02*

In order to assess bioremediation potential of the newly isolated *Dunaliella* strain, we performed kinetic experiments. The effect of pH is one the most important factors for metal adsorption onto both organic and inorganic surfaces. Therefore we first experimented the pH effect. The effect of media pH on metal adsorption process is shown in Figure 2a. The highest adsorption of each heavy metal with *Dunaliella sp. Tuz KS\_02* was obtained at higher pH values which are also favorable for proper algae growth. This is probably related to the degree of protonation of the binding sites on the membrane surface of *Dunaliella* cells. Moreover, the lower number of H<sup>+</sup> and greater number of surface groups with negative charges resulted to stronger interaction with the heavy metals at higher pH conditions which is in concordance

with the fact that cellular membrane surfaces are mostly negatively charged. At lower pH values heavy metal ions found less chance to form a complex with the adsorbent surfaces due to the competition with hydrogen and heavy metal ions for the adsorption sites. On the other hand, there was certain decrease in the adsorption capacities of Cu (II), Zn (II) and Ni (II) from pH 8.0 to 9.0 and this decrease could be attributed to the precipitation of heavy metals copper, lead and zinc at pH 9.0. Hence, the adsorptions observed at pH >8 were due to the combined process of adsorption and precipitation of metal ions. From this point, in order to achieve both high efficiency of metal adsorption and biomass productivity pH 7.0 was selected for subsequent work.

The kinetic profiles of Cu (II), Zn (II), and Ni (II) were illustrated in Figure 2b-2c suggested that the adsorption of Cu(II), mainly took place within the first 2h, followed by a slow increase of adsorption until the equilibrium was reached. However, the substantial increase in the adsorption of Zn (II) and Ni (II) were observed when contact time was increased from 2 to 24h and the maximum uptakes were obtained at 24h of contact.

In order to determine sorption kinetics, four kinetic models were studied by applying the experimental sorption data to the pseudo-first-order equation (Eq. (1)) [16], the pseudo-second-order equation (Eq. (2)) [17], the Elovich equation (Eq. (3)) [18] and intraparticle diffusion (Eq. (4)) [19].

$$\log(q_e - q_t) = \log(q_e) - \frac{k_1}{2.303} t \quad (1)$$

$$\frac{t}{q_t} = \frac{1}{k_2 q_e^2} + \frac{t}{q_e} \quad (2)$$

$$q_t = \frac{1}{b} \ln(ab) + \frac{1}{b} \ln(t) \quad (3)$$

$$q_t = k_{int} t^{0.5} + C \quad (4)$$

where,  $q_t$  is the amount of adsorbed contaminant (mg/g) at time  $t$ ,  $q_e$  is the maximum adsorption capacity (mg/g) for the pseudo-first-order adsorption and pseudo-second-order adsorption,  $k_1$  is the pseudo-first-order rate constant for the adsorption process (1/min),  $k_2$  is the pseudo-second-order rate constant (g/mg.min), constant  $\alpha$  (mg/(g.min)) is the initial adsorption rate,  $\beta$  (g/mg) is related to surface coverage, and  $k_{int}$  is the constant for the particle

diffusion rate ( $\text{mg/g}\cdot\text{min}^{1/2}$ ). The fitting ability of kinetic and adsorption models were analyzed according to the normalized standard deviation,  $s$ , (Eq. (5)) given in below:

$$s = \sqrt{\frac{\sum_{i=1}^n \left( \frac{q_{\text{exp}} - q_{\text{cal}}}{q_{\text{exp}}} \right)^2}{n-1}} \times 100 \quad (5)$$

Where  $n$  is the number of data points. The subscripts “exp” and “calc” show the experimental and calculated values. Error function was employed in this study to find out the most suitable isotherm model to represent the experimental data. Small values of the normalized standard deviation represent better fits of the model to the data. The sorption modeling parameters and  $s$  values were summarized in Table 1.

Previous studies show that in most cases of biosorption pseudo-second-order equation fit better for the whole range of contact times than the pseudo-first-order. The experimental kinetics of Cu (II), Zn (II), and Ni (II) showed better fit to the pseudo-second-order model and this agreement was corroborated by high  $R^2$  value in Table 1. The consistency of the experimental data with the pseudo-second-order kinetic model indicates that the adsorption of Cu (II), Zn (II), and Ni (II) was controlled by chemical adsorption involving valence forces through sharing or exchange electrons between sorbent and sorbate [16]. On the other hand, the higher  $R^2$  values found in the Elovich model for Zn (II) indicated that the adsorbing surface was heterogenous and therefore exhibited different activation energies for chemisorptions. For comparison purposes, kinetic data were also evaluated using the intraparticle diffusion equation. The intraparticle diffusion can be considered as the rate-determining step, if the linearized curve passes through the origin (0, 0). Although, the obtained  $R^2$  values were comparably high with the pseudo-second-order model for all three adsorbates, the results of fitting did not pass through the origin (0, 0) interpreting that intraparticle diffusion was not the rate-determining step in the adsorption processes. Such a finding was similar to that made in previous works on adsorption [20]. According to the results in Table 1 obtained from the above kinetic studies and based on the  $R^2$  and the normalized standard deviation values considering the entire contact time for the heavy metal ions, it can be concluded that the pseudo-second-order is the adsorption kinetics.

Bioadsorption and removal potentials of redundantly released heavy metals, Cu (II), Zn (II), and Ni (II) from various industrial processes have been subjected by several studies [21]. Sustainable and environmental friendly removal of such metals from water bodies is still an important subject. In this study, the data obtained from the analysis of heavy metal

adsorption of *Dunaliella sp. Tuz KS\_02* demonstrated a good removal potential along with a good biomass productivity due to its highly tolerant nature. This observation strongly suggests that the experimented hypersaline species can be cultivated in heavy metal contaminated secondary effluent of bioremediation process, especially in saline systems. Therefore, two important biotechnological practices can be processed in a combinatory way. Saline water bodies can be remediated and most importantly high biomass production of hypersaline green alga for producing byproducts in various biotechnological industries can be easily achieved.

<b>Model</b>	<b>Parameters</b>	<b>Cu(II)</b>	<b>Ni(II)</b>	<b>Zn(II)</b>
<i>Pseudo First Order</i>	$k_1(1/min)$	0.127	0.132	0.018
	$q_{e1}(mg/g)$	0.568	2.397	2.705
	$R^2$	0.831	0.994	0.978
	$s$ (%)	0.732	0.389	0.781
<i>Pseudo Second Order</i>	$k_2(g/mg.min)$	0.617	0.085	0.080
	$q_{e2}(mg/g)$	1.277	3.224	3.439
	$R^2$	0.996	0.997	0.997
	$s$ (%)	0.147	0.129	0.087
<i>Elovich Equation</i>	$\beta$ (g/mg)	4.277	2.174	1.471
	$\alpha$ (mg/g.min)	1.793	1.554	2.343
	$R^2$	0.858	0.991	0.996
	$s$ (%)	0.203	0.249	0.158
<i>Intraparticle Diffusion</i>	$k_{int}(mg/g.min^{1/2})$	0.186	0.573	0.601
	$R^2$	0.661	0.954	0.944
	$s$ (%)	0.335	0.457	0.448

**Table 1.** The kinetic sorption modelling parameters of Cu (II), Ni (II) and Zn (II) on the *Dunaliella sp. Tuz KS\_02*.

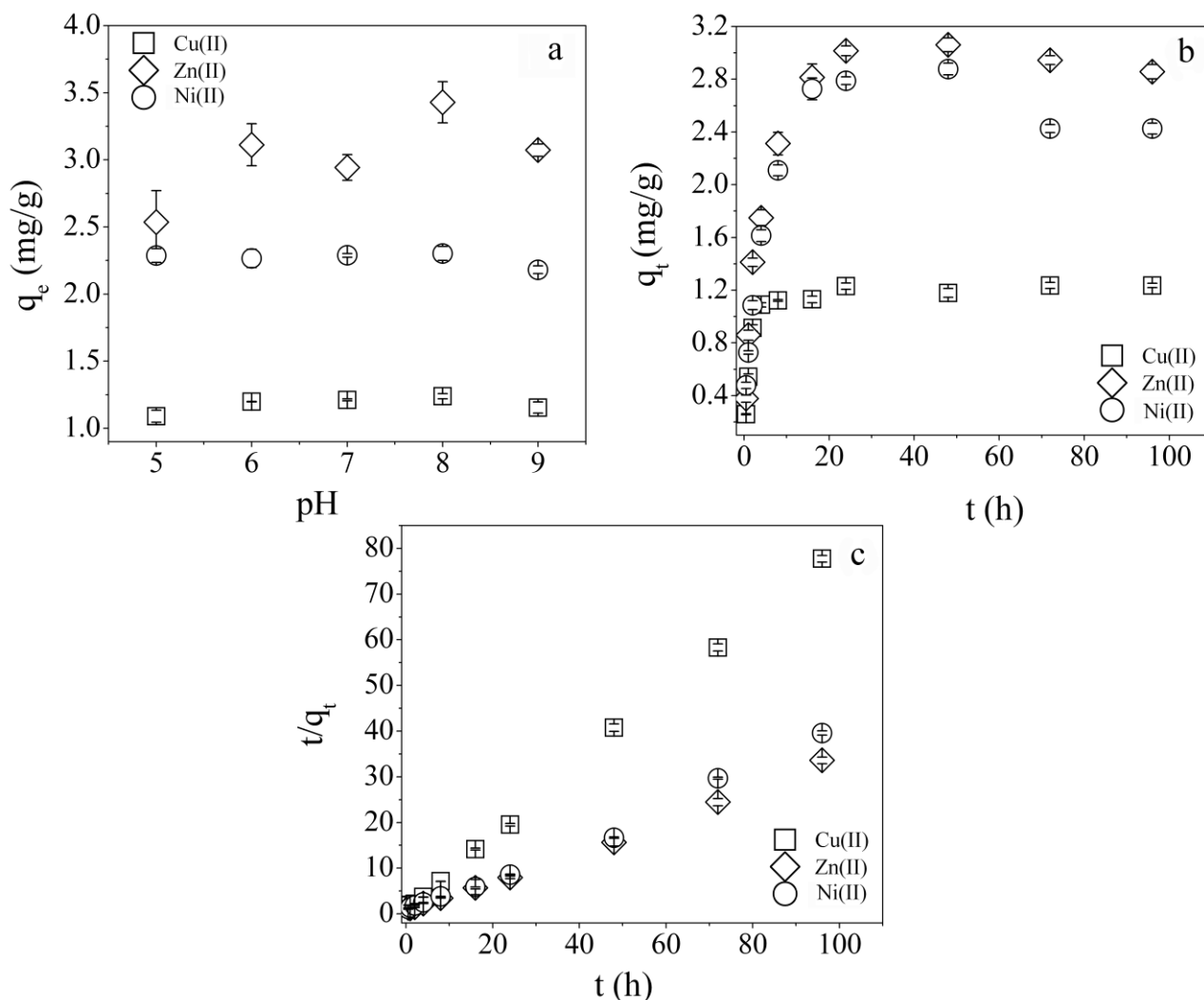


**Figure 2** Heavy metal sorption analyses of *Dunaliella sp. Tuz KS\_02* a) Effect of pH on the sorption of Zn(II), Cu(II), and Ni(II) b) Kinetic modeling of sorption of Zn(II), Cu(II), and Ni(II) onto the *Dunaliella sp. Tuz KS\_02* c) The pseudo-second-order kinetic model for the sorption of Zn(II), Cu(II), and Ni(II) onto the *Dunaliella sp. Tuz KS\_02*. The error bars correspond to  $\pm 1$  SD of triplicates.

### 3.3.3. Growth analysis of the new *Dunaliella sp. Tuz KS\_02* strain under Cu (II), Zn (II), Ni (II) consisting cultivation conditions

The new halotolerant green algae was cultivated with experimented heavy metals, Cu (II), Zn (II), Ni (II), for growth analysis. Biomass productivity is one of the most important parameters for industrial production, especially for algae biofuel production. In order to assess both proliferation and viability of the cells under heavy metal stress, spectrophotometric

growth analysis and fluorometric FDA vital staining were used. Compared to non-treated control, 10 ppm Zn (II) experimental group showed a significant increase in growth rate which facilitate both bioremoval process of Zn (II) and biomass production for biofuel industry. This increase might be the result of the proliferative effect of Zn (II) on the alga. Other experimental groups Cu (II) and Ni (II) demonstrated similar growth characteristics to each other which show slight decrease in growth rates possibly resulted from the mild toxic effects of these heavy metals at 5 ppm and 10 ppm concentrations, respectively. Spectrophotometric measurement is not an informative tool for cell viability and it could be misleading due to the background effect of cell debris generated from fragmented dead cells in cultivation media. Therefore, FDA vital staining which is specific to living population was also used in this study in order to measure the culture condition. According to the data, both measurements found similar growth characteristics. As shown in Figure 3 (left and right) *Dunaliella sp. Tuz KS\_02* cells could proliferate under all experimented heavy metal consisting cultivation conditions. Results indicate that green hypersaline alga *Dunaliella sp. Tuz KS\_02* has a good potential to be successfully cultivated for biomass production. Moreover, unconsumable saline waters which is contaminated by these heavy metals can be used for cultivation in a combined bioremediation and biomass production process.

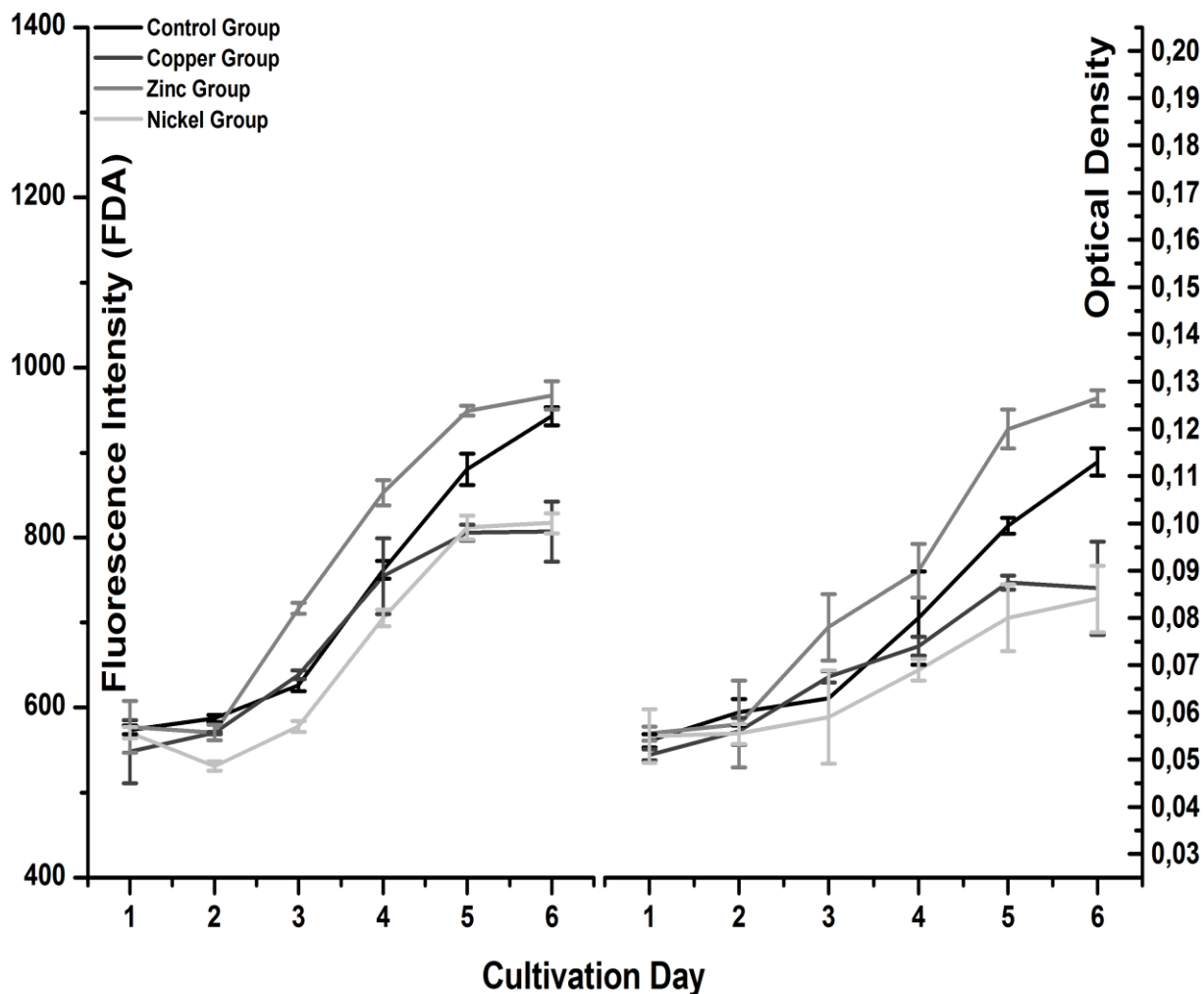


**Figure 3** Fluorometric (left) and spectrophotometric (right) growth analyses of *Dunaliella sp. Tuz KS\_02*. Data represented as relevant fluorescence units and optical density at 600nm wave length for fluorometric and spectrophotometric measurements respectively. The error bars correspond to  $\pm 1$  SD of triplicates.

### 3.3.4. Cellular lipid and ROS accumulation analyses of the new *Dunaliella sp. Tuz KS\_02* strain under Cu (II), Zn (II), Ni (II) consisting cultivation conditions

In order to quantify cellular lipid accumulation and ROS production of *Dunaliella sp. Tuz KS\_02* cultivated with Cu (II), Zn (II), and Ni (II). We used fluorometric microplate NR and DCFH-DA staining methods in comparison with the non-treated control groups at the end of cultivation course. As shown in Fig. 4, all experimented heavy metal treatments result in increased levels of cellular lipid accumulation with increased level of ROS production compared to non-treated control groups. In accordance with recent studies [22,23], under

nitrogen depleted conditions, increased ROS production and lipid accumulation were observed in a parallel manner. This association may suggest that ROS production might lead lipid over accumulation as a survival response against lipid peroxidation or other detrimental effects resulted from ROS production. In this study a similar response was seen in the hypersaline green alga *Dunaliella sp. Tuz KS\_02* cultivated with experimented heavy metals.

Flow cytometric analysis of ROS production and lipid accumulation is another powerful tool in terms of the strong capability of single cell level analysis. According to flow cytometric NR and DCFH-DA analysis shown in Figure 5c and 5d respectively, increased cellular lipid accumulation of all experimental groups accompany increased levels of ROS production in comparison with non-treated control groups. These data suggest that increased ROS production and lipid accumulations have both occurred at single cell level and the data support the findings of previous fluorometric measurements. Therefore, this association might be used as a new lipid accumulation strategy in a combined biotechnological process in order to increase the biofuel production efficiency.

ROS production is a known cause of lipid peroxidation which could be detrimental especially to cellular membranes. In order to assess lipid peroxidation in *Dunaliella sp. Tuz KS\_02* cells, TBARS method was used along with visualization of ROS production by using fluorescence microscopy. Increased level of ROS production visualized by DCFH-DA staining method shown in Figure 6a accompanies with increased MDA concentrations shown in Figure 6b which is an indicator of lipid peroxidation in all experimented heavy metal cultivation conditions compared to non-treated control groups. These data clearly show the association between increased ROS production, lipid peroxidation and cellular lipid accumulation which may be a survival response against membrane integrity loss which is resulted from lipid peroxidation under heavy metal stress conditions.

The use of FT-IR spectroscopy to monitor changes in macromolecular composition of algae cells has been demonstrated [24]. In this study, in addition to the fluorometric and flow cytometric analyses of cellular lipid accumulation, macromolecular composition of *Dunaliella sp. Tuz KS\_02* cells under different heavy metal consisting cultivation conditions was also investigated by using FT-IR spectroscopy at the end of the cultivation period shown in Figure 7. According to the results, all experimented heavy metal treatments increased triacylglycerol levels, especially in Zn (II) groups compared to non-treated control groups which are supported by the previous fluorometric and flow cytometric lipid accumulation analyses. Amide which is related to protein levels demonstrated an increase especially in Zn (II) and Ni (II) heavy metal treatments. Oligosaccharide levels were decreased in especially Cu (II) and

Ni (II) groups where Zn (II) groups showed similar levels. Last of all, polysaccharide levels except Ni (II) groups were increased in Cu (II) and Zn (II) groups. Data indicate that different heavy metal cultivation conditions may result in different macromolecular compositions in algae cells. Especially, increased levels of lipid contents may play an advantageous role in a combination process of bioremediation and biodiesel production.

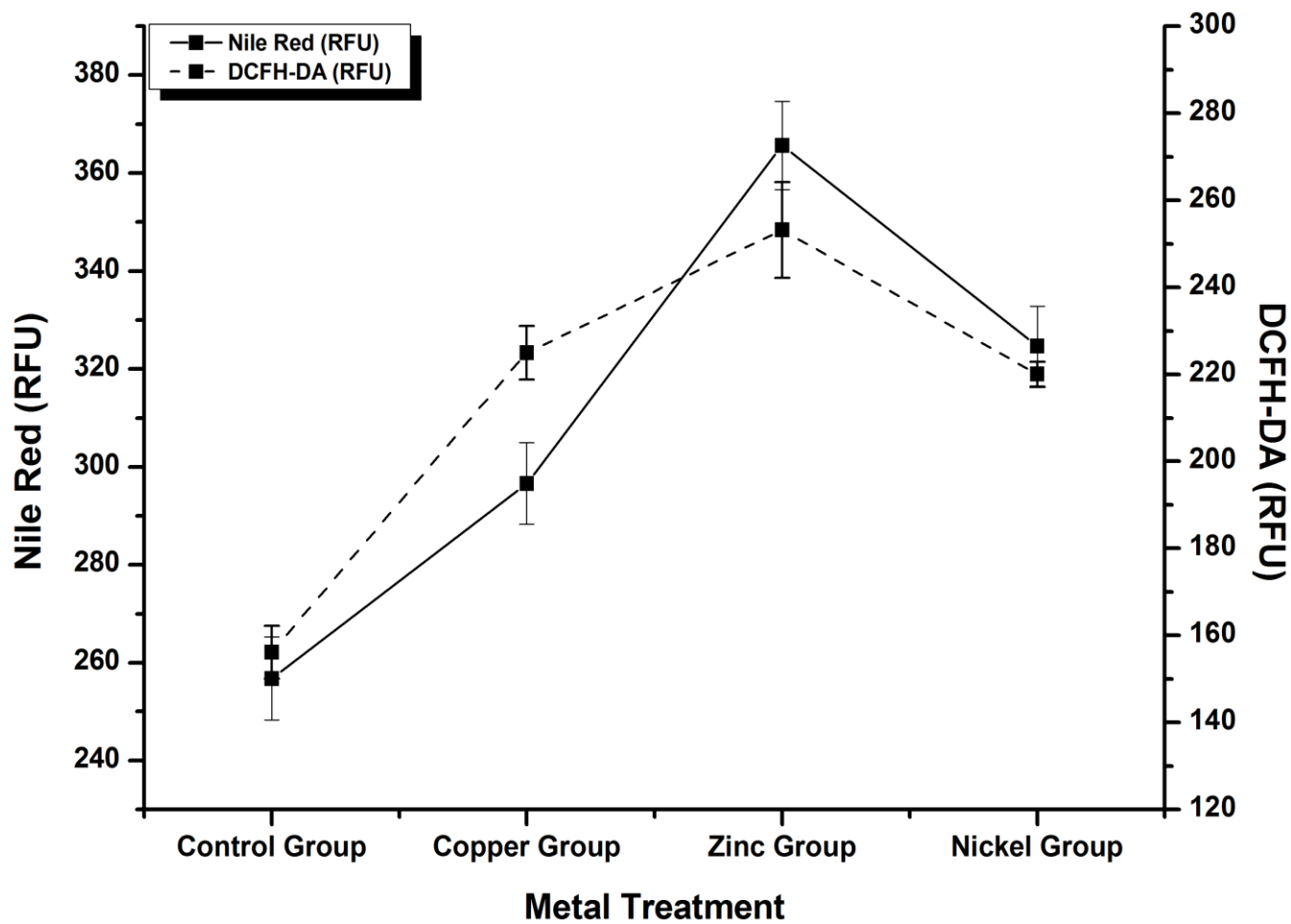


**Figure 4** Fluorometric microplate lipid accumulation (Nile Red) and ROS production (DCFH-DA) analyses of *Dunaliella sp. Tuz KS\_02* cultivated under Cu (II), Zn (II) and Ni (II) treatments.

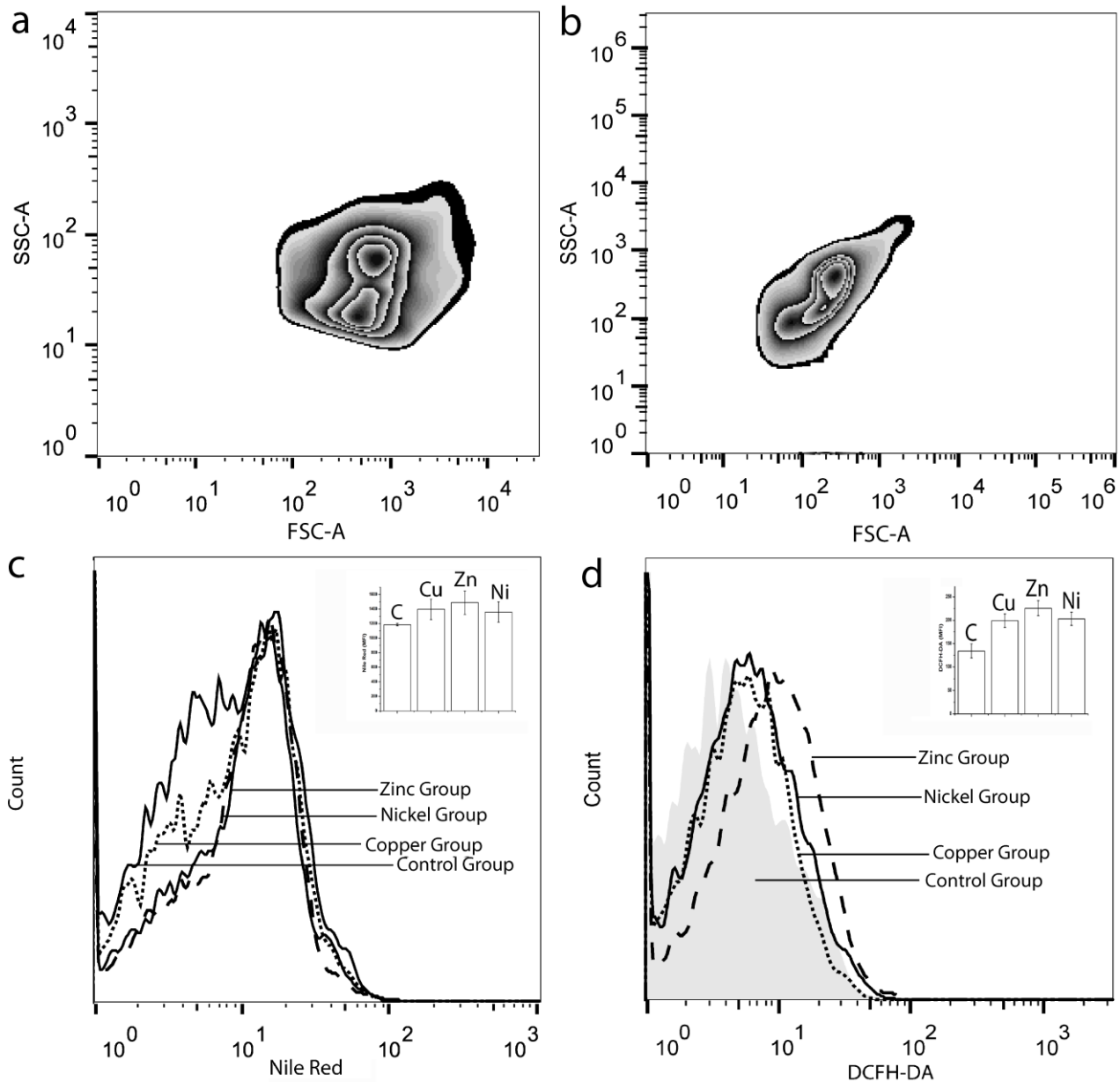


**Figure 5** Flowcytometric lipid accumulation (Nile Red) and ROS production (DCFH-DA) analyses of *Dunaliella sp. Tuz KS\_02* cultivated under Cu (II), Zn (II) and Ni (II) treatments. **a-b)** Zebra-plot of SSC (Side Scatter) and FSC (Forward Scatter) expressing cellular granulation and cellular size, respectively, under the heavy metal treatment conditions **c)** Histogram of flow-cytometric analysis of lipid contents under Cu (II), Zn (II) and Ni (II) treatments **d)** Histogram of flow-cytometric analysis of cellular ROS production under Cu (II), Zn (II) and Ni (II) treatments. Data represent the mean values of triplicates. Standard error for each triplicate corresponds to  $\pm 1$  SE.

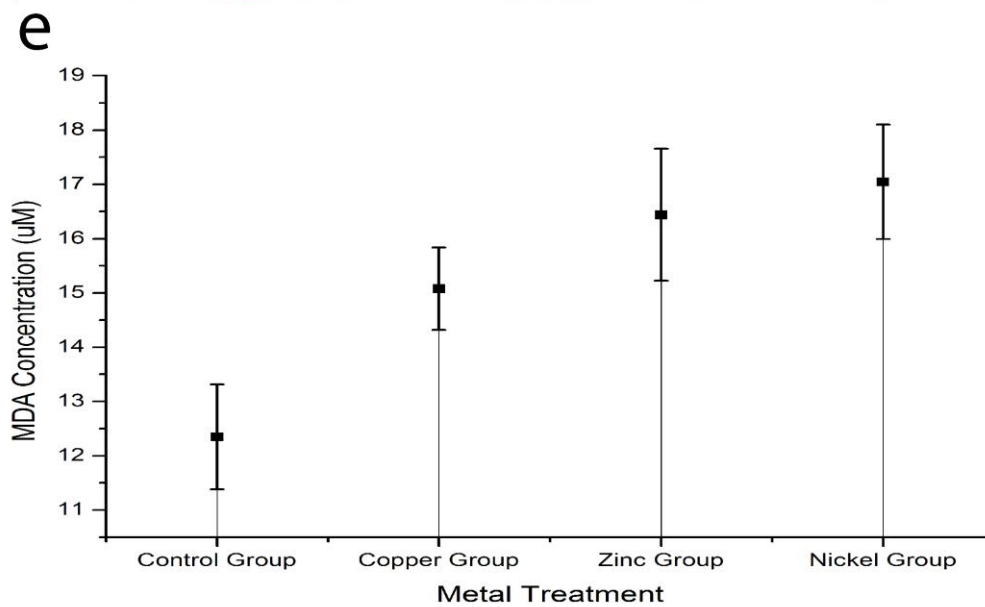
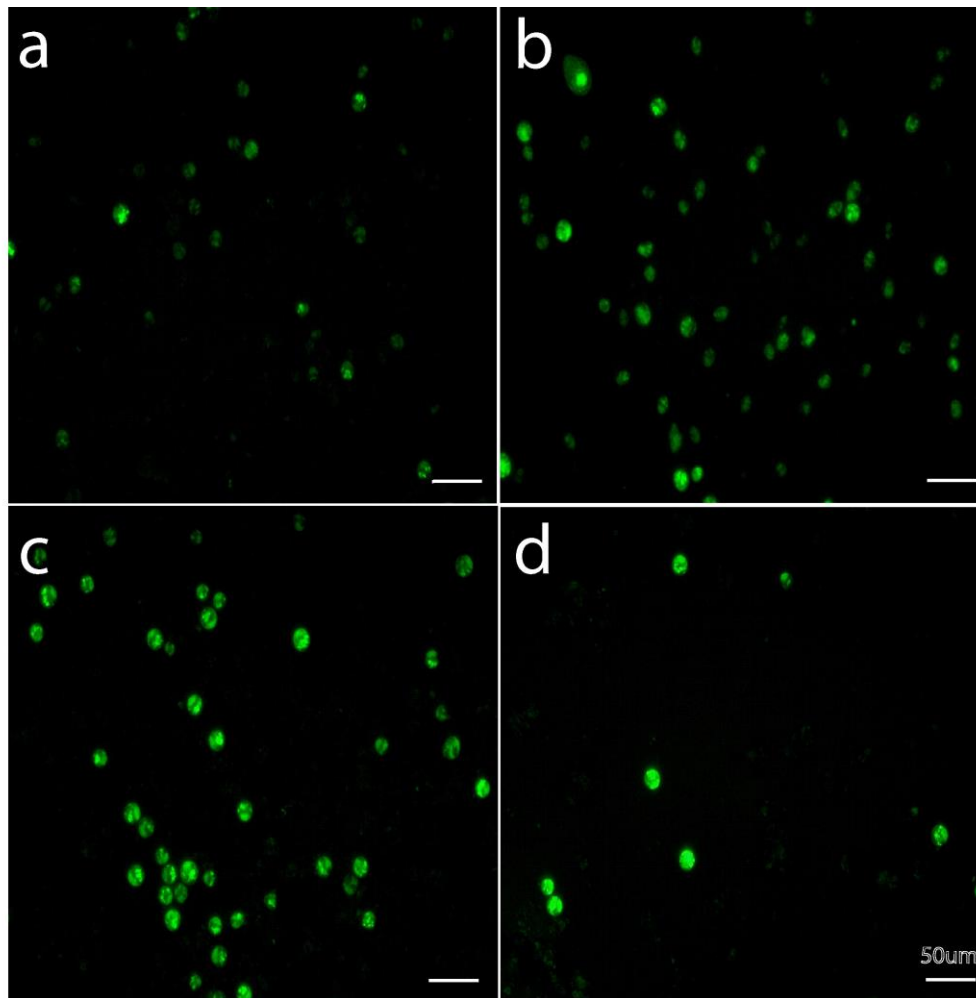


**Figure 6** Fluorescence microscope images of *Dunaliella sp. Tuz KS\_02* cultivated under Cu (II), Zn (II) and Ni (II) treatments. Cells were stained with DCFH-DA, an indicator of ROS production and TBARS assay was used for showing MDA end-product, an indicator of lipid peroxidation

mainly resulted from H<sub>2</sub>O<sub>2</sub> reactants. **a-b-c-d**) Representative fluorescent images of non-treated control, Cu (II), Zn (II), Ni (II) groups stained with DCFH-DA respectively **e**) TBARS analysis of *Dunaliella sp. Tuz KS\_02* cultivated under Cu (II), Zn (II) and Ni (II) treatments. Data represent the mean values of triplicates. Standard error for each triplicate corresponds to  $\pm 1$  SE

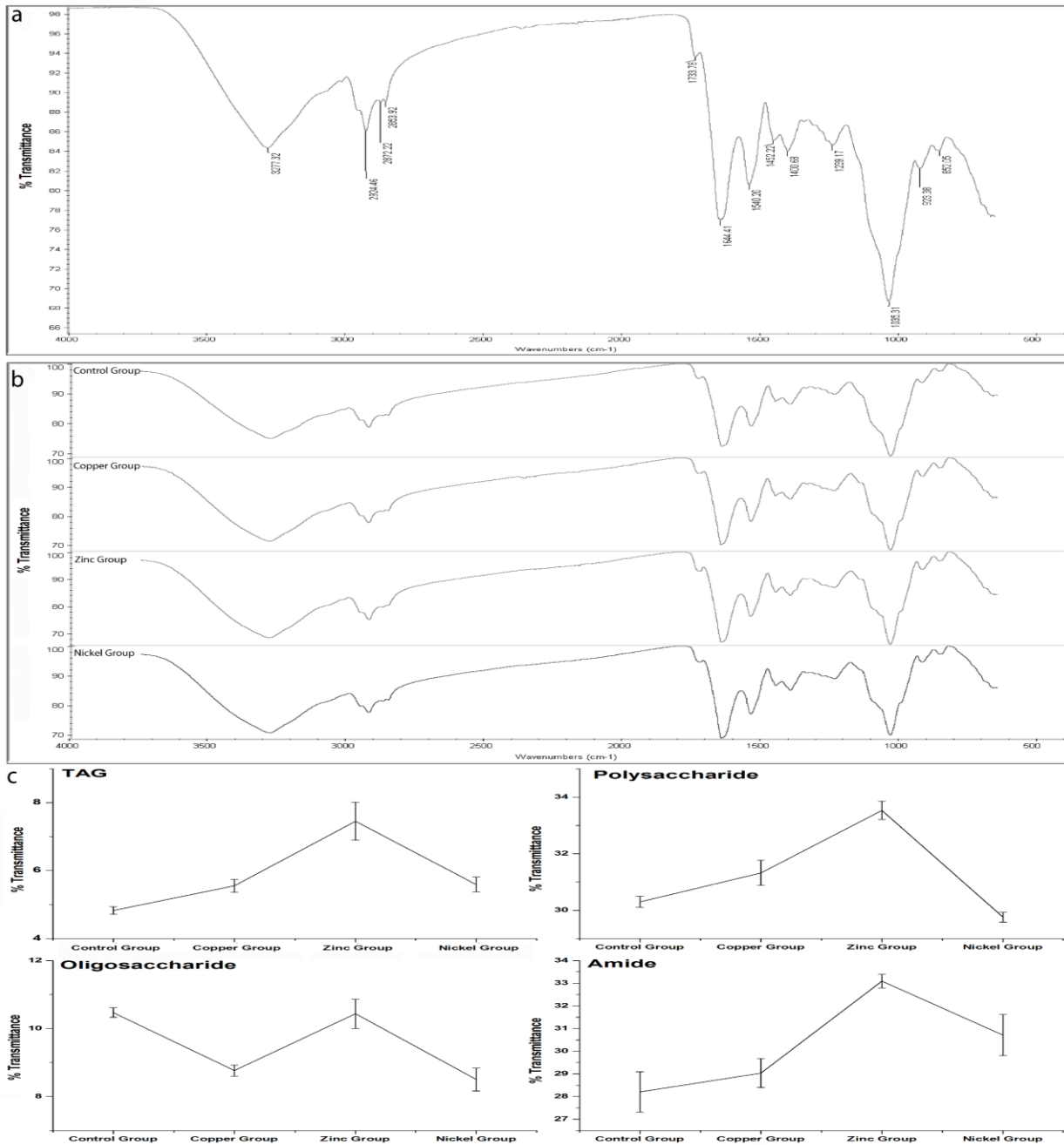


**Figure 7** Representative FT-IR analysis of *Dunaliella sp. Tuz KS\_02* cultivated under Cu (II), Zn (II) and Ni (II) treatments. **a**) Spectra were collected over the wavenumber range 4000–600 cm<sup>-1</sup>. Spectra were baseline corrected using the automatic baseline correction algorithm **b**) Scatter plots of transmittance (%) of TAG, polysaccharide, oligosaccharide and amide

groups c) Overall histogram of transmittance (%) of Cu (II), Zn (II) and Ni (II) treatments in comparison with control group. Data represent the mean values of triplicates. Standard error for each triplicate corresponds to  $\pm 1$  SE.

### **3.3.5 Metabolic Activity and Pigment Analysis of the new *Dunaliella sp. Tuz KS\_02* strain under Cu (II), Zn (II), Ni (II) consisting cultivation conditions**

Fluorescence diacetate (FDA) staining method was previously shown to be used for measuring metabolic activity in algal cells [25]. In order to assess metabolic activity of *Dunaliella sp. Tuz KS\_02* during its growth under heavy metal consisting cultivation conditions, esterase activities of experimental groups were measured by flow cytometric FDA staining method which was modified in this study shown in Figure 8.  $10^6$  cells were counted by using hemocytometer and viable cell population was gated by adjusting FSC and SSC parameters to previously optimized viable cell parameters shown in Figure 6a. According to the data, experimental groups demonstrated similar metabolic activities in comparison with non-treated control groups. This suggests that, none of the experimented heavy metals at around 10 ppm concentrations resulted in dramatic metabolic suppression in *Dunaliella sp. Tuz KS\_02* cells during the cultivation period except of a slight decrease in Cu (II) group which may be resulted from enzymatic inhibition potential of Cu (II).

A further analysis for determination of chlorophyll, carotenoid and total protein contents of the alga was done in order to evaluate other metabolic changes. As shown in Figure 9, Cu (II) group shows a slight decrease in chlorophyll content where Zn (II) group shows increased levels and Ni (II) group has no significant difference. Chlorophyll content is an indicator of both photosynthetic efficiency and metabolic activity [26]. The absence of a drastic change in chlorophyll contents in Cu (II) and Ni (II) groups indicates that the metabolic activity and photosynthetic efficiency were not affected under experimented heavy metal concentrations. Since, the proliferative effect of Zn (II), chlorophyll level increase would be an expected result along with increased growth rates shown in Figure 2. However, Carotenoids can perform an essential role in photoprotection by quenching the triplet chlorophyll and scavenging singlet oxygen and other reactive oxygen species, there was no significant change in carotenoid levels observed under experimented conditions. This might suggest that the photoprotective property of carotenoids were not majorly needed in oxidative stress induced by heavy metals. Indications of successful growth and unaffected metabolic activity of the cells, may suggest that the enzymatic defence mechanism against ROS

accumulation is effective and successful neutralization of ROS can be done under experimented heavy metal concentrations. Last of all, protein contents of the experimental groups showed increased levels in accordance with the previous data obtained from FT-IR analysis. This suggests that the experimented heavy metal concentrations did not inhibit protein metabolism and let the alga proliferate efficiently. Synthesis of some special metal binding proteins like metallothioneins or transporters may be induced by experimented heavy metals with their initial concentrations and this phenomenon may result in increased protein contents of algae cells as another defense mechanism.

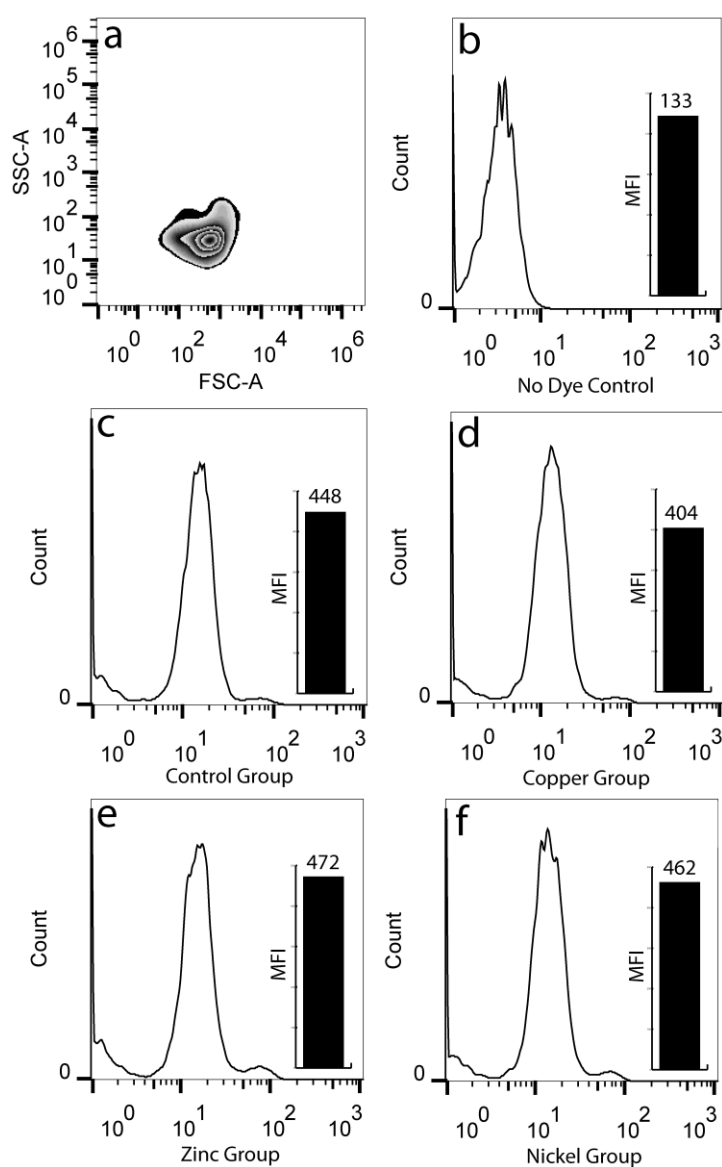


**Figure 8** Flowcytometric metabolic activity analysis of *Dunaliella sp. Tuz KS\_02* cultivated under Cu (II), Zn (II) and Ni (II) treatments. a) Zebra-plot of SSC (Side Scatter) and FSC

(Forward Scatter) expressing cellular granulation and cellular size, respectively, under the heavy metal treatment conditions **b-c-d-e-f**) Histogram and corresponding bar graphs of representative flow-cytometric analysis of metabolic activities of *Dunaliella* cells under Cu (II), Zn (II) and Ni (II) treatments in comparison with no dye and untreated control groups.

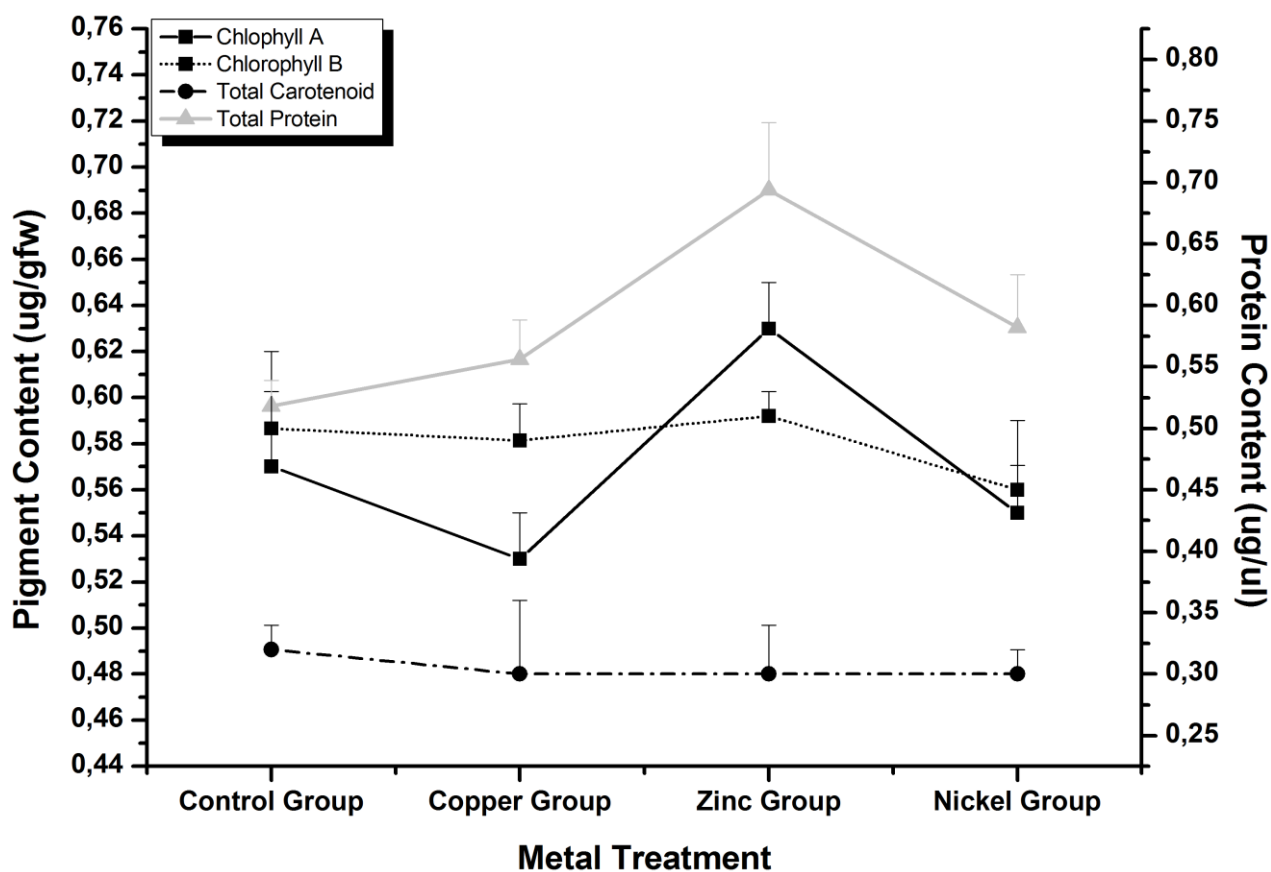


**Figure 9** Total protein and pigment contents of *Dunaliella sp. Tuz Lake KS\_02* strain cultivated under Cu (II), Zn (II) and Ni (II) treatments. Data demonstrate the mean values of triplicates  $\pm$  1 SE

### 3.4 Conclusions

Newly isolated *Dunaliella sp.* cells successfully adsorbed heavy metals at high concentrations without significant disturbance to its growth characteristics along with its increased cellular lipid accumulation. The alga might be suitable in a combinatory way of bioremediation and biofuel feedstock, lipid/biomass, production processes in unusable saline systems with a great advantage of resistancy to contamination issue in open air cultivation systems. ROS might be one of the triggering mechanisms of increased cellular lipid accumulation response under heavy metal stress. This phenomenon might be used as a new cultivation strategy in a combinatory process of bioremediation and biofuel production.

## **CHAPTER 4**

### **4.1 INTRODUCTION**

#### **4.1.1 Genetic Engineering of Microorganisms**

##### **4.1.1.1 General Aspects**

Genetic engineering is broadly accepted definition to introduce genes of interest which enable organisms to have desired traits to a target microorganism's genome. Transformation is the key step of generating transgenic microorganisms. Sterile monocultures namely axenic cultures with a short life cycle under defined environmental conditions are preferred for transformation experiments to introduce new genes to target genomes. After transformation, well-defined expression systems must be established for successful gene introduction. For allowing the selection of transformed cells, a method must also be established or be available that allows for regeneration of the target species from single cells (ideally on agar plates). Some species are photoautotrophs, so they require only light, water and basic nutrients for growth; other species are heterotrophs and can also be grown in the dark if proper nutrients are present in the culture medium. It is mostly advantageous to use microorganisms with separate sexes with well-known sexual life cycles that can be triggered under laboratory conditions for having genetic crosses. In some cases haploid cells also might be favored. In addition, many species have multinucleate cells, but microorganisms with mononucleated cells should be selected for transformation experiments. Moreover, previous molecular, biochemical, physiological or ecological knowledge of the target species and a somewhat developed molecular toolbox is desirable. Existence of extensive sequence information is of utmost importance for transgenics.

Other important strategies for obtaining transgenic microorganisms are targeted or non-targeted mutagenesis such as gene specific mutagenesis or random mutagenesis by using ultraviolet light, gamma radiation and DNA alkylating chemical mutagens. These methods are also extensively used for generating transgenic microorganisms with desired traits of various interest. Selection of generating transgenic strategy is one of the most important steps, but still, availability of genomic information is a crucial part for transgenesis studies besides gene identification or characterization studies in response to various effectors.

Compared to yeast transgenics, the studies conducted with algae are in infant steps due to unavailability of completed sequence and most importantly annotated genome projects. As a model eukaryotic organisms, baker's yeast, *Saccharomyces cerevisiae*, is still most preferred and well-established system in transgenic studies because of its completed and well-known genome and its well-established transformation, expression and selection strategies.

#### 4.1.1.2 Algae Genome Projects

There are several microalgae genome projects, of which the most advanced projects are those for the red alga *Cyanidioschyzon merolae*, the diatom *Thalassiosira pseudonana*, and the three green algae *Chlamydomonas reinhardtii*, *Volvox carteri* and *Ostreococcus tauri*. Sequencing and annotation of the 16.5 Mb *Cyanidioschyzon merolae* genome has been finished [1]. Similarly, sequencing and annotation of the 34 Mb *Thalassiosira pseudonana* genome has been completed [2]. Also, sequencing of the ~120 Mb genome of *Chlamydomonas reinhardtii* has been completed; annotation is proceeding and should soon be finished [3]. The ~140 Mb-sized genome of *Volvox carteri* has been sequenced (8x coverage, unpublished, DOE Joint Genome Institute/JGI, Walnut Creek, CA) and annotation will begin in the near future. Additional algal genome projects are in progress, for example in *Alexandrium tamarense*, *Amphidinium operculatum*, *Aureococcus anophagefferens* (~32 Mb), *Chlorella vulgaris* (~40 Mb), *Cyanophora paradoxa*, *Dunaliella salina* (~130 Mb), *Ectocarpus siliculosus* (~214 Mb), *Emiliana huxleyi* (~220 Mb), *Euglena gracilis*, *Galdieria sulphuraria* (~12 Mb), *Guillardia theta*, *Heterocapsa triquetra*, *Isochrysis galbana*, *Karenia brevis*, *Lotharella amoebiformis*, *Micromonas pusilla* (~15 Mb), *Ochromonas danica*, *Ostreococcus lucimarinus* (~12 Mb), *Pavlova lutheri*, *Phaeodactylum tricorutum* (~30 Mb), *Porphyra purpurea*, and *Porphyra yezoensis*. Finally, due to their small sized genomes, complete genome sequences from ~30 Cyanobacteria are available in different databases; among these are species like *Synechococcus elongatus* (~2.7 Mb), *Anabaena* sp. (6.4 Mb),

*Nostoc punctiforme* (~7.5 Mb), *Synechocystis* sp. (~3.6 Mb), *Thermosynechococcus elongatus* (~2.6 Mb), *Gloeobacter violaceus* (~4.6 Mb), and *Prochlorococcus marinus* (1.7–2.4 Mb; size depends on ecotype).

Several algae genome projects have been continued or finished already. Due to lack of completed gene annotations, the information of completed genome projects are still hardly useful in especially gene identification or characterization studies. For this reason in this part of the study we choose the eukaryotic model organism *Saccharomyces cerevisiae* due to its better annotation information for searching potential responsible genes in increased lipid accumulation response upon mutagenesis.

#### 4.1.1.3 Lipid Metabolism and Metabolic Engineering

The synthesis of the acyl-CoA precursor starts with the production of citrate from the TCA cycle, secreted from the mitochondria, which is then converted to acetyl-CoA by the ATP citrate lyase (ACL1 and ACL2) shown in Figure 1. Part of the acetyl-CoA is converted to malonyl-CoA by the acetyl-CoA carboxylase (ACC1). Synthesis of fatty acids (Acyl-CoA, mainly palmitoyl-CoA and stearic-CoA) is catalyzed, through elongation cycles, by the fatty acid synthase (FAS1 and FAS2) consisting of four successive reactions by the ketoacyl synthase (KS domain), further modified at the  $\beta$ -carbon position by ketoacyl reductase (KR), dehydratase (DH) and the enoyl reductase (ER) from the basic blocks acetyl-CoA and malonyl-CoA. The synthesis of the glycerol-3-phosphate (G3P) is part of the “glycerol pathway” that regulates the concentration of the glycerol (Gly), glycerol-3-Phosphate (G3P), dihydroxyacetone phosphate (DHAP) and dihydroxyacetone (DHA). Dihydroxyacetone phosphate (DHAP) is converted to glycerol-3-phosphate (G3P), by the NAD<sup>+</sup>-dependent G3P dehydrogenases (GPD1) and the reverse reaction G3P, in the mitochondria, is converted to DHAP by the mitochondrial FAD<sup>+</sup>-dependent G3P dehydrogenase (GUT2). Catabolism of glycerol depends on two pathways: (i) the “DHA pathway” in which glycerol is converted to dihydroxyacetone (DHA) by glycerol dehydrogenases (GCY1/YPR1, ARA1 and GRE3). DHA is then phosphorylated to DHAP by the glycerone kinases (DAK1 and DAK2) and (ii) the “G3P pathway” in which glycerol can be phosphorylated into G3P, by the glycerol kinase (GUT1). In *Y. lipolytica*, they are an expansion of homolog genes coding for glycerol dehydrogenase and the absence of homolog to the glycerol-3 phosphatase (GPP1 and GPP2 in *Saccharomyces cerevisiae*). Triacylglycerol (TAG) synthesis follows the Kennedy pathway. FFA are activated to coenzyme A (acyl-CoA) and used for the acylation of the glycerol-3-P

backbone to synthesize TAG. In the first step of TAG assembly, G3P is acylated by G3P acyltransferase (SCT1) to lysophosphatidic acid (LPA), which is then further acylated by LPA acyltransferase (SLC1) to phosphatidic acid (PA). This is followed by dephosphorylation of PA by PA phosphohydrolase (PAP) to release diacylglycerol (DAG). In the final step, DAG is acylated either by DAG acyltransferase (DGA1 and DGA2 with acyl-CoA as an acyl donor) or by phospholipid DAG acyltransferase (LRO1 with glycerophospholipids as an acyl donor) to produce TAG. Free fatty acids (FFA) are activated by fatty acyl-CoA synthetase. The activated acyl-CoA (of N carbon) enter the beta-oxidation corresponding to four reaction catalyzed by the acyl-CoA oxidases (POX1 to POX6) then by the multifunctional enzyme having both the hydratase and the deshydrogenase activity (MFE1) and finally the thiolase realizing an acyl-CoA (of N-2 carbon) and an acetyl-CoA. TAG remobilization could be blocked by inactivation of the triacylglycerol lipases (TGL3 and TGL4) (Figure 1).

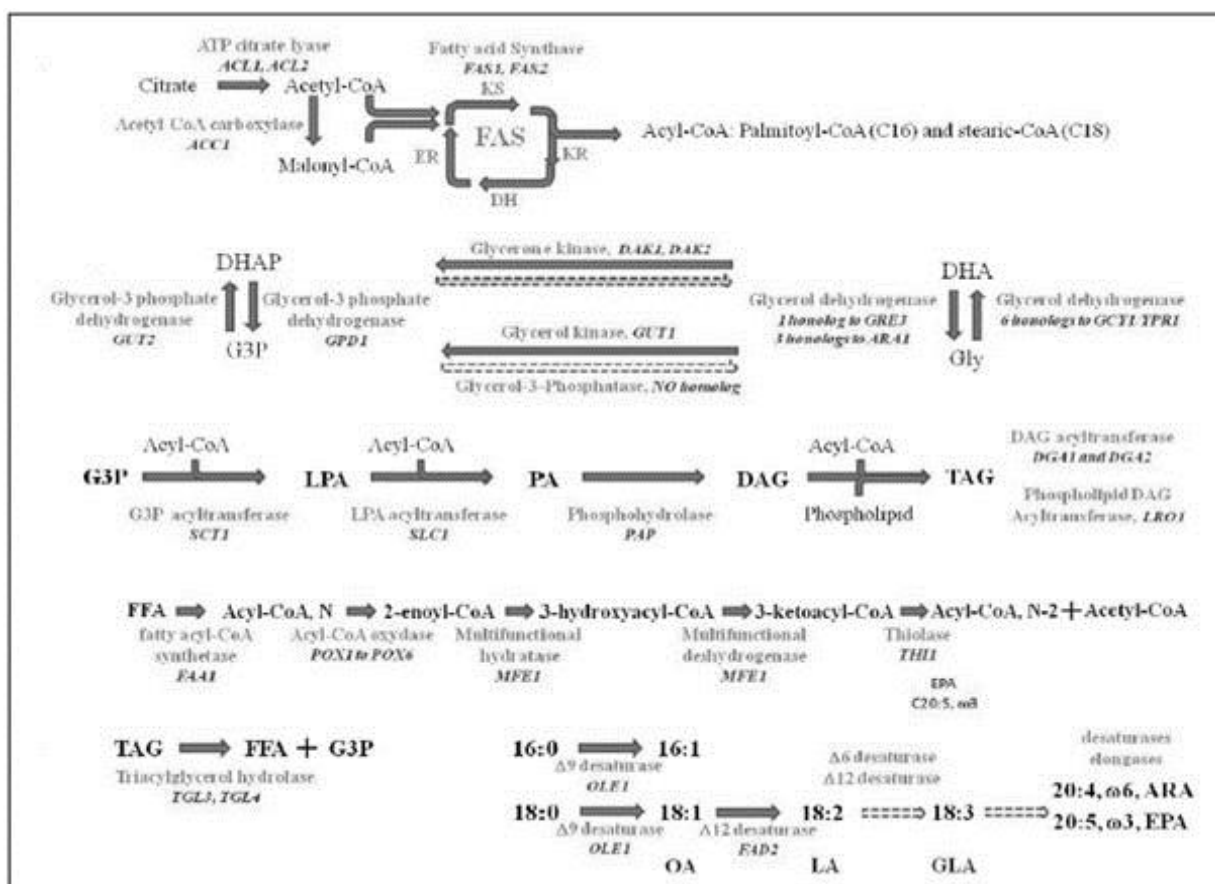


**Figure 1.** Fatty acid synthesis pathway in Baker's yeast, *Saccharomyces cerevisiae* [4].

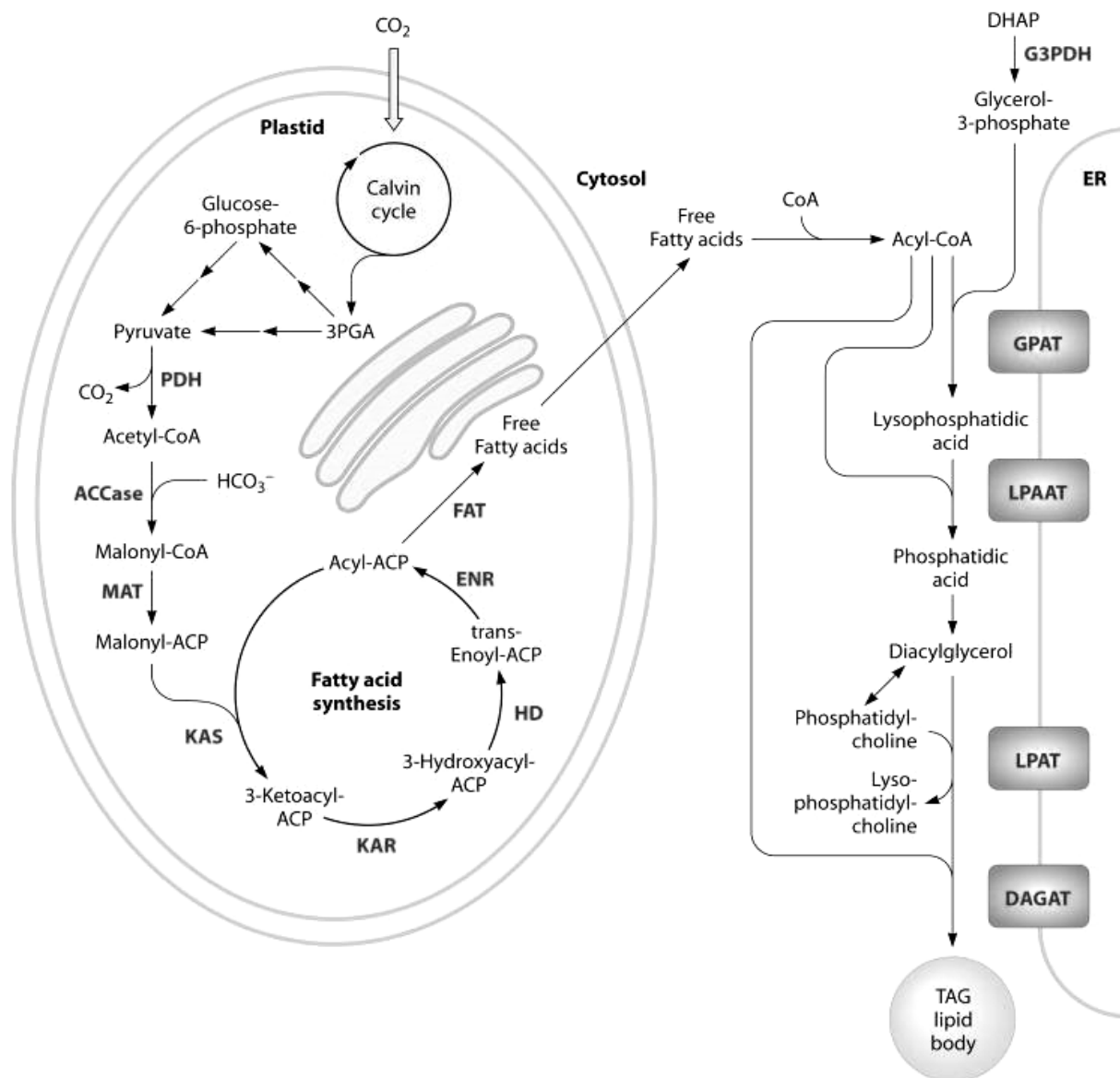


**Figure 2.** Simplified scheme of the metabolites and representative pathways in microalgal lipid biosynthesis. Free fatty acids are synthesized in the chloroplast, while TAGs may be assembled at the ER. ACCase, acetyl-CoA carboxylase; ACP, acyl carrier protein; CoA, coenzyme A; DAGAT, diacylglycerol acyltransferase; DHAP, dihydroxyacetone phosphate; ENR, enoyl-ACP reductase; FAT, fatty acyl-ACP thioesterase; G3PDH, glycerol-3-phosphate dehydrogenase; GPAT, glycerol-3-phosphate acyltransferase; HD, 3-hydroxyacyl-ACP dehydratase; KAR, 3-ketoacyl-ACP reductase; KAS, 3-ketoacyl-ACP synthase; LPAAT, lyso-phosphatidic acid acyltransferase; LPAT, lyso-phosphatidylcholine

acyltransferase; MAT, malonyl-CoA:ACP transacylase; PDH, pyruvate dehydrogenase complex; TAG, triacylglycerols [5].

Understanding microalgal lipid metabolism is of great interest for the ultimate production of diesel fuel surrogates. Both the quantity and the quality of diesel precursors from a specific strain are closely linked to how lipid metabolism is controlled. Lipid biosynthesis and catabolism, as well as pathways that modify the length and saturation of fatty acids, have not been as thoroughly investigated for algae as they have for terrestrial plants and other eukaryotic organisms. However, many of the genes involved in lipid metabolism in terrestrial plants have homologs in the sequenced microalgal genomes. Therefore, it is probable that at least some of the transgenic strategies that have been used to modify the lipid content in higher plants will also be effective with microalgae.

However, several attempts to utilize ACCase overexpression to increase lipid content in various systems have been somewhat disappointing. Dunahay et al. overexpressed native ACCase in the diatom *C. cryptica* [6]. Another study has blocked metabolic pathways that lead to the accumulation of energy-rich storage compounds, such as starch. For example, two different starch-deficient strains of *C. reinhardtii*, the *sta6* and *sta7* mutants, have disruptions in the ADP-glucose pyrophosphorylase or isoamylase genes, respectively [7]. Another starchless mutant of *Chlorella pyrenoidosa* has also been shown to have elevated polyunsaturated fatty acid content [8].

It is reasonable to believe that some of the strategies that result in increased oil seed content in terrestrial plants may be able to increase the lipid content of microalgal cells as well. Many microalgae do not produce large amounts of storage lipids during logarithmic growth. Instead, when they encounter environmental stress, such as a lack of nitrogen, they slow down their proliferation and start producing energy storage products, such as lipids and/or starch. It will be interesting to see how overexpression of lipid synthesis pathway genes will affect microalgal proliferation. It may be that increased lipid synthesis will result in a reduction of cell division. In such a case, overexpression of lipid synthesis genes may still be beneficial if they can be controlled by an inducible promoter that can be activated once the microalgal cells have grown to a high density and have entered stationary phase. Examples of inducible promoters in algae include copper-responsive elements in *C. reinhardtii* and a nitrate-responsive promoter in diatoms. Inhibiting lipid catabolism may also cause problems with proliferation and biomass productivity since microalgae often rely on catabolic pathways to provide energy and precursors for cell division. Genetic engineering studies are comparably

less than that of studies conducted with other eukaryotic microorganisms and higher plants such as *Saccharomyces cerevisiae* and *Arabidopsis thaliana*. Therefore mutagenesis studies are become also important for identification of potential target genes which might be responsible for increased lipid accumulation. After identification of target genes, it might be possible to apply proper genetic manipulations to have desired microorganism strains with increased lipid accumulation.

Lipid production for industrial applications depends on cellular triacylglycerol content accumulated, on the lipid profiles and on the capacity to use cheap resources. Thus, for the advancements of a process, genetic engineering is being used. Enhance of lipid level and modification of lipid profiles were performed by targeting the four following approaches namely increasing the level on the two main precursors G3P and acyl-CoA; boosting the TAG synthesis pathway; preventing TAG remobilization and acyl-CoA degradation and modification of the fatty acid profiles. In yeast, there are numerous studies which applies mentioned strategies for increasing lipid accumulation.

In the yeast *Yarrowia lipolytica*, when carbon is in excess and nitrogen is deprived, the carbon is redirected toward citric acid, which under the activity of the ACL, cytoplasmic ATP citrate lyase (ACL1 and ACL2 genes), resulted in the production of acetyl-CoA. Part of this pool is converted to malonyl-CoA by the ACC, cytoplasmic acetyl-CoA carboxylase (ACC1 gene). Then, the multi-enzymatic complex subunits that constitute the fatty acid synthase FAS encoded by two genes (FAS1 and FAS2), from malonyl-CoA add successively acetyl-CoA to elongate the acyl chain by two carbons at each cycle. The reaction is repeated until a chain length of C16 or C18 is reached releasing palmitate or stearate (C16-CoA and C18-CoA, respectively). Recently, one of the studies it was shown that increased lipid production can be achieved by overexpression of the ACC [9]. Another approach was to increase citric acid production through the inactivation of the 2-methyl-citrate dehydratase encoded by the PHD1 gene.

The second limiting step in the Kennedy pathway is at the last step of TAG synthesis. In yeasts, they are a diacylglycerol acyl transferase Dga1p with acyl-CoA as a donor, which belong to the DGAT2 family. In contrast, in the yeast *Y. lipolytica*, they are a second diacylglycerol acyl transferase Dga2p, which belong to the DGAT1 family. Overexpression in *Y. lipolytica* of either DGA1 or DGA2 increases TAG synthesis without modification of the fatty acid profile [10]. Combining overproduction of acyl-CoA by overexpression of ACC and increasing TAG synthesis by overexpression of DGA2 have been recently reported [9].

The third approach to improve TAG accumulation is to abolish free fatty acid (FFA) and Acyl-CoA degradation through inactivation of the beta oxidation or the inactivation of TAG degradation. *Y. lipolytica* is the yeast having the highest content of acyl CoA encoding gene. Deleting of the six genes improved lipid accumulation even more if both POX genes and GUT2 deletion were combined [11]. Similar improvements were obtained also by combining POX or MFE deletion together with GPD over expression [12]. However, in  $\Delta$ pox1-6 strain, we observed induction of TGL4 and TGL3, suggesting that depending on genetic background, induction of TAG remobilization could be induced even during the accumulation phase. Indeed; deletion of TAG remobilization increases TAG accumulation in *Y. lipolytica* [12].

Finally, the four metabolic engineering steps are to modify the fatty acid profiles of the TAG accumulated. In *Y. lipolytica* they are only two fatty acid desaturases ( $\Delta$ 9 desaturase, OLE1 and  $\Delta$ 12 desaturase, FAD2) allowing to accumulate about nearly 50% linoleic acid in define condition [11]. Significant level of GLA was synthesized in *Y. lipolytica* from endogenous linoleic acid (LA) and oleic acid (OA) by over expression of *M. alpina*  $\Delta$ 12-desaturase and  $\Delta$  6-desaturase [13]. The key steps for lipid accumulation and the effort in metabolic engineering by multi-gene approach have been reviewed recently [14].

#### **4.1.1.4 Existing Problems in Genetic Engineering**

During production of transgenic microorganisms, researchers often have to struggle with the problem that a gene construct is not expressed as desired, even though all elements required for transcription and translation have been included and the construct was integrated into the genome. Gene silencing might be occurred through methylation, and is caused by positional effects and epigenetic mechanisms. It is often related to the control of development and to the response of a cell to viruses, transposable elements, or other foreign DNA or unnaturally placed DNA. Often, screening of a larger number of transformants for a transformant with high expression solves this problem. Heterologous genes should not contain their own introns as they will likely not be spliced correctly; cDNAs should be used. However, genes without introns are often poorly expressed. This problem can be solved by introducing homologous introns into the heterologous coding region. Additional problems have been reported concerning insufficient DNA delivery, failure to integrate into the genome, or improper transport into the chloroplast or through the plasma membrane into the extracellular compartment. These problems are conquerable and, actually, they are not

specific to only algal systems since they are also known to occur with plants or other eukaryotes such as yeast.

Due to the problematic nature of genetic engineering studies mentioned above, we believe that desired phenotype selection based methodologies upon applying mutagenesis are more efficient strategies compared to unexpected genetic manipulations with a slight chance of success for obtaining desired traits. Upon random or targeted mutagenesis, selection of a desired character such as increased lipid content might be more time consuming and labor intensive method but the result would be more expected and precise in terms of obtaining interested traits.

#### **4.1.1.5 Directed Evolution**

Directed evolution is a powerful method for improving proteins and other biological molecules and systems, and involves an iterative process of applying selective pressure to a library of variants to identify mutants with desirable properties. Since its development in the early 1990s, directed evolution has become a valuable tool used in protein engineering, metabolic engineering, and biosynthetic pathway engineering and synthetic biology.

Over the past 20 years, directed evolution has been used successfully to improve protein activity, stability, substrate specificity, enantioselectivity, soluble expression, and binding affinity. Directed evolution relies on the simple yet powerful Darwinian principles of mutation and selection and is comprised of three essential steps: functional expression of the target protein, generation of DNA diversity, and development of a reliable high-throughput screening assay. Expression of a foreign gene in a non-native host is frequently limited by differences in the expression systems from the native organism. These differences in expression can be caused by a number of factors such as different codon usage, missing chaperones, and posttranslational modifications such as glycosylation or disulfide bridges. Some incompatibilities between the target gene and heterologous host, such as recognition of signal sequences or codon usage, can often be overcome by codon optimization of the target gene sequence. Therefore, even if genetic engineering and gene expression in a non-native host organisms to apply directed evolution strategy seem to be best ways to manipulate microorganisms to obtain desired modified strains with various useful characteristics, this might not be the easiest way due to the mentioned bottlenecks.

Although in theory any organism might serve as a host for directed evolution, in reality only a handful have been used. The most popular host organisms for directed evolution

are *Escherichia coli* and *Saccharomyces cerevisiae* because of their high transformation efficiencies, rapid growth rates, well-established manipulation tools, and ability to maintain stable plasmids. Other host organisms such as *Bacillus subtilis*, *Bacillus thuringiensis*, *Thermus thermo.*, *Lactococcus lactis*, *Pichia pastoris*, mammalian cells (CHO, 3T3, Ramos B-cells), and insect cells (*Spodoptera frugiperda* Sf9) and most importantly microalgae cells have also been used, but on a more limited basis.

*S. cerevisiae* is used routinely as a host in directed evolution and several recent articles have demonstrated its effectiveness. Bulter et al. improved the expression (8-fold) and total activity (170-fold) of a laccase from *Myceliophthora thermophila* in *S. cerevisiae* after nine generations of evolution [15]. In another study, a horseradish peroxidase (HRP) enzyme was engineered in *S. cerevisiae* for enhanced activity [16]. After three rounds of directed evolution by random mutagenesis and screening, a 40-fold increase in total HPR activity was obtained. Recently, a xylose isomerase from *Piromyces* sp. was evolved in *S. cerevisiae* through three rounds of mutagenesis and growth-based screening for improved xylose catabolism and fermentation [17]. A strain expressing the engineered enzyme improved its aerobic growth rate by 61-fold and both ethanol production and xylose consumption rates by 8-fold. The mutant enzyme also enabled ethanol production under oxygen-limited conditions, unlike the wild-type enzyme.

Bacterial, yeast, mammalian, and even insect cell lines have all been used as hosts for directed evolution, but surprisingly no published reports have focused on using microalgae as of yet. Currently, there are intensive global research efforts aimed at increasing or modifying hydrocarbons and other energy storage compounds in microalgae. In the past, a lack of genetic tools and genetic information hampered researcher's ability to engineer enzymes and metabolic pathways in microalgae; however, there now exists a wide array of new genetic manipulation tools, genomic sequences, and high-throughput analytical techniques that should allow scientists to use microalgae as a host for directed evolution studies.

Cyanobacteria, also known as blue-green algae, are photosynthetic bacteria that use light, water, and carbon dioxide to synthesize their energy storage components, i.e. lipids, carbohydrates, and proteins. Cyanobacteria are considered to be a promising feedstock for bioenergy generation based on their lipid accumulation, simple and inexpensive cultivation, and fast growth rates compared to other algae and higher plants. Being prokaryotes, cyanobacteria are also much more amenable to genetic engineering approaches compared to eukaryotic algae. *Synechocystis* sp. PCC 6803 is one of the most widely studied cyanobacteria and serves as a model system for studying photosynthesis, adaptability to environmental

stresses, the evolution of plant plastids, and carbon and nitrogen assimilation. This freshwater cyanobacterium can be grown either autotrophically or heterotrophically (using glucose as a carbon source; however, even though it can grow in complete darkness, for unknown reasons it still requires a small amount of light daily under a wide range of conditions).

The doubling rate of *Synechocystis* sp. PCC 6803 under optimal conditions is ~12 hours. *Synechocystis* sp. PCC 6803 has a relatively simple genome and was the first photosynthetic organism to have its entire genome fully sequenced. This strain can efficiently integrate foreign DNA into its genome by homologous recombination and thus allows for targeted gene replacement. Using this feature, a large number of deletion mutants have been created that aid in the study of gene function in cyanobacteria [18]. Low transformation efficiency would limit the size of a mutant library and make a directed evolution effort extremely challenging. Another possible limitation is the strong codon bias often observed for the *Synechocystis* genome [19], thus codon bias in *Synechocystis* is unlikely to seriously hamper a directed evolution effort.

Green algae are a large group of algae that share a common ancestry with higher plants. This group of algae has been used extensively in industrial aquaculture, primarily for the production of nutraceuticals, such as omega-3 fatty acids and  $\beta$ -carotene. *Chlamydomonas reinhardtii* is the most widely studied green algae and serves as a model algal organism in the study of photosynthesis, cellular division, flagellar biogenesis, and mitochondrial function. *C. reinhardtii* can be grown either autotrophically or heterotrophically (using acetate as a carbon source) and has a doubling time of 8 hours under optimal conditions. *C. reinhardtii* was the first green algae species to have its nuclear, chloroplast, and mitochondrial genomes fully sequenced. Transformation methods have been developed that effectively target each of the three genomes; however, researchers have mainly focused on transforming the nuclear and chloroplast genomes. Cyanobacterium *Synechocystis* and the green alga *C. reinhardtii* indeed will be used as host organisms for directed evolution based on their assortment of well-established genetic tools and the widespread interest in algal biofuels and co-products, but presently, number of studies conducted with microalgae is unfortunately limited.

In this study, we conducted directed evolution experiments using ethyl methyl sulfonate induced mutagenesis strategy to obtain fatty acid synthesis regulator enzyme, ACC CoA carboxylase specific chemical inhibitor resistant algae strains. Increased cellular lipid production by evolving targeted fatty acid synthesis regulator enzyme with selective pressure effect of selective chemical inhibitors was tried to be obtained. In addition, model eukaryotic yeast, *Saccharomyces cerevisiae*, was subjected to the same strategy for obtaining sterol

biosynthesis, fenpropimorph, resistant strain in order to assess the lipid synthesis response upon directed evolution application. Resistant strains were also whole-genome sequenced and increased lipid accumulation responsible genes were tried to be revealed.

## **4.2 Materials and Methods**

### **4.2.1 Semi-Quantitative RT-PCR Analysis of Fatty Acid Synthesis Genes under Nitrogen Depleted Cultivation Conditions**

#### **4.2.1.1 RNA isolation and RT Reaction**

Total RNA was isolated from approximately 100mg *Dunaliella salina* biomass using TRIzol reagent (Life Technologies) according to the manufacturer's instructions. One microgram of total RNA was reverse transcribed using Oligo dT primers (0.1 µg), 200 units M-MLV reverse transcriptase (Invitrogen), 40 units RNase inhibitor, 5 mM MgCl<sub>2</sub> and 1 mM dNTP mix, in a total volume of 20 µL. The reaction tube was first incubated at 25 °C for 10 min, followed by incubation at 37 °C for 50 min. The reaction was inactivated by heating at 70 °C for 15 min.

#### **4.2.1.2 Semi-Quantitative RT-PCR Analysis**

To assess the expression of BC: Biotin carboxylase; ACP: Acyl carrier protein; MCTK: Malonyl-CoA:ACP transacylase; KAS: 3-ketoacyl- ACP synthase; FATA: Acyl-ACP thioesterase; SAD: Stearoyl-ACP-desaturase; FAD: ω-3 fatty acid desaturase, ACT: Actin, 1 µL of the reverse transcription reaction was used as template in subsequent PCR reactions in 25 µL reaction volumes. Parameters for polymerase chain reaction were as follows: denaturation at 95°C for 60s, annealing at 55°C for 60s, and extension at 72°C for 60s for 27 cycles. PCR was performed with the addition of 8% dimethyl sulfoxide (DMSO). The sequence of the primers were shown in Table 3. PCR products were electrophoresed on 1% agarose gels and visualized by staining with ethidium bromide.

Gene name	Primers for real time PCR (5'--3')	Product length (bp)
BC	F CAAGAAGGTGATGATCGCCA R GACGTGCAGCGAGTTCTTGTC	120
ACP	F CAGCTCGGCACTGACCTTG R CAAGGGTCAGCTCGAACTTCTC	120
MCTK	F GGTGAGGACAAGGCGGTG R TCATCCTGGCCTTGAAGCTC	120
KAS	F CACCCCACTCTGAACCAGGA R GACCTCCAAACCCGAAGGAG	120
FATA	F AGACTCGTTCAGCGAGGAGC R CATGCCCACAGCATGGTTC	120
SAD	F CCGAGCCCAAGCTTCTAGTG R TTTGCCTCCATGTAATCCCC	120
FAD	F GTAGGTCACCACGTCCAGCC R CTTGATAGGCATGCTGGGTGT	120
ACT	F ACCTCAGCGTTCAGCCTTGT R TGGTCCACGACACCATCAAC	120

**Table 1.** Primers for semi-quantitative real time PCR in this study [20].

#### **4.2.2 Obtaining Fatty Acid Metabolism Specific Inhibitor Resistant Algae and Yeast Strains**

Specific chemical compounds that inhibit the fatty acid synthesis regulator enzyme Acetyl-CoA Carboxylase; quizalofop, diclofop, fenoxaprop have been assessed for their EC<sub>50</sub> values for *Dunaliella salina* KS\_01. After EC<sub>50</sub> doses were determined, cells were again treated and survival of the cells were assessed by using FDA fluorometric analysis with mentioned inhibitors for 24, 48 and 96 hours in order to confirm previously found EC<sub>50</sub> values. Cells then sub-cultured continuously with gradually increased concentrations beginning from the EC<sub>50</sub> of specific inhibitors for applying selective pressure on the algae cells until obtaining resistant strains. Resistant algae species were treated with the chemical inhibitors for two or three weeks long periods and measurements will be taken monitoring the lipid content of the algae. Nile Red (9-Diethylamino-5Hbenzo[alpha]phenoxazine-5-one) which is the most suitable dye for measurement of intracellular lipid content was used for monitoring cellular lipid accumulation of experimented algae during selective pressure applications.

Same strategy was used for obtaining sterol biosynthesis inhibitor, fenpropimorph, resistant *Saccharomyces cerevisiae* strains. After application of selective pressure on yeast using EC<sub>50</sub> of chemical inhibitor, fenpropimorph; resistant strains were selected and plated on inhibitor consisting YPD agar plates, single colonies were then picked and cultured in liquid media consisting EC<sub>50</sub> of chemical inhibitor for confirming the resistance. Then strains were sub-cultured at gradually increased concentrations of inhibitor for obtaining resistant strains. Nile Red staining was again used for analysis of lipid content of resistant yeast strains at the end of the one day cultivation of resistant strains.

#### **4.2.3 Flowcytometric Analysis of Lipid Content**

5 µl of Nile Red (Sigma, USA) from stock solution (0.5 mg/mL) was added to 1 ml of a cell suspension at an OD<sub>600</sub> of 0.3 after washing cells twice with fresh medium. This mixture was gently vortexed and incubated for 20 minutes at room temperature in dark. Nile Red uptake was determined using a BD-FACS Canto flow cytometer (Becton Dickinson Instruments) equipped with a 488 nm argon laser. Upon excitation by a 488 nm argon laser,

NR exhibits intense yellow-gold fluorescence when dissolved in neutral lipids. The optical system used in the FACS Canto collects yellow and orange light (560–640 nm, corresponding to neutral lipids). Approximately 10,000 cells were analysed using a log amplification of the fluorescent signal. Non-stained cells were used as an autofluorescence control. Nile Red fluorescence was measured using a 488 nm laser and a 556 LP+585/42 band pass filter set on a FACS Canto Flow Cytometer. Data were recorded as mean fluorescence intensity (MFI).

#### **4.2.4 Fluorometric Microplate Lipid Content Analysis**

A stock solution of Nile Red (NR) (Sigma, 72485) was prepared by adding 5 mg of NR to 10 ml of acetone. The solution was kept in a dark colored bottle and stored in the dark at -20 °C. 1 ml of algal cells from a culture of 250 ml glass erlenmeyer flasks containing 100 ml growth media with different nitrogen concentrations were transferred to 1.5 ml eppendorf tubes for 5 min centrifugation at 5,000 rpm, washed twice with fresh medium, and measured in a spectrophotometer at 600 nm. Each sample was adjusted to an OD<sub>600</sub> of 0.3 in a 1 ml final volume by dilution with fresh medium. 5µl of Nile Red solution was added to each tube and mixed well, followed by 20 min incubation in the dark. Finally, cellular neutral lipids were quantified using a 96-well microplate spectrofluorometry (SpectraMAX GEMINI XS) with an excitation wavelength of 485 nm and an emission wavelength of 612 nm.

#### **4.2.5 Fluorometric FDA Growth Kinetics Analysis**

Vital staining for determination of cell survival was done by using fluorescein diacetate (FDA) (Sigma, USA). 0.5 mg/ml stock solution was prepared in acetone. The solution was kept in a dark colored bottle and stored in the dark at -20 °C. 1 ml of algal cells from a culture of 250 ml glass erlenmeyer flasks containing 100 ml growth media were transferred to 1.5 ml eppendorf tubes for 5 min centrifugation at 5,000 rpm, washed twice with fresh medium, and measured in a spectrophotometer at 600 nm. Each sample was adjusted to an OD<sub>600</sub> of 0.3 in a 1 ml final volume by dilution with fresh medium. 5µl of FDA solution was added to each tube and mixed well, followed by 20 min incubation in the dark. Finally, cell survivals were quantified using a 96-well microplate spectrofluorometry (SpectraMAX GEMINI XS) with an excitation wavelength of 485 nm and an emission wavelength of 535 nm compared with non-treated control groups.

#### 4.2.6 Illumina Whole Genome Sequencing

Fenpropimorph resistant strain of *Saccharomyces cerevisiae* was isolated after ~150 generations of a Fenpropimorph continuous culture. Illumina sequencing libraries were constructed from the native and three resistant *Saccharomyces cerevisiae* genomic DNA following standard procedures instructed by the manufacturer. Briefly, 10 $\mu$ g of yeast genomic DNA were sonicated to fragment sizes below 2000 bp, concentrated and end-repaired using the End-It DNA repair kit (EPICENTRE Biotechnologies). End-repaired DNA was A-tailed with GoTaq DNA polymerase (Promega) and ligated to Illumina adapters (QuickLigase, NEB). Ligation products between 300-400 bp were excised from a 6% polyacrylamide gel, eluted and ethanol precipitated. Fragment libraries were PCR amplified, cleaned following AMPure (Agencourt) and Qiaquick PCR clean-up procedures, and submitted for sequencing.

#### 4.2.7 Analysis of Illumina Sequencing Data

We collected 14,555,852, 15,901,121, 14,432,333, 14,333,526, 14,465,222 single-end, 30 bp, quality-filtered reads from two native (C) and 3 resistant strains (A, B, C) respectively, using the Illumina Genome Analyzer II platform. Reads were aligned to the UCSC sacCer1 reference sequence using *Maq* with default parameters for single-end reads to a coverage of  $\geq 99.8\%$ . We filtered reads with low mapping quality (score  $< 10$ ) and obtained a final coverage of  $\geq 93.5\%$  with an average read-depth of 35 $\times$  and 28 $\times$  in the non-gap regions of the evolved and parental genomes, respectively.

For SNP-calling, we settled on a approach that required a nucleotide read depth  $\geq 6\times$  per position, with  $\geq 80\%$  base-calls supporting a SNP in the evolved genome data and  $\geq 5\times$  read depth, with  $\geq 70\%$  base-calls supporting a different base in the parental genome data. These nucleotide read depth thresholds allowed us to examine 90.99% of the mappable genome for SNPs. A parallel analysis relying on consensus base quality, quality of adjacent bases, and read mapping quality filters yielded similar SNP calls, but the fraction of the genome compliant with the analysis criteria was slightly reduced.

We searched for small insertions and deletions by performing gapped alignment (*BLAT*) of the *Maq*-unmapped reads to the reference genome and recovering coordinates at which multiple unmapped reads show a bipartite alignment -an alignment to flanking sequences- as the best alignment. Candidate indel coordinates were reduced to sets specific to the evolved or ancestor genome. These strain-specific, candidate indels were then refined to maintain sites at

which wild-type sequences are not observed in the *Maq*-alignment in the corresponding genome sequencing data, but are obtained in the comparison strain.

## 4.3 Results and Discussion

### 4.3.1 Semi-Quantitative RT-PCR Analysis of Fatty Acid Synthesis Genes under Nitrogen Depleted Cultivation Conditions in Algae

#### 4.3.1.1 Determination of Target Gene for Directed Evolution Experiments

Increasing effect of nitrogen starvation on lipid accumulation of algae species is well-known literature knowledge shown in previous studies many times [21]. In order to analyze potential alterations in gene expression under lipid accumulator stress factor, nitrogen depletion, we conducted semi-quantitative RT-PCR experiments on *Dunaliella salina KS\_01* hypersaline green microalgae. For this analysis, we screened eight different fatty acid synthesis genes namely, BC: Biotin carboxylase; ACP: Acyl carrier protein; MCTK: Malonyl-CoA: ACP transacylase; KAS: 3-ketoacyl- ACP synthase; FATA: Acyl-ACP thioesterase; SAD: Stearoyl-ACP-desaturase; FAD:  $\omega$ -3 fatty acid desaturase shown in Figure 3. According to results, all experimented genes were found to be over-expressed under nitrogen depleted conditions as shown in Figure 4. This suggests that nitrogen depletion results to increased lipid accumulation by altering expression of fatty acid synthesis genes. A recent study conducted with *Haematococcus pluvialis*, it was also demonstrated that various types of stress factors including nitrogen starvation, high temperature, iron deficiency leads to over-expression of fatty acid synthesis genes in a parallel manner of the findings obtained from this study [20]. This data might be important for the selection of potential genetic engineering and/or directed evolution targets of fatty acid synthesis pathway. We further selected BC: Biotin carboxylase enzyme for directed evolution studies due to availability of its specific chemical inhibitors. For other experimented enzymes, there are limited options for their chemical inhibitors. Even if there is a defined inhibitor, its specificity to that enzyme of interest is generally unclear. Owing to regulatory characteristics of biotin carboxylase in fatty acid synthesis, various studies were already conducted besides specific chemical inhibitors were clearly defined to the enzyme which are already used as herbicides for higher plants, especially against weed species. Therefore, because of regulatory characteristics and

availability of its specific inhibitors, our choice was biotin carboxylase enzyme for further directed evolution experiments.

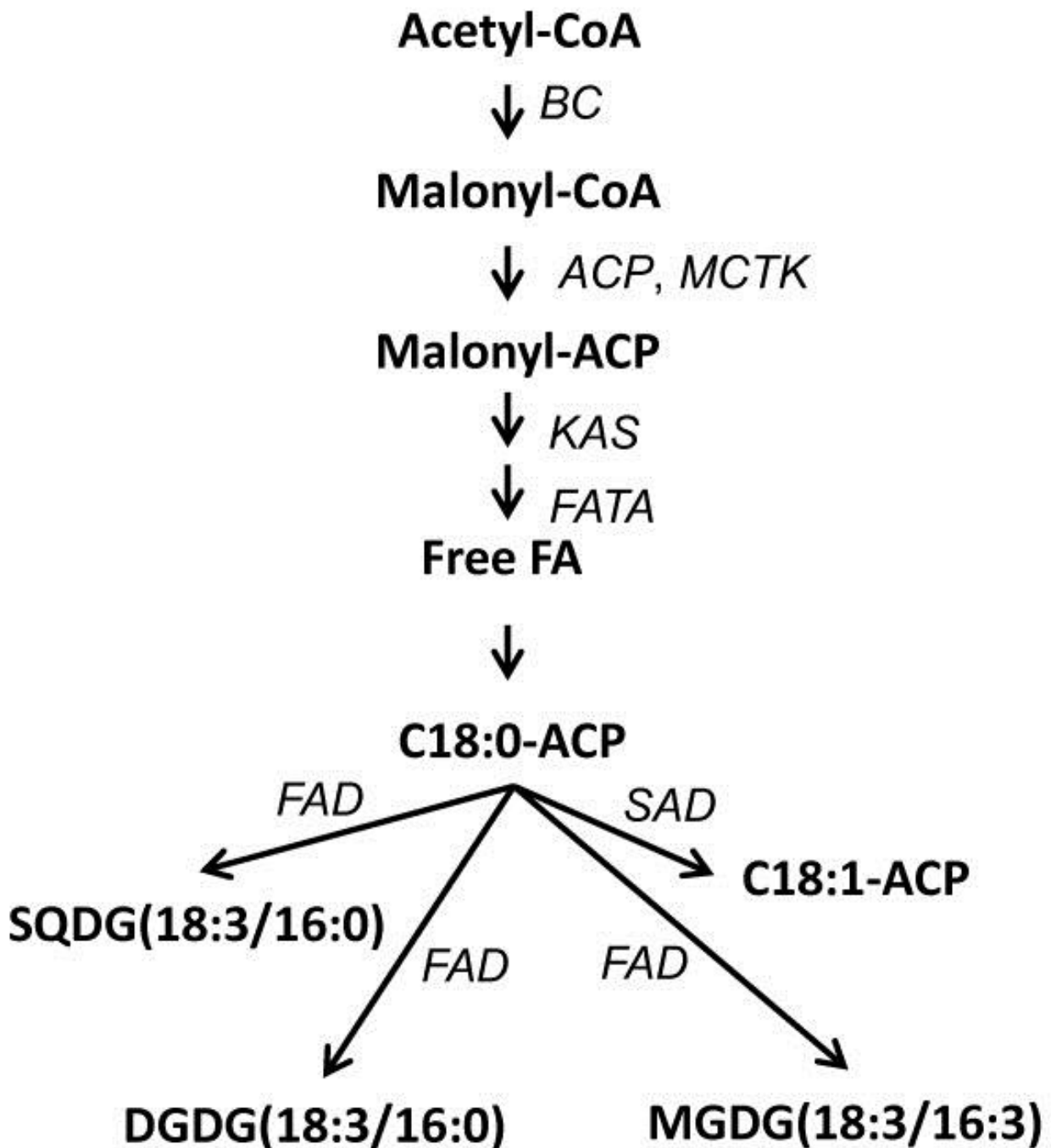


**Figure 3. Pathways of lipid biosynthesis and acyl chain desaturation which are known or hypothesized to occur in green microalgae.** The assignment of candidate genes encoding enzymes catalyzing the reactions were also shown in the diagram in this study Abbreviations: ACP, acyl

carrier protein; CoA, coenzyme A; DGDG, digalactosyldiacylglycerol; FA, fatty acid; MGDG, monogalactosyldiacylglycerol; SQDG, sulfoquinovosyldiacylglycerol [20].

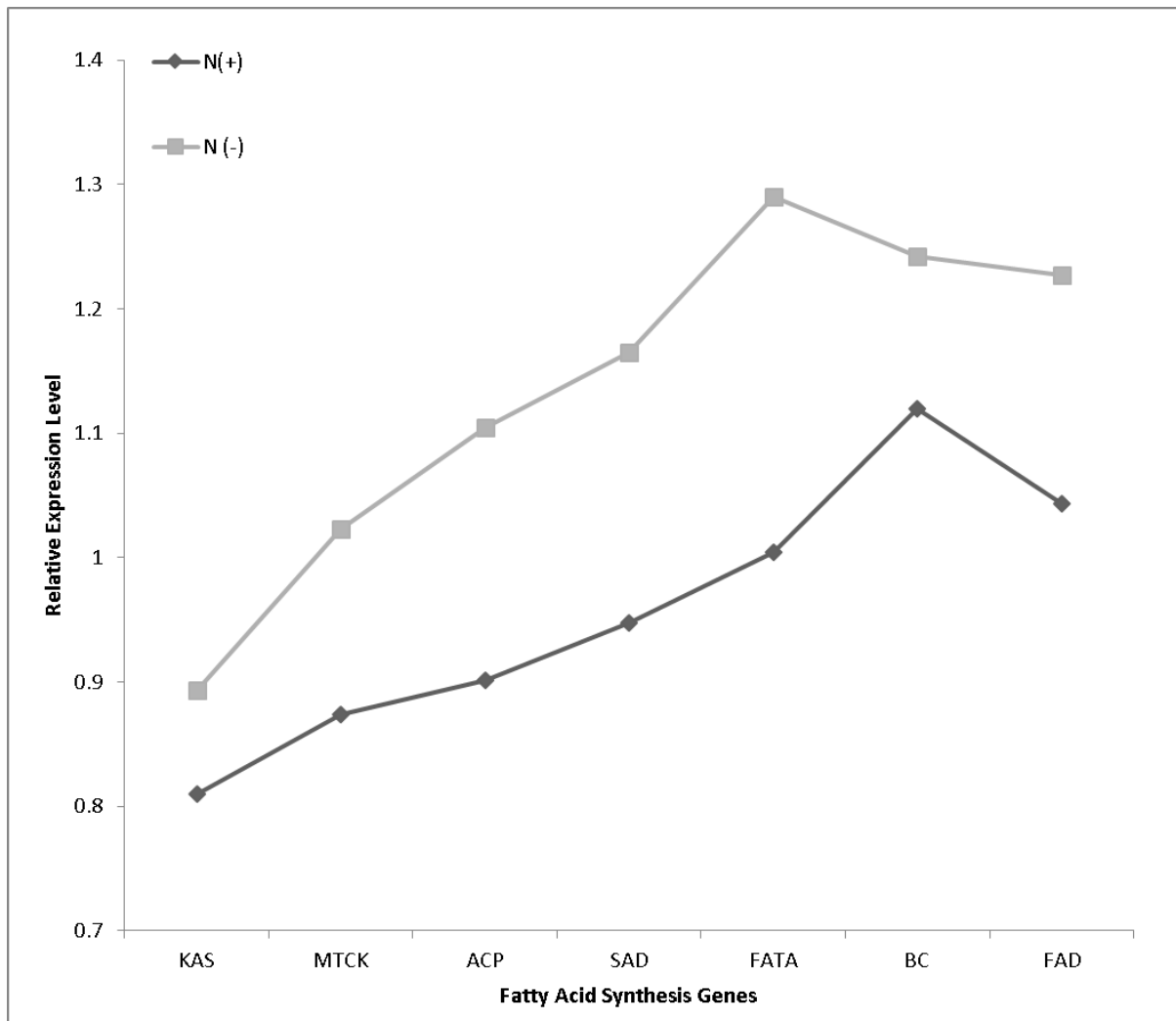


**Figure 4.** Semi-quantitative RT-PCR experiments on *Dunaliella salina* KS\_01 hypersaline green microalgae under nitrogen depleted conditions compared with normal cultivation conditions. BC: Biotin carboxylase; ACP: Acyl carrier protein; MCTK: Malonyl-CoA: ACP transacylase; KAS: 3-ketoacyl- ACP synthase; FATA: Acyl-ACP thioesterase; SAD: Stearoyl-ACP-desaturase; FAD:  $\omega$ -3 fatty acid desaturase.

### 4.3.2 Obtaining Acetyl-CoA Carboxylase Specific Inhibitor Quizalofob Resistant Algae Strains

Most essential step for the fatty acid biosynthetic pathway, Acetyl-CoA Carboxylase catalyzes the first committed step in fatty acid synthesis which converts acetyl-CoA to malonyl-CoA. Because of its rate-limiting role in lipid production, Acetyl-CoA Carboxylase has been studied for its potential on lipid biosynthesis, including some efforts to overexpression the native enzyme [6]. This was the first attempt to increase lipid accumulation by using a genetic engineering strategy in algae, but the success was limited due to the complex nature of the lipid biosynthesis in microorganisms. Direct genetic alterations needs complex understanding of the certain changes in gene expression interested, along with proper knowledge of precisely how those changes will contribute to the related phenotype. As such, first attempts by using targeted genetic manipulation which introducing extra copies of the Acetyl-CoA Carboxylase gene into *Cyclotella cryptica* for improving lipid synthesis, unfortunately have met with only limited success [5]. Instead of a specific, unpredictable genetic manipulations, applying a selective pressure to fatty acid synthetic pathway by using specific chemical inhibitors through phenotypic selection, directing the microorganism to independently change the related metabolic processes to increase lipid production was the new strategy we found shown in Figure 5.

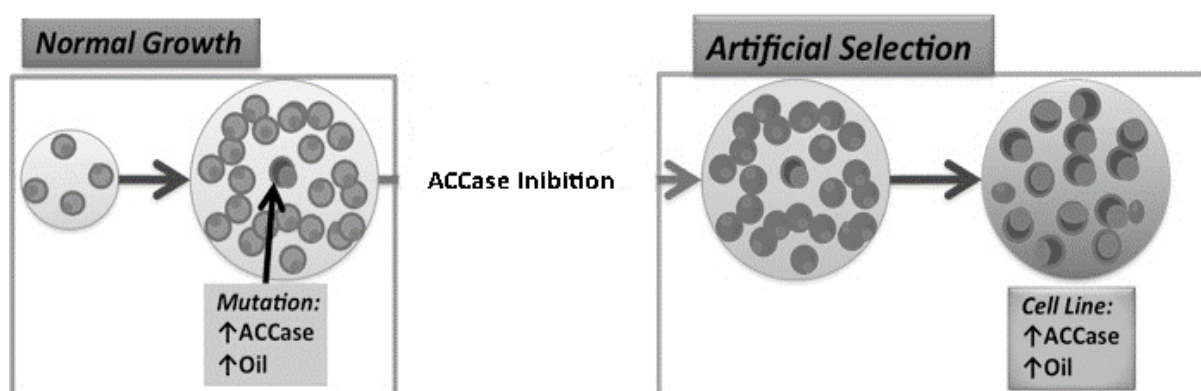


**Figure 5.** Selective pressure to fatty acid synthetic pathway by using specific chemical inhibitors through phenotypic selection.

Instead of direct genetic manipulation by transformation, this study used natural selection to achieve obtaining algae strains with increased cellular lipid accumulation. The

herbicide quizalofop inhibits Acetyl-CoA Carboxylase by competing for its binding site with acetyl-CoA. In order to cope with the stress, algae needs to increase the activity of Acetyl-CoA carboxylase, generating higher copy number of the related gene, increasing the expression level of the enzyme, modified the protein by post-translational modifications or other mechanisms not mentioned here to overcome impaired lipid production process. Hypothetically, subjecting algae populations with gradually increasing levels of Acetyl-CoA Carboxylase inhibitor would select for cells which can cope with the stress by increasing their lipid productivity by alterations mentioned above. Obtaining strains with Acetyl-CoA Carboxylase inhibitor resistance through artificial selection would then isolate populations with heightened activity or expression of Acetyl-CoA Carboxylase, with concomitant increases in lipid synthesis. A similar selection strategy was applied to foxtail millet cell cultures and resulted in strains with not only increased Acetyl-CoA Carboxylase gene expression, but with increased lipid accumulation [22].

After four weeks cultivation in 20 $\mu$ m, 40 $\mu$ m, 80 $\mu$ m concentrations of quizalofop consisting liquid media, we achieved selecting resistant/tolerant *Dunaliella* strain. As shown in Figure 6, first seven days, experimented *Dunaliella* cells cannot tolerate the inhibitor for all concentrations. But at the end of the cultivation, natural selection is occurred and resistant/tolerant cells overcome the inhibitor stress and can continue to proliferate.

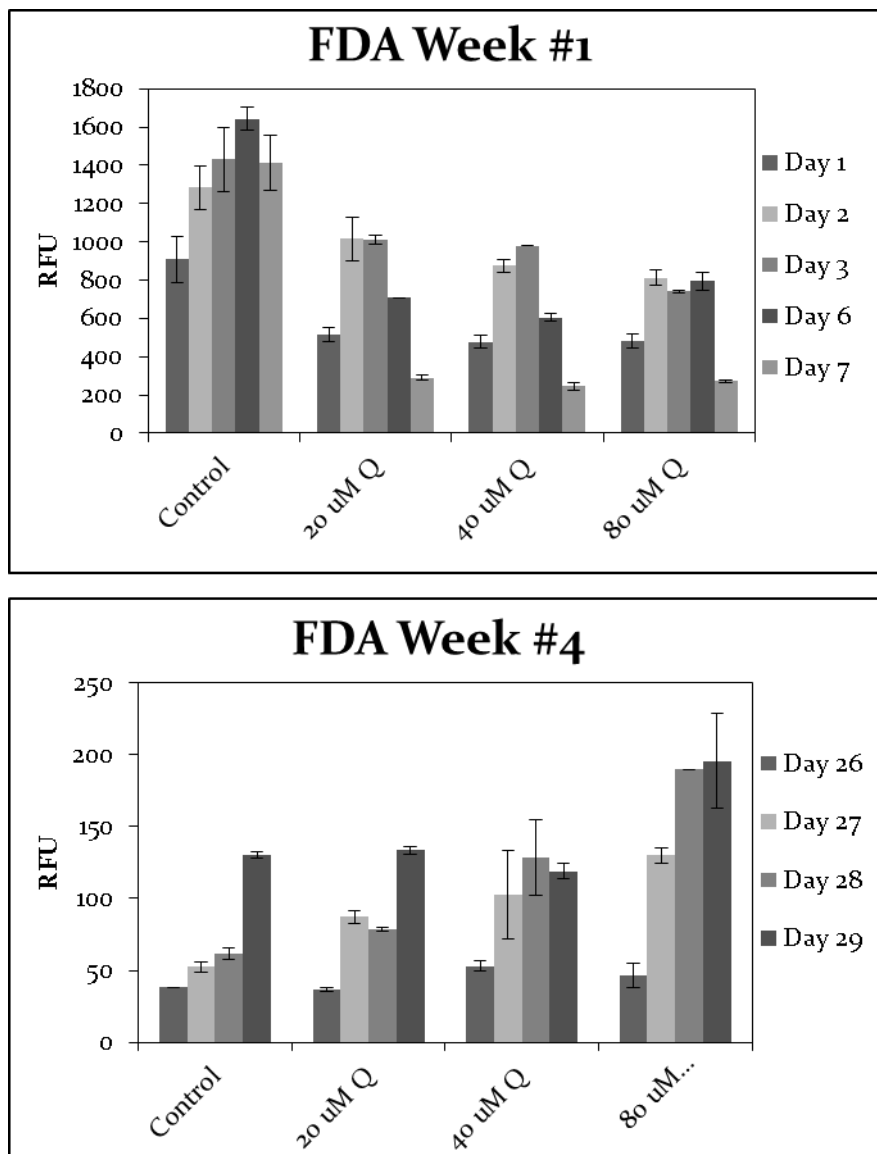


**Figure 6.** Selection of Acetyl-CoA carboxylase inhibitor quizalofob resistant/tolerant *Dunaliella salina* KS\_01 cells by application of selective pressure.

#### 4.3.3 Fluorometric Microplate and Flow-cytometric Nile Red Lipid Content Analysis of Acetyl-CoA Carboxylase Inhibitor Resistant Algae Strains

During four week cultivation period, lipid contents of experimented *Dunaliella salina* KS\_01 groups were analyzed in the first and the last week of cultivation course by using Nile red fluorometric methods shown in Figure 7. Previous results demonstrated that it is highly possible to select Acetyl-CoA carboxylase inhibitor, quizalofob resistant *Dunaliella salina* KS\_01 cells. Our main aim was to obtain quizalofob resistant *Dunaliella* cells with increased

cellular lipid accumulation. According to first measurement of lipid contents in the first cultivation week, it was confirmed that the lipid production was impaired with quizialofob as expected. According to the measurement of lipid contents in the last week of cultivation showed elevated levels of lipid accumulation in quizialofob resistant/tolerant *Dunaliella salina* KS\_01 cells compared to the non-treated control groups. This result may suggest that, *Dunaliella* cells survive by elevating their cellular lipid production upon Acetyl-CoA carboxylase inhibitor, quizialofob treatment.

Experiments were repeated with other acetyl-CoA carboxylase inhibitors namely diclofob and fenoxaprob. Findings supported the previous results obtained from quizialofob experiments. We found elevated levels of lipid accumulation in diclofob and fenoxaprob resistant/tolerant experimental groups compared to the non-treated control groups shown in Figure 8 and Figure 9, respectively. In addition we, interestingly realized that short cultivation periods with Acetyl-CoA carboxylase inhibitors, could be also used for selection of resistant/tolerant sub-populations. Moreover, this resistant sub-populations were also demonstrated with increased lipid contents as well. This observation suggest that, short cultivation periods with specific acetyl-CoA carboxylase inhibitors can be applied as a lipid over production strategy like nitrogen depletion or heating up culture temperatures.

We also conducted flow-cytometric Nile red lipid content analysis for analyzing cellular lipid accumulations at single cell level. Therefore, another reliable method would have supported our findings. According to results, all inhibitors result to increased cellular lipid accumulation at the end of the cultivation course even the period is very short (Figure 10).

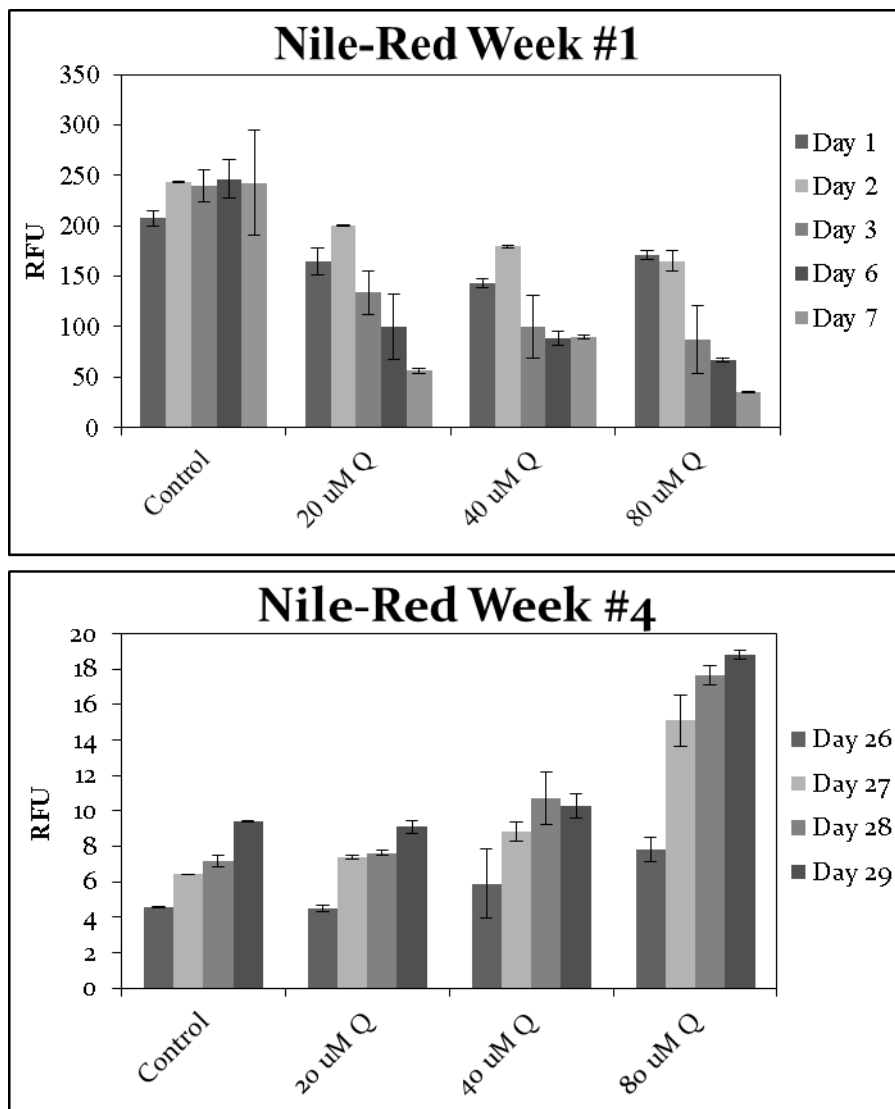


**Figure 7.** Nile red microplate fluorometric lipid content analysis of acetyl-CoA carboxylase inhibitor quizalofob resistant/tolerant *Dunaliella salina* KS\_01 cells upon application of selective pressure.

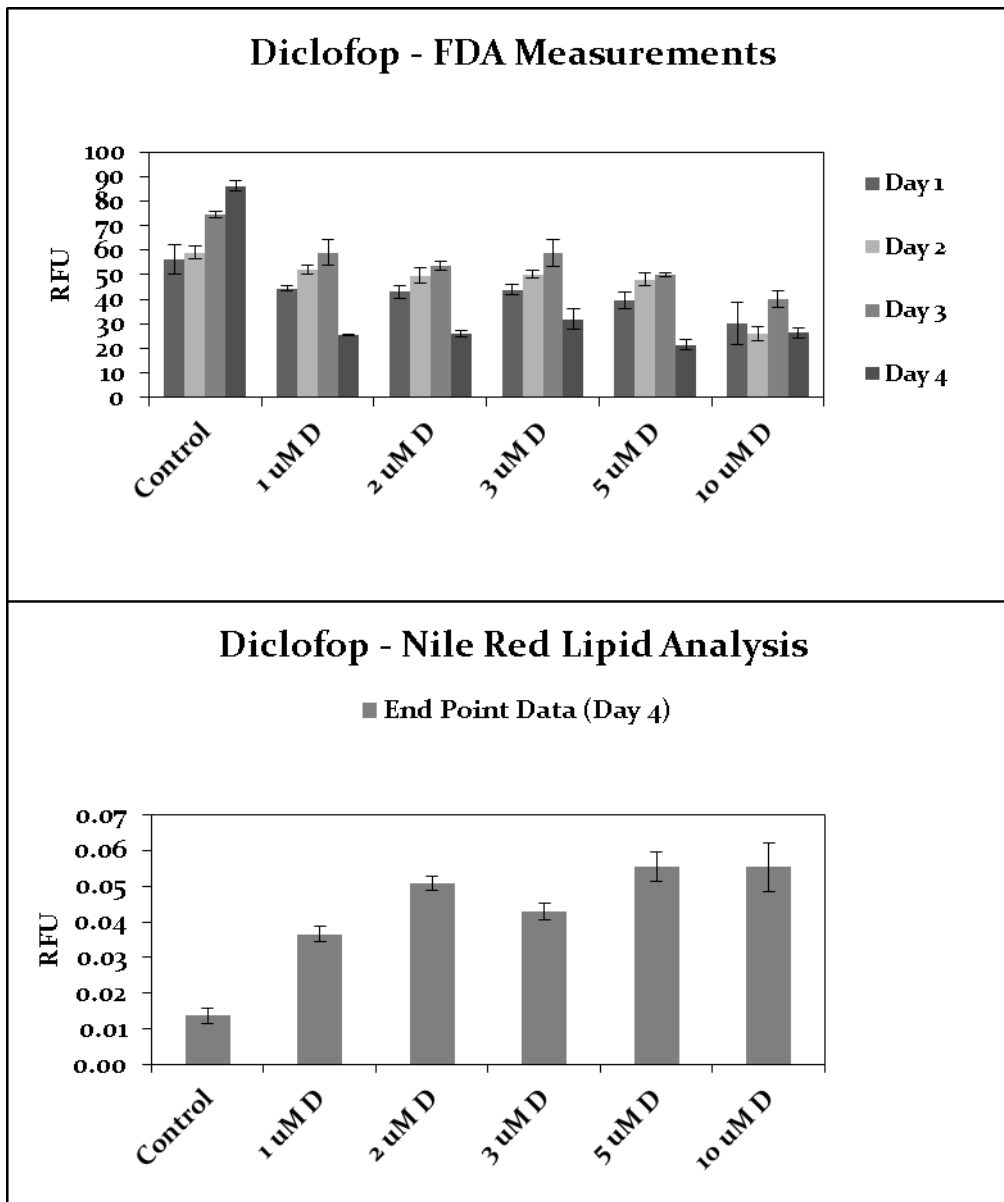


**Figure 8.** Growth and lipid content analysis of *Dunaliella salina* KS\_01 cells upon application of selective pressure with acetyl-CoA carboxylase inhibitor Diclofop.

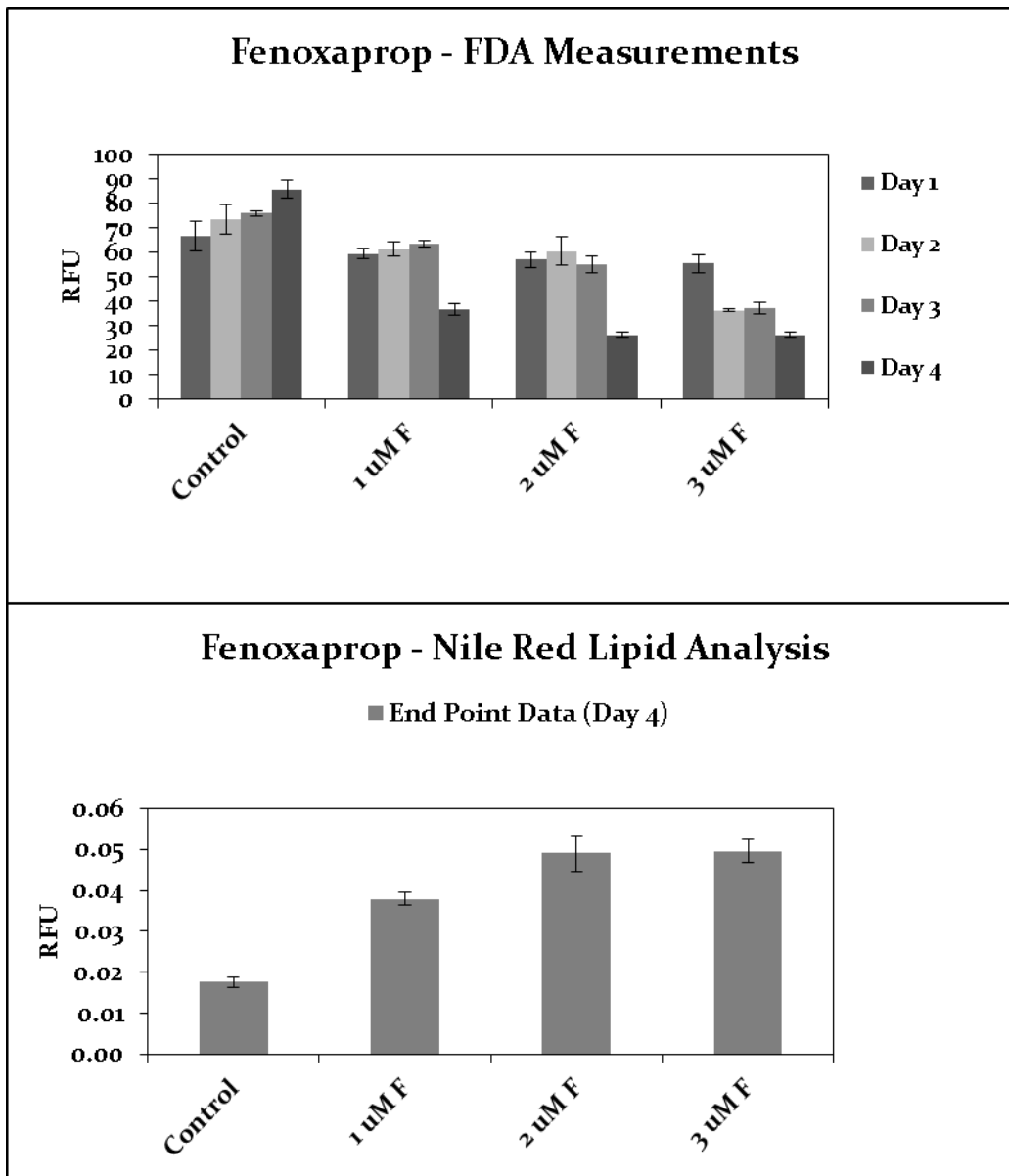


**Figure 9.** Growth and lipid content analysis of *Dunaliella salina* KS\_01 cells upon application of selective pressure with acetyl-CoA carboxylase inhibitor Fenoxaprop.

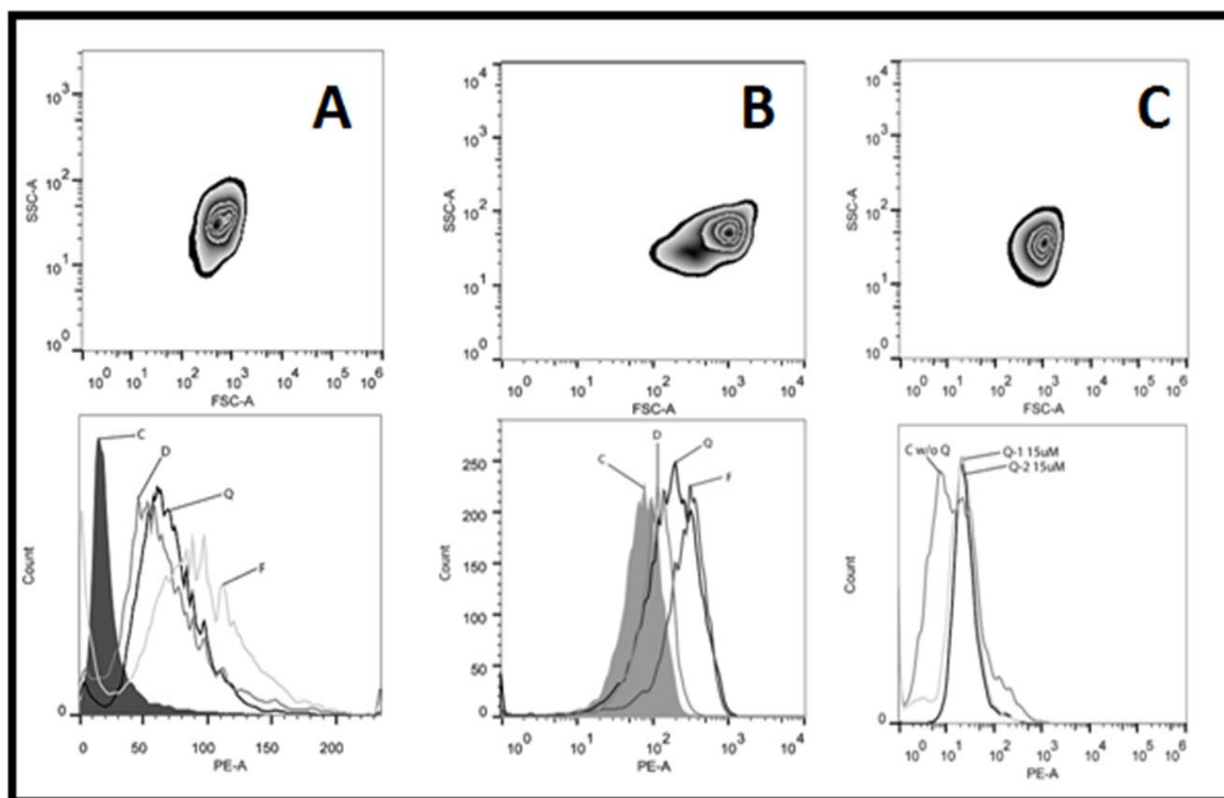


**Figure 10.** A) Nile red flow-cytometry analysis of lipid contents of *Dunaliella salina* KS\_01 cells upon application of selective pressures with acetyl-CoA carboxylase inhibitors Quizalofob, Diclofop and Fenoxaprop. Control groups (C), Quizalofob (Q), Diclofop (D) and Fenoxaprop (F) resistant cells on March, 2013. B) Control groups (C), Quizalofob (Q), and Diclofop (D) and Fenoxaprop (F) resistant cells on May, 2013. C) Control groups (C), Quizalofob (Q) resistant cells treated with 15µM Q and 20µM Q.

#### 4.3.4 Obtaining Ergosterol Biosynthesis Inhibitor, Fenpropimorph Resistant Yeast Strains

Continuous cultivation of wild-type *S. cerevisiae* in gradually increasing concentrations of fenpropimorph starting from its initial  $\frac{1}{2}$  MIC value for 3 to 4 weeks, resistant strains were selected by streak plating of remaining living cells upon drug treatment. Colonies were picked after overnight incubation on fenpropimorph consisting YPD agar plates and cultured in liquid YPD media overnight. Then cells were again subjected to MIC experiments to confirm their resistance to maximum concentration of previously found MIC value. All drugs namely benomyl (BEN), bromopyruvate (BRO), and dyclonine (DYC), fenpropimorph (FEN), and

haloperidol (HAL), methyl-methane sulfonate (MMS), pentamidine (PEN), rapamycin (RAP), staurosporine (STA), terbinafine (TER) and tunicamycin (TUN) were assessed for cross resistance and confirmation of resistance of the strains to different drugs besides their fenpropimorph resistance to obtain more information about underlying resistance mechanisms shown in Figure 11.

Dose-response experiments were conducted for 11 antifungal drugs in wild-type *S. cerevisiae* and three strains of *in-vitro* selected fenpropimorph-resistant *S. cerevisiae* (FenR-A, B, C). Resistance score is equal to the  $\log_2$  of resistant strain minimal inhibitory concentration (MIC) divided by wild type MIC for each drug. A score of +/- 0.35 corresponds to resistance or sensitivity, respectively. Strains A and C showed similar patterns of resistance, exhibiting no resistance to any drug in the panel besides fenpropimorph. Strains A and C showed increased sensitivity to dyclonine despite sharing the ERG2 drug target with fenpropimorph (ERG2 and ERG24). Strain A also showed sensitivity to tunicamycin and Strain C also showed sensitivity to pentamidine and rapamycin. Strain B showed evidence of multidrug-resistance, surviving in elevated concentrations of dyclonine, haloperidol, terbinafine and tunicamycin.

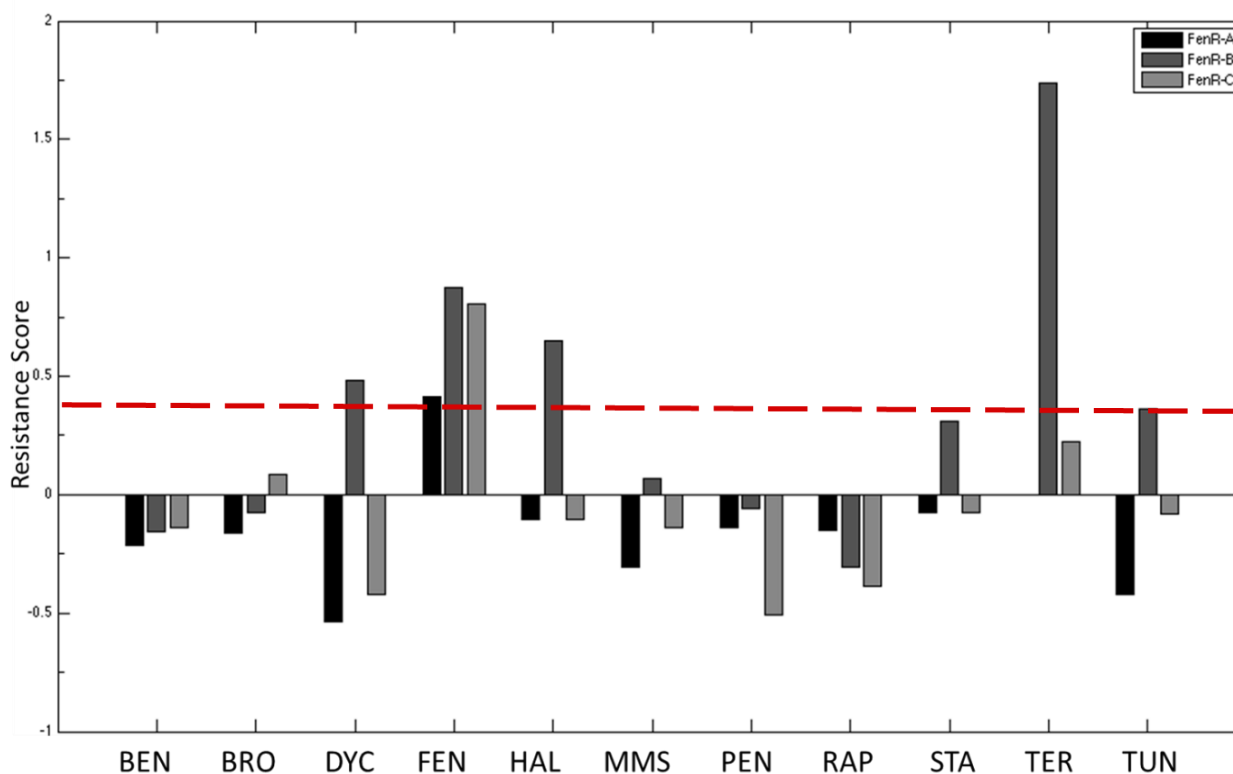


**Figure 11.** Cross-resistance of three Fenpropimorph-resistant strains.

As shown in Figure 11, all three strains demonstrated resistance to fenpropimorph besides multi-resistance characteristics of strain B. After successful selection of resistant strains, we analyzed lipid contents of the strain compared to non-resistant control groups.

Steryl esters and triacylglycerol (TAG) are the main storage lipids in eukaryotic cells. In the yeast *Saccharomyces cerevisiae*, these storage lipids accumulate during stationary growth phase within organelles known as lipid bodies. Lipids are important storage compounds in plants, animals, and fungi. The main storage lipids in eukaryotes are triacylglycerol (TAG) and steryl esters. Storage lipids are usually found within special organelles known as lipid particles or lipid bodies. In yeast, these lipid bodies accumulate during stationary phase, and they can constitute up to 70% of the total lipid content of the cell. Several lipid-metabolizing enzymes are preferentially localized to the lipid bodies in yeast, and it has therefore been proposed that they do not solely serve as a depot for lipids but instead may have a more complex role in lipid biosynthesis, metabolism, degradation, and trafficking.

Storage lipids, steryl esters, the esterified form of sterols linked to a long chain fatty acid, are synthesized by the enzyme acyl-CoA: sterol acyltransferase (ASAT) in the yeast,

*Saccharomyces cerevisiae*. We aimed to obtain main yeast sterol molecule, ergosterol, biosynthesis inhibitor resistant strains by applying a selective pressure to ergosterol synthesis pathway by using its specific chemical inhibitor, fenpropimorph, through phenotypic selection. By using this strategy, we aimed to direct the microorganism to independently change the related metabolic processes to increase overall lipid production by increasing storage steryl esters in order to achieve a new strategy for increasing lipid accumulation for biodiesel production.

#### **4.3.4.1 Flowcytometric Lipid Content Analysis of Resistant Yeast Strains**

Flow-cytometric analysis was conducted in order to assess cellular lipid contents of resistant yeast strains at single cell level compared to non-resistant control groups. According to results, resistance to ergosterol biosynthesis inhibitor, fenpropimorph resulted to increased cellular lipid accumulation as shown in Figure 12.

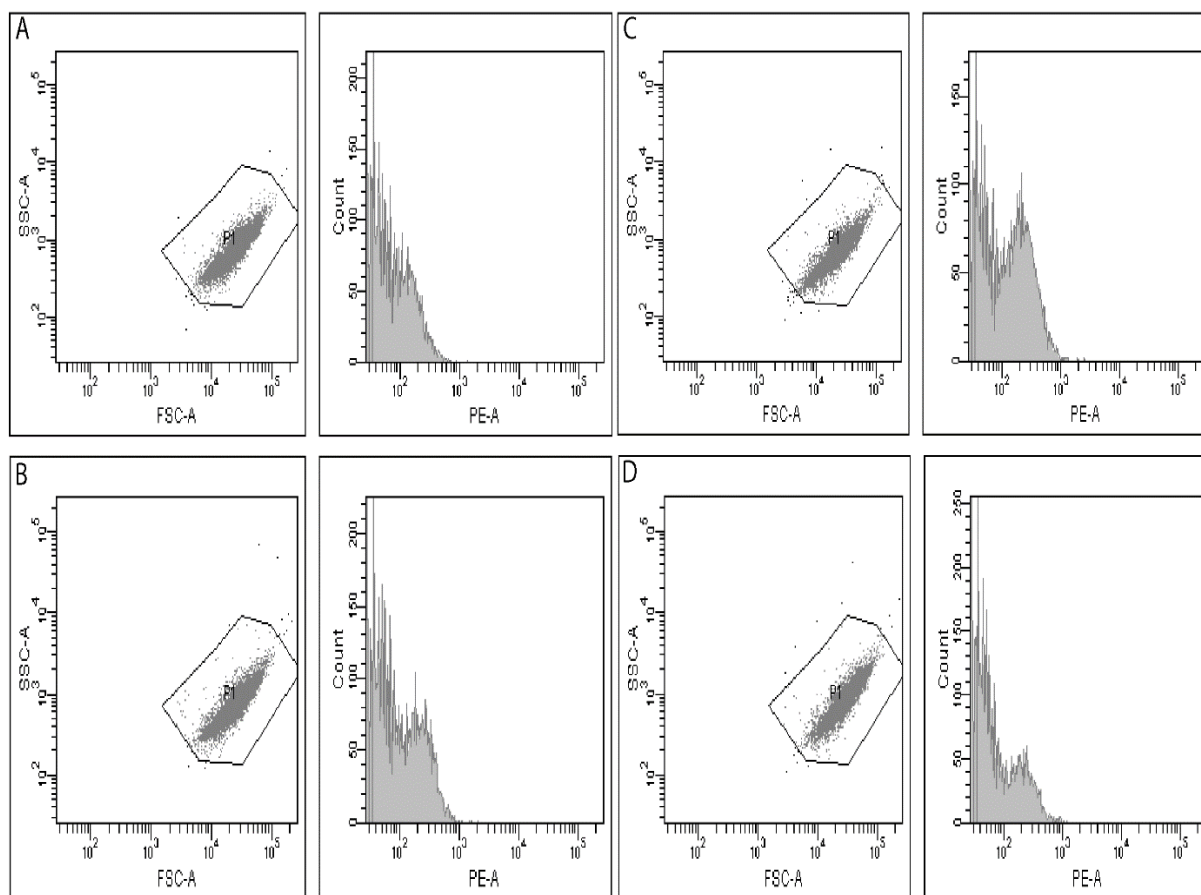


**Figure 12.** Flow-cytometric lipid content analysis of fenpropimorph resistant yeast strains. A, B, C, D is demonstrating; non-resistant control, resistant A strain, resistant B strain and resistant C strain respectively.

#### 4.3.4.2 Illumina Sequencing Data Analysis

##### 4.3.4.2.1 Finding Candidate Genes which might be Responsible for Increased Lipid Accumulation in Fenpropimorph Resistant Yeast Strains

According to flow-cytometric lipid content analysis of resistant yeast strains, A and especially B strains showed increased cellular lipid accumulation response compared to resistant C strain and non-resistant control groups. In order to find potential genes responsible for the increase in lipid production, we conducted whole genome sequencing analysis of wild type non-resistant and resistant A, B, C strains.

#### 4.3.4.2.1.1 *Saccharomyces cerevisiae* FENR-A Strain Whole Genome Sequence Analysis

Mutations were manually analyzed. Mutation quality scores, FQ, obtained from reference strain gene alignment and sequence analysis were set over -90 which is defined as the mutations have strong signals. After removing background mutations which are presented in wild-type non-resistant control strain. Remaining mutations were analyzed by using UCSC Genome Browser (<http://genome.ucsc.edu>).

For fenpropimorph resistant A strain, mutation analysis is given as following:

##### 1-Description:

Lectin-like protein with similarity to Flo1p, thought to be expressed and involved in flocculation

**Transcript (Including UTRs) Position:** chrI:24,000-27,968 **Size:** 3,969

**Total Exon Count:** 1 **Strand:** - **Coding Region Position:** chrI: 24,000-27,968 **Size:** 3,969 **Coding Exon Count:** 1

**Mutation 1:** 25506, C, T SNP

**Mutation 2:** 27099, T, C SNP

**ID:** FLO9\_YEAST

**DESCRIPTION:** RecName: Full=Flocculation protein FLO9; Short=Flocculin-9; Flags: Precursor;

**FUNCTION:** Cell wall protein that participates directly in adhesive cell-cell interactions during yeast flocculation, a reversible, asexual and Ca(2+)-dependent process in which cells adhere to form aggregates (flocs) consisting of thousands of cells. The lectin-like protein sticks out of the cell wall of flocculent cells and selectively binds mannose residues in the cell walls of adjacent cells.

**SUBCELLULAR LOCATION:** Secreted, cell wall (Probable). Membrane; Lipid-anchor, GPI-anchor (Potential). Note=Covalently-linked GPI- modified cell wall protein (GPI-CWP).

**DOMAIN:** The number of the intragenic tandem repeats varies between different *S.cerevisiae* strains. There is a linear correlation between protein size and extend of adhesion: the more repeats, the stronger the adhesion properties and the greater the

fraction of flocculating cells (By similarity). The Ser/Thr-rich repeats are also important for proper cell wall targeting of the protein.

**PTM:** The GPI-anchor is attached to the protein in the endoplasmic reticulum and serves to target the protein to the cell surface. There, the glucosamine-inositol phospholipid moiety is cleaved off and the GPI-modified mannoprotein is covalently attached via its lipidless GPI glycan remnant to the 1, 6-beta-glucan of the outer cell wall layer (By similarity).

**SIMILARITY:** Belongs to the flocculin family.

**2- Description:** Protein similar to mammalian oxysterol-binding protein contains ankyrin repeats localizes to the Golgi and the nucleus-vacuole junction

**Transcript (Including UTRs) Position:** chrI: 192,619-196,185 **Size:** 3,567

**Total Exon Count:** 1 **Strand:** +

**Coding Region Position:** chrI: 192,619-196,185 **Size:** 3,567 **Coding Exon Count:** 1

**Mutation:** 194513, TAAAA, TAAAAA INDEL

**ID:** OSH1\_YEAST

**DESCRIPTION:** RecName: Full=Oxysterol-binding protein homolog 1;

**FUNCTION:** Lipid-binding protein involved in maintenance of intracellular sterol distribution and homeostasis. Binds to phosphoinositides. May be involved in formation of PMN vesicles by altering the membrane lipid composition.

**SUBUNIT:** Interacts with NVJ1.

**SUBCELLULAR LOCATION:** Cytoplasm. Golgi apparatus membrane. Nucleus outer membrane. Note=Soluble protein that accumulates on the surface of late Golgi membranes and at nucleus-vacuole (NV) junctions, interorganelle interfaces between the nuclear envelope and the vacuole membrane formed during piecemeal microautophagy of the nucleus (PMN). Targeted exclusively to NV junctions in stationary phase.

**DOMAIN:** The ankyrin repeats are required for targeting the protein to the NV junction.

**DOMAIN:** The PH domain is required for targeting the protein to the late Golgi.

**DOMAIN:** The FFAT motif is required for interaction with SCS2 and proper localization of the protein.

**SIMILARITY:** Belongs to the OSBP family.

**SIMILARITY:** Contains 3 ANK repeats.

**SIMILARITY:** Contains 1 PH domain.

**3-Description:** Vacuolar membrane antiporter with Ca<sup>2+</sup>/H<sup>+</sup> and K<sup>+</sup>/H<sup>+</sup> exchange activity, involved in control of cytosolic Ca<sup>2+</sup> and K<sup>+</sup> concentrations has similarity to sodium/calcium exchangers, including the bovine Na<sup>+</sup>/Ca<sup>2+</sup>,K<sup>+</sup> antiporter

**Transcript (Including UTRs) Position:** chrIV:232,652-233,887 **Size:** 1,236 **Total Exon Count:** 1 **Strand:** +

**Coding Region Position:** chrIV: 232,652-233,887 **Size:** 1,236 **Coding Exon Count:** 1

**Mutation:** 233330, G, A SNP

**ID:** VCX1\_YEAST

**DESCRIPTION:** RecName: Full=Vacuolar calcium ion transporter; AltName: Full=High copy number undoes manganese protein 1; AltName: Full=Manganese resistance 1 protein; AltName: Full=Vacuolar Ca (2+)/H (+) exchanger;

**FUNCTION:** Has a role in promoting intracellular calcium ion sequestration via the exchange of calcium ions for hydrogen ions across the vacuolar membrane. Involved also in manganese ion homeostasis via its uptake into the vacuole.

**SUBCELLULAR LOCATION:** Vacuole membrane; Multi-pass membrane protein.

**MISCELLANEOUS:** Present with 7770 molecules/cell in log phase SD medium.

**SIMILARITY:** Belongs to the sodium/potassium/calcium exchanger family.

**4- Description:** NADP-cytochrome P450 reductase involved in ergosterol biosynthesis associated and coordinately regulated with Erg11p

**Transcript (Including UTRs) Position:** chrVIII:190,543-192,618 **Size:** 2,076

**Total Exon Count:** 1 **Strand:** +

**Coding Region Position:** chrVIII:190,543-192,618 **Size:** 2,076

**Coding Exon Count:** 1

**Mutation:** 190623, C, A SNP

**ID:** NCPR\_YEAST

**DESCRIPTION:** RecName: Full=NADPH--cytochrome P450 reductase; Short=CPR; Short=P450R; EC=1.6.2.4;

**FUNCTION:** This enzyme is required for electron transfer from NADP to

cytochrome P450 in microsomes. It can also provide electron transfer to heme oxygenase and cytochrome B5. Involved in ergosterol biosynthesis. Has NADPH-dependent ferrireductase activity on the plasma membrane.

**CATALYTIC ACTIVITY:** NADPH + n oxidized hemoprotein = NADP(+) + n reduced hemoprotein.

**COFACTOR:** Binds 1 FAD per monomer.

**COFACTOR:** Binds 1 FMN per monomer.

**BIOPHYSICOCHEMICAL PROPERTIES:** Kinetic parameters:  $K_M=1.59$   $\mu\text{M}$  for cytochrome c;  $K_M=1.46$   $\mu\text{M}$  for NADPH; Note=The  $V_{\text{max}}$  of the reaction is 721 pmol/min/pmol enzyme towards cytochrome c, and 662 pmol/min/pmol enzyme toward NADPH;

**SUBUNIT:** Interacts with PCL1.

**SUBCELLULAR LOCATION:** Endoplasmic reticulum membrane; Single-pass membrane protein. Mitochondrion outer membrane; Single-pass membrane protein. Cell membrane; Single-pass membrane protein. Microsome.

**INDUCTION:** By galactose and on the plasma membrane by iron or copper deficiency. Repressed by glucose.

**PTM:** Phosphorylated by the cyclin-CDK PCL1-PHO85.

**DISRUPTION PHENOTYPE:** Accumulates 20% of ergosterol of wild type.

**MISCELLANEOUS:** Present with 46600 molecules/cell in log phase SD medium.

**SIMILARITY:** In the C-terminal section; belongs to the flavoprotein pyridine nucleotide cytochrome reductase family.

**SIMILARITY:** Contains 1 FAD-binding FR-type domain.

**SIMILARITY:** Contains 1 flavodoxin-like domain.

- 5- Description:** Putative protein of unknown function YPL216W is not an essential gene  
**Transcript (Including UTRs) Position:** chrXVI:143,821-147,129 **Size:** 3,309 **Total Exon Count:** 1 **Strand:** +  
**Coding Region Position:** chrXVI: 143,821-147,129 **Size:** 3,309  
**Coding Exon Count:** 1  
**Mutation:** 144717, GGAAACGTCA, G INDEL  
**ID:** YP216\_YEAST  
**DESCRIPTION:** RecName: Full=Putative ISWI chromatin-remodeling complex

subunit YPL216W;

**FUNCTION:** May be required for the activity of an ISWI chromatin- remodeling complex (By similarity).

**SUBCELLULAR LOCATION:** Nucleus (By similarity).

**MISCELLANEOUS:** Present with 3060 molecules/cell in log phase SD medium.

**SIMILARITY:** Contains 1 DDT domain.

**SIMILARITY:** Contains 1 WAC domain.

#### 4.3.4.2.1.2 *Saccharomyces cerevisiae* FENR-B Strain Whole Genome Sequence Analysis

Mutations were manually analyzed. Mutation quality scores, FQ, obtained from reference strain gene alignment and sequence analysis were set over -90 which is defined as the mutations have strong signals. After removing background mutations which are presented in wild-type non-resistant control strain. Remaining mutations were analyzed by using UCSC Genome Browser (<http://genome.ucsc.edu>).

For fenpropimorph resistant B strain, mutation analysis is given as following:

**1- Description:** Sphinganine C4-hydroxylase, catalyses the conversion of sphinganine to phytosphingosine in sphingolipid biosynthesis.

**Transcript (Inc. UTRs) Position:** chrIV: 1,056,551-1,057,600 **Size:** 1,050

**Total Exon Count:** 1 **Strand:** +

**Coding Region Position:** chrIV: 1,056,551-1,057,600 **Size:** 1,050

**Coding Exon Count:** 1

**Mutation:** 1056577, AG, A INDEL

**ID:** SUR2\_YEAST

**DESCRIPTION:** RecName: Full=Sphingolipid C4-hydroxylase SUR2; EC=1.-.-.;  
AltName: Full= Syringomycin response protein 2;

**FUNCTION:** Required for hydroxylation of C-4 in the sphingoid moiety of ceramide  
Involved in the response to syringomycin.

**PATHWAY:** Membrane lipid metabolism; sphingolipid bio-synthesis.

**SUBCELLULAR LOCATION:** Endoplasmic reticulum membrane; Multi-pass membrane protein (Probable).

**MISCELLANEOUS:** Present with 54300 molecules/cell in log phase SD medium.

**SIMILARITY:** Belongs to the sterol desaturase family.

#### 4.3.4.2.1 *Saccharomyces cerevisiae* FENR-C Strain Whole Genome Sequence Analysis

- 1- **Description:** Lectin-like protein with similarity to Flo1p, thought to be expressed and involved in flocculation

**Transcript (Including UTRs) Position:** chrI: 24,000-27,968 **Size:** 3,969

**Total Exon Count:** 1 **Strand:** -

**Coding Region Position:** chrI: 24,000- 27,968 **Size:** 3,969

**Coding Exon Count:** 1

**Mutation 1:** 25506, C, T SNP

**Mutation 2:** 27099, T, C SNP

**ID:** FLO9\_YEAST

**DESCRIPTION:** RecName: Full=Flocculation protein FLO9;

**FUNCTION:** Cell wall protein that participates directly in adhesive cell-cell interactions during yeast flocculation, a reversible, asexual and Ca(2+)-dependent process in which cells adhere to form aggregates (flocs) consisting of thousands of cells. The lectin-like protein sticks out of the cell wall of flocculent cells and selectively binds mannose residues in the cell walls of adjacent cells.

**SUBCELLULAR LOCATION:** Secreted, cell wall (Probable). Membrane; Lipid-anchor, GPI-anchor (Potential). Note=Covalently-linked GPI- modified cell wall protein (GPI-CWP).

**DOMAIN:** The number of the intragenic tandem repeats varies between different *S.cerevisiae* strains. There is a linear correlation between protein size and extend of adhesion: the more repeats, the stronger the adhesion properties and the greater the fraction of flocculating cells (By similarity). The Ser/Thr-rich repeats are also important for proper cell wall targeting of the protein.

**PTM:** The GPI-anchor is attached to the protein in the endoplasmic reticulum and serves to target the protein to the cell surface. There, the glucosamine-inositol phospholipid moiety is cleaved off and the GPI-modified mannoprotein is covalently attached via its lipidless GPI glycan remnant to the 1, 6-beta-glucan of the outer cell wall layer (By similarity).

**SIMILARITY:** Belongs to the flocculin family.

**2- Description:** Protein similar to mammalian oxysterol-binding protein contains ankyrin repeats localizes to the Golgi and the nucleus-vacuole junction

**Transcript (Including UTRs) Position:** chrI: 192,619-196,185 **Size:** 3,567

**Total Exon Count:** 1 **Strand:** +

**Coding Region Position:** chrI: 192,619-196,185 **Size:** 3,567 **Coding**

**Exon Count:** 1

**Mutation:** 194513, TAAAA, TAAAAA INDEL

**ID:** OSH1\_YEAST

**DESCRIPTION:** RecName: Full=Oxysterol-binding protein homolog 1;

**FUNCTION:** Lipid-binding protein involved in maintenance of intracellular sterol distribution and homeostasis. Binds to phosphoinositides. May be involved in formation of PMN vesicles by altering the membrane lipid composition.

**SUBUNIT:** Interacts with NVJ1.

**SUBCELLULAR LOCATION:** Cytoplasm. Golgi apparatus membrane. Nucleus outer membrane. Note=Soluble protein that accumulates on the surface of late Golgi membranes and at nucleus-vacuole (NV) junctions, interorganelle interfaces between the nuclear envelope and the vacuole membrane formed during piecemeal microautophagy of the nucleus (PMN). Targeted exclusively to NV junctions in stationary phase.

**DOMAIN:** The ankyrin repeats are required for targeting the protein to the NV junction.

**DOMAIN:** The PH domain is required for targeting the protein to the late Golgi.

**DOMAIN:** The FFAT motif is required for interaction with SCS2 and proper localization of the protein.

**SIMILARITY:** Belongs to the OSBP family.

**SIMILARITY:** Contains 3 ANK repeats.

**SIMILARITY:** Contains 1 PH domain.

**3- Description:** No description available

**Transcript (Including UTRs) Position:** chrXVI:

101,608- 102,702 **Size:** 1,095 **Total**

**Exon Count:** 1 **Strand:** -

**Coding Region Position:** chrXVI: 101,608-102,702 **Size:** 1,095

**Coding Exon Count:** 1

**Mutation:** 102464, GA, G INDEL

**ID:** KP236\_YEAST

**DESCRIPTION:** RecName: Full=Serine/threonine-protein kinase  
YPL236C; EC=2.7.11.1;

**CATALYTIC ACTIVITY:** ATP + a protein = ADP + a phosphoprotein.

**SUBCELLULAR LOCATION:** Vacuole membrane; Peripheral membrane protein.

**SIMILARITY:** Belongs to the protein kinase superfamily. Ser/Thr protein kinase family.

**SIMILARITY:** Contains 1 protein kinase domain.

In order to propose a possible hypothesis for increased lipid accumulation in fenpropimorph resistant B strain, we analyze sphingolipid biosynthesis pathway. SUR2 gene which encodes sphinganine C4-hydroxylase enzyme, catalyses the conversion of sphinganine to phytosphingosine in sphingolipid biosynthesis shown in Figure 13. Deletion mutation of SUR2 gene might have taken an important role in increased lipid accumulation response since one of the major branches of the pathway is highly related to palmitate biosynthesis. Downstream blockage of dihydroshingosine conversion into phytosphingosine may result in increased palmitate biosynthesis in order to rescue the sphingolipid synthesis which in turn results in lipid over-accumulation since palmitate is one of the most abundant fatty acid types in eukaryotic cells.

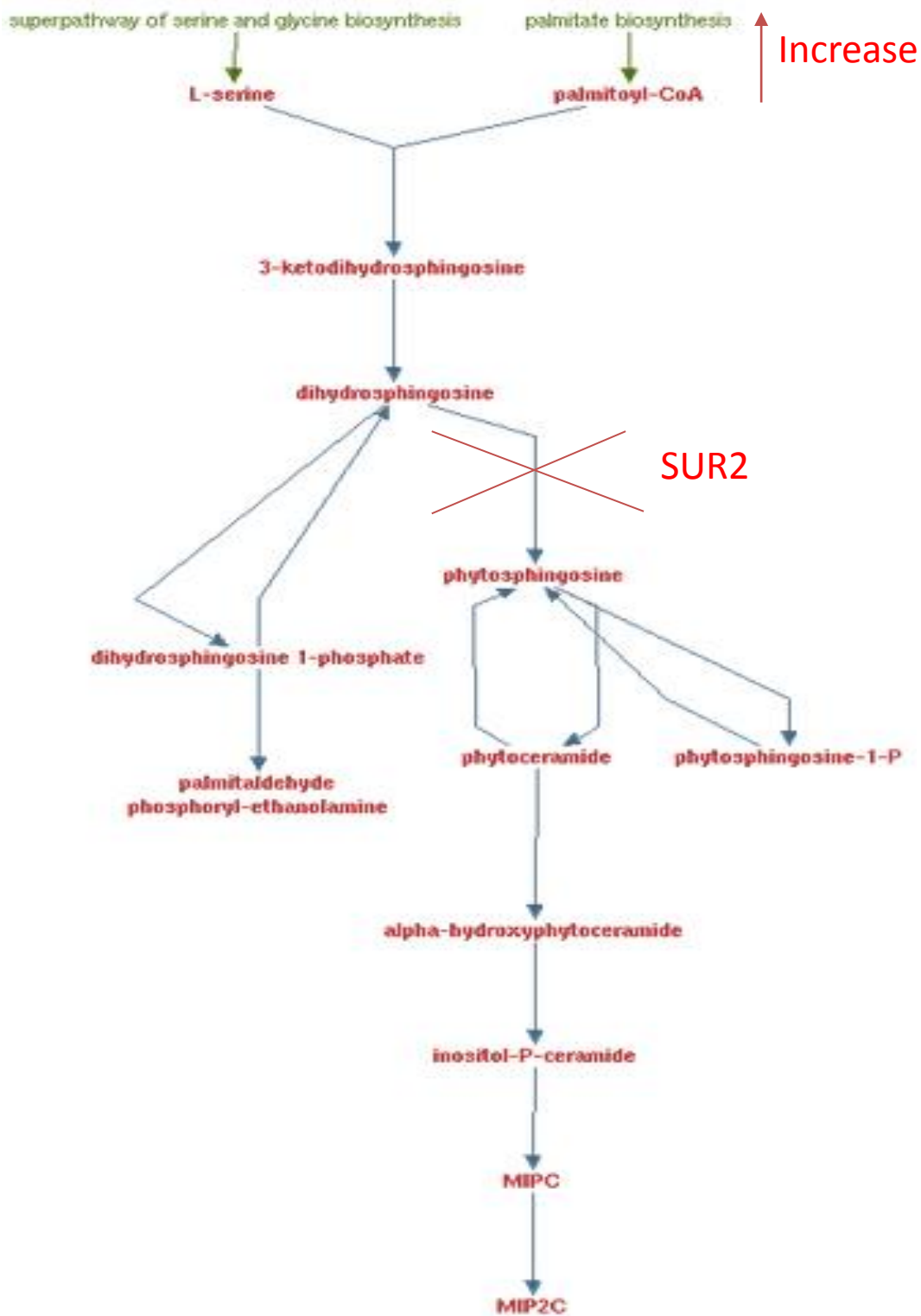


**Figure 13.** Sphingolipid biosynthesis pathway. Hypothesis for increased lipid accumulation response of fenpropimorph resistant *Saccharomyces cerevisiae*

## REFERENCES

### CHAPTER 1

1. Field CB, Behrenfeld MJ, Randerson JT, Falkowski P (1998) Primary production of the biosphere: integrating terrestrial and oceanic components. *Science* 281: 237-240.
2. Christaki E, Karatzia M, Florou-Paneri P (2010) The use of algae in animal nutrition. *Journal of the Hellenic Veterinary Medical Society* 61: 267-276.
3. Pulz O, Gross W (2004) Valuable products from biotechnology of microalgae. *Applied Microbiology and Biotechnology* 65: 635-648.
4. Benemann J (2013) Microalgae for Biofuels and Animal Feeds. *Energies* 6: 5869-5886.
5. Spolaore P, Joannis-Cassan C, Duran E, Isambert A (2006) Commercial applications of microalgae. *Journal of Bioscience and Bioengineering* 101: 87-96.
6. Chojnacka K (2009) Technological use of algae in the food and chemical industries. *Przemysl Chemiczny* 88: 414-418.
7. Rao AR, Baskaran V, Sarada R, Ravishankar GA (2013) In vivo bioavailability and antioxidant activity of carotenoids from microalgal biomass - A repeated dose study. *Food Research International* 54: 711-717.
8. Chisti Y (2007) Biodiesel from microalgae. *Biotechnol Adv* 25: 294-306.
9. Ziolkowska JR, Simon L (2014) Recent developments and prospects for algae-based fuels in the US. *Renewable & Sustainable Energy Reviews* 29: 847-853.
10. Gressel J (2008) Transgenics are imperative for biofuel crops. *Plant Science* 174: 246-263.
11. Huber GW, Dale BE (2009) Grassoline at the Pump. *Scientific American* 301: 52-56.
12. Guschina IA, Harwood JL (2006) Lipids and lipid metabolism in eukaryotic algae. *Progress in Lipid Research* 45: 160-186.
13. Hu Q, Sommerfeld M, Jarvis E, Ghirardi M, Posewitz M, et al. (2008) Microalgal triacylglycerols as feedstocks for biofuel production: perspectives and advances. *Plant Journal* 54: 621-639.
14. Bahadar A, Khan MB (2013) Progress in energy from microalgae: A review. *Renewable & Sustainable Energy Reviews* 27: 128-148.

15. Yildiz M, Soganci AS (2010) Evaluation of geotechnical properties of the salt layers on the Lake Tuz. *Scientific Research and Essays* 5: 2656-2663.
16. Olmos J, Paniagua J, Contreras R (2000) Molecular identification of *Dunaliella* sp utilizing the 18S rDNA gene. *Letters in Applied Microbiology* 30: 80-84.
17. Fredslund J (2006) PHY center dot FI: fast and easy online creation and manipulation of phylogeny color figures. *Bmc Bioinformatics* 7.
18. Krohn BJ, McNeff CV, Yan B, Nowlan D (2011) Production of algae-based biodiesel using the continuous catalytic Mcgyan process. *Bioresour Technol* 102: 94-100.
19. Singh A, Nigam PS, Murphy JD (2011) Renewable fuels from algae: an answer to debatable land based fuels. *Bioresour Technol* 102: 10-16.
20. Metzger P, Largeau C (2005) *Botryococcus braunii*: a rich source for hydrocarbons and related ether lipids. *Appl Microbiol Biotechnol* 66: 486-496.
21. Chiu SY, Kao CY, Tsai MT, Ong SC, Chen CH, et al. (2009) Lipid accumulation and CO<sub>2</sub> utilization of *Nannochloropsis oculata* in response to CO<sub>2</sub> aeration. *Bioresour Technol* 100: 833-838.
22. Chen M, Tang H, Ma H, Holland TC, Ng KY, et al. (2011) Effect of nutrients on growth and lipid accumulation in the green algae *Dunaliella tertiolecta*. *Bioresour Technol* 102: 1649-1655.
23. Damiani MC, Popovich CA, Constenla D, Leonardi PI (2010) Lipid analysis in *Haematococcus pluvialis* to assess its potential use as a biodiesel feedstock. *Bioresour Technol* 101: 3801-3807.
24. Liu ZY, Wang GC, Zhou BC (2008) Effect of iron on growth and lipid accumulation in *Chlorella vulgaris*. *Bioresour Technol* 99: 4717-4722.
25. Li Y, Horsman M, Wang B, Wu N, Lan CQ (2008) Effects of nitrogen sources on cell growth and lipid accumulation of green alga *Neochloris oleoabundans*. *Appl Microbiol Biotechnol* 81: 629-636.
26. Ho SH, Chen WM, Chang JS (2010) *Scenedesmus obliquus* CNW-N as a potential candidate for CO<sub>2</sub> mitigation and biodiesel production. *Bioresour Technol* 101: 8725-8730.
27. Mandal S, Mallick N (2009) Microalga *Scenedesmus obliquus* as a potential source for biodiesel production. *Appl Microbiol Biotechnol* 84: 281-291.
28. Lin Q, Lin J (2011) Effects of nitrogen source and concentration on biomass and oil production of a *Scenedesmus rubescens* like microalga. *Bioresour Technol* 102: 1615-1621.

29. Hsieh CH, Wu WT (2009) Cultivation of microalgae for oil production with a cultivation strategy of urea limitation. *Bioresour Technol* 100: 3921-3926.
30. Xin L, Hu HY, Ke G, Sun YX (2010) Effects of different nitrogen and phosphorus concentrations on the growth, nutrient uptake, and lipid accumulation of a freshwater microalga *Scenedesmus* sp. *Bioresour Technol* 101: 5494-5500.
31. Romek M, Gajda B, Krzysztofowicz E, Kepczynski M, Smorag Z (2011) New technique to quantify the lipid composition of lipid droplets in porcine oocytes and pre-implantation embryos using Nile Red fluorescent probe. *Theriogenology* 75: 42-54.
32. Siaux M, Cuine S, Cagnon C, Fessler B, Nguyen M, et al. (2011) Oil accumulation in the model green alga *Chlamydomonas reinhardtii*: characterization, variability between common laboratory strains and relationship with starch reserves. *BMC Biotechnol* 11: 7.
33. da Silva TL, Reis A, Medeiros R, Oliveira AC, Gouveia L (2009) Oil production towards biofuel from autotrophic microalgae semicontinuous cultivations monitored by flow cytometry. *Appl Biochem Biotechnol* 159: 568-578.
34. Chen W, Zhang C, Song L, Sommerfeld M, Hu Q (2009) A high throughput Nile red method for quantitative measurement of neutral lipids in microalgae. *J Microbiol Methods* 77: 41-47.

## CHAPTER 2

1. Camacho FG, Rodriguez JG, Miron AS, Garcia MC, Belarbi EH, et al. (2007) Biotechnological significance of toxic marine dinoflagellates. *Biotechnol Adv* 25: 176-194.
2. Li Y, Horsman M, Wang B, Wu N, Lan CQ (2008) Effects of nitrogen sources on cell growth and lipid accumulation of green alga *Neochloris oleoabundans*. *Appl Microbiol Biotechnol* 81: 629-636.
3. Csavina JL, Stuart BJ, Riefler RG, Vis ML (2011) Growth optimization of algae for biodiesel production. *J Appl Microbiol* 111: 312-318.
4. Spolaore P, Joannis-Cassan C, Duran E, Isambert A (2006) Commercial applications of microalgae. *J Biosci Bioeng* 101: 87-96.
5. Alscher RG, Donahue JL, Cramer CL (1997) Reactive oxygen species and antioxidants: Relationships in green cells. *Physiologia Plantarum* 100: 224-233.

6. Mallick N, Mohn FH (2000) Reactive oxygen species: response of algal cells. *Journal of Plant Physiology* 157: 183-193.
7. Liu WH, Huang ZW, Li P, Xia JF, Chen B (2012) Formation of triacylglycerol in *Nitzschia closterium* f. *minutissima* under nitrogen limitation and possible physiological and biochemical mechanisms. *Journal of Experimental Marine Biology and Ecology* 418: 24-29.
8. Li X, Hu HY, Zhang YP (2011) Growth and lipid accumulation properties of a freshwater microalga *Scenedesmus* sp. under different cultivation temperature. *Bioresour Technol* 102: 3098-3102.
9. Hong Y, Hu HY, Li FM (2008) Physiological and biochemical effects of allelochemical ethyl 2-methyl acetoacetate (EMA) on cyanobacterium *Microcystis aeruginosa*. *Ecotoxicol Environ Saf* 71: 527-534.
10. Gordillo FL, Goutx M, Figueroa F, Niell FX (1998) Effects of light intensity, CO<sub>2</sub> and nitrogen supply on lipid class composition of *Dunaliella viridis*. *Journal of Applied Phycology* 10: 135-144.
11. Olmos J, Paniagua J, Contreras R (2000) Molecular identification of *Dunaliella* sp utilizing the 18S rDNA gene. *Letters in Applied Microbiology* 30: 80-84.
12. Fredslund J (2006) PHY center dot FI: fast and easy online creation and manipulation of phylogeny color figures. *Bmc Bioinformatics* 7.
13. Levasseur M, Thompson PA, Harrison PJ (1993) Physiological acclimation of marine-phytoplankton to different nitrogen-sources. *Journal of Phycology* 29: 587-595.
14. Greenspan P, Mayer EP, Fowler SD (1985) Nile red: a selective fluorescent stain for intracellular lipid droplets. *J Cell Biol* 100: 965-973.
15. Govender T, Ramanna L, Rawat I, Bux F (2012) BODIPY staining, an alternative to the Nile Red fluorescence method for the evaluation of intracellular lipids in microalgae. *Bioresour Technol* 114: 507-511.
16. Chen W, Sommerfeld M, Hu Q (2011) Microwave-assisted Nile red method for in vivo quantification of neutral lipids in microalgae. *Bioresour Technol* 102: 135-141.
17. Chen W, Zhang C, Song L, Sommerfeld M, Hu Q (2009) A high throughput Nile red method for quantitative measurement of neutral lipids in microalgae. *J Microbiol Methods* 77: 41-47.
18. Cole TA, Fok AK, Ueno MS, Allen RD (1990) Use of Nile red as a rapid measure of lipid content in ciliates. *Eur J Protistol* 25: 361-368.

19. Kimura K, Yamaoka M, Kamisaka Y (2004) Rapid estimation of lipids in oleaginous fungi and yeasts using Nile red fluorescence. *J Microbiol Methods* 56: 331-338.
20. Kalyanaraman B, Darley-Usmar V, Davies KJA, Dennery PA, Forman HJ, et al. (2012) Measuring reactive oxygen and nitrogen species with fluorescent probes: challenges and limitations. *Free Radical Biology and Medicine* 52: 1-6.
21. Liang ZJ, Ge F, Zeng H, Xu Y, Peng F, et al. (2013) Influence of cetyltrimethyl ammonium bromide on nutrient uptake and cell responses of *Chlorella vulgaris*. *Aquatic Toxicology* 138: 81-87.
22. Schonswetter P, Tribsch A, Barfuss M, Niklfeld H (2002) Several Pleistocene refugia detected in the high alpine plant *Phyteuma globulariifolium* sternb & hoppe (Campanulaceae) in the European Alps. *Mol Ecol* 11: 2637-2647.
23. Barbarino E, Lourenco SO (2005) an evaluation of methods for extraction and quantification of protein from marine macro- and microalgae. *Journal of Applied Phycology* 17: 447-460.
24. Bradford MM (1976) A rapid and sensitive method for the quantitation of microgram quantities of protein utilizing the principle of protein-dye binding. *Anal Biochem* 72: 248-254.
25. Wellburn AR (1994) the spectral determination of chlorophyll-A and chlorophyll-b, as well as total carotenoids, using various solvents with spectrophotometers of different resolution. *Journal of Plant Physiology* 144: 307-313.
26. Sabatini SE, Juarez AB, Eppis MR, Bianchi L, Luquet CM, et al. (2009) Oxidative stress and antioxidant defenses in two green microalgae exposed to copper. *Ecotoxicology and Environmental Safety* 72: 1200-1206.
27. Dhindsa RS, Plumbdhindsa P, Thorpe TA (1981) Leaf senescence - correlated with increased levels of membrane-permeability and lipid-peroxidation, and decreased levels of superoxide-dismutase and catalase. *Journal of Experimental Botany* 32: 93-101.
28. Aebi H (1984) Catalase invitro. *Methods in Enzymology* 105: 121-126.
29. Nakano Y, Asada K (1981) Hydrogen-peroxide is scavenged by ascorbate-specific peroxidase in spinach-chloroplasts. *Plant and Cell Physiology* 22: 867-880.
30. Tang HY, Abunasser N, Garcia MED, Chen M, Ng KYS, et al. (2011) Potential of microalgae oil from *Dunaliella tertiolecta* as a feedstock for biodiesel. *Applied Energy* 88: 3324-3330.

31. Ho SH, Chen WM, Chang JS (2010) *Scenedesmus obliquus* CNW-N as a potential candidate for CO<sub>2</sub> mitigation and biodiesel production. *Bioresource Technology* 101: 8725-8730.
32. Griffiths MJ, van Hille RP, Harrison STL (2012) Lipid productivity, settling potential and fatty acid profile of 11 microalgal species grown under nitrogen replete and limited conditions. *Journal of Applied Phycology* 24: 989-1001.
33. Chen M, Tang HY, Ma HZ, Holland TC, Ng KYS, et al. (2011) Effect of nutrients on growth and lipid accumulation in the green algae *Dunaliella tertiolecta*. *Bioresource Technology* 102: 1649-1655.
34. Sharma KK, Schuhmann H, Schenk PM (2012) High Lipid Induction in Microalgae for Biodiesel Production. *Energies* 5: 1532-1553.
35. Lee SJ, Yoon BD, Oh HM (1998) Rapid method for the determination of lipid from the green alga *Botryococcus braunii*. *Biotechnology Techniques* 12: 553-556.
36. Lin QA, Lin JD (2011) Effects of nitrogen source and concentration on biomass and oil production of a *Scenedesmus rubescens* like microalga. *Bioresource Technology* 102: 1615-1621.
37. Bhaduri AM, Fulekar MH (2012) Antioxidant enzyme responses of plants to heavy metal stress. *Reviews in Environmental Science and Bio-Technology* 11: 55-69.
38. Alscher RG, Erturk N, Heath LS (2002) Role of superoxide dismutases (SODs) in controlling oxidative stress in plants. *Journal of Experimental Botany* 53: 1331-1341.
39. Del Rio LA, Sandalio LM, Corpas FJ, Palma JM, Barroso JB (2006) Reactive oxygen species and reactive nitrogen species in peroxisomes. Production, scavenging, and role in cell signaling. *Plant Physiology* 141: 330-335.
40. Miller SR, Martin M, Touchton J, Castenholz RW (2002) Effects of nitrogen availability on pigmentation and carbon assimilation in the cyanobacterium *Synechococcus* sp strain SH-94-5. *Archives of Microbiology* 177: 392-400.
41. Singh SP, Hader DP, Sinha RP (2010) Cyanobacteria and ultraviolet radiation (UVR) stress: Mitigation strategies. *Ageing Research Reviews* 9: 79-90.
42. Courchesne NMD, Parisien A, Wang B, Lan CQ (2009) Enhancement of lipid production using biochemical, genetic and transcription factor engineering approaches. *Journal of Biotechnology* 141: 31-41.
43. Msanne J, Xu D, Konda AR, Casas-Mollano JA, Awada T, et al. (2012) Metabolic and gene expression changes triggered by nitrogen deprivation in the photoautotrophically

- grown microalgae *Chlamydomonas reinhardtii* and *Coccomyxa* sp C-169. *Phytochemistry* 75: 50-59.
44. Tsukagoshi H (2012) Defective root growth triggered by oxidative stress is controlled through the expression of cell cycle-related genes. *Plant Science* 197: 30-39.
  45. Cash TP, Pan Y, Simon MC (2007) Reactive oxygen species and cellular oxygen sensing. *Free Radical Biology and Medicine* 43: 1219-1225.
  46. Converti A, Casazza AA, Ortiz EY, Perego P, Del Borghi M (2009) Effect of temperature and nitrogen concentration on the growth and lipid content of *Nannochloropsis oculata* and *Chlorella vulgaris* for biodiesel production. *Chemical Engineering and Processing* 48: 1146-1151.
  47. Hu Q, Sommerfeld M, Jarvis E, Ghirardi M, Posewitz M, et al. (2008) Microalgal triacylglycerols as feedstocks for biofuel production: perspectives and advances. *Plant Journal* 54: 621-639.
  48. Kobayashi M (2003) Astaxanthin biosynthesis enhanced by reactive oxygen species in the green alga *Haematococcus pluvialis*. *Biotechnology and Bioprocess Engineering* 8: 322-330.
  49. Pinto E, Sigaud-Kutner TCS, Leitao MAS, Okamoto OK, Morse D, et al. (2003) Heavy metal-induced oxidative stress in algae. *Journal of Phycology* 39: 1008-1018.
  50. Zhang YM, Chen H, He CL, Wang Q (2013) Nitrogen starvation induced oxidative stress in an oil-producing green alga *Chlorella sorokiniana* C3. *PLoS One* 8: e69225.
  51. Zhang ZD, Shrager J, Jain M, Chang CW, Vallon O, et al. (2004) Insights into the survival of *Chlamydomonas reinhardtii* during sulfur starvation based on microarray analysis of gene expression. *Eukaryotic Cell* 3: 1331-1348.
  52. Nishiyama Y, Yamamoto H, Allakhverdiev SI, Inaba M, Yokota A, et al. (2001) Oxidative stress inhibits the repair of photodamage to the photosynthetic machinery. *EMBO J* 20: 5587-5594.
  53. Garcia-Ferris C, Moreno J (1993) Redox regulation of enzymatic activity and proteolytic susceptibility of ribulose-1, 5-bisphosphate carboxylase/oxygenase from *Euglena gracilis*. *Photosynth Res* 35: 55-66.
  54. Cakmak T, Angun P, Ozkan AD, Cakmak Z, Olmez TT, et al. (2012) Nitrogen and sulfur deprivation differentiate lipid accumulation targets of *Chlamydomonas reinhardtii*. *Bioengineered* 3: 343-346.

### CHAPTER 3

1. Malik A (2004) Metal bioremediation through growing cells. *Environment international* 30: 261-278.
2. Gupta VK, Rastogi A (2008) Biosorption of lead from aqueous solutions by green algae *Spirogyra* species: kinetics and equilibrium studies. *J Hazard Mater* 152: 407-414.
3. Davis T, Volesky B, Mucci A (2003) A review of the biochemistry of heavy metal biosorption by brown algae. *Water research* 37: 4311-4330.
4. Torres E, Cid A, Herrero C, Abalde J (1998) Removal of cadmium ions by the marine diatom *Phaeodactylum tricornutum* bohlin accumulation and long-term kinetics of uptake. *Bioresource Technology* 63: 213-220.
5. Flouty R, Estephane G (2012) Bioaccumulation and biosorption of copper and lead by a unicellular algae *Chlamydomonas reinhardtii* in single and binary metal systems: a comparative study. *Journal of environmental management* 111: 106-114.
6. Liu Y, Cao Q, Luo F, Chen J (2009) Biosorption of Cd<sup>2+</sup>, Cu<sup>2+</sup>, Ni<sup>2+</sup> and Zn<sup>2+</sup> ions from aqueous solutions by pretreated biomass of brown algae. *Journal of hazardous materials* 163: 931-938.
7. Chisti Y (2008) Biodiesel from microalgae beats bioethanol. *Trends in biotechnology* 26: 126-131.
8. Li Y, Horsman M, Wu N, Lan CQ, Dubois-Calero N (2008) Biofuels from microalgae. *Biotechnol Prog* 24: 815-820.
9. Sivakumar G, Xu J, Thompson R, Yang Y, Randol-Smith P, et al. (2012) Integrated green algal technology for bioremediation and biofuel. *Bioresource technology* 107: 1-9.
10. Tsukahara K, Sawayama S (2005) Liquid fuel production using microalgae. *J Jpn Pet Inst* 48: 251.
11. Elenkov I, Stefanov K, Popov S, Dimitrova-Konaklieva S Effect of salinity on lipid composition of *Cladophora vagabunda*. *Phytochemistry* 42: 39-44.
12. Liu W, Au DWT, Anderson DM, Lam PKS, Wu RSS (2007) Effects of nutrients, salinity, pH and light:dark cycle on the production of reactive oxygen species in the alga *Chattonella marina*. *Journal of Experimental Marine Biology and Ecology* 346: 76-86.
13. Liu W, Ming Y, Li P, Huang Z (2012) Inhibitory effects of hypo-osmotic stress on extracellular carbonic anhydrase and photosynthetic efficiency of green alga *Dunaliella salina* possibly through reactive oxygen species formation. *Plant Physiology and Biochemistry* 54: 43-48.

14. Mallick N, Mohn FH (2000) Reactive oxygen species: response of algal cells. *Journal of Plant Physiology* 157: 183-193.
15. Olmos J, Paniagua J, Contreras R (2000) Molecular identification of *Dunaliella* sp. utilizing the 18S rDNA gene. *Lett Appl Microbiol* 30: 80-84.
16. Lagergren S (1898) Zur theorie der sogenannten adsorption gelöster stoffe. *Handlingar* 24: 1-39.
17. Ho YS, McKay G (1999) Pseudo-second order model for sorption processes. *Process Biochemistry* 34: 451-465.
18. Chien SH, Clayton WR (1980) Application of elovich equation to the kinetics of phosphate release and sorption in soils. *Soil Science Society of America Journal* 44: 265-268.
19. Weber J, W. J., Morris, J. C. (1963) Kinetics of adsorption on carbon from solution. *Journal of the Sanitary Engineering Division* 89: 31-39.
20. Abramian L, El-Rassy H (2009) Adsorption kinetics and thermodynamics of azo-dye Orange II onto highly porous titania aerogel. *Chemical Engineering Journal* 150: 403-410.
21. Mudhoo A, Garg VK, Wang SB (2012) Removal of heavy metals by biosorption. *Environmental Chemistry Letters* 10: 109-117.
22. Liu WH, Huang ZW, Li P, Xia JF, Chen B (2012) Formation of triacylglycerol in *Nitzschia closterium* f. *minutissima* under nitrogen limitation and possible physiological and biochemical mechanisms. *Journal of Experimental Marine Biology and Ecology* 418: 24-29.
23. Menon KR, Balan R, Suraishkumar GK (2013) Stress induced lipid production in *Chlorella vulgaris*: Relationship with specific intracellular reactive species levels. *Biotechnology and Bioengineering* 110: 1627-1636.
24. Dean AP, Sigeo DC, Estrada B, Pittman JK (2010) Using FTIR spectroscopy for rapid determination of lipid accumulation in response to nitrogen limitation in freshwater microalgae. *Bioresource Technology* 101: 4499-4507.
25. Li J, Ou DY, Zheng LL, Gan NQ, Song LR (2011) Applicability of the fluorescein diacetate assay for metabolic activity measurement of *Microcystis aeruginosa* (Chroococcales, Cyanobacteria). *Phycological Research* 59: 200-207.
26. Miller SR, Martin M, Touchton J, Castenholz RW (2002) Effects of nitrogen availability on pigmentation and carbon assimilation in the cyanobacterium *Synechococcus* sp. strain SH-94-5. *Arch Microbiol* 177: 392-400.

## CHAPTER 4

1. Matsuzaki M, Misumi O, Shin-I T, Maruyama S, Takahara M, et al. (2004) Genome sequence of the ultrasmall unicellular red alga *Cyanidioschyzon merolae* 10D. *Nature* 428: 653-657.
2. Armbrust EV, Berges JA, Bowler C, Green BR, Martinez D, et al. (2004) The genome of the diatom *Thalassiosira pseudonana*: Ecology, evolution, and metabolism. *Science* 306: 79-86.
3. Shrager J, Hauser C, Chang CW, Harris EH, Davies J, et al. (2003) *Chlamydomonas reinhardtii* genome project. A guide to the generation and use of the cDNA information. *Plant Physiology* 131: 401-408.
4. France Thevenieau J-MN (2013) Microorganisms as sources of oils. *OCL* 20: 8.
5. Radakovits R, Jinkerson RE, Darzins A, Posewitz MC (2010) Genetic Engineering of Algae for Enhanced Biofuel Production. *Eukaryotic Cell* 9: 486-501.
6. Dunahay TG, Jarvis EE, Roessler PG (1995) Genetic transformation of the diatoms *Cyclotella cryptica* and *Navicula saprophila*. *Journal of Phycology* 31: 1004-1012.
7. Zabawinski C, Van den Koornhuysen N, D'Hulst C, Schlichting R, Giersch C, et al. (2001) Starchless mutants of *Chlamydomonas reinhardtii* lack the small subunit of a heterotetrameric ADP-glucose pyrophosphorylase. *Journal of Bacteriology* 183: 1069-1077.
8. Ramazanov A, Ramazanov Z (2006) Isolation and characterization of a starchless mutant of *Chlorella pyrenoidosa* STL-PI with a high growth rate, and high protein and polyunsaturated fatty acid content. *Phycological Research* 54: 255-259.
9. Tai M, Stephanopoulos G (2013) Engineering the push and pull of lipid biosynthesis in oleaginous yeast *Yarrowia lipolytica* for biofuel production. *Metabolic Engineering* 15: 1-9.
10. Rani SH, Saha S, Rajasekharan R (2013) A soluble diacylglycerol acyltransferase is involved in triacylglycerol biosynthesis in the oleaginous yeast *Rhodotorula glutinis*. *Microbiology-Sgm* 159: 155-166.
11. Beopoulos A, Haddouche R, Kabran P, Dulermo T, Chardot T, et al. (2012) Identification and characterization of DGA2, an acyltransferase of the DGAT1 acyl-CoA:diacylglycerol acyltransferase family in the oleaginous yeast *Yarrowia lipolytica*.

- New insights into the storage lipid metabolism of oleaginous yeasts. *Applied Microbiology and Biotechnology* 93: 1523-1537.
12. Dulermo T, Nicaud JM (2011) Involvement of the G3P shuttle and beta-oxidation pathway in the control of TAG synthesis and lipid accumulation in *Yarrowia lipolytica*. *Metabolic Engineering* 13: 482-491.
  13. Chuang LT, Chen DC, Nicaud JM, Madzak C, Chen YH, et al. (2010) Co-expression of heterologous desaturase genes in *Yarrowia lipolytica*. *New Biotechnology* 27: 277-282.
  14. Liang MH, Jiang JG (2013) Advancing oleaginous microorganisms to produce lipid via metabolic engineering technology. *Progress in Lipid Research* 52: 395-408.
  15. Bulter T, Alcalde M, Sieber V, Meinhold P, Schlachtbauer C, et al. (2003) Functional expression of a fungal laccase in *Saccharomyces cerevisiae* by directed evolution. *Applied and Environmental Microbiology* 69: 987-995.
  16. Morawski B, Quan S, Arnold FH (2001) Functional expression and stabilization of horseradish peroxidase by directed evolution in *Saccharomyces cerevisiae*. *Biotechnology and Bioengineering* 76: 99-107.
  17. Lee SM, Jellison T, Alper HS (2012) Directed Evolution of Xylose Isomerase for Improved Xylose Catabolism and Fermentation in the Yeast *Saccharomyces cerevisiae*. *Applied and Environmental Microbiology* 78: 5708-5716.
  18. Vermaas W (1996) Molecular genetics of the cyanobacterium *Synechocystis* sp. PCC 6803: Principles and possible biotechnology applications. *Journal of Applied Phycology* 8: 263-273.
  19. Das S, Roymondal U, Chottopadhyay B, Sahoo S (2012) Gene expression profile of the cyanobacterium *synechocystis* genome. *Gene* 497: 344-352.
  20. Lei AP, Chen H, Shen GM, Hu ZL, Chen L, et al. (2012) Expression of fatty acid synthesis genes and fatty acid accumulation in *Haematococcus pluvialis* under different stressors. *Biotechnology for Biofuels* 5.
  21. Lamers PP, Janssen M, De Vos RCH, Bino RJ, Wijffels RH (2012) Carotenoid and fatty acid metabolism in nitrogen-starved *Dunaliella salina*, a unicellular green microalga. *Journal of Biotechnology* 162: 21-27.
  22. Dong ZG, Zhao HJ, He JG, Huai JL, Lin H, et al. (2011) Overexpression of a foxtail millet Acetyl-CoA carboxylase gene in maize increases sethoxydim resistance and oil content. *African Journal of Biotechnology* 10: 3986-3995.